Neuro-biomécanique de la redondance musculaire – Modélisation musculo-squelettique et contrôle moteur de la co-contraction agoniste / antagoniste

David Amarantini

Rapport de Synthèse

En vue de l'obtention de l'

Habilitation à Diriger des Recherches

Discipline : **Sciences et Techniques des Activités Physiques et Sportives**
Spécialités : **Biomécanique & Neurosciences**

Présenté et soutenu le 18/06/2019 par

David AMARANTINI

Neuro-biomécanique de la redondance musculaire

Modélisation musculo-squelettique et contrôle moteur de la co-contraction agoniste / antagoniste

Devant le jury composé de :

Éric BERTON	PU	ISM UMR 7287, Aix-Marseille Université	Parrain
Laurence CHÈZE	PU	LBMC UMR T9406, Université de Lyon	Rapporteure
François HUG	PU	MIP EA 4334, Université de Nantes	Rapporteur
Philippe MARQUE	PU-PH	ToNIC UMR 1214, Université de Toulouse	Examinateur
Alain MARTIN	PU	CAPS U 1093, Université de Bourgogne	Examinateur
Stéphane PERREY	PU	Euromov EA 2991, Université de Montpellier	Rapporteur

phd.stanford.edu/comics

Remerciements

« Tout vient à point à qui sait attendre » ou « tout ça pour ça », le lecteur naïf ou spécialiste curieux saura trouver le sous-titre le plus adapté à ce rapport de synthèse. Toujours est-il que la légende voudrait qu'Eric Berton s'écria « Alleluiacciu » du sommet du Monte Cinto à la réception de ce manuscrit. Si la réalité ne laisse aucun doute sur le fait qu'Eric Berton entreprend régulièrement la traditionnelle ascension du Monte Cinto (NDR (et non MDR !) : plus haut sommet de Corse culminant à 2706 m), force est de reconnaitre que, peu conscient de l'importance du diplôme d'Habilitation à Diriger les Recherches (j'invite le lecteur à lire le chapitre consacré à ce sujet dans le mémoire présenté par Eric Dufrêne en 2007 [1]), je n'ai cessé d'en repousser la rédaction depuis 2012. *Mea culpa*, mon Ecole Doctorale ! Je prends pour excuse – valable ! – d'avoir – à raison ! – consacré le maximum des heures « Recherche » que mes métiers de maître de conférences m'accordent encore au plaisir d'autres activités qui m'ont permis de construire le cheminement scientifique dont il m'est aujourd'hui donné l'occasion de faire la synthèse.

Mon parcours scientifique, puisqu'il est le personnage principal de ce récit, n'aurait pas été le même sans certaines rencontres décisives. Il leur revient de fait d'être ajoutées au casting de cette Odyssée ; par ordre chronologique d'apparition.

Merci à toi…
♫ *Salut à toi – Joyeux Merdier (Bérurier Noir, 1985)*

… Jean Pierre Blanchi, Luc Martin, Violaine Cahouët, François Prince, Hugo Centomo, Eric Berton, Guillaume Rao, Bernard Thon, Manh-Cuong Do, Jessica Tallet, Marieke Longcamp, Fabien Dal Maso, Jérémie Bigot, David Gasq, Sylvain Cremoux, Julien Duclay, Camille Charissou, Robin Baurès, Philippe Marque, Isabelle Loubinoux, Alexandre Chalard, Joseph Tisseyre, Maxime Fauvet, …

… tous les collaborateur·trice·s proches et moins proches avec qui j'ai eu, j'ai et j'aurai encore plaisir à échanger et travailler, que je préfère ne pas citer de peur d'en oublier (la mémoire, à mon âge...).

Et merci ❤ à vous, Anne-Laure, Orso, Lou et Viggo.

---

[1] Dufrêne, E. (2007). Mémoire pour l'obtention d'une Habilitation à Diriger des Recherches. Université Paris-Sud. Repéré à : http://max2.ese.u-psud.fr/publications/2007dufre_HDR.pdf.

Table des matières

Introduction

I. Introduction

Ce document est la synthèse du cheminement scientifique que j'ai suivi depuis que j'ai soutenu ma thèse en 2003 (dir. : Luc Martin ; Laboratoire Sport et Performance Motrice (SPM), EA 597, Université Joseph Fourier Grenoble I, Grenoble), d'abord en tant qu'attaché temporaire d'enseignement et de recherche à l'Université de la Méditerranée Aix-Marseille II (2003-2004), puis comme maître de conférences à l'Université Paul Sabatier Toulouse III.

J'ai été successivement rattaché au Laboratoire d'Aérodynamique et de Biomécanique du Mouvement (LABM, USR 2164 CNRS, Marseille), au Laboratoire Adaptation Perceptivo Motrice et Apprentissage (LAPMA (EA 3691) puis PRISSMH-LAPMA (EA 4561), Toulouse) et au Toulouse NeuroImaging Center (ToNIC, UMR 825 puis UMR 1214 Inserm / UPS, Toulouse). J'y ai (co-)encadré 5 thèses de Doctorat et 18 Master 2 Recherche déjà soutenus, ainsi que 16 Master 2 Professionnel dans l'offre de formation en « Entrainement Sportif » à la Faculté des Sciences du Sport et du Mouvement Humain (Université Paul Sabatier Toulouse III, Toulouse). L'ensemble de mes travaux ont conduit à la publication de 59 articles (36), chapitre (1), rapports d'études (3) et résumés (19), et la présentation de 100 communications orales (69) et affichées (31).

Au sein de chacune des équipes auxquelles j'ai été intégré, j'ai participé au développement des activités des recherche dans le domaine de la biomécanique puis de la neuro-biomécanique, en centrant mes travaux sur la question de la redondance musculaire. Cette propriété anatomo-fonctionnelle est liée au fait que le système musculo-squelettique dispose de plus de muscles que de degrés de liberté articulaires, avec en moyenne 2,6 actionneurs musculaires par degré de liberté cinématique. La redondance musculaire confère ainsi une extrême complexité au système neuro-musculo-squelettique, mais apparaît également comme un atout majeur pour adapter la coordination motrice aux contraintes externes et internes du mouvement (Gelfand & Latash, 1998 ; Latash, 2012 ; Roby-Brami *et al.,* 2005). C'est un sujet de recherche au cœur des questions fondamentales et appliquées dans les domaines de la biomécanique et du contrôle moteur, où il fait notamment référence aux problèmes de la « redondance motrice » ('problem of motor redundancy' ; Bernstein,

1967) et de la « distribution des forces musculaires » ('force-sharing problem' ; p. ex., Chao & An, 1978 ; Prilutsky, 2000). En termes mécanique, la redondance musculaire implique qu'il existe une infinité de combinaisons de forces (ou de moments de forces) musculaires individuelles possibles pour produire un même effort résultant dans une direction donnée autour d'une articulation. La complexité du problème sous-déterminé qui en découle est d'autant plus importante que la redondance musculaire ne concerne pas que les muscles synergistes agonistes qui exercent un effort dans le sens de l'effort résultant, mais également les muscles synergistes antagonistes qui agissent simultanément dans le sens opposé. Même si de nombreux modèles musculo-squelettiques ont été proposés – y compris ceux que nous avons développés dans le cadre de mon travail de thèse (Amarantini & Martin, 2004 ; Cahouët *et al.,* 2002) – pour trouver une solution à ce problème et fournir une estimation physiologiquement réaliste des efforts résultant, agoniste et antagoniste, et musculaires, la question de la quantification de l'action mécanique produite par les muscles lors d'une action isométrique ou dynamique n'est pas résolue. C'est dans ce contexte que j'ai initié mes travaux dans le but de contribuer à une meilleure caractérisation et une meilleure compréhension du phénomène de co-contraction entre les muscles agonistes et antagonistes en utilisant une approche biomécanique. L'objectif était à la fois de proposer un modèle musculo-squelettique fournissant une estimation fiable de la contribution mécanique des muscles antagonistes à la production d'un effort résultant, et d'étudier les facteurs susceptibles d'expliquer la modulation de cette contribution dans une double perspective clinique et d'optimisation de la performance. Dans la continuité de mon travail de thèse, ces travaux ont donné lieu à la co-direction de la thèse de Guillaume Rao (Rao, 2006 ; co-dir. : Eric Berton) et ma participation active à celle d'Hugo Centomo (Centomo, 2006 ; dirs. : François Prince & Luc Martin) qui m'a par ailleurs permis d'établir une collaboration internationale durable et productive avec le Département de kinésiologie de l'Université de Montréal. Les études que nous avons menées ont contribué à une meilleure compréhension du rôle fonctionnel et des conséquences d'une altération du niveau d'activité des muscles antagonistes lors de la production d'un effort musculaire chez des sujets sains (Amarantini & Bru, 2015 ; Rao *et al.,* 2009) et des patients souffrant d'un déficit moteur (Centomo *et al.,* 2007, 2008). Elles feront l'objet du premier chapitre de cette note de synthèse pour

l'habilitation à diriger des recherches, intitulé « La biomécanique, c'est génial ! »[2] à la suite de mon curriculum vitae détaillé.

Dans le même temps, ces travaux ont fait émerger de nouveaux questionnements qui m'ont conduit à développer, en étroite collaboration avec Marieke Longcamp (Laboratoire de Neurosciences Cognitives, UMR 7291 CNRS / Aix-Marseille Université, Marseille) et Jérémie Bigot (Institut de Mathématiques de Bordeaux, UMR 5251 CNRS / Université de Bordeaux, Bordeaux), une nouvelle approche pluridisciplinaire au croisement de la biomécanique et des neurosciences pour aborder la question des mécanismes nerveux centraux sous-jacents au contrôle de l'activité musculaire antagoniste chez l'homme. Cette conversion, ou plutôt cette extension thématique a été opérée au regard de deux constats. Le premier concerne la difficulté d'arriver à un consensus clair dans la communauté scientifique en biomécanique quant à la définition d'un modèle musculo-squelettique de référence pour l'estimation des efforts musculaires « au-delà » du moment musculaire résultant. Même si dans ce domaine l'innovation doit rester une priorité énoncée de longue date (Yeadon & Challis, 1994), on peut questionner, et regretter en ce qui me concerne, le caractère analytique des nombreux modèles musculo-squelettique proposés dans le domaine de la biomécanique du mouvement au détriment d'un modèle synthétique. Le second constat est, comme l'illustre parfaitement la réflexion de Désiré Mégot (Tome & Janry, 2010 ; p. 20) et l'affirme Latash (2016), la nécessité réciproque d'étudier les mécanismes nerveux sous-jacents la modulation de l'activité musculaire pour comprendre le fonctionnement biomécanique du système musculo-squelettique. Dans cette logique, la stratégie de recherche que j'ai priorisée se fonde sur l'analyse combinée de données électroencéphalographiques (EEG), électromyographiques (EMG) et d'efforts musculaires pour aborder la problématique clé du contrôle moteur de la redondance musculaire lors de contractions normales et altérées chez l'homme. J'ai fait le choix de privilégier l'analyse de cohérence entre les signaux électrophysiologiques (EEG-EMG et EMG-EMG) comme un outil approprié pour étudier la contribution des mécanismes nerveux centraux (Boonstra, 2013 ; Dai *et al.,* 2017) à la régulation du niveau d'activité des muscles antagonistes chez des sujets sains contrôles ou experts dans une spécialité sportive, et des patients présentant des déficiences motrices. Nous avons développé une méthode originale d'analyse de cohérence temps-fréquence (Bigot *et al.,* 2011), combinée à la mesure des efforts

---

[2] Adapté du titre complet de la première édition du livre intitulé « analyse du mouvement humain par la biomécanique » (Allard & Blanchi, 1996), co-écrit par mon non moins génial directeur de DEA Jean-Pierre Blanchi.

musculaires et/ou à la modélisation biomécanique. Cette démarche a permis d'étudier de manière globale le rôle fonctionnel de la co-contraction entre les muscles agonistes et antagonistes, et de mieux comprendre les mécanismes impliqués dans la distribution des efforts musculaires en fonction des contraintes externes et internes de la contraction musculaire. Ces travaux ont été concrétisés par les thèses de Fabien Dal Maso (Dal Maso, 2012 ; co-dir. : Marieke Longcamp), Sylvain Cremoux (Cremoux, 2013 ; co-dir. : Eric Berton) et Camille Charissou (Charissou, 2018 ; co-dirs. : Laurent Vigouroux & Eric Berton) que j'ai co-encadrées. Ces problématiques seront développées dans le deuxième chapitre de cette note de synthèse pour l'habilitation à diriger des recherches, intitulé « La neuro-biomécanique, c'est magique ! ».

Je tiens à souligner que, de manière transversale à l'ensemble de mes travaux de recherche, j'ai porté un soin tout particulier au développement de mes propres scripts de traitement de données, en faisant appel pour certains aux techniques les plus avancées dans les domaines du calcul numérique et du traitement du signal. Ce choix est central dans les questions qui jalonnent mon parcours scientifique et dans ma pratique d'encadrement, comme dans le cadre de la co-direction de la thèse de David Gasq (Gasq, 2015 ; co-dir. : Pier-Giorgio Zanone) qui a par ailleurs permis de diversifier mes travaux sur des problématiques cliniques chez les patients cérébro-lésés en phase chronique, et de les valoriser dans le domaine industriel. Cet aspect de mon travail de recherche a pour défauts d'être addictif, chronophage et plus difficile à valoriser directement en termes de productions scientifiques reconnues, mais il présente à mon sens plusieurs avantages qui marquent ma stratégie de recherche. Le premier est l'acquisition de compétences et des connaissances déterminantes en vue d'obtenir des résultats fiables et reproductibles, condition indispensable pour en faire une interprétation adéquate. Le second est la maitrise de chacune des étapes et des paramètres du traitement des données, évitant ainsi, comme le recommande McClelland *et al.* (2012) concernant la rectification du signal EMG pour l'analyse de cohérence, de perpétuer des méthodes d'analyse inappropriées qui peuvent biaiser les résultats. Le troisième est de participer au développement d'outils d'analyse novateurs à disposition de l'ensemble de la communauté scientifique en biomécanique et neurosciences comportementales, avec un haut niveau de confiance pouvant être accordé aux résultats dont ils sont issus. Cette démarche fait partie intégrante de mon cheminement scientifique et a permis de me forger une compétence forte en traitement avancé des signaux cinématiques, dynamiques, électromyographiques et électroencéphalographiques déterminante pour le

développement de mes axes de recherche en biomécanique, contrôle moteur, neurophysiologie et neurosciences. Le regard rétrospectif qu'offre la rédaction de ce mémoire de synthèse est l'occasion de souligner l'importance de la confiance et du soutien que m'a apporté Eric Berton (Institut des Sciences du Mouvement Etienne-Jules Marey, UMR 7287 CNRS / Aix-Marseille Université, Marseille) après ma thèse, qui m'ont permis de renforcer cette stratégie et de développer de manière durable mes principaux axes de recherche dans un environnement privilégié, notamment en matière d'encadrement. Je suis très reconnaissant à vous, Pr. Berton ![3] L'expertise que j'ai ainsi acquise dans le domaine du traitement des données, et que je m'attache à transmettre aux étudiants de Master 2 et aux doctorants que j'encadre et avec lesquels je collabore, a été un vecteur de développement de mes travaux de recherche, d'interactions et de collaborations riches et productives. Elle m'a permis d'accéder à une forte autonomie y compris du point de vue financier grâce aux projets auxquels j'ai participé en tant qu'investigateur principal ou de partenaire. Dans ce contexte, le contrat de prestation établi avec Airbus © contribue au transfert industriel et clinique de mes activités de recherche dans le domaine des exosquelettes. Ces travaux s'inscrivent dans une double perspective d'amélioration de la santé et la sécurité d'opérateurs sur ligne d'assemblage, et du développement d'une neuroprothèse visant la facilitation des mouvements du membre supérieur chez le patient post-accident vasculaire cérébral en collaboration avec David Gasq (ToNIC UMR 1214 Inserm / UPS & service des explorations fonctionnelles physiologiques de l'hôpital Rangueil (CHU de Toulouse), Toulouse).

Le troisième chapitre de cette note de synthèse pour l'habilitation à diriger des recherches sera consacré aux perspectives scientifiques, et à l'exposé synthétique des axes de recherche auxquels je souhaite donner priorité à l'avenir. Une partie de ces projets sont déjà engagés, dans le cadre de la co-direction de la thèse de Joseph Tisseyre (co-dir. : Jessica Tallet) et ma participation active à la thèse CIFRE d'Alexandre Chalard (dirs. : David Gasq & Philippe Marque). La thèse de Joseph Tisseyre a pour objet central l'étude des mécanismes sous-jacents aux mouvements miroirs, définis comme des mouvements ou contractions involontaires se produisant dans les muscles homologues controlatéraux à ceux du mouvement volontaire (Armatas *et al.,* 1994 ; Cernacek, 1961). Les objectifs sont d'explorer, d'une part, les corrélats cérébraux associés à l'asymétrie des mouvements miroirs et, d'autre part, le lien entre les fonctions attentionnelles et exécutives et les mouvement miroirs chez des adultes sains et des patients cérébro- lésés (Tisseyre *et al.,*

---

[3] Adapté de l'anglicisme consacré par Jolitorax s'adressant à Panoramix (Goscinny & Uderzo, 1966) : « Je suis très reconnaissant à vous, druide Panoramix ».

2018). La thèse d'Alexandre Chalard vise à étudier l'effet d'injections de toxine botulique dans les fléchisseurs du coude sur la réduction des co-contractions spastiques au cours d'un mouvement d'extension active de coude chez des patients hémiplégiques vasculaires chroniques. Ce travail a déjà permis de formuler des recommandations méthodologiques pour normaliser de manière adaptée les données EMG chez les patients présentant des patterns d'activation musculaire atypiques (Chalard *et al.,* 2018a), et de clarifier les facteurs fonctionnels et cliniques les plus déterminants dans la limitation des mouvements du membre supérieur suite à un accident vasculaire cérébral (AVC) (Chalard *et al.,* 2018b). Plus globalement, ce projet fait appel à une approche multimodale pour étudier la modulation de l'indice de co-contraction spastique ainsi que celles, concomitantes, de l'activité corticale et de l'excitabilité cortico-spinale avant et à court et long terme après injection de toxine botulique. L'ensemble de ces travaux sont réalisés en étroite collaboration avec David Gasq et Philippe Marque au sein des services des Explorations Fonctionnelles Physiologiques et de Médecine Physique et de Réadaptation à l'hôpital Rangueil du Centre Hospitalier Universitaire de Toulouse. Mon engagement dans ces projets est en totale cohérence avec le cheminement scientifique que j'ai suivi depuis ma thèse, mais marquent l'extension de mes travaux de recherche à une définition élargie de la redondance musculaire et à des problématiques fondamentales et appliquées dans le domaine médical. Ces orientations de recherche sont dans la logique de mon rattachement depuis septembre 2013 à l'équipe iDREAM (dir. : Isabelle Loubinoux) de l'Unité de Recherche Mixte Inserm / UPS ToNIC, et se placent dans la perspective de contribuer au développement de thérapeutiques innovantes chez le patient post-accident vasculaire cérébral, pour restituer une préhension fonctionnelle notamment. Dans la continuité des travaux que j'ai déjà menés (Bigot *et al.,* 2011 ; Blais *et al.,* 2018 ; Charissou *et al.,* 2016 ; Charissou *et al.,* 2017 ; Cremoux *et al.,* 2017 ; Cremoux *et al.,* 2018 ; Dal Maso *et al.,* 2017), l'axe de recherche central que je souhaite développer en priorité vise à explorer la contribution des centres nerveux supra-spinaux et spinaux dans le contrôle de la redondance musculaire en faisant appel à l'analyse de cohérence. Pour traiter cette question, le premier projet est conduit par Maxime Fauvet dans le cadre d'une thèse qui vient de débuter à l'Université de Toulouse (co-dir. : Philippe Marque), avec pour but d'étudier au cours du temps le couplage entre le cortex et les muscles, entre les muscles et au sein du cortex via la mesure des cohérences cortico-musculaire (EEG-EMG), intermusculaire (EMG-EMG) et cortico-corticales (EEG-EEG) lors de contractions isométriques et de mouvements volontaires. Ces résultats permettront de mieux comprendre les liens fonctionnels entre les différentes structures centrales

impliquées dans le contrôle du mouvement et leur dynamique au cours de l'action motrice. Le second projet sera développé par Emilie Mathieu (co-dirs. : Sylvain Cremoux & Philippe Pudlo ; Laboratoire d'Automatique, de Mécanique et d'Informatique Industrielles et Humaines, UMR 8201 CNRS / Université Polytechnique des Hauts-de-France, Valenciennes) dans le cadre d'une thèse de l'Université de Valenciennes, déjà associée au projet de thèse CIFRE d'Alexandre Chalard. L'objectif central de ce travail sera d'étudier le lien entre la modulation de la cohérence intermusculaire et la plasticité de la coordination motrice chez des sujets sains et des patients hémiplégiques vasculaires chroniques. Il visera également à développer un modèle neuro-biomécanique d'estimation des forces musculaires, au sein duquel la cohérence intermusculaire pourrait être introduite comme donnée d'entrée afin apporter une redondance d'information supplémentaire qui réduirait la dimensionnalité du problème d'optimisation numérique formulé pour estimer les efforts musculaires. Finalement, deux stages de Master 2 Recherche, co-dirigés respectivement avec Julien Duclay et Lilian Fautrelle (ToNIC UMR 1214 Inserm / UPS, Toulouse), initient des travaux autour de deux problématiques qui permettront de mieux comprendre le rôle fonctionnel et les mécanismes impliqués dans la modulation des cohérences cortico-musculaire et intermusculaire. Le premier comparera la cohérence cortico-musculaire entre des contractions isométriques et concentriques et des contractions excentriques au cours desquelles l'excitabilité cortico-spinale est diminuée en lien avec l'intervention de mécanismes nerveux d'inhibition au niveau médullaire (Duclay *et al.,* 2011, 2014). Le second étudiera l'effet du contexte émotionnel sur la cohérence intermusculaire lors de mouvement de pointage par une approche pluridisciplinaire, au croisement de la psychologie cognitive, des neurosciences et de la biomécanique. Ce travail contribuera à meilleure compréhension des processus nerveux centraux impliqués dans les comportements moteurs d'approche ou d'évitement selon la valence émotionnelle, respectivement positive ou négative, perçue lors de la tâche (Elliot, 2006). L'intérêt est fondamental, mais également pratique et clinique dans une double perspective de maximiser la performance motrice chez le sportif et de faciliter la rééducation chez des patients présentant une altération de la fonction motrice.

A la suite de ma thèse soutenue le 7 juillet 2003, j'ai été recruté comme ATER au sein de la Faculté de Sciences du Sport de l'Université de la Méditerranée Aix-Marseille II, puis comme maître de conférences à l'UFR STAPS de l'Université Paul Sabatier Toulouse III. Au sein des structures de recherche auxquelles j'ai été successivement rattaché, actuellement le Toulouse NeuroImaging Center (UMR 1214 ToNIC Inserm / UPS, http://tonic.inserm.fr/), l'objet central de mes travaux de recherche est la « redondance musculaire », avec des visées dans les domaines entrecroisés de l'optimisation de la performance motrice chez le sujet sain et l'amélioration de la fonction motrice chez le patient cérébro- ou médullo-lésé. Tout au long de mon parcours scientifique, j'ai approfondi ce sujet en m'intéressant de manière privilégiée aux rôles fonctionnels de la co-contraction agoniste / antagoniste et aux mécanismes nerveux centraux de contrôle de l'activité musculaire antagoniste lors de contractions volontaires et involontaires chez l'homme. Pour traiter cette question cruciale en contrôle moteur, mon cheminement scientifique m'a fait passer d'une approche strictement biomécanique à une approche multimodale réellement pluridisciplinaire au croisement de la biomécanique, des neurosciences et du traitement du signal. Chronologiquement, les principales thématiques de recherche que j'ai développées, et qui sont pour partie présentées de manière détaillée dans ce rapport de synthèse, sont :

- La modélisation musculo-squelettique de la redondance musculaire ;
- L'étude des facteurs de modulation de la co-contraction agoniste / antagoniste saine et pathologique ;
- L'étude des corrélats cérébraux de l'activité des muscles antagonistes ;
- La contribution des interactions cortico-musculaires et intermusculaires au contrôle de la co-contraction agoniste / antagoniste.

J'ai toujours cherché à mener ces travaux dans un esprit de partage de compétences, d'interactions réciproques et de collaborations désintéressées, ce qui constitue à mon sens une des clés de mon parcours scientifique. Mes activités de recherche ont ainsi donné lieu un total de 59 publications et 100 communications en date du 28 février 2019, et m'a offert le privilège de co-encadrer 5 thèses de Doctorat et 18 Master 2 Recherche déjà soutenus. Au-delà des aspects bibliométriques, cette riche pratique d'encadrement a directement contribué au développement de mes axes de recherche et à l'élaboration de ceux auxquels je souhaite donner priorité à l'avenir. En poursuivant la démarche originale dans laquelle je m'inscris dans le domaine de la neuro-biomécanique, ces travaux approfondiront l'analyse de la co-contraction à travers une définition élargie et une vision ouverte à de nouveaux champs scientifiques. Ils contribueront également à mieux comprendre le rôle fonctionnel et les mécanismes impliqués dans le contrôle de la redondance musculaire dans une double perspective fondamentale et clinique.

Curriculum vitae

II. Curriculum vitae [4]

David AMARANTINI, PhD

Né le 6 aout 1975 à Chambéry (73), pacsé, 3 enfants.

✉   Université Toulouse III - Paul Sabatier
     Faculté des Sciences du Sport et du Mouvement Humain
     118 route de Narbonne
     31062 Toulouse Cedex 9
     France
☎   +33 (0)5 61 55 65 46 / +33 (0)5 62 74 61 85
🖷   +33 (0)5 61 55 82 80 / +33 (0)5 62 74 61 63
✆   david.amarantini@univ-tlse3.fr / david.amarantini@inserm.fr
✍   Page web 🇫🇷 | 🇬🇧 / Citations *Google Scholar* / Profil *ResearchGate*

CURSUS

➢ **PARCOURS PROFESSIONNEL**

- **2011 - 2014 : Professeur associé**, Département de kinésiologie, Université de Montréal, Montréal, Canada (du 01/08/2011 au 31/05/2014).

- **2010 - 2011 : Congé pour recherche**. Laboratoire de Simulation et Modélisation du Mouvement, Université de Montréal, Montréal, Québec, Canada.

- **2004 - … : Maître de conférences**, Université Paul Sabatier Toulouse 3 (UPS), Université de Toulouse (UFTMiP), Toulouse, France.
  - *Composante :* UFR STAPS puis Faculté des Sciences du Sport et du Mouvement Humain (F2SMH).
  - *Laboratoire :* LAPMA (EA 3691) de sept. 2004 à déc. 2010 ;
    PRISSMH-LAPMA (EA 4561) de janv. 2011 à août 2013 ;
    UMR 825 (Inserm / UPS) puis Toulouse NeuroImaging Center (ToNIC, UMR 1214 Inserm / UPS) depuis sept. 2013.

- **2003 - 2004 : Attaché Temporaire d'Enseignement et de Recherche à temps partiel**, Université de la Méditerranée Aix-Marseille II, Marseille, France.
  - *Composante :* Faculté des Sciences du Sport.
  - *Laboratoire :* LABM, USR 2164 CNRS.

- **2003 : Ingénieur de recherche**. Contrat de prestation établi entre le Laboratoire SPM et la Fonderie Moulaire pour « l'analyse comparative du pédalier « CG-BR ». CDD à temps plein du 01/03/2003 au 31/07/2003.

---

[4] Mise à jour : 28 février 2019.

- ➢ **PARCOURS UNIVERSITAIRE**

  - **2008 : Autorisation à diriger les recherches à titre individuel**, Ecole Doctorale CLESCO (ED 326). Doctorant : Dal Maso, F..

  - **1999 - 2003 : Doctorat STAPS** (allocataire MENRT 1999 - 2002, soutenu le 07/07/2003), Université Joseph Fourier Grenoble 1, Grenoble, France. Dir. : Martin, L..

  - **1998 - 1999 : DEA STAPS**, « Sport et Performance - Facteurs biomécaniques, biologiques et socio-économiques », Université Joseph Fourier Grenoble 1, Grenoble, France. Dirs. : Blanchi, J.P., Martin, L..

  - **1997 - 1998 : Maîtrise STAPS**, « Education et Motricité », Université Joseph Fourier Grenoble 1, Grenoble, France.

  - **1996 - 1997 : Licence STAPS**, « Education et Motricité », Université Joseph Fourier Grenoble 1, Grenoble, France.

  - **1994 - 1996 : DEUG STAPS**, Université Joseph Fourier Grenoble 1, Grenoble, France.

  - **1993 - 1994 : Classe Préparatoire aux Grandes Ecoles PTSI**, Lycée Louis Lachenal, Argonay (74).

  - **1993 : Baccalauréat série E**, lycée Louis Lachenal, Argonay (74).

DISTINCTIONS

- **2016 - 2020 : Prime d'Encadrement Doctoral et de Recherche**.
- **2012 - 2016 : Prime d'Excellence Scientifique**.
- **2008 - 2012 : Prime d'Encadrement Doctoral et de Recherche**.
- **2004 : Qualification aux fonctions de maître de conférences**. Section 74 - STAPS, N° 04274147390.

FORMATIONS

- **2007 : Journées Inter-Régions de Formation en Neuro-Imagerie.**
  Formation EEG/MEG : Introduction à l'acquisition et au traitement du signal. Application et travaux dirigés. 24-28 Septembre 2007, Marseille, France.

- **2007 : 4th EEGLAB Workshop.**
  Atelier de formation sur le traitement avancé des données électro-physiologiques. 26-29 Juin 2007, Aspet, France.

- **1999 - 2001 : Modules de formation scientifique**.
  Ecole Doctorale « Ingénierie pour le Vivant », Université Joseph Fourier Grenoble 1, Grenoble, France.

THÉMATIQUES DE RECHERCHE

- Etude **neuro-biomécanique des mécanismes de contrôle de l'activité musculaire**.

- Quantification et **analyse des cohérences électrophysiologiques**.

- **Modélisations biomécaniques** pour l'estimation des efforts musculaires.

- Etude des **mécanismes de contrôle de la coordination** multi-musculaire et de la posture.

- *Mots clés :* Biomécanique ; neurosciences ; contrôle moteur ; traitement du signal ; mouvement humain sain et pathologique.

PRODUCTION SCIENTIFIQUE

- **Publications :**
  - 36 articles.
  - 1 chapitre d'ouvrage.
  - 19 résumés publiés.
  - 3 rapports d'études.

- **Communications :**
  - 69 communications orales, dont 9 conférences et séminaires invités.
  - 31 communications affichées.

- **Indicateurs d'impact (source : *Google Scholar*) :**
  - Citations : 898.
  - h / i10-index : 15 / 18.

- **Encadrements :**
  - 6 thèses de doctorat, dont 1 en cours.
  - 21 mémoires de Master 2 Recherche et Master of Science, dont 3 en cours.
  - 19 mémoires de Master 2 Professionnel, dont 3 en cours.

➢ **ARTICLES**

- Fauvet, M., Cremoux, S., Chalard, A., Tisseyre, J., Gasq, D.*, **Amarantini, D.*** (* co-derniers auteurs) (accepted for publication). A novel method to generalize time-frequency coherence analysis between EEG or EMG signals during repetitive trials of different durations. In *2019 9th International IEEE/EMBS Conference on Neural Engineering (NER)*.

- Chalard, A., **Amarantini, D.**, Tisseyre, J., Marque, P., Tallet, J., Gasq, D. (epub ahead of print). Spastic co-contraction, rather than spasticity, is associated with impaired active function in adults with acquired brain injury: A pilot study. *Journal of Rehabilitation Medicine*.

- Tisseyre, J., Marquet-Doléac, J., Barral, J., **Amarantini, D.***, Tallet, J.* (* co-derniers auteurs) (2019). Lateralized inhibition of symmetric contractions is associated with motor, attentional and executive processes. *Behavioural Brain*

Research, 361, 65-73.

- Gimenez, P., Chicoine, E., **Amarantini, D.**, Dal Maso, F., Tremblay, J. (2018). Unilateral conditioning contractions enhance power output in elite short track speed skaters. *Sports Medicine International Open*, 2(6): E185-E190.

- Blais, M., **Amarantini, D.**, Albaret, J.M., Chaix, Y., Tallet, J. (2018). Atypical inter-hemispheric communication correlates with altered motor inhibition during learning of a new bimanual coordination pattern in developmental coordination disorder. *Developmental Science*, 21(3), e12563.

- Tisseyre, J., **Amarantini, D.**, Chalard, A., Marque, P., Gasq, D., Tallet, J. (2018). Mirror movements are linked to executive control in healthy and brain-injured adults. *Neuroscience*, 379, 246-256.

- Charissou, C., **Amarantini, D.**, Baurès, R., Berton, E., Vigouroux, L. (2017). Effects of hand configuration on muscle force coordination, co-contraction and concomitant intermuscular coupling during maximal isometric flexion of the fingers. *European Journal of Applied Physiology*, 117(11), 2309-2320.

- Dal Maso, F., Longcamp, M., Cremoux, S., **Amarantini, D.** (2017). Effect of training status on corticomuscular beta-range coherence with agonist vs. antagonist muscles during knee isometric contractions. *Experimental Brain Research*, 235(10), 3023-3031.

- Cremoux, S., Tallet, J., Dal Maso, F., Berton, E., **Amarantini, D.** (2017). Impaired corticomuscular coherence during isometric elbow flexion contractions in human with cervical Spinal Cord Injury. *European Journal of Neuroscience*, 46(4), 1991-2000.

- Lajante, M., Droulers, O., **Amarantini, D.** (2017). How reliable are "state-of-the-art" facial EMG processing methods? Guidelines for improving the assessment of emotional valence in advertising research. *Journal of Advertising Research*, 57(1) 28-37.

- Daviaux, Y., Cremoux, S., Tallet, J., **Amarantini, D.**, Cornu, C., Deschamps, T. (2016). I can't reach it! Focus on theta sensorimotor rhythm toward a better understanding of impaired action-perception coupling. *Neuroscience*, 339, 32-46.

- Barrué-Belou, S., **Amarantini, D.**, Marque, P., Duclay, J. (2016). Neural adaptations to submaximal isokinetic eccentric strength training. *European Journal of Applied Physiology*, 116(5), 1021-1030.

- Charissou, C., Vigouroux, L., Berton, E., **Amarantini, D.** (2016). Fatigue- and training-related changes in 'beta' intermuscular interactions between agonist muscles. *Journal of Electromyography and Kinesiology*, 27, 52-59.

- Daviaux, Y., Cremoux, S., Tallet, J., **Amarantini, D.**, Cornu, C., Deschamps, T. (2016). An enhanced experimental procedure to rationalize on the impairment of perception of action capabilities. *Psychological Research*, 80(2), 224-234.

- Cremoux, S., **Amarantini, D.**, Tallet, J., Dal Maso, F., Berton, E. (2016). Increased antagonist muscle activity in cervical SCI patients suggests altered reciprocal inhibition during elbow contractions. *Clinical Neurophysiology*, 127(1), 629-634.

- **Amarantini, D.**, Bru, B. (2015). Training-related changes in the EMG-moment relationship during isometric contractions: Further evidence of improved control of

muscle activation in strength-trained men? *Journal of Electromyography and Kinesiology*, 25(4), 697-702.

- Zorgati, H., Prieur, F., Vergniaud, T., Cottin, F., Do, M.-C., Labsy, Z., **Amarantini, D.**, Gagey, O., Lasne, F., Collomp, K. (2014). Ergogenic effect of oral glucocorticoid intake during repeated bouts of high- intensity exercise. *Steroids*, 86, 10-15.

- Gasq, D., Labrunée, M., **Amarantini, D.**, Dupui, P., Montoya, R., Marque, P. (2014). Between-day reliability of centre of pressure measures for balance assessment in hemiplegic stroke patients. *Journal of NeuroEngineering and Rehabilitation*, 11(1), 39.

- Cremoux, S., Tallet, J., Berton, E., Dal Maso, F., **Amarantini, D.** (2013). Motor-related cortical activity after cervical spinal cord injury: multifaceted EEG analysis of isometric elbow flexion contractions. *Brain Research*, 1533, 44-51.

- Cremoux, S., Tallet, J., Berton, E., Dal Maso, F., **Amarantini, D.** (2013). Does the force level modulate the cortical activity during isometric contractions after a cervical spinal cord injury? *Clinical Neurophysiology*, 124, 1005-1012.

- Lajante, M., Droulers, O., Dondaine, T., **Amarantini, D.** (2012). Opening the "Black Box" of Electrodermal Activity in Consumer Neuroscience. *Journal of Neuroscience, Psychology, and Economics*, 5(4), 238-249.

- Dal Maso, F., Longcamp, M., **Amarantini, D.** (2012). Training-related decrease in antagonist muscles activation is associated with increased motor cortex activation: evidence of central mechanisms for control of antagonist muscles. *Experimental Brain Research*, 220, 287-295.

- **Amarantini, D.**, Rao, G., Martin, L., Cahouët, V., Berton, E. (2012). EMG-based estimation of muscular efforts exerted during human movements. *Movement & Sport Sciences*, 75, 27-37.

- Bigot, J., Longcamp, M., Dal Maso, F., **Amarantini, D.** (2011). A new statistical test based on the wavelet cross-spectrum to detect time-frequency dependence between non-stationary signals: application to the analysis of cortico-muscular interactions. *NeuroImage*. 55(4), 1504-1518.

- Rao, G., Berton, E., **Amarantini, D.**, Vigouroux, L., Buchanan, T.S. (2010). An EMG-driven biomechanical model that accounts for the decrease in moment generation capacity during a dynamic fatigued condition. *Journal of Biomechanical Engineering*, 132(7), 071003.

- **Amarantini, D.**, Rao, G., Berton, E. (2010). A two-step EMG-and-optimization process to estimate muscle force during dynamic movement. *Journal of Biomechanics*, 43(9), 1827-1830.

- Rao, G., **Amarantini, D.**, Berton, E. (2009). Influence of additional load on the moments of the agonist and antagonist muscle groups at the knee joint during closed chain exercise. *Journal of Electromyography and Kinesiology*, 19(3), 459-466.

- Noé, F., **Amarantini, D.**, Paillard, T. (2009). How experienced alpine-skiers cope with restrictions of ankle degrees-of-freedom when wearing ski-boots in postural exercises. *Journal of Electromyography and Kinesiology*, 19(2), 341-346.

- Centomo, H., **Amarantini, D.**, Martin, L., Prince, F. (2008). Differences in the coordination of agonist and antagonist muscle groups in below-knee amputee and

able-bodied children during dynamic exercise. *Journal of Electromyography and Kinesiology*, 18(3), 487-494.

- Centomo, H., **Amarantini, D.**, Martin, L., Prince, F. (2007). Kinematic and kinetic analysis of a stepping-in-place task in below-knee amputee children compared to able-bodied children. *IEEE Transactions on Neural Systems and Rehabilitation Engineering*, 15(2), 258-265.

- Vigouroux, L., Quaine, F., Labarre-Vila, A., **Amarantini, D.**, Moutet, F. (2007). Using EMG data to constrain optimization procedure improves finger tendon tension estimations during static fingertip force production. *Journal of Biomechanics*, 40(13), 2846-2856.

- Centomo, H., **Amarantini, D.**, Martin, L., Prince, F. (2007). Muscle adaptation patterns of below-knee amputee children during walking. *Clinical Biomechanics*, 22(4), 457-463.

- Huffenus, A.F., **Amarantini, D.**, Forestier, N. (2006). Effects of distal and proximal arm muscles fatigue on multi-joint movement organization. *Experimental Brain Research*, 170(4), 438-447.

- Rao, G., **Amarantini, D.**, Berton, E., Favier, D. (2006). Influence of body segments' parameters estimation models on inverse dynamics solutions during gait. *Journal of Biomechanics*, 39(8), 1531-1536.

- **Amarantini, D.**, Martin, L. (2004). A method to combine numerical optimization and EMG data for the estimation of joint moments under dynamic conditions. *Journal of Biomechanics*, 37(9), 1393-1404.

- Cahouët, V., Martin, L., **Amarantini, D.** (2002). Static optimal estimation of joint accelerations for inverse dynamic problem solution. *Journal of Biomechanics*, 35(11), 1507-1513.

➢ **CHAPITRES D'OUVRAGES**

- Bouisset, S., Rao, G., **Amarantini, D.**, Berton, E. (2006). Etude et modélisation du mouvement humain. In: Fuchs P. and Moreau G. (Eds.). *Traité de la Réalité Virtuelle – Vol. 1 : L'Homme et l'environnement virtuel*. ODILE-JACOB, Paris, pp. 109-117.

➢ **RÉSUMÉS PUBLIÉS**

- Chalard, A., **Amarantini, D.**, Picaut, P., Pons, L., Marque, P., Gasq, D. (2018). Assessment of upper limb active movement facilitation and neuromuscular plasticity induced by abobotulinumtoxinA in chronic poststroke: A study protocol. *Toxicon*, 156(Suppl. 1), S15-S16.

- Chalard, A., **Amarantini, D.**, Belle, M., Montané, E., Gasq, D. (2018). Impact of different EMG normalisation methods on muscle activations and cocontraction index in adults with chronic post-stroke hemiparesis. *Annals of Physical and Rehabilitation Medicine*, 61(Suppl.), e444.

- Chalard, A., **Amarantini, D.**, Tisseyre, J., Marque, P., Tallet, J., Gasq, D. (2018). Is spasticity or spastic cocontraction of the elbow flexors associated with the limitation of voluntary elbow extension in adults with acquired hemiparesis? *Annals of Physical*

and Rehabilitation Medicine, 61(Suppl.), e439.

- Cremoux, S., Charissou, C., Tallet, J., Abade-Moreira, A., Dal Maso, F., **Amarantini, D.** (2018). T80. Alteration of intermuscular coherence in synergistic muscle pairs during actual elbow flexion contractions after cervical spinal cord injury. *Clinical Neurophysiology*, 129(Suppl. 1), e33.

- Gasq, D., Montastruc, J., Lambert, V., Dupui, P., **Amarantini, D.** (2016). Facteurs déterminants de l'asymétrie d'appui en posture statique chez le patient hémiparétique. *Neurophysiologie Clinique / Clinical Neurophysiology*, 46(4-5), 260-261.

- Gasq, D., Lainard, M., Kaluza, L., Dupui, P., **Amarantini, D.** (2016). Identification of a voluntary overcontrol of postural sway from static stabilometric assessment. *Annals of Physical and Rehabilitation Medicine*, 59(Suppl.), e124.

- Montastruc, J., **Amarantini, D.**, Lambert, V., Castel-Lacanal, E., Marque, P., Gasq, D. (2016). Main determinants of weight-bearing asymmetry in hemiplegic stroke patients. *Annals of Physical and Rehabilitation Medicine*, 59(Suppl.), e69.

- Achour-Benallegue, A., Paubel, P.V., **Amarantini, D.**, Pelletier, J., Kaminski, G. (2016). Could the diversity of facial expressions representations in visual art be the subject of a harmonized aesthetic relation? *International Journal of Psychology*, 51(Suppl. 1), 60-61.

- Gasq, D., Dupui, P., Marque, P., Zanone, P.-G., **Amarantini, D.** (2015). Pourquoi faire appel à l'analyse temps-fréquence pour quantifier la stabilité posturale de patients neurologiques ? *Neurophysiologie Clinique / Clinical Neurophysiology*, 45(4-5), 404-405.

- Kaluza, L., **Amarantini, D.**, Lainard, M., Dupui, P., Gasq, D. (2015). Quels paramètres stabilométriques pour objectiver un surcontrôle volontaire des oscillations posturales ? *Neurophysiologie Clinique / Clinical Neurophysiology*, 45(4-5), 400.

- Cremoux, S., **Amarantini, D.**, Tallet, J., Dal Maso, F., Berton, E. (2014). P76: Increased antagonist muscular activations in cervical SCI participants: evidence of altered reciprocal inhibition during voluntary elbow contractions. *Clinical Neurophysiology*, 125(Suppl. 1), S68.

- Gasq, D., Labrunée, M., **Amarantini, D.**, Dupui, P., Montoya, R., Marque, P. (2013). Between-day reliability of centre of pressure measures in hemiplegic stroke patients. *Fundamental & Clinical Pharmacology*, 27(Suppl. 1), 54-55.

- Cremoux, S., Tallet, J., Berton, E., Dal Maso, F., **Amarantini, D.** (2012). Atypical EMG activation patterns of the elbow extensors after complete C6 tetraplegia during isometric contractions: a case report. *Computer Methods in Biomechanics and Biomedical Engineering*, 15(Suppl. 1), 266-268.

- **Amarantini, D.**, Rao, G., Martin, L., Cahouët, V., Berton, E. (2009). Optimization- and EMG-assisted estimation of joint moments and muscle forces during dynamic movements. In: Lacouture, P., Colloud, F., Monnet, T., *La machine humaine au regard de la performance humaine*, Société de Biomécanique, France, pp. 17-22.

- Bru, B., **Amarantini, D.** (2008). Influence of sporting expertise on the EMG-torque relationship during isometric contraction in man. *Computer Methods in Biomechanics and Biomedical Engineering*, 11(Suppl. 1), 43-44.

- Rao, G., **Amarantini, D.**, Vigouroux, L., Berton, E. (2006). Influence of muscular fatigue on agonist and antagonist muscle groups moments during loaded squats. *Journal of Biomechanics*, 39(Suppl. 1), S74-S75.

- Rao, G., Berton, E., **Amarantini, D.** (2005). Effect of load on agonist and antagonist muscle moments during dynamic squats. *Computer Methods in Biomechanics and Biomedical Engineering*, 8(Suppl. 1), 233-234.

- **Amarantini, D.**, Martin, L. (2003). Estimation of knee muscle moments from an EMG-assisted optimization method during dynamic contractions. *Archives of Physiology and Biochemistry*, 111(1), 106.

- **Amarantini, D.**, Martin, L., Blanchi, J.P. (1999). Biomechanical analysis of inter-joint coordination. *Archives of Physiology and Biochemistry*, 107(Suppl.), 93.

➢ **MONOGRAPHIES**

- Guebba, S.[†], Carrere-Casajus, P.[†], Gasq, D.[‡], **Amarantini, D.**[‡] (2018). A review of promising technologies for the worker's future 'exosuit'. *Rapport final de recherche*, Inserm / Airbus, Toulouse, France ([†] co-premiers auteurs ; [‡] co-superviseurs).

- Gasq, D., **Amarantini, D.** (2017). Evaluation ergonomique de l'apport pour la santé d'un exosquelette assistant une tâche de crabotage. *Rapport final de recherche*, Inserm / Airbus, Toulouse, France.

- **Amarantini, D.**, Martin, L. (2003). Analyse comparative du pédalier Chichignoud G. – Bardin R. « CG – BR ». *Rapport final de recherche*, Université Joseph Fourier Grenoble 1 / Fonderie Moulaire, Grenoble, France.

- **Amarantini, D.** (2003). Estimation des efforts musculaires à partir de données périphériques : Application à l'analyse de la coordination pluri-articulaire. *Thèse de doctorat*, Université Joseph Fourier Grenoble 1, Grenoble, France.

➢ **COMMUNICATIONS ORALES**

- **Amarantini, D.**, Rieu, I., Simonetta-Moreau, M.*, Durif, F.* (* co-derniers auteurs) (2018). Analyse comparative accélérométrie / vidéo dans les tremblements du chef. *Colloque NEURO-MD*, Allergan Medical Institute®, Paris, France. Présentation orale.

- Tisseyre, J., **Amarantini, D.**, Chalard, A., Marque, P., Gasq, D., Tallet, J. (2018). Alteration of executive control is associated with greater mirror movements in healthy and brain-injured adults. *20èmes Journées Toulousaines de Psychomotricité*, Toulouse, France. Présentation orale.

- Cremoux, S., Tallet, J., Dal Maso, F., Charissou, C., **Amarantini, D.** (2018). Potential of corticomuscular and intermuscular interactions to evaluate and detect alteration of motor control in healthy people and people with cervical spinal cord injury. *31st International Congress of Clinical Neurophysiology*, Washington, DC, USA. Présentation orale en symposium.

- Chalard, A., **Amarantini, D.**, Tisseyre, J., Marque, P., Tallet, J., Gasq, D. (2018). Spastic cocontraction, spasticity and impairment of motor function during active elbow extension in adults with hemiparesis. *XVIIème congrès de la SOFAMEA*, Toulouse, France. Présentation orale.

- Cremoux, S., Dal Maso, F., Longcamp, M., Bigot, J., Berton, E., Tallet, J., **Amarantini, D.** (2017). L'ElectroEncéphaloGraphie – Couplage cortico-musculaire et mécanismes de contrôle de la contraction musculaire. *17ème Congrès International de l'Association des Chercheurs en Activités Physiques et Sportives*, Dijon, France. Présentation orale en symposium.

- Charissou, C., **Amarantini, D.**, Baurès, R., Berton, E., Vigouroux, L. (2017). Contribution of pair-specific intermuscular coupling to the regulation of agonist-antagonist co-contraction during maximal isometric flexion of the fingers. *17ème Congrès International de l'Association des Chercheurs en Activités Physiques et Sportives*, Dijon, France. Présentation orale.

- Tisseyre, J., **Amarantini, D.**, Chalard, A., Marque, P., Gasq, D., Tallet J. (2017). Mirror movements of upper limbs are correlated with attentional and executive functions in healthy subjects and brain injury patients. *17ème Congrès International de l'Association des Chercheurs en Activités Physiques et Sportives*, Dijon, France. Présentation orale.

- Blais, M., **Amarantini, D.**, Albaret, J.M., Chaix, Y., Tallet, J. (2017). Inter-hemispheric communication is altered during learning of a new bimanual coordination in teenagers with developmental coordination disorder. *12th Developmental Coordination Disorder Conference*, Perth, Western Australia, Australia. Présentation orale.

- Charissou, C., Vigouroux, L., Berton, E., **Amarantini, D.** (2017). Functional relevance of correlated neural inputs in the regulation of antagonist activity during submaximal isometric fingers flexion tasks. *13ème colloque de la Journée de l'École Doctorale des Sciences du Mouvement Humain*, Montpellier, France. Présentation orale.

- Gasq, D., Montastruc, J., Lambert, V., Dupui, P., **Amarantini, D.** (2016). Facteurs déterminants de l'asymétrie d'appui en posture statique chez le patient hémiparétique. *Congrès Posture Equilibre Mouvement (PEM)*, Nancy, France. Présentation orale.

- Gasq, D., Lainard, M., Kaluza, L., Dupui, P., **Amarantini, D.** (2016). Identification of a voluntary overcontrol of postural sway from static stabilometric assessment. *31ème Congrès de la Société Française de Médecine Physique et de Réadaptation*, Saint Etienne, France. Présentation orale.

- Montastruc, J., **Amarantini, D.**, Lambert, V., Castel-Lacanal, E., Marque, P., Gasq, D. (2016). Main determinants of weight-bearing asymmetry in hemiplegic stroke patients. *31ème Congrès de la Société Française de Médecine Physique et de Réadaptation*, Saint Etienne, France. Présentation orale.

- Achour-Benallegue, A., Paubel, P.V., **Amarantini, D.**, Pelletier J., Kaminski G. (2016). Could the diversity of facial expressions representations in visual art be the subject of a harmonized aesthetic relation? *31st International Congress of Psychology*, Yokohama, Japan. Présentation orale.

- Lamaud, M., Bonneval, F., Destruhaut, P., Rodriguez, A., **Amarantini, D.**, Darmana, R. (2016). Effects of padding material and thickness on second metatarsal head discharge. *FIP World Congress of Podiatry*, Montréal, Canada. Présentation orale.

- Auzias, P., Seitz, C., Escalle, Y., Rodriguez, A., **Amarantini, D.**, Darmana, R. (2016). Shod, barefoot and minimalist shoes running: A comparative study. *FIP World*

Congress of Podiatry, Montréal, Canada. <u>Présentation orale</u>.

- **Amarantini, D.** (2015). Quantification of synchronization processes between electrophysiological signals by coherence. *Movement to Health Laboratory - Euromov*, Université de Montpellier 1, Montpellier, France. <u>Séminaire invité</u>.

- Cremoux, S., **Amarantini, D.** (2015). Time-frequency coherence analysis between electrophysiological signals provides new insights into the mechanisms underlying the control and perception of motor action. *16ème Congrès International de l'Association des Chercheurs en Activités Physiques et Sportives*, Nantes, France. <u>Symposium</u>.

- <u>Blais, M.</u>, **Amarantini, D.**, Albaret, J.M., Chaix, Y., Tallet, J. (2015). EEG-EEG coherence as a marker of motor learning in adults and teenagers with and without motor impairments. *16ème Congrès International de l'Association des Chercheurs en Activités Physiques et Sportives*, Nantes, France. <u>Présentation orale en symposium</u>.

- <u>Charissou, C.</u>, Vigouroux, L., Berton, E., **Amarantini, D.** (2015). Effects of fatigue on EMG-EMG coherence between agonist muscles during isometric contractions in trained and untrained participants: Evidence for the importance of intermuscular coupling in motor control. *16ème Congrès International de l'Association des Chercheurs en Activités Physiques et Sportives*, Nantes, France. <u>Présentation orale en symposium</u>.

- <u>Cremoux, S.</u>, Daviaux, Y., **Amarantini, D.**, Deschamps, T., Cornu, C., Tallet, J. (2015). Cortico-cortical coherence elicits neurophysiological processes underlying impaired action-perception coupling. *16ème Congrès International de l'Association des Chercheurs en Activités Physiques et Sportives*, Nantes, France. <u>Présentation orale en symposium</u>.

- <u>Cremoux, S.</u>, Tallet, J., Berton, E., Dal Maso, E., **Amarantini, D.** (2015). Altered corticomuscular coherence after cervical spinal cord injury. *16ème Congrès International de l'Association des Chercheurs en Activités Physiques et Sportives*, Nantes, France. <u>Présentation orale en symposium</u>.

- <u>Gasq, D.</u>, Dupui, P., Marque, P., Zanone, P.-G., **Amarantini, D.** (2015). Pourquoi faire appel à l'analyse temps-fréquence pour quantifier la stabilité posturale de patients neurologiques ? *22ème Congrès de la Société Francophone Posture Equilibre Locomotion*, Paris, France. <u>Présentation orale</u>.

- <u>Kaluza, L.</u>, **Amarantini, D.**, Lainard, M., Dupui, P., Gasq, D. (2015). Quels paramètres stabilométriques pour objectiver un surcontrôle volontaire des oscillations posturales ? *22ème Congrès de la Société Francophone Posture Equilibre Locomotion*, Paris, France. <u>Présentation orale</u>.

- **Amarantini, D.**, Lajante, M. (2014). The hidden face of consumers' experience: an EMG-based method for continuous measurement of emotion. *International Workshop on Neuroscience and Consumer Behavior: New Insights in Attention and Emotion Research*, Graduate School of Management of Rennes, Rennes, France. <u>Conférence invitée</u>.

- Droulers, O., <u>Lajante, M.</u>, **Amarantini, D**. (2014). Paradigme neuroscientifique : Applicabilité des mesures psychophysiologiques en marketing. *Atelier d'approfondissement proposé par l'Association Française du Marketing*, Institut de Gestion de Rennes, Université de Rennes 1, Rennes, France. <u>Atelier</u>.

- Daviaux, Y., Cremoux, S., Tallet, J., **Amarantini, D.**, Cornu, C., Deschamps, T. (2014). Effects of anxiety on the perception of action capabilities towards a sensorimotor integration perspective. *19th Annual Congress of the European College of Sport Science*, Amsterdam, The Netherlands. Mini-présentation orale.

- **Amarantini, D.** (2013). Mesurer la valence des réactions émotionnelles du consommateur avec l'électromyographie faciale. *29ᵉ Congrès International de l'Association Française du Marketing – « Apports de la psychophysiologie à l'étude des cognitions et des affects du consommateur : vers un renouveau de la discipline »*, La Rochelle, France. Présentation orale en session spéciale.

- Barrué-Belou, S., **Amarantini, D.**, Duclay, J. (2013). Modulations de l'excitabilité spinale suite à un entrainement excentrique sous-maximal. *15ème Congrès International de l'Association des Chercheurs en Activités Physiques et Sportives*, Grenoble, France. Présentation orale.

- Cremoux, S., **Amarantini, D.**, Tallet, J., Dal Maso, F., Berton, E. (2013). Effets d'une lésion médullaire sur la modulation de l'activation musculaire agonistes et antagonistes lors de contractions isométriques sous-maximales. *15ème Congrès International de l'Association des Chercheurs en Activités Physiques et Sportives*, Grenoble, France. Présentation orale.

- Dal Maso, F., Longcamp, M., Cremoux, S., **Amarantini, D.** (2013). Corticomuscular interactions with antagonist muscles – Direct evidence of supraspinal control of antagonist muscles. *15ème Congrès International de l'Association des Chercheurs en Activités Physiques et Sportives*, Grenoble, France. Présentation orale.

- Marquet-Doléac, J., **Amarantini, D.**, Albaret, JM., Barral, J., Tallet, J. (2013). Motor overflows to investigate behavioral and cerebral asymmetries. *15ème Congrès International de l'Association des Chercheurs en Activités Physiques et Sportives*, Grenoble, France. Présentation orale.

- **Amarantini, D.** (2013). Neuro-biomécanique des muscles antagonistes. *Journée du GT8 Robotique et Neurosciences « Génération de mouvement et contrôle moteur »*, Toulouse, France. Présentation orale.

- **Amarantini, D.** (2012). A neurobiomechanical approach to understanding the mechanisms involved in the regulation of agonist-antagonist cocontraction during voluntary activity. *Movement to Health Laboratory*, Université de Montpellier 1, Montpellier, France. Séminaire invité.

- Prince, F., Gasq, D., **Amarantini, D.** (2012). Comment interpréter une évaluation stabilométrique ? *27ème Congrès de la Société Française de Médecine Physique et de Réadaptation*, Toulouse, France. Atelier.

- Duclay, J., **Amarantini, D.**, Martin, A. (2012). Recurrent inhibition of synergistic muscles during maximal voluntary anisometric contraction. *17th Annual Congress of European College of Sport Science*, Bruges, Belgium. Présentation orale.

- Lajante, M., Droulers, O., Dondaine, T., **Amarantini, D.** (2012). Opening the "Black Box" of Electrodermal Activity in Consumer Neuroscience. *2012 NeuroPsychoEconomics Conference*, Rotterdam, The Netherlands. Présentation orale.

- Cremoux, S., Tallet, J., Berton, E., Dal Maso, F., **Amarantini, D.** (2012). Modulation de l'activité corticale lors de contractions isométriques à différents niveaux de force

après une lésion médullaire cervicale. *XVIèmes Journées d'Etudes Francophones en Activités Physiques Adaptées*, Orsay, France. Présentation orale.

- **Amarantini, D.** (2011). Modélisation musculosquelettique & approche « neuro-biomécanique » de la fonction musculaire. *Laboratoire Motricité, Interactions, Performance*, Université de Nantes, Nantes, France. Séminaire invité.

- **Amarantini, D.** (2011). EMG-based estimation of muscular efforts exerted during human movements. *Sport, Measure & Simulation 2011*, Poitiers, France. Conférence invitée.

- **Amarantini, D.** (2011). Modélisations biomécaniques de la fonction musculaire : applications pour l'optimisation de la préparation physique. *Atelier entraînement spécialisé et préparation physique*, Centre National Multisport Montréal, Montréal, Canada. Conférence invitée.

- **Amarantini, D.** (2011). Modélisations biomécaniques pour l'étude des mécanismes de contrôle et de régulation de la cocontraction. *Unité de recherche CIAMS-RIME*, Université Paris-Sud 11, Orsay, France. Séminaire invité.

- **Amarantini, D.** (2011). Modélisations des forces musculaires utilisant l'électromyographie comme information redondante. *Xèmes Journées de la SOFAMEA – Journée thématique : « regards croisés sur la modélisation de la fonction musculaire »,* Saint-Etienne, France. Conférence invitée.

- Cremoux, S., Tallet, J., Berton, E., Dal Maso, F., **Amarantini, D.** (2011). Désynchronisation corticale lors de contractions isométriques volontaires sous maximales chez le sujet tétraplégique. *14ème Congrès International de l'Association des Chercheurs en Activités Physiques et Sportives*, Rennes, France. Présentation orale.

- Dal Maso, F., Longcamp, M., **Amarantini, D.** (2011). Modulation of cortical oscillatory suppression is associated with decreased activation of antagonist muscles in strength-trained athletes. *14ème Congrès International de l'Association des Chercheurs en Activités Physiques et Sportives*, Rennes, France. Présentation orale.

- Duclay, J., **Amarantini, D.**, Martin, A. (2011). Changes in recurent inhibition during maximal voluntary anisometric contraction. *16th Annual Congress of the European College of Sport Science*, Liverpool, United Kingdom. Présentation orale.

- **Amarantini, D.** (2010). Biomechanical modeling and analysis of force distribution patterns in isometric and dynamic muscle contractions. *6th World Congress on Biomechanics*, Singapore, Singapore. Présentation orale en symposium.

- Dal Maso, F., Longcamp, M., **Amarantini, D.** (2010). Influence of agonist-antagonist muscle coactivation on corticomuscular coherence during submaximal isometric contractions. *IXes Journées de la SOFAMEA*, Toulouse, France. Présentation orale.

- Gasq, D., Dal Maso, F., Prince, F., Montoya, R., **Amarantini, D.** (2010). Medio-lateral control of the centre of pressure in healthy subjects under asymmetric conditions: preliminary results. *IXes Journées de la SOFAMEA*, Toulouse, France. Présentation orale.

- Dal Maso, F., Longcamp, M., **Amarantini, D.** (2009). Influence of agonist-antagonist cocontraction on cortico-muscular coherence in strength-trained and

untrained men during submaximal isometric knee contractions. *13ème Congrès International de l'Association des Chercheurs en Activités Physiques et Sportives*, Lyon, France. Présentation orale.

- **Amarantini, D.**, Rao, G., Martin, L., Cahouët, V., Berton, E. (2009). Optimization- and EMG-assisted estimation of joint moments and muscle forces during dynamic movements. *Journée Thématique de la Société de Biomécanique : La machine humaine au regard de la performance sportive*, Poitiers, France. Présentation orale.

- **Amarantini, D.** (2008). Optimization-based and EMG-assisted estimation of muscle forces and joint moments under isometric and dynamic contractions. *8th World Congress on Computational Mechanics & 5th. European Congress on Computational Methods in Applied Sciences and Engineering*, Venice, Italy. Présentation orale en symposium.

- **Amarantini, D.** (2008). Modélisation(s) biomécanique(s) pour l'estimation des efforts musculaires : applications cliniques. *Journée Scientifique 2008 de l'IFR 96*, Toulouse, France. Présentation orale.

- Bru, B., **Amarantini, D.** (2008). Sporting expertise influences the EMG-torque relationship during isometric contraction. *Journées Nationales de la Robotique Humanoïde*, Aéroclub de France, Paris, France. Présentation orale.

- **Amarantini, D.**, Rao, G., Berton, E. (2007). A two-step EMG-assisted minimax optimization process to estimate individual muscle forces in dynamic movements. *12ème Congrès International de l'Association des Chercheurs en Activités Physiques et Sportives*, Leuven, Belgium. Présentation orale.

- **Amarantini, D.** (2007). Changes in multi-muscle and multi-joint coordination during perturbed locomotor-like rhythmic movement. *24ème Congrès du Club Locomotion et Motricité Rythmique*, Toulouse, France. Présentation orale.

- Centomo, H., **Amarantini, D.**, Martin, L., Prince, F. (2006). Differences in agonist and antagonist muscle groups coordination between below-knee amputee and able-bodied children during dynamic exercise. *14th Biennial Conference for the Canadian Society for Biomechanics*, University of Waterloo, Waterloo, Canada. Présentation orale.

- Rao, G., **Amarantini, D.**, Vigouroux, L., Berton, E. (2006). Influence of muscular fatigue on agonist and antagonist muscle groups moments during loaded squats. *5th World Congress of Biomechanics*, Munich, Germany. Présentation orale.

- Centomo, H., **Amarantini, D.**, Martin, L., Prince, F. (2006). Differences in the coordination of agonist and antagonist muscle groups in below-knee amputee and able-bodied children during dynamic exercise. *Journée scientifique du Programme MENTOR des IRSC (Programme de formation stratégique sur les troubles de la mobilité et de la posture)*, École de technologie supérieure, Montréal, Canada. Présentation orale.

- **Amarantini, D.** (2005). Modélisations biomécaniques pour l'estimation des efforts musculaires. *11ème Congrès International de l'Association des Chercheurs en Activités Physiques et Sportives*, Paris, France. Présentation orale en symposium.

- Rao, G., **Amarantini, D.**, Favier, D., Berton, E. (2005). Estimation du niveau de co-contraction et des forces articulaires au genou lors d'un exercice de squat en charge. *11ème Congrès International de l'Association des Chercheurs en Activités Physiques*

et Sportives, Paris, France. <u>Présentation orale</u>.

- <u>Rao, G.</u>, Berton, E, **Amarantini, D.** (2005). Effect of load on agonist and antagonist muscle moments during dynamic squats. *30th Congress of the Société de Biomécanique*, Brussels, Belgium. <u>Présentation orale</u>.

- **Amarantini, D.** (2004). Développement de modèles biomécaniques pour l'analyse du mouvement humain. *Laboratoire Mouvement et Perception*, Université Aix-Marseille 2, Marseille (Luminy), France. <u>Séminaire invité</u>.

- Gonzalez, D., **Amarantini, D.**, Dietrich, G., Micallef, J.P., Favier, D. (2004). 3D Kinematics and kinetics analysis of javelin throwing performance. *XXIInd International Symposium of Biomechanics in Sports*, University of Ottawa, Ottawa, Ontario, Canada. <u>Présentation orale</u>.

- Rao, G., Berton, E., **Amarantini, D.**, Favier, D. (2004). A Kinematic and Dynamic Analysis of Elite Alpine Skiers. *XXIInd International Symposium of Biomechanics in Sports*, University of Ottawa, Ottawa, Ontario, Canada. <u>Présentation orale</u>.

- Rao, G., **Amarantini, D.**, Berton, E., Favier, D. (2004). Influence of Anthropometric Prediction Models on Inverse Dynamics Solutions. *13th Biennial Conference of the Canadian Society for Biomechanics*, Halifax, Nova Scotia, Canada. <u>Présentation orale</u>.

- **Amarantini, D.**, Martin, L., Cahouët, V. (2004). Optimization-based Procedures for the Prediction of Joint Muscular Efforts. *13th Biennial Conference of the Canadian Society for Biomechanics*, Halifax, Nova Scotia, Canada. <u>Présentation orale</u>.

- **Amarantini, D.**, Martin, L. (2003). Détermination des moments musculaires agoniste et antagoniste au cours de mouvements dynamiques : utilisation de l'optimisation numérique et des signaux électromyographiques. *10ème Congrès International de l'Association des Chercheurs en Activités Physiques et Sportives*, Toulouse, France. <u>Présentation orale</u>.

- **Amarantini, D.**, Martin, L. (2003). Estimation of knee muscle moments from an EMG-assisted optimization method during dynamic contractions. *28ème Congrès de la Société de Biomécanique*, Poitiers, France. <u>Présentation orale</u>.

- **Amarantini, D.**, Cahouët, V., Martin, L. (2001). Method for solving inverse dynamic problems using static optimisation of joint accelerations. *9ème Congrès International de l'Association des Chercheurs en Activités Physiques et Sportives*, Valence, France. <u>Présentation orale</u>.

➢ **COMMUNICATIONS AFFICHEES**

- Chalard, A., **Amarantini, D.**, Picaut, P., Pons, L., Marque, P., Gasq, D. (2019). Assessment of upper limb active movement facilitation and neuromuscular plasticity induced by abobotulinumtoxinA in chronic poststroke: A study protocol. *4th International Neurotoxin Association Conference*, Copenhagen, Denmark. <u>Poster</u>.

- Chalard, A., **Amarantini, D.**, Tisseyre, J., Marque, P., Tallet, J., Gasq, D. (2018). Is spasticity or spastic cocontraction of the elbow flexors associated with the limitation of voluntary elbow extension in adults with acquired hemiparesis? *12th World Congress of the International Society of Physical and Rehabilitation Medicine*, Paris, France. <u>E-Poster</u>.

- Chalard, A., **Amarantini, D.**, Belle, M., Montané, E., Gasq, D. (2018). Impact of different EMG normalisation methods on muscle activations and cocontraction index in adults with chronic post-stroke hemiparesis. *12th World Congress of the International Society of Physical and Rehabilitation Medicine*, Paris, France. E-Poster.

- Cremoux, S., Charissou, C., Tallet, J., Abade-Moreira, A., Dal Maso, F., **Amarantini, D.** (2018). Alteration of intermuscular coherence in synergistic muscle pairs during actual elbow flexion contractions after cervical spinal cord injury. *31st International Congress of Clinical Neurophysiology*, Washington, DC, USA. Poster.

- Cremoux, S., **Amarantini, D.**, Dal Maso, F., Tallet, J. (2017). Etude neuro-physiologique des mouvements miroirs chez le sujet traumatisé médullaire cervical. *17ème Congrès International de l'Association des Chercheurs en Activités Physiques et Sportives*, Dijon, France. Poster.

- Blais, M., **Amarantini, D.**, Albaret, J.M., Chaix, Y., Tallet, J. (2016). Inter-hemispheric communication is altered during learning of a new bimanual coordination in teenagers with developmental coordination disorder. *Journée de l'Ecole Doctorale Comportement, Langage, Education, Socialisation, Cognition*, Toulouse, France. Poster.

- Charissou, C., **Amarantini, D.**, Berton, E., Vigouroux, L. (2016). Effects of grip type on EMG-EMG coherence between hand flexor and extensor muscles during maximal isometric contractions. *12ème colloque de la Journée de l'Ecole Doctorale des Sciences du Mouvement Humain*, Marseille (Luminy), France. Poster.

- Charissou, C., Vigouroux, L., Berton, E., **Amarantini, D.** (2015). Fatigue- and training-related modulation of "β" EMG-EMG coherence between synergist agonist muscles during isometric contractions: New evidence of the significance of intermuscular coupling in motor control. *Progress in Motor Control X*, Budapest, Hungary. Poster.

- Daviaux, Y., Cremoux, S., Tallet, J., **Amarantini, D.**, Cornu, C., Deschamps, T. (2015). Impaired perception of reaching capabilities involves an atypical sensorimotor activity over the contralateral premotor area. *9th IBRO World Congress of Neuroscience*, Rio de Janeiro, Brazil. Poster.

- Gimenez, P., Chicoine, E., **Amarantini, D.**, Dal Maso, F., Tremblay, J. (2014). Effect of lower-body pre-activation on performance during repeated jump squats in short-track speed skaters. *SPIN Summit 2014*, Montréal, Canada. Poster.

- Cremoux, S., **Amarantini, D.**, Tallet, J., Dal Maso, F., Berton, E. (2014). Increased antagonist muscular activations in cervical SCI participants: evidence of altered reciprocal inhibition during voluntary elbow contractions. *30th International Congress of Clinical Neurophysiology*, Berlin, Germany. Poster.

- Zorgati, H., Collomp, K., Cottin, F., Vergniaud, T., Do, M.-C., **Amarantini, D.**, Labsy, Z., Gagey, O., Prieur, F. (2013). Effet d'une prise de courte durée de corticoïde sur l'oxygénation musculaire du vastus lateralis lors d'exercices brefs et intenses. *15ème Congrès International de l'Association des Chercheurs en Activités Physiques et Sportives*, Grenoble. Poster.

- Gasq, D., Labrunée, M., **Amarantini, D.**, Dupui, P., Montoya, R., Marque, P. (2013). Between-day reliability of centre of pressure measures in hemiplegic stroke patients.

VIIIème Congrès de Physiologie, de Pharmacologie et de Thérapeutique (P2T), Angers, France. Poster.

- Cremoux, S., Tallet, J., Berton, E., Dal Maso, F., **Amarantini, D.** (2012). Atypical EMG activation patterns of the elbow extensors after complete C6 tetraplegia during isometric contractions: a case report. *37ème Congrès de la Société de Biomécanique (en collaboration avec 27ème Congrès de Médecine Physique et de Réadaptation)*, Toulouse, France. Poster.

- Cremoux, S., Tallet, J., Berton, E., Dal Maso, F., **Amarantini, D.** (2012). Modulation of the cortical activity during isometric contractions at different force levels after a cervical spinal cord injury. *2012 Summer School on Neurorehabilitation*, Nuévalos (Zaragoza), Spain. Poster.

- Cremoux, S., Tallet, J., Berton, E., Dal Maso, F., **Amarantini, D.** (2012). Evolution de l'activité corticale lors de contractions isométriques à différents niveaux de force après une tétraplégie. *8ème Journée de l'Ecole Doctorale en Sciences du Mouvement Humain*, Montpellier, France. Poster, prix de la meilleure communication affichée.

- Dal Maso, F., Longcamp, M., **Amarantini, D.** (2011). Effect of strength-training on cortical oscillatory activity modulations in isometric contractions. *17th Annual Meeting of the Organization for Human Brain Mapping*, Québec, Canada. Poster.

- Cremoux, S., Tallet, J., Berton, E., Dal Maso, F., **Amarantini, D.** (2011). Effets d'une lésion médullaire sur la désynchronisation corticale lors de contractions isométriques volontaires sous-maximales. *7ème Journée de l'Ecole Doctorale Sciences du Mouvement Humain, Faculté des Sciences du Sport*, Marseille, France. Poster.

- Dal Maso, F., **Amarantini, D.**, Longcamp, M. (2009). Influence of agonist/antagonist cocontraction on the cortico-muscular coherence during knee isometric contractions. *Progress in Motor Control VII*, Marseille, France. Poster.

- Dal Maso, F., Longcamp, M., **Amarantini, D.** (2008). Influence de la coactivation des muscles agonistes et antagonistes sur la cohérence corticomusculaire chez l'expert en production de force. *1ère journée « Gilles Cometti » - La force : pourquoi, comment ?*, Dijon, France. Poster.

- Dedieu, P., **Amarantini, D.**, Doutreloux, J.P., Zanone, P.-G. (2008). Changes in ankle kinematics during walking/running with or without swinging arms. *1st i-FAB Congress*, Bologne, Italie. Poster.

- Bru, B., **Amarantini, D.** (2008). Influence of sporting expertise on the EMG-torque relationship during isometric contraction in man. *33ème Congrès annuel de la Société de Biomécanique*, Compiègne, France. Poster.

- Bru, B., **Amarantini, D.** (2007). Influence de l'expertise sur la nature de la relation moment résultant–EMG en conditions isométriques. *12ème Congrès International de l'Association des Chercheurs en Activités Physiques et Sportives*, Leuven, Belgium. Poster.

- Rao, G., **Amarantini, D.**, Berton, E., Vigouroux, L. (2007). Biomechanical investigation of the muscular redundancy through internal and external perturbations. *12ème Congrès International de l'Association des Chercheurs en Activités Physiques et Sportives*, Leuven, Belgium. Poster.

- Bru, B., **Amarantini, D.** (2007). Influence de l'expertise sur la relation

moment - EMG en conditions isométriques : étude préliminaire. *Journée IFR 96 Jeunes Chercheurs*, Institut des Sciences du Cerveau de Toulouse, Université Paul Sabatier Toulouse 3, Toulouse, France. <u>Poster</u>.

- Vigouroux, L., **Amarantini, D.**, Dion, F, Quaine, F. (2004). Finger muscle recruitment by the min/max optimization procedure. *29th Congrès de la Société de Biomécanique*, Créteil, France. <u>Poster</u>.

- Rao, G., Berton, E., **Amarantini, D.**, Favier, D. (2004). A Biomechanical Analysis of Turning Motion of Elite Alpine Skiers. *9th Annual Congress of the European College of Sport Science*, Clermont-Ferrand, France. <u>Poster</u>.

- **Amarantini, D.**, Martin, L. (2002). Procédure d'optimisation non linéaire pour l'estimation des moments musculaires agoniste et antagoniste à l'articulation du genou à partir des signaux EMG. *Congrès REPAR 2002*, Montréal, Canada. <u>Poster</u>.

- Termoz, N., Martin, L., **Amarantini, D.**, Prince, F. (2002). Modélisation biomécanique pour l'analyse des tâches d'interaction posture/mouvement. *III ème Congrès annuel des stagiaires de recherche en santé de la Faculté de médecine et des Centres hospitaliers de l'Université de Montréal*, Montréal, Canada. <u>Poster</u>.

- **Amarantini, D.**, Martin, L., Blanchi, J.P. (1999). Analyse biomécanique de la coordination interarticulaire. *24ème Congrès de la Société de Biomécanique*, Dijon, France. <u>Poster</u>.

- **Amarantini, D.**, Martin, L., Blanchi, J.P. (1999). Analyse biomécanique des coordinations interarticulaires : Application à la rééducation. *Journées des Sciences de la Vie et de la Santé*, Université Joseph Fourier Grenoble 1, Grenoble, France. <u>Poster, prix du Meilleur Poster</u>.

➢ ACTIVITES DE DIFFUSION, VULGARISATION SCIENTIFIQUE

- **Amarantini, D.** (2018). Bouge ton cerveau ! – Gérer mes mouvements : Que fait mon cerveau ? *Festival Pint of Science*, Toulouse, France. <u>Vulgarisation scientifique</u>.

ENCADREMENT DE THÈSE

- **2016 - … : Tisseyre, J.** (co-dir. : Tallet, J.).
  Etude longitudinale des liens entre attention et syncinésies chez des patients cérébro-lésés : marqueurs de la récupération ? ***Thèse de doctorat***, Université Paul Sabatier Toulouse 3, Toulouse, France.

- **2014 - 2018 : Charissou, C.** (co-encadrant ; co-dirs. : Berton, E., Vigouroux, L.).
  Etude de la contribution du couplage intermusculaire au contrôle de l'activité des muscles synergistes agonistes et antagonistes lors de contractions isométriques volontaires. ***Thèse de doctorat***, Université d'Aix-Marseille, Marseille, France ; soutenue le 30/03/2018.
  <u>Situation :</u> ATER ; Département STAPS, Institut National Universitaire Champollion, Rodez, France.

- **2011 - 2015 : Gasq, D.** (co-dir. : Zanone, P.-G.).
  Application de l'analyse temps-fréquence à l'évaluation de l'instabilité posturale chez le patient neurologique. ***Thèse de doctorat***, Université Paul Sabatier Toulouse 3, Toulouse,

France ; soutenue le 11/12/2015.
Situation : MCU-PH ; Université Paul Sabatier Toulouse 3 - CHU Toulouse (Rangueil), Toulouse, France.

- **2010 - 2013 : Cremoux, S.** (co-dir. : Berton, E.).
Contrôle de la contraction musculaire volontaire après un traumatisme médullaire cervical : Etude de la réorganisation des activations musculaires et corticales. *Thèse de doctorat*, Université d'Aix-Marseille, Marseille, France ; soutenue le 2/12/2013.
Situation : MCF ; Université de Valenciennes, Valenciennes, France.

- **2008 - 2012 : Dal Maso, F.** (co-dir. : Longcamp, M.).
Implication du cortex moteur primaire dans la régulation de la coactivation musculaire – Etude de la modulation des oscillations corticales et des interactions cortico-musculaires. *Thèse de doctorat*, Université Paul Sabatier Toulouse 3, Toulouse, France ; soutenue le 20/09/2012.
Situation : *Assistant professor ;* Université de Montréal, Montréal, Canada.

- **2003 - 2006 : Rao, G.** (co-dir. : Berton, E.).
Biomécanique de la coordination motrice : Modélisations et analyses en réponse à une perturbation interne ou externe. *Thèse de doctorat*, Université de la Méditerranée Aix-Marseille II, Marseille, France ; soutenue le 17/11/2006, prix de thèse 2006 de l'Université de la Méditerranée.
Situation : MCF ; Université d'Aix-Marseille, Marseille, France.

ENCADREMENT DE MASTER 2 RECHERCHE & MASTER OF SCIENCE

- **2018 - 2019 : Glories, D.** (co-dir. : Duclay, J.).
Effet du mode de contraction sur la cohérence corticomusculaire lors de flexions plantaires sous-maximales à différents niveaux de force. *Master 2 Recherche, Optimisation de la Performance Sportive et Entraînement*, Université Paul Sabatier Toulouse 3, Toulouse, France.

- **2018 - 2019 : Pierrieau, E.** (co-dir. : Fautrelle, L. ; co-encadrante : Charissou, C.).
Influence du contexte émotionnel sur le contrôle moteur lors de mouvements dirigés complexes : apport de l'étude de la cohérence intermusculaire. *Master 2 Recherche, Neuropsychologie et Neurosciences Cliniques*, Université Paul Sabatier Toulouse 3, Toulouse, France.

- **2018 - 2019 : Soulhol, M.** (co-dir. : Duclay, J.).
Influence du mode et de l'intensité de contraction sur la réactivité des rythmes électroencéphalographiques lors de flexions plantaires sous-maximales chez le sujet sain. *Master 2 Recherche, Optimisation de la Performance Sportive et Entraînement*, Université Paul Sabatier Toulouse 3, Toulouse, France.

- **2017 - 2018 : Carrère-Casajus, P.** (co-dir. : Gasq, D. ; co-encadrant : Gimenez, C. (R&T Manufacturing Engineering / Exoskeleton, Airbus Group)).
Establishment of a review: promising technologies for the worker's future 'exosuit'. *Master 2 Recherche, mention « Sciences Pour l'Ingénieur », programme international « Mechatronic System for Rehabilitation »*, Université Franco-Italienne (Université Pierre et Marie Curie, Paris, France & Università di Brescia, Brescia, Italia).

- **2017 - 2018 : Guebba, S.** (co-dir. : Gasq, D. ; co-encadrant : Gimenez, C. (R&T

Manufacturing Engineering / Exoskeleton, Airbus Group)).
Review of promising technologies for the worker's future 'exosuit'. ***Master of Science,*** *Mechatronics of complex systems*, Institut Supérieur de Mécanique de Paris (Supméca), Saint-Ouen, France.

- **2017 - 2018 : Fauvet, M.** (co-dir. : Gasq, D.).
Etude du lien entre les cocontractions spastiques et le couplage corticomusculaire chez le patient post AVC. ***Master 2 Recherche*** *« Neuropsychologie et Neurosciences Cliniques »*, Université Paul Sabatier Toulouse 3, Toulouse, France.
Poursuite d'études : Thèse de doctorat, Université Paul Sabatier Toulouse 3, Toulouse, France.

- **2016 - 2017 : Belle, M.** (co-dir. : Gasq, D.).
Etude des cocontractions spastiques et limitation du mouvement actif du membre supérieur des patients post-AVC : étude pilote. ***Master 2 Recherche*** *« Neuropsychologie et Neurosciences Cliniques »*, Université Paul Sabatier Toulouse 3, Toulouse, France.

- **2015 - 2016 : Chalard, A.** (co-dir. : Gasq, D.).
Etude du lien entre la modulation de la coactivation musculaire et l'altération des capacités fonctionnelles chez le patient hémiplégique. ***Master 2 Recherche****, mention « Sciences du Sport et du Mouvement Humain », spécialité « Optimisation de la Performance Sportive et Entraînement »*, Université Paul Sabatier Toulouse 3, Toulouse, France ; lauréat du 3ème Prix de l'Ordre des masseurs-kinésithérapeutes 2018 dans la catégorie Sénior.
Poursuite d'études : Thèse de doctorat CIFRE, Université Paul Sabatier Toulouse 3, Toulouse, France.

- **2015 - 2016 : Tisseyre, J.** (co-dir. : Tallet, J.).
Étude des liens entre le profil attentionnel et exécutif et le degré de syncinésies chez des adultes sains et des patients neurologiques. ***Master 2 Recherche*** *« Neuropsychologie et Neurosciences Cliniques »*, Université Paul Sabatier Toulouse 3, Toulouse, France.
Poursuite d'études : Thèse de doctorat, Université Paul Sabatier Toulouse 3, Toulouse, France.

- **2014 - 2015 : Carmet, D.** (co-dir. : Accadbled, F. ; co-encadrant : Cavaignac E.).
Modification des caractéristiques neuromusculaires induites par la chirurgie du LCA en utilisant la TMG. ***Master 2 Recherche****, mention « Sciences du Sport et du Mouvement Humain », spécialité « Optimisation de la Performance Sportive et Entraînement »*, Université Paul Sabatier Toulouse 3, Toulouse, France.

- **2014 - 2015 : Marrier, B.** (co-dir. : Le Meur, Y. ; co-encadrant : Piscione, J.).
Effet de la fatigue neuromusculaire sur les propriétés mécaniques d'un système poly-articulé lors d'une course en sprint : application en rugby à VII. ***Master 2 Recherche****, mention « Sciences du Sport et du Mouvement Humain », spécialité « Optimisation de la Performance Sportive et Entraînement »*, Université Paul Sabatier Toulouse 3, Toulouse, France.
Poursuite d'études : Thèse de doctorat, Université Paris Descartes, Paris, France.

- **2013 - 2014 : Charissou, C.** (co-dir. : Duclay, J.).
Influence de la fatigue sur la cohérence intermusculaire : effets de la spécialité sportive. ***Master 2 Recherche*** *« Mécanique pour le Vivant »*, Université Paul Sabatier Toulouse 3, Toulouse, France.
Poursuite d'études : Thèse de doctorat, Université d'Aix-Marseille, Marseille, France.

- **2012 - 2013 : Gov, T.**.
  Etude du délai électromécanique - Aspects méthodologiques et influence des paramètres d'exécution lors d'une contraction volontaire. ***Master 2 Recherche***, *mention « Sciences du Sport et du Mouvement Humain », spécialité « Optimisation de la Performance Sportive et Entraînement »*, Université Paul Sabatier Toulouse 3, Toulouse, France.

- **2012 - 2013 : Raynaldy, L.** (co-dir. : Hamaoui, A.).
  Effets de la modification de la position de la tête et du focus attentionnel sur la performance posturale lors d'une tâche posturo-cinétique : Etude préliminaire. ***Master 2 Recherche***, *mention « Sciences du Sport et du Mouvement Humain », spécialité « Activités Physiques Adaptées à la Prévention en Santé Publique »*, Université Paul Sabatier Toulouse 3, Toulouse, France.

- **2012 - 2013 : Chicoine, E.** (co-dir. : Tremblay, J.).
  Effet d'une présollicitation maximale isométrique des muscles stabilisateurs sur la coordination intermusculaire lors d'un exercice pluriarticulaire épuisant. ***Maîtrise en Sciences de l'activité physique***, Université de Montréal, Montréal, Canada.

- **2009 - 2010 : Cremoux, C.** (co-dir. : Tallet, J.).
  Effets d'une lésion médullaire sur la cohérence corticomusculaire et la coactivation lors de contractions isométriques volontaires. ***Master 2 Recherche*** *« Sport, Motricité, Santé et Société »*, Université Paul Sabatier Toulouse 3, Toulouse, France.
  Poursuite d'études : Thèse de doctorat, Université d'Aix-Marseille, Marseille, France.

- **2008 - 2009 : Gasq, D.**.
  Mécanismes de contrôle du centre de pression résultant, selon l'axe médio-latéral, en conditions d'asymétries chez le sujet sain : résultats préliminaires. ***Master 2 Recherche*** *« Sport, Motricité, Santé et Société »*, Université Paul Sabatier Toulouse 3, Toulouse, France.
  Poursuite d'études : Thèse de doctorat, Université Paul Sabatier Toulouse 3, Toulouse, France.

- **2007 - 2008 : Dal Maso, F.** (co-dir. : Longcamp, M.).
  Influence de la co-activation des muscles agonistes et antagonistes sur la cohérence cortico-musculaire lors de contractions isométriques chez l'homme. ***Master 2 Recherche*** *« Sport, Motricité, Santé et Société »*, Université Paul Sabatier Toulouse 3, Toulouse, France.
  Poursuite d'études : Thèse de doctorat, Université Paul Sabatier Toulouse 3, Toulouse, France.

- **2007 - 2008 : Zélic, G.**.
  Influence de l'interface homme-environnement sur les mécanismes de stabilisation active et les efforts articulaires subis lors d'activités physiques et sportives à impacts. ***Master 2 Recherche*** *« Sport, Motricité, Santé et Société »*, Université Paul Sabatier Toulouse 3, Toulouse, France.
  Poursuite d'études : Thèse de doctorat, Université de Montpellier 1, Montpellier, France.

- **2006 - 2007 : Bru, B.**.
  Influence de l'expertise sportive sur la relation fondamentale entre électromyographie et effort musculaire. ***Master 2 Recherche*** *« Sport, Motricité, Santé et Société »*, Université Paul Sabatier Toulouse 3, Toulouse, France.
  Poursuite d'études : Thèse de doctorat, Université Pierre-et-Marie-Curie, Paris, France.

- **2004 - 2005 : Martin, E.** (co-dir. : Do, M.-C.).

Effet d'une raideur articulaire sur le contrôle de l'équilibre postural. ***Master 2 Recherche « Sport, Motricité, Santé et Société »***, Université Paul Sabatier Toulouse 3, Toulouse, France.

ENCADREMENT DE MASTER 2 PROFESSIONNEL

L'ensemble des mémoires ci-dessous ont été soutenus dans le cadre de l'offre de formation en Master 2 du département « Entraînement Sportif » de la Faculté des Sciences du Sport et du Mouvement Humain (Université Paul Sabatier Toulouse III, Toulouse, France).

- **2018 - 2019 : Braconnier, A.**.
  Effets de différents types d'entraînements intermittents sur la capacité à répéter des efforts à haute intensité chez le jeune rugbyman.

- **2018 - 2019 : Dupreys, P.**.
  Apport de l'ajustement de l'articulation talo-crurale sur le développement de la détente verticale par un entrainement « pliométrie-vitesse » en rugby à XIII.

- **2018 - 2019 : Maiau, R.**.
  Effets d'une préactivation des muscles des membres inférieurs sur l'optimisation des dix derniers mètres de la course d'élan en saut en longueur.

- **2017 - 2018 : Baudraz, V.**.
  Le développement de la puissance musculaire des membres inférieurs par la pliométrie chez le jeune rugbyman.

- **2017 - 2018 : Gayrard, V.**.
  Les effets d'un entrainement en pliométrie chez de jeunes footballeuses.

- **2016 - 2017 : Nuttman, M.**.
  Le développement de la puissance neuromusculaire par le biais de répétitions de sprints.

- **2016 - 2017 : Point, G.**.
  Développement de la puissance des membres inférieurs en vue d'augmenter la détente verticale et maintenir la qualité de vitesse chez des jeunes footballeurs.

- **2016 - 2017 : Sans, J.**.
  Effet d'un entraînement en pliométrie sur la performance en sprint chez des jeunes footballeurs U10-U11.

- **2015 - 2016 : Lepretre, S.-A.** (co-dir. : Vaucelle, S.).
  Effets d'un entrainement intermittent « vitesse-pliométrie » sur la relation force-vitesse-puissance en sprint

- **2015 - 2016 : Maris, L.** (co-dir. : Vaucelle, S.).
  Amélioration de la performance en répétition de sprints par un entrainement aérobie.

- **2015 - 2016 : Nsiri, S.** (co-dir. : Vaucelle, S.).
  Effet d'un entrainement combiné en force et sprint résisté et/ou non résisté sur le démarrage en sprint.

- **2015 - 2016 : Rey, J.**.
  Amélioration de l'équilibre du judoka par un travail de proprioception.

- **2014 - 2015 : Doumerc, J.** (co-dir. : Vaucelle, S.).

Effet d'un entrainement de sprints résistés sur les propriétés de force-vitesse-puissance et sur l'efficacité mécanique lors du sprint.

- **2014 - 2015 : Galiègue, W.**.
  L'effet d'un entraînement pliométrique sur la phase de départ et de virage en natation lors d'un 50 mètres nage libre.

- **2014 - 2015 : Maillot, R.**.
  Développement de la force maximale des membres inférieurs à travers des résistances variables.

- **2012 - 2013 : Ganot, R.**.
  Développement de l'explosivité des membres inférieurs chez le karatéka.

- **2012 - 2013 : Lénard, T.**.
  Développement spécifique de la puissance des membres inférieurs afin d'augmenter la vitesse de course.

- **2011 - 2012 : Bouchfira, Z.**.
  Effets d'un entrainement excentrique sur l'hypertrophie et la force explosive des membres inférieurs en karaté.

- **2011 - 2012 : Gauthier, J.**.
  Variables déterminantes de la performance du jeu au pied en rugby à XV.

PROJETS DE RECHERCHE ET DE FORMATION

- **Contrat de prestations Inserm / Airbus (1/07/2016 – 1/07/2019).**
  <u>Responsable scientifique</u> (co-resp. : David Gasq (ToNIC, Université Paul Sabatier Toulouse 3)) du contrat de prestation de recherche entre Airbus et l'Inserm relatif au développement et à l'étude biomécanique d'exosquelettes. Partenaire industriel : Gimenez, C. (R&T Manufacturing Engineering / Exoskeleton, Airbus Group).
  – **2017 : « ErgoAirbus » |** Evaluation ergonomique de l'apport pour la santé d'un exosquelette assistant une tâche de crabotage.
  – **2018 : « Wearable of the future » |** A review of promising technologies for the worker's future 'exosuit'.

- **Programme IDEX Toulouse, volet Formation 2016 - 2017, axe « parcours innovants en licence ».**
  <u>Participant</u> au projet *Enseigner Par les Outils (EPO) : Plateforme pédagogique et expérimentale des sciences du mouvement*, financé par le 4ème appel à projets « Innovations en Licence » de l'IDEX de Toulouse. Porteurs : Robin Baurès (CerCo, Université Paul Sabatier Toulouse 3) et Bruno Watier (LAAS, Université Paul Sabatier Toulouse 3).

- **PHRC National 2014.**
  <u>Participant</u> au projet *Evaluation of botulinum toxin injection efficacy in the treatment of head essential tremor by a multi-center, randomized, double-blind, parallel-group, placebo-controlled study (Btx-HT)* financé par le Ministère des Affaires sociales, de la Santé et des Droits des femmes. Porteur : Durif, F. (NPsy-Sydo, CHU de Clermont-Ferrand).

- **ANR, Appel à projets générique 2014, Défi 4 « Santé et bien-être ».**

Participant au projet *Improving the evaluation of comatose and post-comatose patients and boosting their cognitive functions (CogniComa)* sélectionné par l'ANR. Porteur : Perrin, F. (CRNL, Université Lyon 1 Claude Bernard).

- **World Anti-Doping Agency (WADA) research grant 2011.**
  Participant au projet *Effects of glucocorticoid during repeated bouts of high-intensity exercise* financé par l'Agence mondiale antidopage. Porteur : Do, M.-C. (CIAMS, Université Paris Sud).

- **Clusters de recherche Rhône-Alpes 2008.**
  Participant (responsable modélisation biomécanique) au projet *Prévention des troubles musculo squelettiques du membre supérieur (TMS - MS)* financé par la Région Rhône-Alpes. Porteur : Forestier, N. (EMAS, Université de Savoie).

- **Opérations scientifiques UPS 2006-2008.**
  Co-porteur du projet *Neuro-Biomécanique de la cohérence cortico-musculaire (NeuroBiomeCo)* financé par l'Université Paul Sabatier Toulouse 3 dans le cadre du 1er appel d'offre du Conseil Scientifique « opérations scientifiques 2006-2008 ». Porteur : Longcamp, M. (LAPMA, Université Paul Sabatier Toulouse 3).

ACTIVITÉS D'EXPERTISES

➢ **REVIEWER**

Journal	Nb.
BMC Neuroscience	1
BioMedical Engineering OnLine	1
British Journal of Sports Medicine	1
Communications in Nonlinear Science and Numerical Simulation	1
Computer Methods in Biomechanics and Biomedical Engineering	3
European Journal of Applied Physiology	4
Experimental Techniques	1
Frontiers in Human Neuroscience	1
Gait & Posture	3
Innovation and Research in BioMedical engineering	1
Journal of Biomechanics	5
Journal of Physical Therapy Science	1
Mécanique et Industries	3
Medicine and Science in Sports and Exercise	1
Movement & Sport Sciences - Science & Motricité	1
Perceptual and Motor Skills	1
PLoS ONE	1

➢ **JURYS DE DOCTORATS (PHD ET MD, HORS ENCADREMENTS)**

- **Daviaux, Y.** (18/09/2015). <u>Membre invité</u> du jury de *Thèse de Doctorat STAPS, spécialité Neurosciences, de l'Université de Nantes Angers Le Mans (Nantes, France)* intitulée « Intégration sensorimotrice et contexte somatosensoriel – Vers une meilleure compréhension des processus neuronaux impliqués dans le couplage action-perception ».

- **Montastruc, J.** (19/06/2015). <u>Membre invité</u> du jury de *Thèse pour le Diplôme d'Etat de Docteur en Médecine de l'Université Paul Sabatier Toulouse 3 (Toulouse, France)* intitulée « Etude des déterminants de l'asymétrie d'appui chez le patient hémiplégique suite à un AVC ».

- **Chotard, C.** (21/10/2014). <u>Membre invité</u> du jury de *Thèse pour le Diplôme d'Etat de Docteur en Médecine de l'Université Paul Sabatier Toulouse 3 (Toulouse, France)* intitulée « Analyse cinématique tridimensionnelle du mouvement du membre supérieur : faisabilité, résultats préliminaires chez le sujet sain et le sujet hémiplégique, perspectives ».

- **Lajante, M.** (4/12/2013). <u>Examinateur</u> de la *Thèse de Doctorat en Sciences de Gestion de l'Université de Rennes 1 (Rennes, France)* intitulée « Contribution des neurosciences à l'étude de l'émotion en persuasion publicitaire : concepts, méthodes et mesures ».

- **Huchez, A.** (22/01/2013). <u>Examinateur</u> de la *Thèse de Doctorat STAPS de l'Université de Valenciennes et du Hainaut-Cambrésis (Valenciennes, France)* intitulée « Etude de la gestion et du contrôle de l'inertie lors de la réalisation d'une tâche acrobatique complexe en gymnastique ».

- **Bru, B.** (27/09/2012). <u>Examinateur</u> de la *Thèse de Doctorat STAPS de l'Université de Pierre et Marie Curie - Paris VI (Paris, France)* intitulée « Contribution à l'identification des paramètres géométriques et inertiels pour la modélisation dynamique du corps humain ».

- **Gérus, P.** (26/09/2011). <u>Examinateur</u> de la *Thèse de doctorat STAPS de l'Université de la Méditerranée (Marseille, France)* intitulée « Modélisation biomécanique de l'interaction tendon-aponévrose-fibre pour estimer les forces musculaires : apport des mesures échographiques ».

- **Domalain, M.** (19/02/2010). <u>Examinateur</u> de la *Thèse de doctorat STAPS de l'Université de la Méditerranée (Marseille, France)* intitulée « Modélisation biomécanique de la main pour l'estimation des contraintes du système musculo-squelettique lors de la préhension pouce-index ».

- **Billot, M.** (8/12/2009). <u>Examinateur</u> de la *Thèse de doctorat STAPS de l'Université de Bourgogne (Dijon, France)* intitulée « Estimation des contributions mécaniques agonistes et antagonistes à l'articulation de la cheville dans différentes conditions de sollicitations ».

➢ **AGENCES, FONDATIONS, FONDS ET ORGANISMES**

- **Expert auprès du Haut Conseil de l'Évaluation de la Recherche et de l'Enseignement Supérieur (HCÉRES) :** Campagne d'évaluation des entités de recherche de la 2018-2019 (vague E).

- **Expert auprès de l'Agence Nationale de la Recherche :** Programme « Blanc » 2008, 2009, 2010, 2012 ; Programme « TecSan » 2008.

- **Expert auprès de l'Association Nationale de la Recherche Technique :** Programme « CIFRE » 2007.

- **Expert auprès de l'Université Paul Sabatier Toulouse 3 :** Appel d'offre du Conseil Scientifique « opérations scientifiques 2011 - 2012 ».

- **Expert auprès de la Fondation de l'Avenir** : Appel d'offres « Recherche Médicale Appliquée » 2015.

- **Expert auprès de la Fondation universitaire « Santé, Sport et Développement Durable » de l'Université de la Méditerranée :** Appel d'offres 2011.

- **Expert auprès du <u>Mitacs</u> :** Programme « Accélération » 2014.

➢ **CONGRÈS SCIENTIFIQUES**

- **Membre du comité scientifique** des *20èmes Journées Toulousaines de Psychomotricité*, 2018, Toulouse.

- **Organisateur** du *XVIIème congrès de la Société Francophone d'Analyse du Mouvement chez l'Enfant et l'Adulte (SOFAMEA)*, 24-26 Janvier 2018, Toulouse, France. Co-orgs. : Darmana, R., Gasq, D..

- **Membre du comité scientifique** du *16ème Congrès International de l'Association des Chercheurs en Activités Physiques et Sportives (ACAPS)*, 26-28 octobre 2015, Nantes, France.

- **Membre du comité scientifique** du *15ème Congrès International de l'Association des Chercheurs en Activités Physiques et Sportives (ACAPS)*, 29-31 Octobre 2013, Grenoble, France.

- **Membre du comité d'organisation** du *37ème Congrès de la Société de Biomécanique (SB)*, 16-19 octobre 2012, Toulouse, France.

- **Membre du comité d'évaluation** du *27ème Congrès de Médecine Physique et de Réadaptation (SOFMER)*, 18-20 Octobre 2012, Toulouse, France.

- **Membre du comité d'organisation** du *XVIIIème Congrès de l'Association Posture et Equilibre (APE)*, 2-3 Décembre 2011, Albi, France.

ACTIVITÉS D'ENSEIGNEMENT

➢ **SITUATIONS**

- **2004 - … : Maître de conférences** (192 h eq. TD par an), Faculté des Sciences du Sport et du Mouvement Humain (UFR STAPS), Université Paul Sabatier Toulouse 3, Toulouse, France.

- **2003 - 2004 : Attaché Temporaire d'Enseignement et de Recherche** (mi-temps, 96 h eq. TD), Faculté des Sciences du Sport, Université de la Méditerranée Aix-Marseille 2, Marseille, France.

- **1999 - 2003 : Vacataire** (145 h eq. TD), UFR STAPS, Université Joseph Fourier Grenoble 1, Grenoble, France.

➢ **DISCIPLINES ENSEIGNÉES**

- **Biomécanique et analyse du mouvement humain, anatomie :**
  - Licence et Master 1, Faculté des Sciences du Sport et du Mouvement Humain (UFR STAPS), Université Paul Sabatier Toulouse 3, Toulouse, France ;
  - Institut de Formation en Psychomotricité de Toulouse (2ème année), Université Paul Sabatier Toulouse 3, Toulouse, France.

- **Programmation et analyse de données, traitement du signal :**
  - Master 2, Faculté des Sciences du Sport et du Mouvement Humain (UFR STAPS) et Faculté des Sciences et Ingénierie, Université Paul Sabatier Toulouse 3, Toulouse, France.

- **Bioénergétique de l'activité physique :**
  - Licence et Master 1, Faculté des Sciences du Sport et du Mouvement Humain (UFR STAPS), Université Paul Sabatier Toulouse 3, Toulouse, France.

- **Approche scientifique de la préparation physique :**
  - Master 2 *Entraînement Sportif*, Faculté des Sciences du Sport et du Mouvement Humain (UFR STAPS), Université Paul Sabatier Toulouse 3, Toulouse, France.

- **Notes et mémoires de recherche, mémoires professionnels :**
  - Licence 3 *Entraînement Sportif* et *Activités Physiques Adaptées*, Faculté des Sciences du Sport et du Mouvement Humain (UFR STAPS), Université Paul Sabatier Toulouse 3, Toulouse, France.
  - Master 1 *Entraînement Sportif*, Faculté des Sciences du Sport et du Mouvement Humain (UFR STAPS), Université Paul Sabatier Toulouse 3, Toulouse, France.
  - Master 1 *Biosanté*, Faculté des Sciences et Ingénierie, Université Paul Sabatier Toulouse 3, Toulouse, France.
  - Master 2 *Entraînement Sportif*, Faculté des Sciences du Sport et du Mouvement Humain (UFR STAPS), Université Paul Sabatier Toulouse 3, Toulouse, France.

ACTIVITÉS D'ADMINISTRATION

➢ **RESPONSABILITÉS ADMINISTRATIVES ET COLLECTIVES**

- **2017 - … : Membre de la commission pédagogique**, Faculté des Sciences du Sport et du Mouvement Humain, Université Paul Sabatier Toulouse 3, Toulouse, France.

- **2016 - … : Responsable de l'axe de recherche « Axe 3 : Neurobiomécanique. Motricité volontaire et involontaire »** (co-resp. : Gasq, D.), équipe « iDREAM Plasticité Neuromotrice, Médecine Régénérative et Médicaments innovants post-AVC » (dir. : Loubinoux, I.), Toulouse NeuroImaging Center (ToNIC, UMR 1214 Inserm / UPS).

- **2014 - … : Membre de la Commission des Thèses**, Ecole Doctorale « Comportement, Langage, Education, Socialisation, Cognition » (ED 326), Université Paul Sabatier Toulouse 3, Toulouse, France.

- **2014 - … : Membre élu au Conseil de Laboratoire**, collège MCF ou MCU-PH, Laboratoire « Imagerie Cérébrale et Handicaps Neurologiques » (UMR 825 Inserm / UPS) puis Toulouse NeuroImaging Center (ToNIC, UMR 1214 Inserm / UPS).

- **2014 - 2017 : Membre nommé au Groupe d'Avancement (GA) « SHS - STAPS »**, Université Paul Sabatier Toulouse 3, Toulouse, France.

- **2010 - 2013 : Membre nommé au Groupe d'Avancement et Primes (GAP) « SHS - STAPS »**, Université Paul Sabatier Toulouse 3, Toulouse, France.

- **2008 - 2012 : Membre élu au Conseil Scientifique de l'Université Paul Sabatier**, Université Paul Sabatier Toulouse 3, Toulouse, France.

- **2008 - 2012 : Membre élu au Conseil Scientifique de l'UFR STAPS de Toulouse**, Université Paul Sabatier Toulouse 3, Toulouse, France.

- **2008 - … : Membre de la Commission Informatique, Multimédia et Nouvelles Technologies**, Faculté des Sciences du Sport et du Mouvement Humain, Université Paul Sabatier Toulouse 3, Toulouse, France.

➢ **COMMISSIONS / COMITÉS DE RECRUTEMENT**

- **2019 : Comité de sélection pour le poste de maître de conférences 485**, profil *Biomécanique du mouvement humain*. UFR STAPS, GIPSA-lab, Université Grenoble Alpes, Grenoble, France.

- **2018 : Comité de sélection pour le poste de maître de conférences 659**, profil *Biomécanique et/ou physiologie de l'exercice*. Faculté des Sciences du Sport, Institut des Sciences du Mouvement, Aix-Marseille Université, Marseille, France.

- **2015 : Comité de sélection pour le poste de maître de conférences 370**, profil *Vieillissement, approche neuromécanique et système dynamique*. Faculté des Sciences du Sport, Institut des Sciences du Mouvement, Aix-Marseille Université, Marseille, France.

- **2014 : Comité de sélection pour le poste de maître de conférences 4241**, profil *Neurosciences, électrophysiologie (EEG, MEG, EMG...), santé, physiologie et analyse du mouvement*. UFR STAPS, Centre de recherches sur le sport et le mouvement, Université Paris Ouest Nanterre La Défense, Nanterre, France.

- **2014 : Commission de recrutement MAST**, profil *APA, éducation pour la santé, éducation thérapeutique et institutions sanitaires et sociales (médico-social, sanitaire, réseaux)*. Faculté des Sciences du Sport et du Mouvement Humain, Université Paul Sabatier Toulouse 3, Toulouse, France.

- **2014 : Commission de recrutement MAST**, profil *APA, promotion pour la santé, éducation thérapeutique et création de services APA-Santé (collectivités, fédérations, entreprises)*. Faculté des Sciences du Sport et du Mouvement Humain, Université Paul Sabatier Toulouse 3, Toulouse, France.

- **2013 : Comité de sélection pour le poste de maître de conférences 1033**, profil

Analyse du mouvement, activité physique. Faculté des Sciences du Sport, Laboratoire « Motricité Humaine, Éducation, Sport, Santé », Université Nice Sophia Antipolis, Nice, France.

- **2012 : Comité de sélection pour le poste de maître de conférences 4096**, profil *Analyses cinématique et dynamique de la locomotion, amélioration des modèles articulaires et introduction des modèles musculaires*. Faculté des sciences du sport, Institut Pprime, Université de Poitiers, Poitiers, France.

- **2012 : Comité de sélection pour le poste de maître de Conférences 4094**, profil *Analyses cinématique et dynamique de la locomotion, personnalisation des modèles pour des applications en milieu sévère*. Faculté des sciences du sport, Institut Pprime, Université de Poitiers, Poitiers, France.

- **2012 : Comité de sélection pour le poste de maître de Conférences 0563**, profil *Approche comportementale de l'expertise motrice et apprentissage*. Faculté des Sciences du Sport et du Mouvement Humain, PRISSMH - Laboratoire Adaptation Perceptivo-Motrice et Apprentissage, Université Paul Sabatier Toulouse 3, Toulouse, France.

- **2010 : Comité de sélection pour le poste de maître de Conférences 1551**, profil *Biomécanique des matériaux et des structures*. Faculté des Sciences du Sport, Institut des Sciences du Mouvement, Université Aix-Marseille 2, Marseille, France.

- **2010 : Comité de sélection pour le poste de maître de Conférences 1437**, profil *Sociologie et psychologie sociale des pratiques physiques et sportives : Etude du rapport à la norme*. Faculté des Sciences du Sport, Institut des Sciences du Mouvement, Université Aix-Marseille 2, Marseille, France.

- **2009 : Comité de sélection pour le poste de maître de Conférences 0769**, profil *Biomécanique et mécanique musculaire*. UFR STAPS, Laboratoire Adaptation Perceptivo-Motrice et Apprentissage, Université Paul Sabatier Toulouse 3, Toulouse, France.

- **2008 : Comité de sélection pour le poste de maître de Conférences 0907**, profil *Neurosciences de la motricité humaine*. UFR STAPS, Laboratoire Adaptation Perceptivo-Motrice et Apprentissage, Université Paul Sabatier Toulouse 3, Toulouse, France.

- **2008 - 2011 : Commission de recrutement des enseignants du 2nd degré**, UFR STAPS, Université Paul Sabatier Toulouse 3, Toulouse, France.

- **2007 : Commission de spécialistes pour le poste de maître de Conférences 0437 S**, profil *Interactions posture-mouvement et vieillissement des fonctions sensori-motrices*. UFR STAPS, Université Joseph Fourier Grenoble 1, Grenoble, France.

- **2007 : Commission de spécialistes pour le poste de maître de Conférences 1292 S**, profil *Ingénierie pour la santé*. UFR STAPS, Université Joseph Fourier Grenoble 1, Grenoble, France.

➢ **RESPONSABILITÉS PÉDAGOGIQUES**

- **2017 - … : Responsable de la Licence 3 « Entrainement Sportif » (L3 ES)**, Faculté des Sciences du Sport et du Mouvement Humain, Université Paul Sabatier Toulouse 3, Toulouse, France.

- **2014 - 2016 : Coordinateur du parcours « Recherche » du Master 2 mention « Sciences du Sport et du Mouvement Humain »**, Domaine « Sciences, Technologies, Santé », Faculté des Sciences du Sport et du Mouvement Humain, Université Paul Sabatier Toulouse 3, Toulouse, France. Co-coord. : Garcia, M.C..

- **2012 - 2013 : Responsable du parcours « Recherche » du Master 2 mention « Sciences du Sport et du Mouvement Humain »**, Domaine « Sciences, Technologies, Santé », Faculté des Sciences du Sport et du Mouvement Humain, Université Paul Sabatier Toulouse 3, Toulouse, France.

- **2004 - … : Responsabilités d'UE dans les formations :**

  - **Licence 1 STAPS**. Faculté des Sciences du Sport et du Mouvement Humain (UFR STAPS), Université Paul Sabatier Toulouse 3, Toulouse, France.

  - **Licence 3 STAPS spécialité « Entraînement Sportif »**. Faculté des Sciences du Sport et du Mouvement Humain (UFR STAPS), Université Paul Sabatier Toulouse 3, Toulouse, France.

  - **Master 1 STAPS**. Faculté des Sciences du Sport et du Mouvement Humain (UFR STAPS), Université Paul Sabatier Toulouse 3, Toulouse, France.

  - **Master 2 STAPS spécialité « Entraînement Sportif »**. Faculté des Sciences du Sport et du Mouvement Humain (UFR STAPS), Université Paul Sabatier Toulouse 3, Toulouse, France.

Petit préambule à l'usage du lecteur

Le prochain chapitre intitulé « La biomécanique, c'est génial ! », comme celui intitulé « La neuro-biomécanique, c'est magique ! » (cf. V.), est complété par des publications jointes au format des revues dans lesquelles elles ont été publiées. Cette prise de partie assumée, autorisée par les recommandations du conseil scientifique restreint de l'Université Toulouse 3 Paul Sabatier [5], n'est en rien une solution de facilité retenue en raison d'un manque d'exigence. Elle relève au contraire de l'affirmation que les produits de la recherche des étudiants que j'encadre sont le fruit d'un travail collaboratif et d'interactions continues dans lesquels je m'implique totalement, à toutes les étapes, quitte à reconnaître être parfois – sans doute – trop intrusif dans leur démarche. Sans aucunement prétendre être le parfait directeur de thèse [6], ce fonctionnement fait partie intégrante de ma stratégie de recherche et de ma pratique d'encadrement.

Si l'HDR se veut didactique, alors autant éviter les redites, même en travaillant sur la question de la redondance !

---

[5] Page synthétique de recommandations du conseil scientifique restreint de l'Université Toulouse 3 Paul Sabatier aux candidats à l'Habilitation à Diriger des Recherches (HDR). Repéré à : http://www.univ-tlse3.fr/medias/fichier/recommandations_hdr_du_cs_ups_1351766448335.pdf.

[6] Le guide du parfait directeur de thèse. Ecole Doctorale des Sciences de la Mer et du Littoral, Université Bretagne Loire. Repéré à : https://ed-sml.u-bretagneloire.fr/sites/default/files/u51/le_guide_du_parfait_directeur_de_these_edition_2017.pdf.

La biomécanique, c'est génial !

III.　La biomécanique, c'est génial ![7]

Comme je l'ai rappelé en *Introduction*, le système musculo-squelettique est doté d'une grande redondance, tout particulièrement au niveau musculaire avec en moyenne 2,6 actionneurs musculaires par degré de liberté cinématique. Cette propriété singulière lui confère de très grandes capacités d'adaptation pour produire une action motrice isométrique ou dynamique adaptée aux contraintes internes et externes de la tâche. Elle implique également qu'il existe une infinité de combinaisons d'efforts musculaires pour produire un même effort résultant autour d'une articulation (Challis, 1997 ; Prilutsky & Zatsiorsky, 2002). Du point de vue biomécanique, ce sujet renvoie à un niveau de complexité d'autant plus important que le problème sous-déterminé qui en résulte concerne à la fois les muscles agonistes agissant mécaniquement dans le sens de l'effort résultant, et les muscles antagonistes agissant dans le sens opposé.

Cette activation des muscles antagonistes lors de contractions volontaires est systématique et définie le phénomène de « co-activation » (ou « coactivation ») ou de « co-contraction » (ou « cocontraction ») entre les muscles agonistes et antagonistes (Figure 1). Si les deux termes renvoient généralement au même phénomène dans la littérature scientifique francophone et anglophone, la différence n'est toutefois pas uniquement sémantique. Le terme « co-activation » fait le plus souvent référence au rapport d'activité EMG entre les muscles antagonistes et les muscles agonistes (p. ex., Amarantini & Bru, 2015 ; Kellis *et al.,* 2003). Le terme « co-contraction » semble plus adapté quand cet indice est quantifié à partir de l'estimation des efforts musculaires, que ce soit en matière de forces ou de moments de forces (p. ex., Amarantini & Martin, 2004 ; Centomo *et al.,* 2007, 2008 ; Charissou *et al.,* 2017 ; Falconer & Winter, 1985 ; Goislard de Monsabert *et al.,* 2012 ; Rao *et al.,* 2009, 2010 ; Winter, 1990)[8]. Du point de vue fonctionnel, l'indice de co-activation ou de co-contraction peut être quantifié par le rapport entre l'activité EMG d'un muscle

---

[7] Collection *Un mémoire de synthèse présenté en vue de l'obtention de l'HDR dont vous êtes le Héros*. Si vous voulez plus d'informations à propos de ce titre, retournez auprès des Prs. Paul Allard et Jean-Pierre Blanchi à la note de bas de page n° 2 (p. 4). Sinon, poursuivez votre activité de lecture sur cette page.

[8] De là à penser que mon collègue et encore ami Laurent Vigouroux (Vigouroux *et al.,* 2019) a fait exprès de prendre le contrepied de cette désambiguïsation sémantique pour contrarier le regard rétrospectif que je porte aujourd'hui sur mon parcours scientifique, il n'y a qu'un pas – d'escalade – que je ne franchirai pas.

agissant comme antagoniste et celle de ce même muscle activé volontairement de manière maximale (p. ex., Barrué-Belou *et al.,* 2016 ; Billot *et al.,* 2014 ; Duclay *et al.,* 2011, 2014 ; Kluka *et al.,* 2015, 2016 ; Vinti *et al.,* 2012). Pour les travaux que j'ai menés sur la question de la redondance musculaire, la préférence a été donnée aux recommandations méthodologiques élaborées pour quantifier de la manière la plus appropriée l'indice de co-activation (Kellis *et al.,* 2003) ou de co-contraction (Winter, 1990) par un rapport entre les muscles antagonistes et les muscles agonistes agissant simultanément autour de la ou les articulations étudiées.
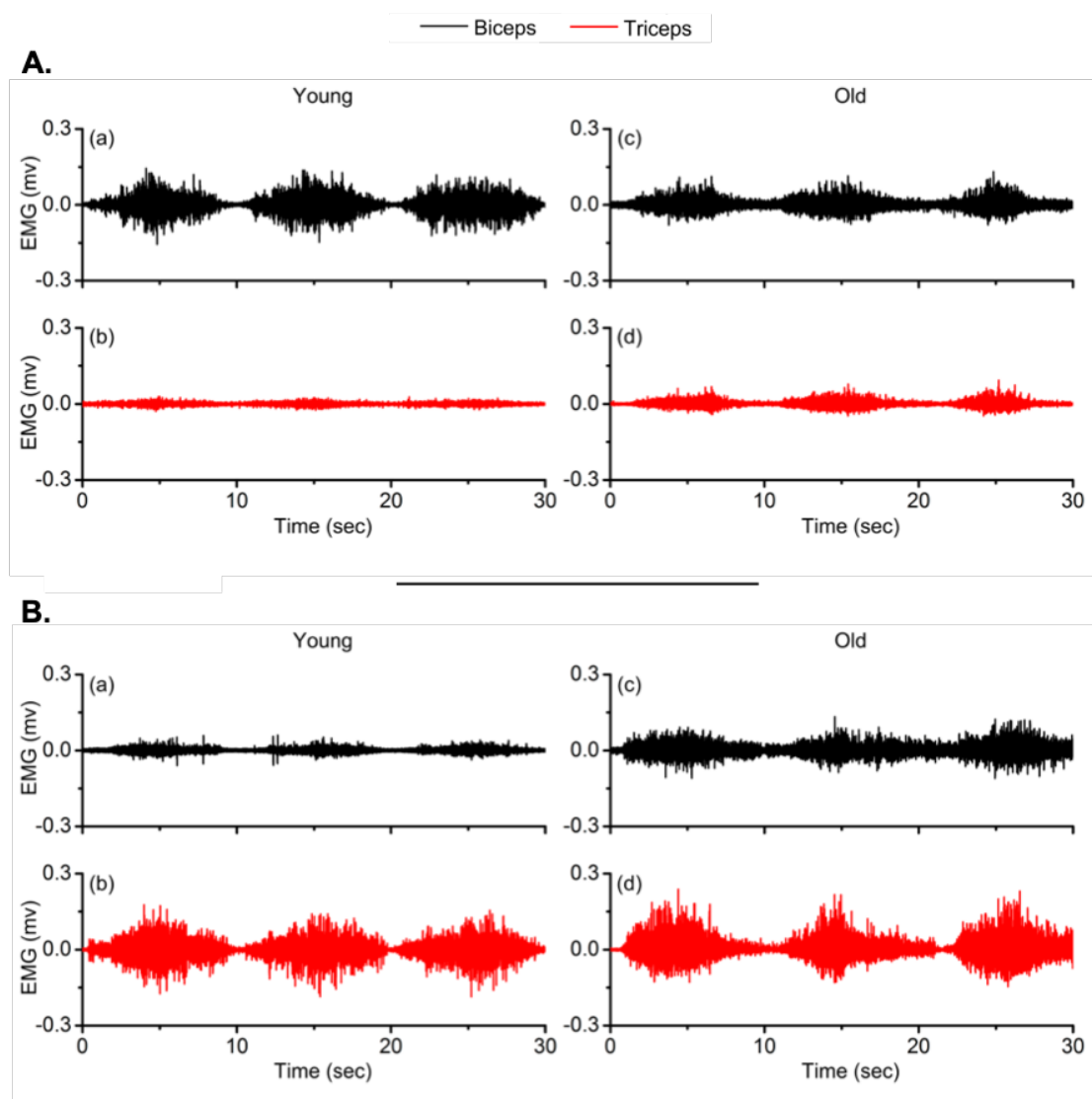
Figure 1, adaptée de Sun *et al.* (2016). Illustration du phénomène de co-contraction agoniste / antagoniste à partir d'enregistrements électromyographiques des muscles biceps (tracés noirs) et triceps (tracés rouges) brachiaux lors de trois mouvements consécutifs de flexion (A.) et d'extension (B.) du coude chez des participants jeunes (panneaux de gauche) et âgés (panneaux de droite). Quelle que soit la direction du mouvement, l'activité du muscle agoniste est systématiquement associée à celle de l'antagoniste agissant dans le sens opposé.

43

Mon intérêt à approfondir le sujet de de la redondance musculaire et la co-contraction agoniste / antagoniste comme objet central de mes activités de recherche ne se réduit évidemment pas à ces considérations sémantico-méthodologiques. Cette problématique a été au cœur de mes travaux dès les stages de recherche que j'ai réalisés en Maîtrise (dir. : Jean-Pierre Blanchi) et en DEA (dirs. : Luc Martin & Jean-Pierre Blanchi) au sein du Laboratoire Sport et Performance Motrice (SPM, EA 597) de l'UFR STAPS de Grenoble (Université Joseph Fourier Grenoble I). Dans une double perspective clinique (Allard *et al.,* 1981) et robotique en collaboration avec Bernard Espiau (projet robot bipède BIP ; Inria Grenoble - Rhône-Alpes, Grenoble, France) (Espiau *et al.,* 1998 ; Espiau & Oudeyer, 2008), l'objectif était d'évaluer les effets du port d'une orthèse du genou équipée d'un système élastique d'aide à la flexion sur les paramètres spatio-temporels, cinématiques et cinétiques d'une tâche posturo-cinétique de piétinement (Amarantini *et al.,* 1999 ; Amarantini, 2003, p. 78-115). Dans ce contexte, l'analyse de la co-contraction agoniste / antagoniste s'est avérée essentielle pour étudier de manière pertinente les changements de coordinations multi-segmentaire et multi-musculaire dans des configurations mécaniques où l'ajout d'un système élastique externe participe, avec les muscles, à la production du mouvement.

Le choix de centrer mes travaux de recherche sur la thématique de la redondance musculaire et de la co-contraction agoniste / antagoniste s'est également imposé à partir du constat contradictoire que la contribution de l'activité antagoniste à la performance motrice a été le plus souvent négligée, alors que de nombreux travaux ont clairement établi que leur contribution est loin d'être négligeable (Carolan & Cafarelli, 1992). Même si cette question a donné matière à débat (Kellis, 1998), les muscles antagonistes peuvent être activés entre 10 % et 35 % de leurs activations maximales au cours de contractions maximales isométriques (Beltman *et al.,* 2003 ; Kubo *et al.,* 2004) ou dynamiques (Baratta *et al.,* 1988 ; Grabiner *et al.,* 1989). D'autres travaux ont permis d'estimer à 30 N·m le moment de force développé par les muscles fléchisseurs du genou lors d'extensions isocinétiques de la jambe à 30 °·s^{-1} au cours desquelles le moment musculaire résultant atteignait 250 N·m (Aagaard *et al.,* 2000). En plus de ces aspects quantitatifs, les conclusions de la littérature sur les rôles fonctionnels de la co-contraction agoniste / antagoniste permettent d'établir sans ambiguïté que cette dernière ne peut pas être réduite à un épiphénomène, et qu'elle revêt au contraire une importance majeure dans la contraction musculaire (Falconer & Winter, 1985 ; Kellis *et al.,* 2003).

D'une manière générale, la co-contraction agoniste / antagoniste à un double rôle stabilisateur et protecteur de l'articulation. L'augmentation de la contrainte articulaire due à la co-contraction confère une meilleure stabilité de l'articulation (Granata & Marras, 2000 ; Mengarelli *et al.,* 2018). En augmentant la raideur de cette dernière (Carolan et Cafarelli, 1992 ; Remaud *et al.,* 2007), la co-contraction des groupes musculaires agoniste et antagoniste agirait de manière à stabiliser « activement » l'articulation en assistant les structures jouant un rôle « passif » de stabilisation articulaire (Alkjaer *et al.,* 2002 ; Basmajian & De Luca, 1985 ; Cholewicki *et al.,* 1997 ; Kingma *et al.,* 2004 ; Li *et al.,* 1999 ; Rudolph *et al.,* 2001 ; Shelburne *et al.,* 2005). La co-contraction des ischio-jambiers contribue à la fonction du ligament croisé antérieur pour maintenir la stabilité articulaire du genou et produire une force opposée au mouvement de translation antérieure du tibia (Miller *et al.,* 2000 ; Yanagawa, *et al.,* 2002). A l'inverse, un manque de co-contraction pourrait donc entraîner une diminution de la stabilité articulaire, en créant un stress supplémentaire aux structures internes du genou (Miller *et al.,* 2000). Lors d'activités dynamiques des membres inférieurs, le manque de stabilité articulaire semble ainsi à l'origine de certaines pathologies musculo-squelettiques (Miller *et al.,* 2000) et le développement à long terme de troubles ostéo-articulaires (Felson *et al.,* 2000 ; Issa & Sharma, 2006).

Comme l'ensemble des travaux que j'ai encadrés ont permis de le documenter de manière approfondie, de nombreuses études ont mis en évidence d'autres rôles fonctionnels bénéfiques de la co-contraction agoniste / antagoniste. Il a notamment été montré que l'activation simultanée des muscles ischio-jambiers simultanée à celle du quadriceps lors d'une extension du genou permet d'une part une répartition plus homogène des pressions sur le plateau tibial (Aagaard *et al., 2*000 ; Remaud *et al., 2*007) et, d'autre part, de limiter les tensions au sein des capsules articulaires (Baratta *et al.,* 1988 ; Solomonow *et al.,* 1988). La co-contraction agoniste / antagoniste joue également un rôle important dans le contrôle moteur (Kellis, 1998 ; Minetti, 1994 ; Osternig *et al.,* 1986 ; Psek & Cafarelli, 1993) et la stabilisation de la posture (Goislard de Monsabert *et al.,* 2012 ; Mora *et al.,* 2003). Finalement, elle apparaît comme un mécanisme nécessaire à l'apprentissage de nouvelles tâches et à la réalisation de mouvements nécessitant un haut degré de précision (De Luca et Mambrito, 1987 ; Gribble *et al.,* 2003 ; Heald *et al.,* 2018). De nombreux résultats soutiennent ainsi l'hypothèse proposée par Levine et Kabat (Levine & Kabat, 1952) selon laquelle la co-contraction agoniste / antagoniste pourrait améliorer la fluidité et la précision du mouvement produit par la contraction des muscles agonistes (da Fonseca *et al.,* 2006 ; Gribble *et al.,* 2003 ; Hagood *et al.,* 1990 ; van Soest *et al.,* 2003).

Certes, la présence de co-contraction agoniste / antagoniste implique une altération de l'efficience de la contraction musculaire car, pour un même moment résultant, la demande métabolique associée à l'effort produit par groupe musculaire agoniste augmente pour s'opposer à la contribution des muscles antagonistes (Baratta *et al.,* 1988 ; Remaud *et al.,* 2005), ce qui peut entraîner une diminution de la performance (Olney & Winter, 1985). Il est cependant intéressant de noter que, pour les mouvements impliquant des changements rapides et successifs de direction, il apparaît plus économique de moduler conjointement le niveau d'activation de l'ensemble des muscles agonistes et antagonistes plutôt que de les solliciter alternativement (Engelhorn, 1983 ; Hasan, 1986). Ainsi, dans certaines conditions, la co-contraction agoniste / antagoniste pourrait participer à une stratégie de contrôle qui permettrait de diminuer la dépense énergétique de la tâche.

Dans ce contexte, la principale contribution de mon travail de thèse (Amarantini, 2003) a été le développement d'un modèle musculo-squelettique « assisté » ou « piloté » par EMG (Amarantini & Martin, 2004) permettant d'estimer de manière physiologiquement réaliste les moments de force développés autour d'une articulation par les groupes musculaires agoniste et antagoniste, et donc la co-contraction agoniste / antagoniste. Dans la perspective d'analyser les coordinations multi-musculaire et pluri-articulaire d'un mouvement complexe dans des conditions perturbées (Amarantini *et al.,* 1999), l'objectif était également d'optimiser l'estimation du moment résultant classiquement obtenu par dynamique inverse (Winter, 1990 ; Cahouët *et al.,* 2002), en tenant compte de manière appropriée du phénomène de co-contraction. Sans redétailler ici le formalisme proposé, il est important de rappeler que ce modèle neuro- (au sens où l'EMG y est considérée comme un marqueur de la « commande centrale ») musculo-squelettique présentait l'originalité de combiner de manière précurseur l'utilisation de l'optimisation numérique non linéaire avec l'introduction des données EMG comme donnée d'entrée. Ce travail a permis de lever un verrou important dans la littérature concernant le calcul des efforts musculaires agoniste et antagoniste, « et au-delà » [9] (Amarantini *et al.,* 2010), car les méthodes par approche inverse n'en permettaient alors qu'une estimation en grande partie insatisfaite (Brand *et al.,* 1986 ; Buchanan & Shreeve, 1996 ; Challis, 1997 ; Challis & Kerwin, 1993 ; Cholewicki *et al.,* 1995 ; Herzog & Binding, 1992, 1993 ; Raikova & Prilutsky, 2001). Même au détriment d'une procédure de calibration relativement lourde, le modèle proposé fournissait une

---

[9] Adapté de la devise « Vers l'infini, et au-delà ! » que martèle avec force le ranger de l'espace Buzz l'Éclair en mission secrète pour la sauvegarde de l'humanité (Lasseter, 1995).

excellente estimation du moment résultant déterminé par dynamique inverse, ainsi qu'une estimation des moments musculaires tout à fait réaliste d'un point de vue physiologique (Figures 2 et 3).
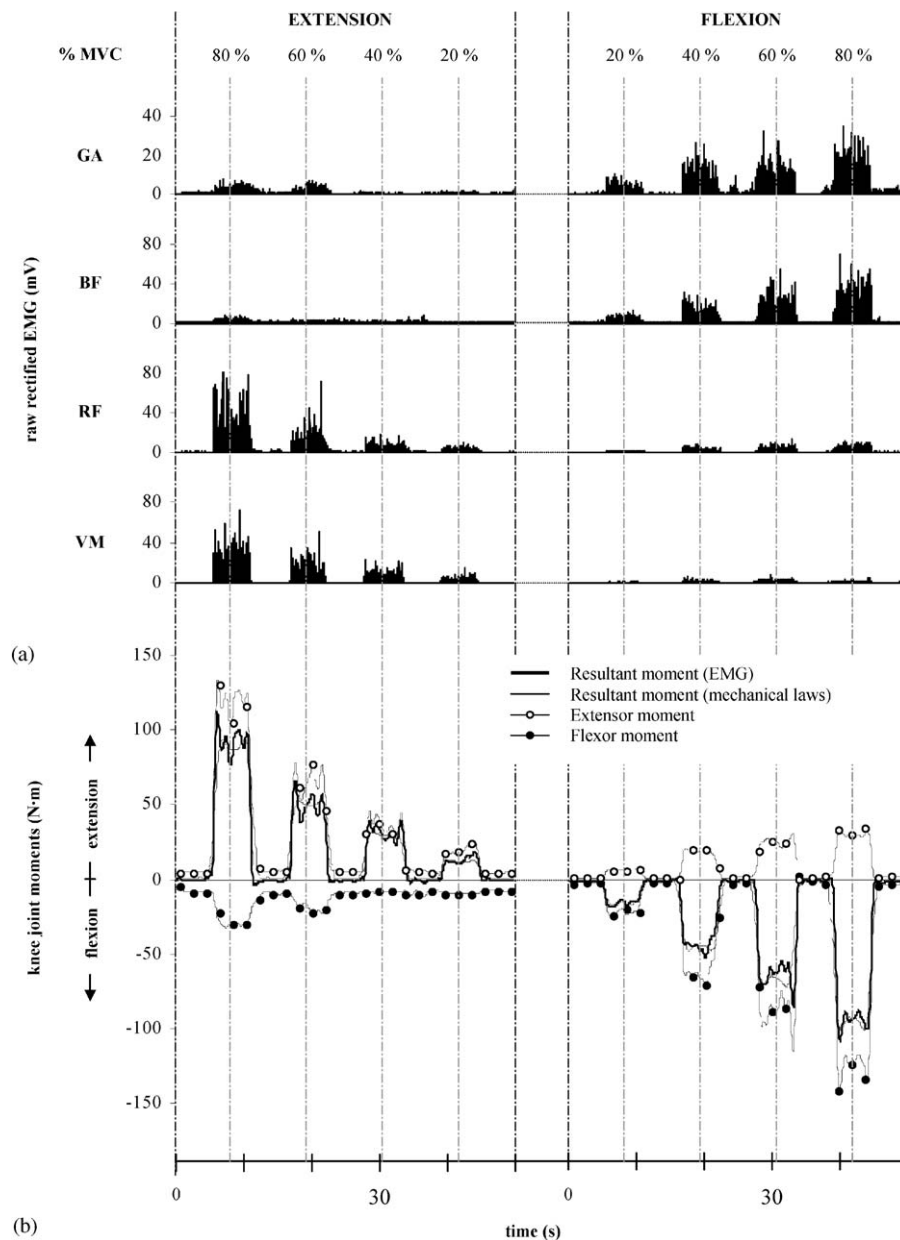
Figure 2, adaptée de Amarantini *et al.* (2004). a. Profils EMG redressés enregistrés au cours de contractions isométriques des muscles extenseurs et des muscles fléchisseurs du genou (*gastrocnemius* (GA), *biceps femoris* (BF), *rectus femoris* (RF) et *vastus medialis* (VM)) à 20, 40, 60 et 80 % de la force maximale volontaire. **b.** Moments musculaires estimés à l'articulation du genou à partir des données EMG en résolvant le problème d'optimisation non linéaire avec contraintes formulé dans le cadre de ma thèse (Amarantini, 2003) en conditions isométriques.
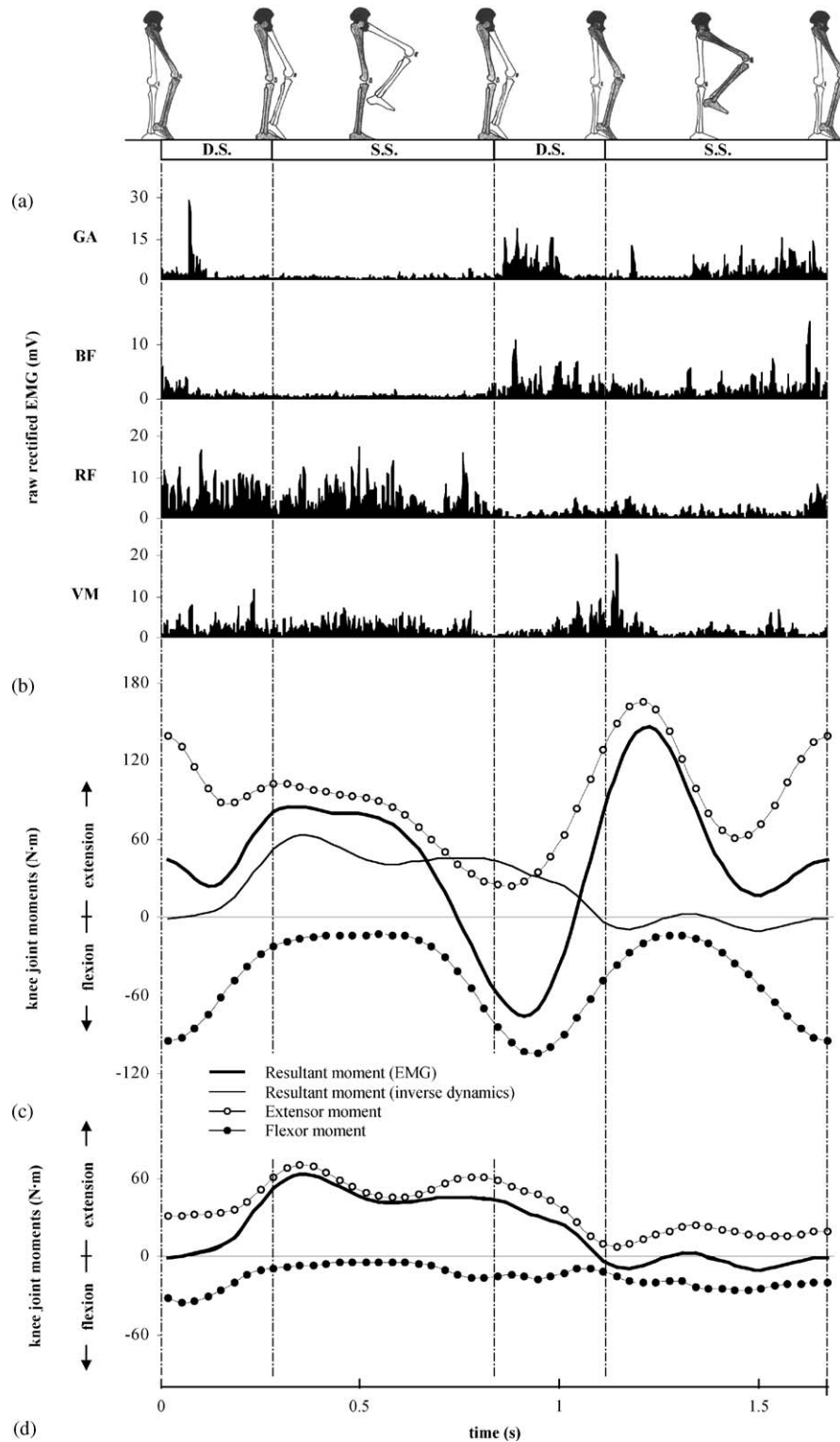
Figure 3, adaptée de Amarantini *et al.* (2004). a. Déplacement des segments du membre inférieur droit lors des phases d'un mouvement de piétinement (SS : simple appui ; DS : double appui). **b.** EMG redressée des muscles *gastrocnemius* (GA), *biceps femoris* (BF), *rectus femoris* (RF) et *vastus medialis* (VM). **c. & d.** Moments musculaires résultant, extenseur et fléchisseur estimés à partir de l'EMG en utilisant : **c.** une méthode de minimisation sans contraintes (Olney & Winter, 1985) et **d.** la procédure d'optimisation non linéaire avec contraintes proposée dans le cadre de mon travail de thèse (Amarantini, 2003).

Au commencement de ma démarche scientifique était donc la modélisation de la co-contraction agoniste / antagoniste, cette dernière étant abordée à la fois comme un modèle d'étude de la redondance musculaire et comme un objet de recherche original et privilégié dans une perspective d'analyse de la coordination motrice. A la suite de mon recrutement comme ATER à la Faculté de Sciences du Sport de Marseille, j'ai poursuivi ces travaux en biomécanique afin d'apporter des éléments de réponse à la question fondamentale de savoir en quoi une exagération ou une atténuation de la co-contraction agoniste / antagoniste pourrait favoriser l'apparition de certaines pathologies, ou, au contraire, contribuer à augmenter l'efficience de la contraction musculaire. Ce cheminement m'a conduit à engager mes activités de recherche dans deux directions qui ont fait l'objet des thèses de Guillaume Rao (Rao, 2006) et d'Hugo Centomo (Centomo, 2006) ainsi que du Master 2 Recherche de Bertrand Bru.

La première est d'ordre méthodologique et visait à réviser le modèle neuro-musculo-squelettique développé au cours de ma thèse (Amarantini *et al.,* 2004) afin d'en simplifier la procédure expérimentale et d'en généraliser l'application chez i) des patients dans une perspective clinique et translationnelle et ii) des sujets sains dans une perspective d'optimisation de la performance. Si les modèles musculo-squelettiques EMG-assistés ont démontré l'avantage de tenir compte de manière appropriée de la co-contraction agoniste / antagoniste (Hoang *et al.,* 2018, 2019 ; Nikooyan *et al.,* 2012), ils présentent cependant une limite importante. En effet, ils requièrent généralement une étape relativement lourde de calibration des signaux EMG afin d'établir, en amont de leur application dans une tâche expérimentale d'intérêt, les paramètres relatifs à la relation force- ou moment-EMG pour chaque muscle. Comme décrit de manière détaillée dans Amarantini *et al.* (2010), Centomo *et al.* (2007, 2008) et Rao *et al.* (2009, 2010), la reformulation du problème d'optimisation, au niveau du critère objectif comme des contraintes, a permis de s'affranchir de cette étape de calibration et ainsi de dépasser une limitation restrictive de l'utilisation des modèles musculo-squelettiques EMG-assistés pour estimer les efforts musculaires. Cette dynamique de recherche a finalement abouti à un modèle permettant de fournir une estimation physiologiquement réaliste, au sens qu'elle reflète la co-contraction agoniste / antagoniste de manière adaptée, les moments résultant, agoniste et antagoniste en conditions isométriques comme en conditions dynamiques, que les capacités de production de force soient intactes ou altérées par la présence de fatigue musculaire (Rao *et al.,* 2010). Cette contribution significative, qui présente également l'originalité de faire appel à

l'analyse temps-fréquence pour la première fois dans le cadre de mes travaux, est présentée de manière détaillée p. 54-62 :

- Rao, G., Berton, E., **Amarantini, D.**, Vigouroux, L., Buchanan, T.S. (2010). An EMG-driven biomechanical model that accounts for the decrease in moment generation capacity during a dynamic fatigued condition. *Journal of Biomechanical Engineering*, 132(7), 071003.

Finalement, pour aller au bout de mon cheminement scientifique sur cette question de la modélisation de la redondance musculaire, il semblait pertinent de prendre en considération le fait que, selon les conditions externes ou internes de réalisation d'une action motrice, le moment développé par un groupe musculaire peut résulter de combinaisons très différentes des forces produites par les muscles qui le composent (Pincivero *et al.,* 2006, 2008).
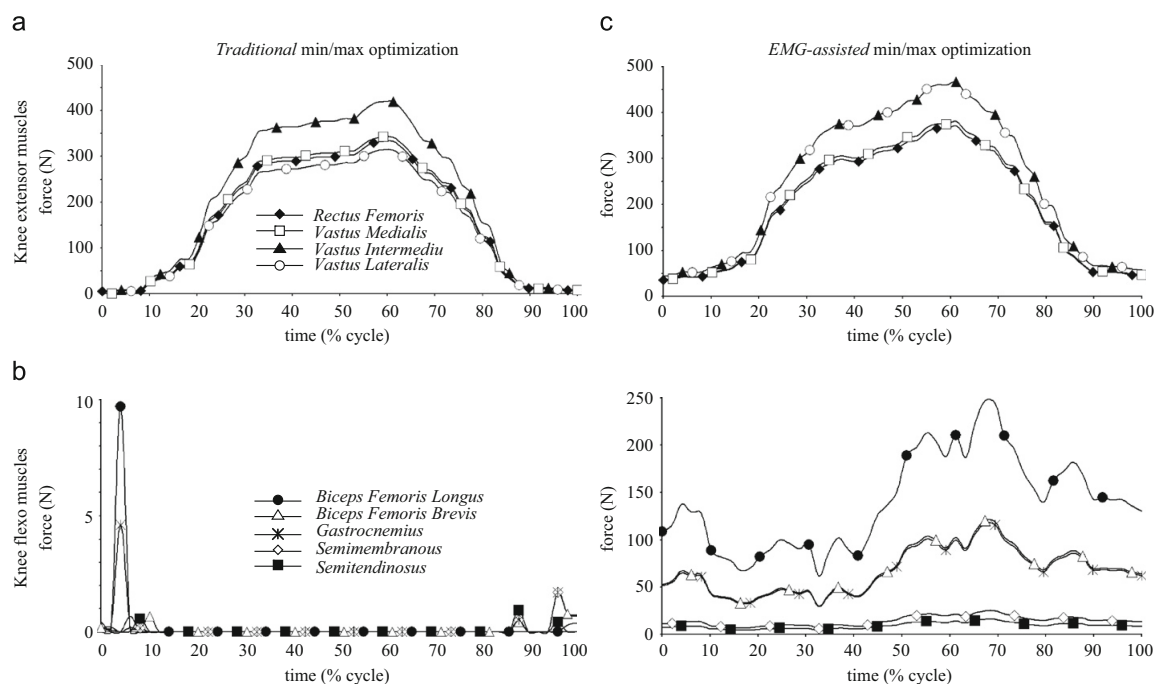
Figure 4, adaptée de Amarantini *et al.* (2010). Profils des forces musculaires produites par les muscles extenseurs (panneaux du haut) et fléchisseurs (panneaux du bas) du genou lors d'une tâche de squat. Les panneaux de gauche représentent les résultats obtenus à l'aide d'une méthode d'optimisation minmax « classique » (Rasmussen *et al.,* 2001) ; les panneaux de droite représentent les solutions fournies en utilisant la méthode d'optimisation minmax assistée par EMG proposée pour estimer les forces produites par chacun des muscles extenseurs et fléchisseurs du genou en tenant compte de manière appropriée de la co-contraction agoniste / antagoniste (Amarantini *et al.,* 2010).

Cet objectif représentait un défi majeur en biomécanique car les méthodes basées sur l'optimisation statique par approche inverse (p. ex., Crowninshield & Brand, 1981) peut conduire à une estimation incohérente des forces musculaires, même en faisant appel à l'optimisation dite « minmax » qui présente pourtant l'avantage de répartir au mieux la tension allouée à chaque muscle (Rasmussen *et al.,* 2001). En effet, les forces musculaires des muscles antagonistes sont incorrectement évaluées à zéro alors que les signaux EMG correspondants montrent une activité significative (Challis, 1997). Cette réflexion a abouti au développement d'un modèle d'optimisation minmax assisté par EMG (Amarantini *et al.,* 2010) qui, utilisé comme une extension au modèle d'estimation des moments agoniste et antagoniste, améliore sensiblement l'estimation des forces musculaires même pour les muscles dont l'EMG n'est pas introduite comme donnée d'entrée (Figure 4).

La deuxième direction de recherche dans laquelle je me suis engagé visait à explorer les facteurs de modulation de la co-contraction agoniste / antagoniste.

Comme évoqué précédemment, la présence de lésions ostéo-articulaires est un des facteurs qui impactent le plus la contribution des muscles antagonistes au cours d'une action motrice. D'autres études ont montré une augmentation significative de la co-contraction agoniste / antagoniste chez des patients neurologiques (Cremoux *et al.,* 2012 ; Farmer *et al.,* 1998 ; Thomas *et al.,* 1998 ; Unnithan *et al.,* 1996a, 1996b), au détriment de l'efficacité du mouvement. Unnithan *et al.* (1996b) ont ainsi observé que la co-contraction des muscles des membres inférieurs est un facteur majeur responsable du plus grand coût énergétique de la marche chez les enfants atteints de paralysie cérébrale. La co-contraction agoniste / antagoniste est également directement dépendante de la nature de la tâche (Escamilla *et al.,* 1998 ; Goislard de Monsabert *et al.,* 2012), des capacités de production de force (Kellis, 1999 ; Kellis *et al.,* 2011 ; Potvin & O'Brien, 1998) et du niveau d'expertise. Basmajian et De Luca (1985) ont mis en évidence que la pratique d'un entraînement en force diminue la contribution des muscles antagonistes. Ce résultat est en accord avec d'autres travaux qui ont montré une diminution de la co-contraction avec l'expertise ou la plasticité induite par un entrainement spécifique (Amiridis *et al.,* 1996 ; Carolan & Caffareli, 1992 ; Griffin et Cafarelli, 2005 ; Hakkinen *et al.,* 1998 ; Hakkinen *et al.,* 2000 ; Tillin *et al.,* 2011). Par ailleurs, plusieurs auteurs ont conclu que la co-contraction joue un rôle définitif dans le développement des habiletés motrices des jeunes enfants (Okamoto *et al.,* 2003 ; Winter, 1979). Le raffinement de la co-contraction agoniste / antagoniste semble ainsi pouvoir être considéré comme un indicateur pertinent de l'amélioration d'une habilité et de son

acquisition (Corser, 1973 ; Tanaka, 1974).

Le niveau de co-contraction agoniste / antagoniste semblent donc constamment ajusté selon les conditions internes et externes de réalisation d'une action motrice. Les travaux de Guillaume Rao (Rao, 2006) et d'Hugo Centomo (Centomo, 2006) ont eu pour objet de contribuer à cette réflexion et à une meilleure compréhension des conséquences fonctionnelles d'une régulation optimale ou inappropriée de la co-contraction. Ils ont donné lieu à plusieurs publications significatives, dont les deux suivantes sont présentées de manière détaillée p. 63-77 :

- Centomo, H., **Amarantini, D.**, Martin, L., Prince, F. (2007). Muscle adaptation patterns of below-knee amputee children during walking. *Clinical Biomechanics*, 22(4), 457-463.

- Rao, G., **Amarantini, D.**, Berton, E. (2009). Influence of additional load on the moments of the agonist and antagonist muscle groups at the knee joint during closed chain exercise. *Journal of Electromyography and Kinesiology*, 19(3), 459-466.

Dans leur ensemble, les résultats de ces travaux ont a renforcé ma conviction dans la pertinence de la démarche scientifique que j'ai adoptée immédiatement à la suite de ma thèse. En effet, ils ont apporté des connaissances essentielles qui enrichissent la compréhension de l'importance fonctionnelle de la co-contraction dans des conditions perturbées par une altération de la fonction motrice (Centomo *et al.,* 2007, 2008 ; Rao *et al.,* 2010), la présence d'une charge externe (Rao *et al.,* 2009) ou d'une plasticité induite par un entrainement (Amarantini & Bru, 2015).

Concernant la co-contraction elle-même, le fait que les enfants amputés trans-tibiaux en présentent une forme d'altération pourrait être un facteur important dans l'étiologie des maladies dégénératives de l'articulation du genou observée chez cette population. La moindre co-contraction agoniste / antagoniste observée chez ces enfants comparativement à des enfants contrôles pourrait entrainer une diminution de stabilité à l'articulation du genou, précurseur du développement asymptomatique d'ostéoarthrite à la jambe amputée mais également à la jambe saine (Burke *et al.,* 1978 ; Melzer *et al.,* 2001). Par ailleurs, le fait que les enfants amputés produisent la même cinématique de piétinement que les enfants contrôles en adoptant une coordination agoniste / antagoniste différente suggère que le système nerveux central exploite la redondance musculaire pour maintenir la performance malgré l'altération des capacités motrices. Cette hypothèse est cohérente avec les travaux qui ont mis en évidence une plasticité au niveau central suite à une amputation

chez l'homme (Chen *et al.,* 2002 ; Flor *et al.,* 1995 ; Knecht *et al.,* 1995). Elle est également en accord avec les conclusions établies dans des conditions de perturbation externe et de fatigue, qui suggèrent que le système neuro-musculo-squelettique exploite la redondance musculaire de manière appropriée au niveau agoniste / antagoniste afin de préserver l'intégrité des articulations tout en conservant une coordination motrice optimale (Rao *et al.,* 2009, 2010). Comme l'ont montré les effets de l'expertise en force sur la co-contraction agoniste / antagoniste (Amarantini & Bru, 2015), ce phénomène pourrait être associé à une modification de la nature de la relation entre les signaux EMG des muscles synergistes et le moment de force développé autour de l'articulation (Figure 5).
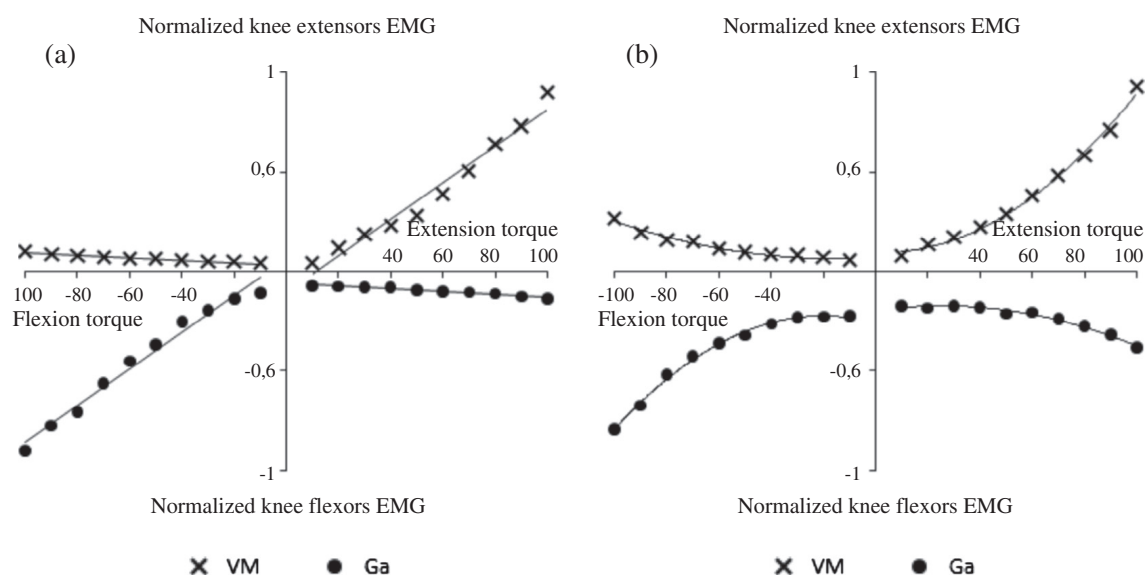
Figure 5, adaptée de Amarantini & Bru (2015). Effet de l'expertise en production de force (**a.** participants experts en haltérophilie / musculation *vs* **b.** participants actifs non spécialistes dans une activité de force) sur la relation EMG-moment des muscles fléchisseurs (×) et extenseurs (•) du genou lors de contractions isométriques réalisées en flexion et en extension à différents niveaux de force. VM : *vastus medialis* ; Ga : *gastrocnemius*.

Guillaume Rao[1]
Institute of Movement Sciences,
University of the Mediterranean,
UMR CNRS 6233,
163, Avenue de Luminy,
13288 Marseille Cedex 09, France;
Department of Mechanical Engineering,
University of Delaware,
126 Spencer Laboratories, Newark, DE 19716
e-mail: guillaume.rao@univmed.fr

Eric Berton
Institute of Movement Sciences,
University of the Mediterranean,
UMR CNRS 6233,
163, Avenue de Luminy,
13288 Marseille Cedex 09, France
e-mail: eric.berton@univmed.fr

David Amarantini
Universite de Toulouse,
UPS, LAPMA,
118, Route de Narbonne,
F-31062 Toulouse Cedex 09, France
e-mail: david.amarantini@cict.fr

Laurent Vigouroux
Institute of Movement Sciences,
University of the Mediterranean,
UMR CNRS 6233,
163, Avenue de Luminy,
13288 Marseille Cedex 09, France
e-mail: laurent.vigouroux@univmed.fr

Thomas S. Buchanan
Fellow ASME
Department of Mechanical Engineering,
University of Delaware,
126 Spencer Laboratories, Newark, DE 19716
e-mail: buchanan@udel.edu

An EMG-Driven Biomechanical Model That Accounts for the Decrease in Moment Generation Capacity During a Dynamic Fatigued Condition

Although it is well known that fatigue can greatly reduce muscle forces, it is not generally included in biomechanical models. The aim of the present study was to develop an electromyographic-driven (EMG-driven) biomechanical model to estimate the contributions of flexor and extensor muscle groups to the net joint moment during a nonisokinetic functional movement (squat exercise) performed in nonfatigued and in fatigued conditions. A methodology that aims at balancing the decreased muscle moment production capacity following fatigue was developed. During an isometric fatigue session, a linear regression was created linking the decrease in force production capacity of the muscle (normalized force/EMG ratio) to the EMG mean frequency. Using the decrease in mean frequency estimated through wavelet transforms between dynamic squats performed before and after the fatigue session as input to the previous linear regression, a coefficient accounting for the presence of fatigue in the quadriceps group was computed. This coefficient was used to constrain the moment production capacity of the fatigued muscle group within an EMG-driven optimization model dedicated to estimate the contributions of the knee flexor and extensor muscle groups to the net joint moment. During squats, our results showed significant increases in the EMG amplitudes with fatigue (+23.27% in average) while the outputs of the EMG-driven model were similar. The modifications of the EMG amplitudes following fatigue were successfully taken into account while estimating the contributions of the flexor and extensor muscle groups to the net joint moment. These results demonstrated that the new procedure was able to estimate the decrease in moment production capacity of the fatigued muscle group. [DOI: 10.1115/1.4001383]

Keywords: EMG, biomechanical model, muscle fatigue, muscle force, frequency shift

1 Introduction

Muscular fatigue is an inevitable feature of muscle activation, such as that which occurs during sporting competitions, rehabilitation exercises, or repetitive tasks (e.g., lifting and material handling). The fatigue starts at the beginning of the muscle activation and is commonly defined as a loss of force production capacity associated with an increase in the perceived level of effort [1]. The multiple physiological mechanisms underlying the decrease in force production capacity have been studied extensively and encompass central fatigue with diminished muscle activation [2] or peripheral fatigue with an increased concentration of inorganic phosphate or a failure in excitation-contraction coupling [3,4]. Changes in the electromyographic (EMG) signal have also been reported in the presence of fatigue. To compensate for the loss of force production capacity, previous work reported an increase in the EMG amplitude during submaximal isometric activities. Consequently, force decreases for constant levels of EMG during

maximal voluntary activations [1]. Related to the development of muscle fatigue, the EMG frequency content is also modified as the mean and median frequencies have been shown to decrease [1,5,6]. During dynamic (i.e., force-varying and/or nonisometric) contractions, the EMG signal has been described as nonstationary because of changes in its frequency content through time [5,6]. Due to these nonstationarities, time-frequency methods that do not rely on a local quasi-stationarity assumption (e.g., Choi–Williams distributions or wavelet transforms) are better suited to the spectral analysis of the EMG signal during fatiguing and/or dynamic contractions than the fast Fourier transforms [5,6].

The muscular redundancy of the human body prevents one from finding a unique combination of muscle forces leading to the net joint moment [7]. Most advanced biomechanical models use geometrical and physiological data (force-length and force-velocity relationships, moment arms, physiological cross sectional area (PCSA), and muscle length), kinematics, dynamics, EMG, and mechanical laws of motion as inputs to optimization processes in order to resolve the redundancy issue [8–10]. These models use the EMG amplitudes as direct or indirect information to compute muscle forces or muscle group contributions to the net joint moment. Despite the quasi-permanent presence of muscle fatigue during daily activities, few studies have attempted to take into account its presence when investigating muscle forces or their

contributions to the net joint moment. Indeed, the major limitation of using the EMG data of fatigued muscles in EMG-driven biomechanical models is the altered EMG-force relationship. A single study reported a method to take into account the changes in the EMG amplitudes due to fatigue during an isokinetic exercise [11]. This method was used as a part of an EMG-driven biomechanical model to estimate the modifications of spinal loading due to fatigue. However, this method required the movement to be performed on a dynamometer because a direct measurement of the force produced during the motion was needed. Its utility would be greatly improved if such a method could be applied to functional nonisokinetic movements.

The aim of the present study was to develop an EMG-driven biomechanical model to obtain the contributions of flexor and extensor muscle groups to the net joint moment during a nonisokinetic functional movement (squat exercise) performed in *nonfatigued* and in *fatigued* conditions. A methodology that aims at balancing the decreased muscle moment production capacity following fatigue was developed. This procedure aims at, first, assessing the changes in the activation level due to the presence of muscle fatigue (i.e., the changes in the EMG-moment relationship) and, second, taking these changes into account while estimating the contributions of the agonist and antagonist muscle groups to the net joint moment. We expected higher EMG amplitudes for the fatigued than for the nonfatigued condition for the same motion. When applying the original methodology developed in this study and assuming few changes in muscle activation patterns, we hypothesized identical outputs of the EMG-driven model (i.e., the contributions of the flexor and extensor muscle groups to the net joint moment) between both conditions. Indeed, given identical inputs in terms of kinematics and dynamics data, increased EMG amplitudes of the agonist muscles under fatigue (required to perform the task due to the low moment production capacity) would be balanced by the methodology presented here.

2 Methods

2.1 Subjects. Nine male subjects participated in this study. Mean ($\pm$s.d.) age, height, and mass were, respectively, 26.9 ($\pm$3.2 years), 1.75 ($\pm$0.05 m), and 70.6 ($\pm$6.2 kg). All subjects were free of known injuries. The project was approved by the University Review Board and all subjects gave written consent after being informed of the experimental procedures.

2.2 Experimental Protocol. The experimental design was comprised of four consecutive steps: an isometric maximal voluntary contraction, 11 cycles of dynamic half squats in a nonfatigued condition, an isometric fatigue session, and 11 cycles of dynamic half squats in a fatigued condition.

The first step involved isometric maximal voluntary contractions. The subjects were standing on a force plate and anchored to the ground using four inextensible ropes. Rope lengths were adjusted so that knee angles were close to 90 deg (Fig. 1). The subjects were instructed to produce the greatest vertical force during 4 s while maintaining their trunks as vertical as possible. In order to obtain a maximal performance, a visual feedback of the performance was provided through an oscilloscope and subjects were given verbal encouragement. The maximal value within three trials of maximal voluntary force (MVF) measured by the force plate was used in the third step of the experiment.

The second step examined dynamic half squats in the nonfatigued condition. The subjects performed 11 cycles of dynamic half squats (beginning in an upright posture and bending the knees until the thighs were parallel to the ground, then going back up) loaded with 20% of their bodyweight. The bar was positioned on the subjects' shoulders. A piece of wood was located below the heels and no motion of the heels was allowed. A metronome was used to keep constant the duration of each squat cycle (0.5 Hz frequency). Online verbal feedbacks were given to the subjects in
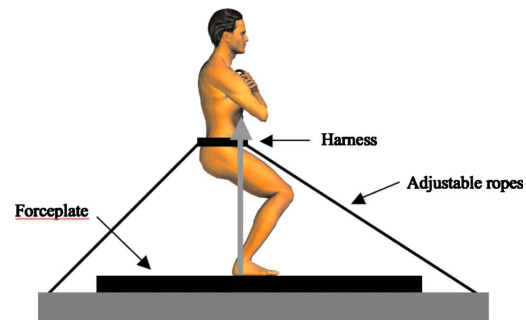

Fig. 1 Typical posture of a subject during the MVC and the isometric fatigue tasks

order for them to control their motions and perform the same squat movements in nonfatigued and fatigued conditions.

The third step was an isometric fatigue session. The subjects had to sustain 60% MVF for as long as possible to create fatigue in the knee extensor muscle group. This isometric fatigue protocol was performed in the same posture as the MVF trials. A visual feedback of the force to sustain was provided using an oscilloscope. The fatigue session was terminated as soon as the force level dropped below 40% MVF.

Finally, the fourth step consisted of dynamic half squats in the fatigued condition. Immediately after the end of the fatigue session, the subjects were loaded with 20% bodyweight and performed another block of 11 squat cycles. The squat cycle duration was also controlled (0.5 Hz pace).

2.3 Data Acquisition. Kinematic data were recorded at 120 Hz using a six camera Vicon 624 system. Trajectories of the foot, shank, thigh, trunk, and barbell segments were recorded from ten passive markers placed over the following landmarks on the right side of the body: the fifth metatarsal head, the lateral malleolus, the lateral femoral condyle, the great trochanter, the head of the clavicle, the epicondyle of the elbow, the wrist, the jaw, the vertex of the head, and the middle of the barbell. The ground reaction data were sampled at 1560 Hz from a six component AMTI force platform. As recommended in Refs. [8,12], electromyographic data for the gastrocnemius medialis (ga), biceps femoris (bf), rectus femoris (rf), and vastus medialis (vm) muscles were recorded at 1000 Hz using a Biopac MP 150 system (gain=500, input impedance=1.0 MΩ, common mode rejection ratio (CMRR) =110 dB, noise=0.5 μV, resolution=16 bits). Ag/Ag–Cl bipolar surface electrodes were placed over bellies of the selected muscles with a 2 cm center-to-center interelectrode distance. Skin preparation and electrode placements were done following the recommendations of the SENIAM group [13]. A TTL signal generated by the EMG acquisition device was later used to synchronize the EMG and the kinematics and dynamics data.

2.4 Data Processing. Ground reaction data were filtered using a fourth-order zero phase-lag Butterworth filter with a 10 Hz net cutoff frequency. Marker trajectories were smoothed using a constrained cubic smoothing spline procedure (MATLAB, SPLINE TOOLBOX, version 3.2.2). Angular time series of the ankle, knee, hip, and trunk angles were computed from smoothed Cartesian coordinates of the markers. Using cubic spline interpolation, angular kinematics, and ground reaction were resampled to 1000 Hz to match the EMG acquisition frequency. Values of joint angular velocities and accelerations were obtained by analytically differentiating the spline functions.

Based on the vertical velocity of the barbell, each variable of the squat cycle was normalized in time from 0% to 100%. The two first and two last cycles were removed from the analysis to

avoid electromyographic and kinematic changes due to movement initiation and termination. The seven remaining cycles were averaged to obtain one representative cycle for each variable (EMG, angular kinematics, and ground reaction) for each subject. In the nonfatigued and fatigued conditions, the knee net joint moment was computed via inverse dynamics [14] using the representative cycles of kinematics and ground reaction data as well as body segment parameters from Ref. [15]. Inverse dynamics were computed using the Langrangian formalism with the human body modeled as a planar four-link system with frictionless hinges.

2.5　Modeling. Based on the modifications of the EMG signal during the isometric fatigue session, a methodology was developed to assess the loss of moment production capacity of the fatigued muscle group during the dynamic session. This methodology was further used as a part of an EMG-driven biomechanical model to estimate the contributions of the flexor and extensor muscle groups to the knee net joint moment under muscle fatigue condition.

First, the isometric fatigue session served as a basis to create a linear relationship representing the loss of force production capacity of the fatigued muscles as a function of the decrease in the EMG mean frequency. Second, an EMG-driven model was used to estimate the flexor and extensor contributions to the knee net joint moment in the nonfatigued condition. Third, the decrease in force production capacity in the fatigued dynamic condition (further referred as the K coefficient) was estimated using the decrease in the EMG mean frequency between the nonfatigued and the fatigued conditions as input to the linear relationship. Finally, the K coefficient was used in the EMG-driven model to constrain the moment production capacity of the fatigued muscle group. These different steps will be detailed in the following paragraphs.

2.5.1　Isometric Fatigue Session. During the isometric fatigue session, the subjects had to sustain 60% of their MVF for as long as possible. During this session, angular kinematics and EMG data were analyzed within windows that were 512 points long and centered every 5% force decrease. These windows corresponded to 60% (nonfatigued condition), 55%, 50%, 45%, and 40% of the MVF. Within each window, the knee angles and the root mean square (RMS) of the EMG signal were computed. Wavelet transforms with Morlet wavelets of 126 points length at the coarsest scale were used to obtain the values of the mean frequency of the myoelectric signal within each window [16,17].

Force plate vertical force, RMS EMG, and mean EMG frequency values were then normalized relative to values of the nonfatigued condition. Because adaptations to fatigue may arise either on EMG or on force signals, a ratio between the normalized force plate vertical force and the normalized RMS EMG signal was computed for each analysis window (normalized force/EMG ratio). Finally, linear regression was used to fit the normalized force/EMG ratio to the normalized mean frequency decrease. Thus, the output of the isometric fatigue session consisted of a linear relationship that represents the normalized force/EMG ratio (the force production capacity of the muscle group) as a function of the normalized mean frequency decrease.

Considering, first, that the fatigue protocol would only affect the extensor muscle group and, second, that the low activation levels of the flexor muscles would produce highly variable frequency content estimates, the linear regression was only computed for the knee extensor muscles (i.e., rectus femoris and vastus medialis muscles).

2.5.2　Dynamic Trials—Nonfatigued Case. The contributions of the knee flexor and extensor muscle groups to the net joint moment were obtained from an EMG-to-moment optimization procedure [8,18]. For the nonfatigued condition, the optimization problem was formulated as follows:

Find

$$\alpha_i^{nf} = \{\alpha_{ga}^{nf}, \alpha_{bf}^{nf}, \alpha_{rf}^{nf}, \alpha_{vm}^{nf}\}, \quad \beta_j^{nf} = \{\beta_A^{nf}, \beta_K^{nf}, \beta_H^{nf}\}, \quad \delta_j^{nf}$$
$$= \{\delta_A^{nf}, \delta_K^{nf}, \delta_H^{nf}\}, \quad \text{and} \quad w_i^{nf}(t) = \{w_{ga}^{nf}(t), w_{bf}^{nf}(t), w_{rf}^{nf}(t), w_{vm}^{nf}(t)\}$$

$$\text{that minimize:} C = \frac{1}{2}(M_K^{nf}(t) - \hat{M}_K^{nf}(t))^2 \tag{1}$$

with

$$\hat{M}_K^{nf}(t) = \sum_i (\alpha_i^{nf} \cdot w_i^{nf}(t) \cdot S_i^{nf}(t))^T \cdot [\mathbf{1} + \mathbf{E} \cdot (\beta_j^{nf} \cdot \Delta\theta_j(t))$$
$$- \mathbf{E} \cdot (\delta_j^{nf} \cdot \dot{\theta}_j(t))], \quad i = \{ga, bf, rf, vm\}, \quad j = \{A, K, H\} \tag{2}$$

subject to:

$$\begin{cases} \alpha_{ga}^{nf}, \alpha_{bf}^{nf} < 0; \quad \alpha_{rf}^{nf}, \alpha_{vm}^{nf} > 0 \\ \quad \beta_j^{nf} \text{ and } \delta_j^{nf} > 0 \\ \quad 0 < w_i^{nf}(t) < 1 \\ \hat{M}_{ga}^{nf}, \hat{M}_{bf}^{nf} < 0; \quad \hat{M}_{rf}^{nf}, \hat{M}_{vm}^{nf} > 0 \end{cases} \text{ as inequality constraints } \tag{3}$$

The "nf" and "f" superscripts correspond, respectively, to the nonfatigued and the fatigued conditions while the indices "i" stand for the muscle investigated (ga, bf, rf, and vm) and the indices "j" represent the joint of concern (ankle, knee, and hip). Bold and italic terms stand for matrix and scalars, respectively. In Eq. (1), $M_K^{nf}(t)$ corresponds to the knee net joint moment computed through inverse dynamics while $\hat{M}_K^{nf}(t)$ stands for the net moment estimated using the EMG data. In Eq. (2), α_i^{nf} represents the isometric EMG-moment coefficient in the nonfatigued condition and $w_i^{nf}(t)$ stands for the individual muscle gains at each time t. $S_i^{nf}(t)$ contains the rectified and filtered (low-pass, fourth-order, 2.5 Hz net cutoff frequency) EMG data of the four selected muscles. $\hat{M}_K^{nf}(t)$ also comprises an identity matrix (1) of size 4, biarticularity matrix (**E**), and β_j^{nf} and δ_j^{nf} terms to take into account that EMG amplitudes may change depending on the origins and insertions of the muscles, respectively, as well as the length and the shortening velocity of the muscle fibers. Additional constraints (Eq. (3)) were added to the procedure to ensure that the sign convention of the outputs (i.e., the contribution of the flexor and extensor muscle groups to the net joint moment) is fulfilled at each time t [8].

2.5.3　Dynamic Trials—Fatigued Case. A schematic representation of the methodology used in the present study to estimate the contributions of the knee flexor and extensor muscle groups to the net joint moment under fatigue condition is presented in Fig. 2.

In the fatigued condition, the formulation of the optimization problem included a supplementary equality constraint that took into account the loss of moment production capacity of the extensor muscle group. The loss of moment production capacity was estimated using the previously described linear relationship (see the *isometric fatigue session* section) with the normalized decrease in the EMG mean frequency between the dynamic nonfatigued and fatigued sessions as input.

The time-frequency spectrums of the EMG signals were obtained from wavelet transforms of the EMG bursts within fixed-length windows for each squat cycle. These windows of 512 samples were centered at the time instants, where the knee joint angle trajectory was the most repeatable, that is the time instants corresponding to the minimum of the knee angle standard deviation (quasi-cyclostationarity hypothesis [5]). The time-frequency spectrum estimates were then averaged over all the cycles to obtain a single estimate of the mean frequency for the selected muscle in either the nonfatigued or the fatigued condition (Fig. 3). The normalized mean frequency decrease was assessed as the dif-
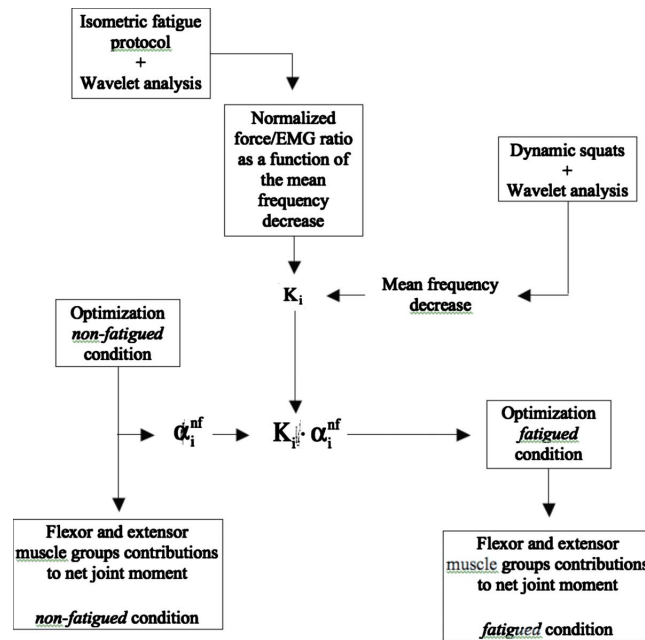
56

Fig. 2 Schematic representation of the methodology used in the study to assess the contributions of the flexor and extensor muscle groups to the net joint moment under fatigue condition

ference between the mean frequency estimates obtained from the nonfatigued and the fatigued conditions normalized by the value in the nonfatigued case. Using the linear regression previously created (see the isometric fatigue session section), an estimate of the moment production capacity of the fatigued muscle (the K coefficient) was obtained for the dynamic squat in the fatigued condition.

In the fatigued condition, the nonlinear constrained optimization problem was formulated as for the nonfatigued case (see Eqs. (1)–(3)) with a supplementary set of equality constraints (Eq. (4)). Hence, the methodology developed in this study to account for the presence of fatigue in the EMG signals was used to constrain the moment production capacity of the extensor muscle group during the resolution of the optimization problem in the fatigued case.

$$\alpha_{ga}^f = \alpha_{ga}^{nf}, \quad \alpha_{bf}^f = \alpha_{bf}^{nf}$$
$$\alpha_{rf}^f = K_{rf} \cdot \alpha_{rf}^{nf}, \quad \alpha_{vm}^f = K_{vm} \cdot \alpha_{vm}^{nf} \tag{4}$$

where the α_i^f coefficient represents the isometric EMG-moment relationship in the fatigued condition and the K coefficients are computed from the mean frequency decrease in the EMG signals (see the *dynamic trials* section).

The optimization problems under the nonfatigued and fatigued conditions were solved using a sequential quadratic programming (SQP) approach [19]. All computations were done using MATLAB software (version 7; Optimization Toolbox, version 3.0.3; Spline Toolbox, version 3.2.2; Time-Frequency Toolbox).

2.6 Statistics. One-way ANOVAs (fatigue effect) were conducted on the minimum, maximum, and mean values of the ankle, knee and hip angular displacements and velocities, as well as on the model parameters. One-way ANOVAs (fatigue effect) were also carried out on the minimal, maximal, and mean values of the knee net joint moment and the contributions of the flexor and

extensor muscle groups to the net joint moment. A significance level of 0.05 was used for all comparisons. Tukey post-hoc tests were used whenever necessary.

3 Results

3.1 Isometric Fatigue Session. The presence of muscle fatigue during the isometric session was revealed by an increase in the EMG amplitudes and a decrease in the EMG mean frequencies. Indeed, mean RMS EMG increased by $4.6 \pm 27.2\%$ and $16.4 \pm 23.7\%$, respectively, for the rectus femoris and the vastus medialis muscles. As mentioned in the Sec. 2, no estimate of the gastrocnemius medialis and biceps femoris mean frequencies was performed due to the low activation level of these muscles and the high variability of this variable under such conditions. Oppositely, decreases in mean frequencies of $36.0 \pm 5.9\%$ and $23.4 \pm 12.5\%$ for the rectus femoris and the vastus medialis muscles, respectively, were observed. These changes corresponded to decreases of $31.8 \pm 19.2\%$ and $40.1 \pm 14.8\%$ of the normalized force/EMG ratio for the rectus femoris and the vastus medialis muscles. During this isometric fatigue session, the knee joint angles showed little variations with maximal discrepancies below 5 deg.

An example of the original methodology developed in this study and consisting of a linear regression between the force production capacity (i.e., the normalized force/EMG ratio) and the normalized mean frequency decrease is illustrated in Fig. 4. All the slopes of the linear regressions were positive with mean values of 0.91 ± 0.69 and 1.28 ± 0.52, respectively, for the rectus femoris and the vastus medialis muscles with corresponding mean coefficients of determination (r^2) of 0.70 ± 0.40 and 0.63 ± 0.38.

3.2 Dynamic Trials. A significant augmentation in the EMG amplitudes was seen between the nonfatigued and the fatigued dynamic conditions with an averaged increase of $29.74 \pm 15.39\%$,
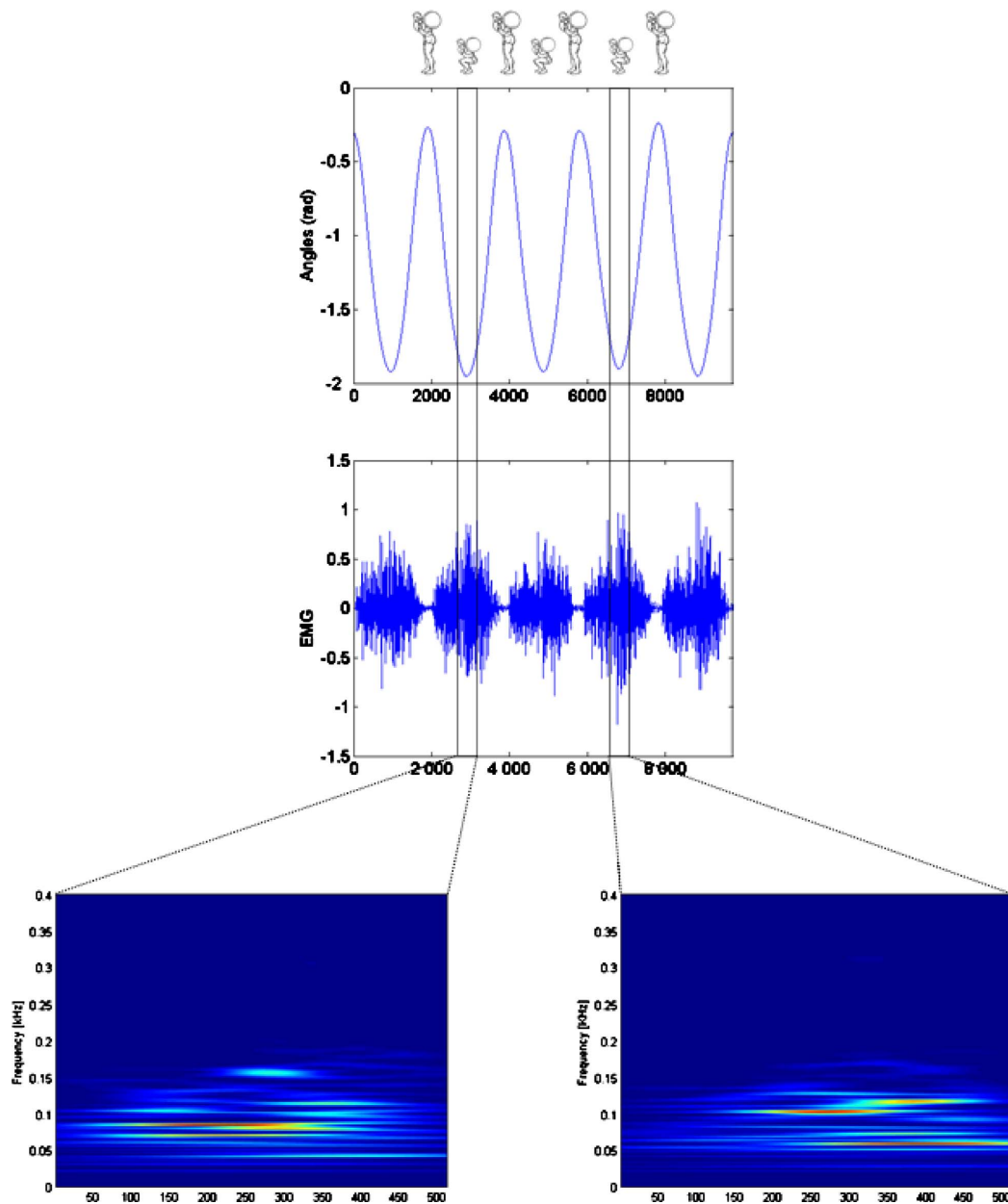
57

Fig. 3 Schematic representation of the methodology used to estimate the frequency content of the EMG signal. Upper graph shows the evolution through time of the knee angle. Middle graph represents the EMG signal of the rectus femoris muscle. Bottom graphs show the outputs of the wavelet analysis. The 512 points analysis windows were centered at the time instants were the knee joint angle trajectory was the most repeatable. For the bottom graphs, the time is along the horizontal axis and the frequency along the vertical one. The amplitude of the signal at any given time and frequency is represented using color scale. Brighter colors inform that the corresponding frequency bandwidth is often found in the signal frequency content.

$18.02 \pm 12.50\%$, $23.63 \pm 25.17\%$, and $21.70 \pm 15.12\%$ for the gastrocnemius medialis, biceps femoris, rectus femoris, and vastus medialis muscles, respectively, $(F_{1,34} > 33.02$ and $p < 0.05$ for all muscles). Despite these modifications, kinematic data of the squat cycles were very similar between the nonfatigued and the fatigued dynamic conditions. Indeed, no statistical influence of the fatigue factor was found on the minimum, mean, and maximum values of the ankle, knee, and hip joint angles and angular velocities. More-

58
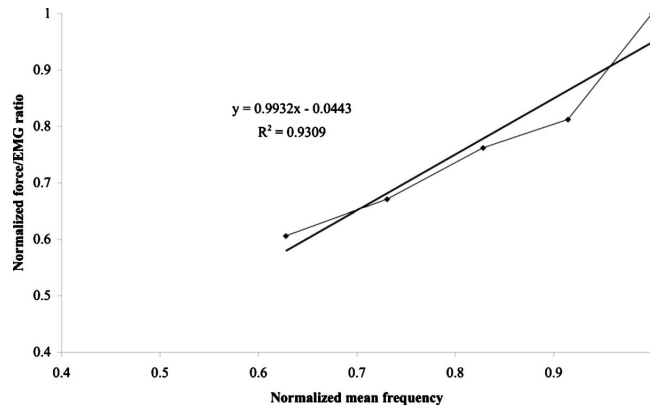
Fig. 4 Representative example for one subject of the isometric linear relationship that links the force production capacity of the rectus femoris muscle (normalized force/EMG ratio) to the normalized mean frequency decrease. Raw data as well as the corresponding linear regression are shown.

over due to the position of the bar, no motion of the upper body was allowed during the squat movement, strengthening the results that the squats were very similar in nonfatigue and fatigue conditions.

The EMG mean frequencies estimated through wavelet transforms during the dynamic squats revealed a significant decrease between the nonfatigued and the fatigued conditions with relative diminutions of $18.28 \pm 7.45\%$ and $7.72 \pm 3.14\%$ for the rectus femoris and the vastus medialis muscles, respectively. Once the normalized mean frequency decreases were input to the linear

regressions, the moment production capacities (K coefficient in Eq. (4)) were estimated to be $82.99 \pm 10.79\%$ and $87.15 \pm 9.81\%$ of the nonfatigued condition for the rectus femoris and vastus medialis muscles, respectively. The moment production capacity of these muscles was significantly affected by the presence of fatigue ($F_{1,34} = 33.44$ and $p < 0.05$).

Despite the presence of fatigue, the EMG-driven optimization model revealed little difference in muscle group contributions to joint moments between the nonfatigued and the fatigued dynamic
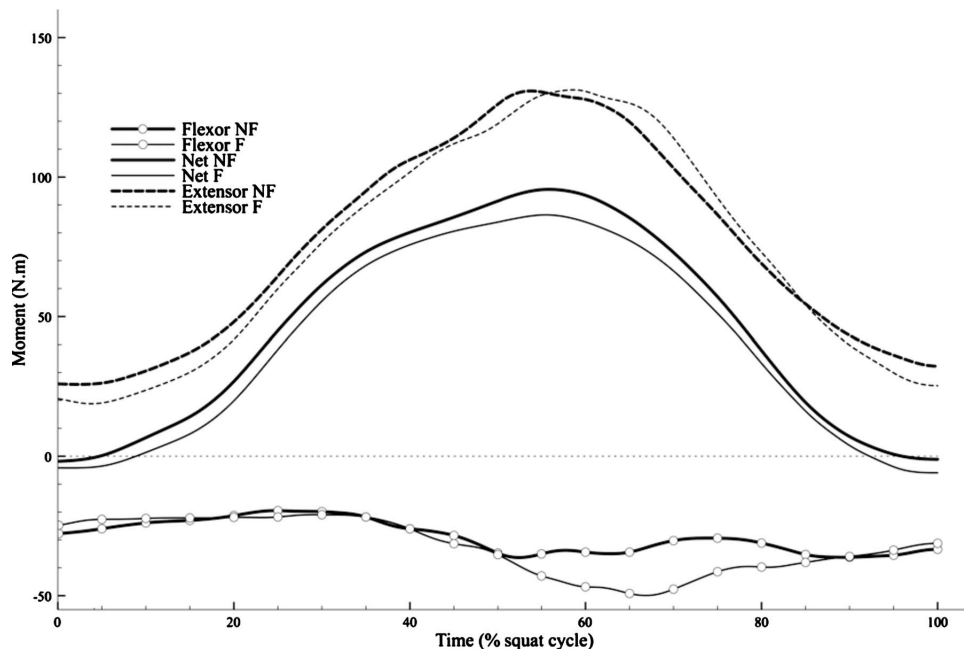
Fig. 5 Evolution through time of the mean values (n=9) of the moments developed by the extensor muscle group (upper curves), the net joint moments (middle curves) and the flexor muscle group moments (lower curves). For each variable, thick lines correspond to the nonfatigued condition and thin lines to the fatigued situation.

59

Table 1 Mean values (±s.d.) of the optimized parameters. α_i, β_i, and δ_i represent, respectively, the isometric EMG-moment coefficient and the terms accounting for the force-length and force-velocity relationships. * indicates a significant influence of the *fatigue* factor (p < 0.05).

	NF	F	
α_{ga}	-80.67 ± 50.51	-80.67 ± 50.51	
α_{bf}	-54.81 ± 25.89	-54.81 ± 25.89	
α_{rf}	154.29 ± 55.15	123.28 ± 45.94	*
α_{vm}	150.76 ± 54.32	130.95 ± 51.08	*
β_A	0.80 ± 0.35	0.95 ± 0.51	
β_K	0.19 ± 0.09	0.09 ± 0.07	*
β_H	0.35 ± 0.13	0.38 ± 0.12	
δ_A	0.14 ± 0.06	0.16 ± 0.09	
δ_K	0.04 ± 0.01	0.03 ± 0.02	
δ_H	0.06 ± 0.03	0.07 ± 0.05	

conditions (Fig. 5). Indeed, the minimum, maximum, and mean values of the knee net joint moments showed no difference due to the fatigue factor. No statistical influence of the fatigue factor was seen on the contributions of the flexor and extensor muscle groups to the net joint moment estimated with either the original version of the model (nonfatigued condition) or the version that included the equality constraint (K coefficient) on the moment production capacity (fatigued condition).

The comparison of the parameters issued from the optimization processes (Eq. (1)–(4)) revealed no influence of the fatigue factor (Table 1), except on the β_K term (i.e., the one that accounts for the changes in the EMG amplitudes due to the force-length relationship at the knee joint). The influence of the fatigue factor was also nonsignificant for the $w_i(t)$ terms. Indeed, the evolutions through time of the $w_i(t)$ coefficients were similar between the nonfatigued and the fatigued dynamic conditions (Fig. 6).

4 Discussion

The aim of the present study was to develop an EMG-driven biomechanical model to obtain the contributions of flexor and extensor muscle groups to the net joint moment during a nonisokinetic functional movement (squat exercise) performed in nonfatigued and in fatigued conditions. An EMG-based methodology that aims at balancing the decreased muscle moment production capacity following fatigue was developed. The outputs of the new
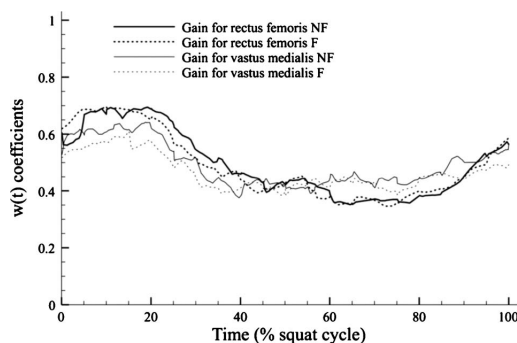
Fig. 6 Evolution through time of the individual muscle gains of the rectus femoris (thick lines) and vastus medialis (thin lines) muscles in the nonfatigued (continuous lines) and fatigued (dashed lines) situations. Note the similar patterns of the $w_i(t)$ coefficients, which imply that the optimization procedure did not take advantage of this variable to compensate for the additional equality constraint.

methodology indicated that the decreases in mean frequency during the fatigued dynamic squats corresponded to moment production capacities of 83% and 87% of the nonfatigued values for the rectus femoris and the vastus medialis muscles, respectively. These values are consistent with the fact that the maximal force depletion was 33% at the end of the isometric fatigue session. It was demonstrated that the model was able to characterize fatigue with a single coefficient for each muscle K_i, which accounted for fatigue-induced frequency shifts obtained using wavelet analysis.

Our working hypothesis stated that with identical kinematics and dynamics data and different EMG inputs, the proposed methodology could estimate the decreased muscle moment production capacity due to fatigue and take this decrease into account in the EMG-to-moment procedure. While the outputs of the optimization procedure were similar, the optimization parameters (Eqs. (2)–(4)) could have been modified during the resolution by the SQP algorithm. The consistency of the present methodology was reinforced by the lack of significant differences between the optimized parameters of the model (compare Table 1), except for the term accounting for the force-length relationship at the knee joint (i.e., β_K). However, the difference on the β_K coefficient is not surprising since a dependence of the force-length relationship to muscle fatigue as been reported by [20]. The stability of the optimized parameters revealed that the optimization procedure did not take advantage of the other variables to compensate for the additional equality constraint. This point is supported by the similar patterns of the $w_i(t)$ coefficients (compare Fig. 6).

Our results showed no influence of the fatigue factor on the flexor and extensor contributions to the net joint moment, though a general increase in the EMG activities was seen between the nonfatigued and the fatigued dynamic conditions. The procedure developed in this study and included in an EMG-driven model aimed at taking into account the changes in the EMG amplitudes due to muscle fatigue (i.e., the changes in the activation level) to estimate the contributions of the knee flexor and extensor muscle group to the net joint moment. Expectedly with no influence of the fatigue factor on the kinematic data, the net knee joint moments were very similar between the nonfatigued and the fatigued sessions. As the net joint torques required to produce the task in both conditions were similar, the central nervous system increased the activation of the fatigued muscle group to reach the necessary extension moment. An increased activation of the agonist group could lead to increased antagonist activation because of a common drive to the agonist-antagonist pairs [21]. In the present study, higher EMG amplitudes were also seen for the antagonist muscle group reinforcing the "common drive" hypothesis. However, as previously stated in Ref. [22] during squats with low loads, the activation levels of antagonist muscles were low (mean values below 10% MVF) and a relative 25% increase in the EMG amplitudes would have little effects on the muscle group moment. The outputs of the EMG-to-moment optimization process showed no difference in the antagonist contribution to the net joint moment between the nonfatigued and the fatigued conditions. Hence, while the EMG of the extensor muscle group is logically increased, the contribution of the extensor muscle group is kept constant through the different conditions. These results satisfied our hypothesis in that the developed procedure was able to take into account the changes in the activation level of the fatigued muscles for their use in an EMG-driven model in the fatigued condition.

The procedure described in this study mainly relied on the estimation of the EMG mean frequencies both during isometric and dynamic contractions. Several factors may influence the estimation of the frequency content of the EMG signals (i.e., nonstationary feature of the EMG signal, muscle activation levels, muscle fiber length, muscle fiber velocity). Although the use of short time fast fourier transform (FFT) may have provided the same results [23], it is likely that the use of wavelet transforms to estimate the EMG frequency content in fatigued isometric and dynamic condi-

60

tions will enhance the accuracy of the spectral estimates [5,6]. The other possible artifacts were also carefully taken into account throughout this study. First, the isometric session was performed at 60% MVC and the EMG analysis windows during the dynamic sessions were located at time instants of high activation (compare Fig. 3), thus removing the activation level as a possible artifact in the estimation of the mean frequencies [24]. Second, the frequency estimates had also shown a strong dependence on muscle fiber length [25]. In our experiment, the variations in knee joint angle (and consequently in muscle length) during the isometric fatigue session were less than 5 deg for all the subjects. During the dynamic sessions, the spectral estimates were carried out within analysis windows located at time instants, where the knee joint angle trajectories were the most repeatable. No influence of the fatigue factor was seen on the kinematics data and the knee angles within the analysis windows were similar between the non-fatigued and the fatigued sessions. Thus, EMG frequency content was estimated at the same muscle length for the nonfatigued and the fatigued dynamic conditions. Third, the time instants, where the knee joint angles were the most repeatable also corresponded to a knee joint velocity close to zero. The EMG mean frequencies in dynamic conditions were thus estimated during a "quasi-isometric" contraction, avoiding the artifacts due to differences in the muscle fiber shortening velocity.

The isometric fatigue session was used to create a linear regression between the moment production capacity of the muscles (i.e., the normalized force/EMG ratio) and the decrease in mean frequency. Indeed, the force production capacity has been shown to decrease linearly with fatigue during submaximal exercises [26] and previous work had represented the mean frequency decrease through time using a linear model and reported a good fit with the experimental data [27]. However, some subjects showed low co-efficients of determination for the linear regression (with a r^2 value of 0.12 for the worst case). In future studies several possibilities are offered to improve these values. First, using different regressions than the linear one (i.e., polynomial, exponential, and logarithmic) may improve the values of the coefficient of determination. Indeed under fatigue condition, previous studies reported that some of physiologic parameters evolved with a nonlinear trend [28]. Second, as the regression was created from raw force/EMG ratios and mean frequency data, this issue may be resolved by modeling previously, and separately, the evolutions through time of the normalized force/EMG ratio and of the mean frequency decrease. Afterward, the previous modeled data could be put all together to create the final regression between the moment production capacity and the decrease in mean frequency. While the present experiment was conducted using an isometric fatigue session, the linear regression between the muscular force production capacity and the mean frequency could be obtained from dynamic fatiguing exercises. Indeed, during a long lasting dynamic exercise, consistent and quasi-linear mean frequency decreases were reported when studying the same joint angle range over the entire range of motion during the fatiguing exercise [25]. This point enhances the applicability of the methodology to different types of muscle fatigue as isometric exercises or repetitive exertion bouts both lead to a decrease in EMG mean frequency and an increase in EMG amplitude for a constant force output.

While some limitations may appear as the choice of the representative muscles or the fact that the level of fatigue of the knee flexors could not be tested, we believe that the methodology developed in this study has several advantages. First, to our knowledge, this work is among the first in attempting to estimate the force production capacity of fatigued muscles during functional dynamic nonisokinetic movements. This feature extends the use of the EMG-driven models to functional activities performed under muscle fatigue. As previous work reported changes in muscle activation patterns during cutting movements following muscle fatigue [29], such a procedure can help in studying the stress experienced by the ligaments in situations usually encountered during

sport exercises. Second, while the described procedure can be applied generally to a wide range of activities and EMG-driven models, the subject-specific trend of the development of muscle fatigue is fully taken into account. Indeed, the linear regression built during an isometric or dynamic fatigue session is tuned specifically to the properties of each muscle.

In conclusion, this study presented an original procedure based on the decrease in the frequency content of the EMG data to assess the force production capacity of a muscle group following a fatiguing exercise. Based on this procedure, an equality constraint was added to an EMG-driven biomechanical model to estimate the contributions of the flexor and extensor muscle group to the net joint moment during dynamic exercise under fatigue condition. The results presented here are promising, as they constitute the first attempt to estimate the force production capacity of a fatigued muscle group during a dynamic, nonisokinetic exercise. The procedure previously described may find applications for the study of several functional activities performed under muscle fatigue such as rehabilitation exercises, walking, jogging, etc. Further studies are necessary to extend the use of the proposed method to other biomechanical models. In particular, more detailed models that aimed at estimating muscle forces [9] could benefit in the use of the procedure described in this study.

References

[1] Basmajian, J. V., and De Luca, C. J., 1985, *Muscle Alive*, 5th ed., Williams and Wilkins, Baltimore.

[2] Gandevia, S. C., 2001, "Spinal and Supraspinal Factors in Human Muscle Fatigue," Physiol. Rev., **81**, pp. 1725–1789.

[3] Cheng, A. J., and Rice, C. L., 2005, "Fatigue and Recovery of Power and Isometric Torque Following Isotonic Knee Extensions," J. Appl. Physiol., **99**, pp. 1446–1452.

[4] Westerblad, H., and Allen, D. G., 2002, "Recent Advances in the Understanding of Skeletal Muscle Fatigue," Curr. Opin. Rheumatol., **14**, pp. 648–652.

[5] Bonato, P., Roy, S. H., Knaflitz, M., and De Luca, C. J., 2001, "Time-Frequency Parameters of the Surface Myoelectric Signal for Assessing Muscle Fatigue During Cyclic Dynamic Contractions," IEEE Trans. Biomed. Eng., **48**, pp. 745–753.

[6] Karlsson, J. S., Ostlund, N., Larsson, B., and Gerdle, B., 2003, "An Estimation of the Influence of Force Decrease on the Mean Power Spectral Frequency Shift of the EMG During Repetitive Maximum Dynamic Knee Extensions," J. Electromyogr. Kinesiol., **13**, pp. 461–468.

[7] Buchanan, T. S., Almdale, D. P., Lewis, J. L., and Rymer, W. Z., 1986, "Characteristics of Synergic Relations During Isometric Contractions of Human Elbow Muscles," J. Neurophysiol., **56**, pp. 1225–1241.

[8] Amarantini, D., and Martin, L., 2004, "A Method to Combine Numerical Optimization and EMG Data for the Estimation of Joint Moments Under Dynamic Conditions," J. Biomech., **37**, pp. 1393–1404.

[9] Buchanan, T. S., Lloyd, D. G., Manal, K., and Besier, T. F., 2005, "Estimation of Muscle Forces and Joint Moments Using a Forward-Inverse Dynamics Model," Med. Sci. Sports Exercise, **37**, pp. 1911–1916.

[10] Cholewicki, J., McGill, S. M., and Norman, R. W., 1995, "Comparison of Muscle Forces and Joint Load From an Optimization and EMG Assisted Lumbar Spine Model: Towards Development of a Hybrid Approach," J. Biomech., **28**, pp. 321–331.

[11] Sparto, P. J., and Parnianpour, M., 1998, "Estimation of Trunk Muscle Forces and Spinal Loads During Fatiguing Repetitive Trunk Exertions," Spine, **23**, pp. 2563–2573.

[12] Olney, S. J., and Winter, D. A., 1985, "Predictions of Knee and Ankle Moments of Force in Walking From EMG and Kinematic Data," J. Biomech., **18**, pp. 9–20.

[13] Hermens, H. J., Freriks, B., Disselhorst-Klug, C., and Rau, G., 2000, "Development of Recommendations for SEMG Sensors and Sensor Placement Procedures," J. Electromyogr. Kinesiol., **10**, pp. 361–374.

[14] Winter, D. A., 1990, *Biomechanics and Motor Control of Human Movements*, Wiley-Interscience, Toronto, Ontario.

[15] Zatsiorsky, V., and Seluyanov, V., 1983, "The Mass and Inertial Characteristics of Main Segments of the Human Body," *Biomechanics VIII-B*, Human Kinetics, Champaign, pp 1152–1159.

[16] Karlsson, J. S., and Gerdle, B., 2001, "Mean Frequency and Signal Amplitude of the Surface EMG of the Quadriceps Muscles Increase With Increasing Torque—A Study Using the Continuous Wavelet Transform," J. Electromyogr. Kinesiol., **11**, pp. 131–140.

[17] Auger, F., Flandrin, P., Goncalves, P., and Lemoine, O., 1996, "Time-Frequency Toolbox-for Use With Matlab," *Reference Guide*, Centre National de la Recherche Scientifique, France.

[18] Centomo, H., Amarantini, D., Martin, L., and Prince, F., 2007, "Differences in the Coordination of Agonist and Antagonist Muscle Groups in Below-Knee Amputee and Able-Bodied Children During Dynamic Exercise," J. Electromyogr. Kinesiol., **18**, pp. 487–494.

[19] Boggs, P. T., and Tolle, J. W., 1995, "Sequential Quadratic Programming," Acta Numerica, **4**, pp. 1–52.

[20] Butterfield, T. A., and Herzog, W., 2005, "Is the Force-Length Relationship a Useful Indicator of Contractile Element Damage Following Eccentric Exercise?," J. Biomech., **38**, pp. 1932–1937.

[21] De Luca, C. J., and Mambrito, B., 1987, "Voluntary Control of Motor Units in Human Antagonist Muscles: Coactivation and Reciprocal Activation," J. Neurophysiol., **58**, pp. 525–542.

[22] Isear, J. A., Erickson, J. C., and Worrell, T. W., 1997, "EMG Analysis of Lower Extremity Muscle Recruitment Patterns During an Unloaded Squat," Med. Sci. Sports Exercise, **29**, pp. 532–539.

[23] Maclsaac, D. T., Parker, P. A., Scott, R. N., Englehart, K. B., and Duffley, C., 2001, "Influence of Dynamic Factors on Myoelectric Parameters," IEEE Eng. Med. Biol. Mag., **20**, pp. 82–89.

[24] Linnamo, V., Strojnik, V., and Komi, P. V., 2002, "EMG Power Spectrum and Features of the Superimposed M-Wave During Voluntary Eccentric and Concentric Actions at Different Activation Levels," Eur. J. Appl. Physiol., **86**, pp. 534–540.

[25] Potvin, J. R., 1997, "Effects of Muscle Kinematics on Surface EMG Amplitude and Frequency During Fatiguing Dynamic Contractions," J. Appl. Physiol., **82**, pp. 144–151.

[26] Stephens, J. A., and Taylor, A., 1972, "Fatigue of Maintained Voluntary Muscle Contraction in Man," J. Physiol. (London), **220**, pp. 1–18.

[27] Coorevits, P. L. M., Danneels, L. A., Ramon, H., Van Audekercke, R., Cambier, D. C., and Vanderstraeten, G. G., 2005, "Statistical Modeling of Fatigue-Related Electromyographic Median Frequency Characteristics of Back and Hip Muscles During a Standardized Isometric Back Extension Test," J. Electromyogr. Kinesiol., **15**, pp. 444–451.

[28] Binder-Macleod, S. A., Lee, S. C. K., Fritz, A. D., and Kucharski, L. J., 1998, "New Look at Force-Frequency Relationship of Human Skeletal Muscle: Effects of Fatigue," J. Neurophysiol., **79**, pp. 1858–1868.

[29] Nyland, J. A., Caborn, D. N., Shapiro, R., and Johnson, D. L., 1997, "Fatigue After Eccentric Quadriceps Femoris Work Produces Earlier Gastrocnemius and Delayed Quadriceps Femoris Activation During Crossover Cutting Among Normal Athletic Women," Knee Surg. Sports Traumatol. Arthrosc, **5**, pp. 162–167.

62

Muscle adaptation patterns of children with a trans-tibial amputation during walking

H. Centomo [a,b], D. Amarantini [d], L. Martin [e], F. Prince [a,b,c,*]

[a] *Department of Kinesiology, Université de Montréal, Montreal, Que., Canada*
[b] *Gait and Posture Laboratory, Centre de réadaptation Marie Enfant, Montreal, Que., Canada*
[c] *Department of Surgery, Faculty of Medicine, Université de Montréal, Montreal, Que., Canada*
[d] *Laboratoire Adaptation Perceptivo-Motrice et Apprentissage, Université Paul Sabatier, Toulouse, France*
[e] *Laboratoire Sport et Performance Motrice, Université Joseph Fourier, Grenoble, France*

Abstract

Background. Many studies have shown that trans-tibial amputation involves modifications of resultant muscle patterns during gait. However, these experiments did not estimate the contribution of simultaneous agonist and antagonist muscle action (co-contraction) during gait tasks. Diminution of co-contraction could create joint instability and, thus, change joint integrity, which is particularly important in the etiology of degenerative diseases, such as osteoarthritis, present at the knees of amputated limbs, and particularly in non-amputated limbs. The purpose of this study was to determine if there is any difference in the production of co-contraction about the knee between able-bodied children and children with a trans-tibial amputation during gait.

Methods. Six children with a trans-tibial amputation vs. six able-bodied children paired for gender, age, weight and height participated in this study. Four one-way ANOVAs ($P < 0.05$) were used to observe differences in resultant, agonist and antagonist moments, power, and co-contraction index during different phases of gait between able-bodied children limbs, the amputated and the non-amputated limbs of children with trans-tibial amputation.

Findings. Children with a trans-tibial amputation modified muscle patterns at their amputated limb and produced smaller co-contraction ($P < 0.05$) during single limb support, for both the non-amputated and amputated limbs when compared to able-bodied children.

Interpretation. These results suggest that children with a trans-tibial amputation altered their muscle patterns to perform locomotion. These changes produced a diminution of co-contraction during single limb support for both the amputated and non-amputated limbs and, thus, could create joint instability.

Crown Copyright © 2006 Published by Elsevier Ltd. All rights reserved.

Keywords: Trans-tibial amputation; Children; Agonist muscles; Antagonist muscles; Co-contraction; Gait; Muscle patterns

1. Introduction

Human locomotion involves complex multi-joint and multi-muscle coordination arising because of the redundancy inherent in the musculoskeletal system. Especially during walking, able-bodied (AB) subjects coordinate motion in the lower limbs at the hip, knee and ankle joints for safer ambulation in their environment (Winter, 1991).

For subjects with a trans-tibial amputation (TTA), loss of the ankle and foot, which is responsible for 80% of the propulsion in normal gait (Winter, 1991), requires changes in hip and knee joint coordination to perform efficient gait (Winter and Sienko, 1988; Sanderson and Martin, 1997; Powers et al., 1998; Sadeghi et al., 2001). Particularly during weight-bearing, Sanderson and Martin (1997) observed significant changes in the resultant knee joint moment between able-bodied adults and six adults with a TTA

(32.8 (SD 6.7) years). The moment pattern showed a transition from extensor to flexor in the control limb (CL) of AB adults and in the non-amputated limb (NAL) of adults with a TTA whereas it remained flexor in the amputated limb (AL) of adults with a TTA. Furthermore, Winter and Sienko (1988) noted a very low or near zero resultant moment in elderly subjects with a TTA for the first half of stance and a normal knee flexor moment for the rest of the stance phase. In contrast, Powers et al. (1998) recorded a knee extensor moment throughout the stance phase in 10 males with a TTA (62.3 (SD 6.9) years). In summary, the findings of the previously mentioned authors were not consistent with one another regarding knee joint kinetics.

On the other hand, it has been demonstrated that the knee joint is commonly affected in joint pathologies associated with TTA (Burke et al., 1978; Melzer et al., 2001). Joint instability (or joint laxity) is a major factor in the etiology of degenerative diseases (Felson et al., 2000; Issa and Sharma, 2006) such as osteoarthritis seen at the knee of the NAL and AL of subjects with a TTA (Burke et al., 1978; Melzer et al., 2001). Articular instability could be attributed to changes in co-contraction (i.e., co-activation of the agonist and antagonist muscles), creating additional stresses on the internal structures of the joints (Arms et al., 1984; Solomonow et al., 1989; Miller et al., 2000). More precisely for AB adults during walking, Falconer and Winter (1985) found a higher percentage of co-contraction during weight acceptance compared to the other phases of the gait cycle. The higher production of co-contraction during weight acceptance is not surprising, given that this phase requires augmented knee joint stability. Hence, the development of premature osteoarthritis at the knees of subjects with a TTA could result from modifications in the activity of the agonist and antagonist muscle groups associated with changes observed in net joint kinetics. Indeed, the human system has more muscles acting around each joint than theoretically needed for coordinated motion, and there are multiple possibilities of muscle coordination to perform a given movement (Prilutsky and Zatsiorsky, 2002). The premature development of osteoarthritis observed in both AL and NAL of subjects with a TTA could be associated with long-term effects of changes induced in muscle patterns following amputation. Hence it could be of special clinical interest to study the modifications in muscle patterns during locomotion as early as childhood in subjects with a TTA.

The purpose of the present study was to investigate differences in the production of co-contraction about the knee between AB children and children with a TTA. To gain insight into how children with a TTA adapted the production of co-contraction during gait, we quantified the resultant, flexor and extensor moments developed at the knee joint in AB children and in the NAL and the AL of children with a TTA. Based on kinematic, kinetic and EMG data, co-contraction was estimated with an updated version of the EMG-assisted optimization model proposed by Amarantini and Martin (2004). The present experiment

tested the hypothesis that children with a TTA have lower production of co-contraction at the knee than AB children because of changes in both agonist and antagonist muscle group moments. For subjects with a TTA, such changes could affect joint stability and, thus, might predispose subjects with an amputation to the development of osteoarthritis in both their AL and NAL.

2. Methods

2.1. Subjects

Six children with a TTA (4 males, 2 females) with age 11 (SD 5) years, height 153.5 (SD 16.1) cm and body mass 53.4 (SD 21.3) kg were selected from the Musculoskeletal Clinic of the Centre de Réadaptation Marie Enfant of Hôpital Sainte-Justine. Four children had congenital limb deficiencies while the other two underwent amputations as a result of meningococcemia disease. A certified prosthetist of the Centre de Réadaptation Marie Enfant conducted individual evaluations to ensure that the lower limb prosthesis performed normally, that each subject was comfortable using it and performed normally with his or her prosthesis. To provide some control over the effect of prosthetic design on gait, children with a TTA using Seattle-Light foot prostheses were recruited. Additionally, amputee recruitment focused on children who were fully ambulatory.

Six age-, height-, mass- and sex-matched AB children (4 males, 2 females; age 12 (SD 4) years; height 1.56 (SD 0.17) m; body mass 55.5 (SD 13.9) kg) with no known musculoskeletal problems that could affect their ability to perform gait participated in this study.

All the children were physically active and in good health. The procedures for this study were approved by the Research Ethics Committee of Hôpital Sainte-Justine, and all parents gave informed, written consent.

2.2. Experimental design

Each subject was instructed to walk along a 10-m walkway at a self-selected speed. Shoes were worn during testing. Three to five practice trials were allowed to familiarize the subjects with the testing environment. Three acceptable trials were recorded for each limb where the subjects were instructed to put each foot on a force platform while walking with fluidity. The equipment employed in this study comprised eight 3D digital cameras (Vicon Peak, CA, USA), two AMTI force platforms (Advance Mechanical Technology Inc., MA, USA) and eight double-differential pre-amplifier EMG electrodes from a multi-channel EMG system (Model MA-300-16, Motion Lab Systems, Inc., LA, USA).

The 2D kinematic data were acquired at 60 Hz. Twenty-four passive, reflective markers were placed bilaterally on anatomical landmarks (front and back of head, acromion, elbow, wrist, anterior superior iliac spines, thigh, knee,

shank, ankle, heel and toe) and one on the sacrum. Raw coordinates were filtered with a zero-lag, low-pass Butterworth filter (4th order, 6 Hz cut-off frequency) before computing joint angular and linear displacements. At each joint, angular velocity and acceleration were calculated by differentiating cubic smoothing splines (De Boor, 2004). Ground reaction forces and moments were recorded at 900 Hz and were filtered with a zero-lag 4th order Butterworth filter with a 9 Hz low-pass cut-off frequency. To collect muscle activity for AB children, EMG electrodes were fixed bilaterally on the rectus femoris, vastus medialis, medial hamstring (MH) and gastrocnemius (GA). For children with a TTA, the EMG electrodes were applied on the same muscles, without the GA electrode for the AL. Thus, only the MH was taken as the representative knee flexor muscle for the AL. The skin was cleaned with alcohol and, when necessary, body hair was shaved. The electrodes were oriented parallel to muscle fibre direction and were positioned on muscle belly. The EMG signals were sampled at 900 Hz, bandpass-filtered (zero-lag, 4th order, 30–300 Hz cut-off frequencies), and then full wave-rectified.

2.3. Gait variables

The vector of resultant moments was calculated at the knee with inverse dynamics, according to Lagrangian formalism (Zajac and Gordon, 1989; Amarantini and Martin, 2004). For sign convention, the moment was positive for knee extension. Net joint power was computed at each joint as the scalar product of angular velocity and net joint moment. Concentric contraction (energy generation) was represented by positive power, while eccentric contraction (energy absorption) was represented by negative power.

Agonist and antagonist moments were estimated with an updated version of the EMG-assisted optimization model proposed by Amarantini and Martin (2004). For the present study, the estimation of the coefficients α establishing the isometric moment-EMG relationships was directly incorporated into the routine used for dynamic conditions. Thus, the *isometric calibration* step was appropriately removed from the experimental design without affecting the results. This improvement is an obvious advantage for clinical application since it reduces the complexity of the experimental setup. The low-pass cut-off frequency and the exponent applied to the EMG signals were respectively set to 2.5 Hz and 1 for all muscles according to the recommendations of Amarantini and Martin (2004). Consequently, the optimization problem was rewritten as:

$$\text{find}: \alpha = \{\alpha_{RF}, \alpha_{VM}, \alpha_{MH}, \alpha_{GA}\}, \quad \beta = \{\beta_h, \beta_k, \beta_a\},$$
$$\delta = \{\delta_h, \delta_k, \delta_a\} \text{ and } w = \{w_{RF}, w_{VM}, w_{MH}, w_{GA}\}$$

$$\text{that minimize:} \quad C = \frac{1}{2} \cdot \sum_t (M_K(t) - \widehat{M}_K(t))^2 \quad (1)$$

α, β, δ and w

with

$$\widehat{M}_k(t) = w_{\text{ext}}(t) \cdot \widehat{M}_{\text{ext}}(t) + w_{\text{flex}}(t) \cdot \widehat{M}_{\text{flex}}(t) \quad (2)$$

$$\widehat{M}_{K_i}(t) = [\alpha_i \cdot r\text{EMG}_i(t)] \cdot [1 \pm E \cdot (\beta \cdot \Delta\theta) \pm E \cdot (\delta \cdot \dot\theta)],$$
$$i = \{RF, VM, MH, GA\} \quad (3)$$

$$\text{subject to:} \begin{cases} \alpha_{MH} \text{ and } \alpha_{GA} < 0, \quad \alpha_{RF} \text{ and } \alpha_{VM} > 0 \\ \beta > 0 \text{ and } \delta > 0 \\ \widehat{M}_{\text{flex}} < 0 \text{ and } \widehat{M}_{\text{ext}} > 0 \\ 0 < w < 1 \end{cases} \quad (4)$$

where rEMG is the vector of EMG signals processed using filter characteristics, and α is the matrix of coefficients establishing EMG-moment relationships. Variable w is the matrix of muscle group gains, and E is the matrix of biarticularity. Unlike the model of Amarantini and Martin (2004), w was applied to the extensor (w_{ext}) and flexor (w_{flex}) muscular groups to gain processing times. This change is possible, given that the model accounts for the total force of each muscular group. β and δ are matrices of stiffness and viscosity coefficients depending respectively upon angular changes ($\theta_j - \theta_{jTiso}$) and angular velocity ($\dot\theta_j$) vectors. $\Delta\theta$ was defined as the difference between the vector of angular displacement (θ) and that of theoretical isometric calibration angles ($\theta_{Tiso} = \langle\theta_{hTiso}, \theta_{kTiso}, \theta_{aTiso}\rangle^t$), calculated as half of the excursion of movement at each joint (van Dieen and Visser, 1999).

The above constrained nonlinear optimization problem was solved by sequential quadratic programming (Boggs and Tolle, 1996) with w, $|\alpha|$, β and δ initially set to 0.5, 50, 5 and 5, respectively. Flexor and extensor moments were used to compute the co-contraction index (CI) at the knee at each time t according to the expression given by Falconer and Winter (1985):

$$\text{CI} = \left(\frac{2 \cdot |M_{\text{antago}}|}{|M_{\text{ago}}| + |M_{\text{antago}}|} \right) \times 100\% \quad (5)$$

where M_{ago} is the knee agonist moment, and M_{antago} is the knee antagonist moment at each time t.

2.4. Statistics

The present study focuses principally on the knee because joint kinetic differences between AB and subjects with a TTA are most apparent at this joint (Sanderson and Martin, 1997), and major musculoskeletal problems occur at the knee joint for subjects with a TTA (Burke et al., 1978; Melzer et al., 2001).

After the calculations, all biomechanical patterns were normalized relative to time, and joint kinetics were normalized by the subjects' mass. For each subject, mean sagittal kinematic and kinetic profiles were obtained by averaging three gait cycles.

For comparisons, the dependent variables were the knee CI (expressed in %), the averaged peaks of knee angular

positions, of the net, agonist and antagonist knee joint moments and of the knee joint power (K1–K4). Each variable was compared during weight acceptance, single limb support, push-off, mid-swing and end of swing period. After having verified the absence of difference between the right and left legs of AB children with one-way repeated measures ANOVA, the data from the left and right sides of each AB subject were averaged to form one set of "control" data called "CL". One-way ANOVAs were then performed on each of the dependent variables to compare AL versus NAL (repeated measures ANOVA), CL versus AL and CL versus NAL (independent ANOVAs). Significant difference was set at $P < 0.05$.

3. Results

3.1. Kinematics

Step length, swing time, stance time and single limb support time were not statistically different between CL, AL and NAL (Table 1). Furthermore, no significant difference was observed for the stride length (Table 1), and for the averaged speed and cadence. Speed and cadence values were respectively 1.12 m/s (SD 0.17) and 113.1 steps/min (SD 12.5) for AB children compared to 1.04 m/s (SD 0.14) and 111.2 steps/min (SD 12.6) for children with a TTA.

No significant differences were observed for peak knee angular excursion values during the support and swing periods (see Fig. 1). This invariance, obtained from the kinematics data, showed high consistency in the behaviour of AB and children with a TTA at the knee during gait.

3.2. Muscular strategies

The updated version of the EMG-assisted optimization model proposed by this study gave an accurate estimation of the resultant moment when compared to the resultant moment obtained by the inverse dynamic calculated with Lagrangian formalism. Indeed, we found a coefficient of determination of 0.97 for AB children and of 0.93 for children with a TTA. Thus, for the rest of this paper, the resultant moment estimated from the EMG signals has been taken to compare the three limbs.

Moments were plotted during the gait cycle, with heel contact representing 0%, toe-off 65%, and just before subsequent heel contact 100% of the gait cycle. As shown in Fig. 1, the CL produced a positive (extensor) moment for the first 0–12% of the gait cycle, as the quadriceps acted eccentrically (negative power K1) to control knee flexion and thus using the quadriceps for agonist muscles. From 12% to 30% of the gait cycle, the knee carried out extension with concentric contraction of the agonist quadriceps muscles (positive power K2) to raise the centre of the mass. Then, the resultant moment changed polarity (flexor) from 30% to 50% of the gait cycle as the agonist hamstring muscles acted eccentrically (negative power) to slow forward progression of the body. From 50% to 75%, the end of the stance phase to the beginning of the swing phase, the resultant moment was extensor, and the agonist quadriceps muscles acted eccentrically (negative power K3) to control knee flexion during push-off, and continued during early swing to decelerate the backward swinging leg. Finally, for the rest of the gait cycle (75–100%), the resultant moment was negative (flexor), and the agonist hamstring muscles acted eccentrically as the hamstring controlled knee extension prior to subsequent heel contact (negative power K4). The NAL showed the same pattern (see Fig. 1).

As illustrated in Fig. 1, the AL did not perform the same muscular pattern during the stance phase compared to the CL and NAL. The AL had a positive resultant moment (extensor) for all of the stance phase compared to the transition (extensor to flexor) observed for the CL and NAL. Indeed, significant differences were apparent for the minimum resultant moment value during stance where CL (-0.21 (SD 0.11) N m/kg) and NAL (-0.32 (SD 0.31) N m/kg) were flexor while AL (0.30 (SD 0.27) N m/kg) was extensor ($P < 0.05$). That is to say, children with a TTA used their extensors as agonist muscles for all of the stance phase. Finally, no significant

Table 1
Spatio-temporal parameters (mean and standard deviation (SD)) for the control limb (CL) in AB children and for the non-amputated (NAL) and the amputated (AL) limbs in children with a TTA

	AB children		Children with a TTA	
	Mean	SD	Mean	SD
Stride length (m)	1.18	0.15	1.15	0.18

	AB children		Children with a TTA			
	CL		NAL		AL	
	Mean	SD	Mean	SD	Mean	SD
Step length (m)	0.60	0.08	0.54	0.10	0.56	0.10
Stance time (%)	65.2	1.2	65.9	0.9	65.3	0.9
Swing time (%)	34.8	1.2	34.1	1.0	34.7	0.9
Single limb support (%)	11–50	2	12–50	3	15–51	3

difference was evident for peak values of the resultant, extensor and flexor moments during the stance and swing phases. Similar results were obtained for the peak muscular power values of K1–K4, where no significant difference was found for the stance and swing phases (see Fig. 1).

3.3. Co-contraction

For the CI, no significant difference was discerned for weight acceptance and change of direction of knee angular displacement. During the single limb support, a significant difference was observed for the CI. Indeed, the CI for the
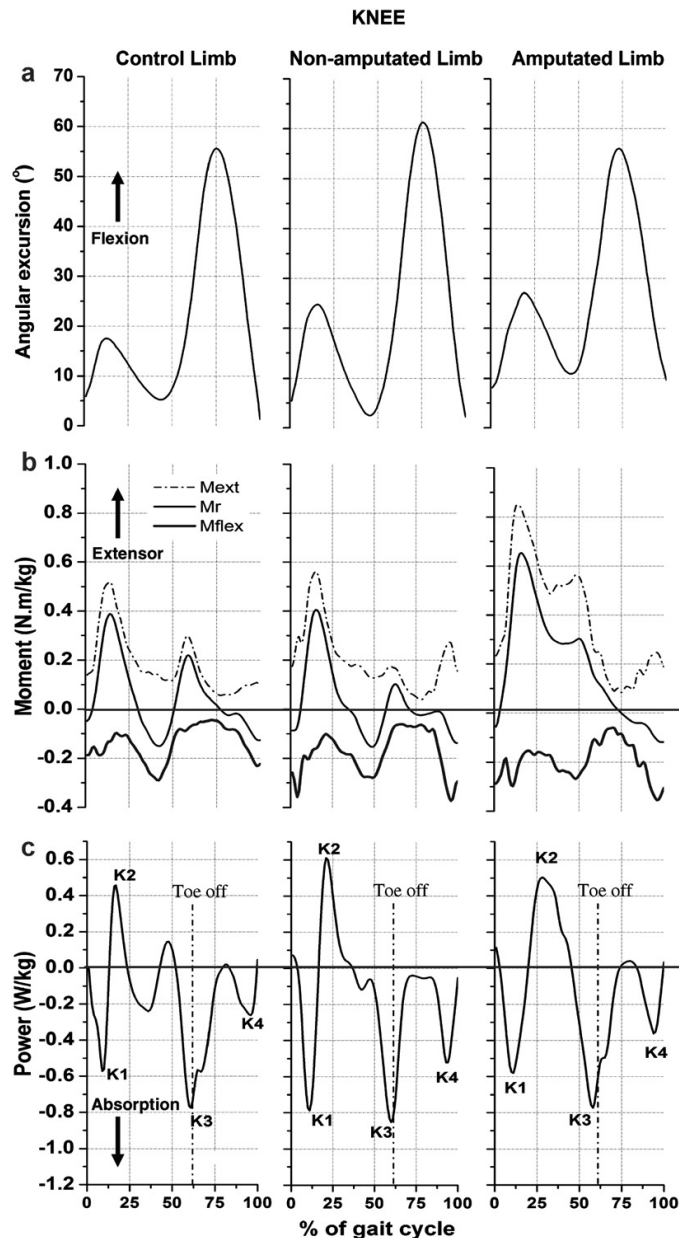
Fig. 1. (a) Knee angular displacement. (b) Resultant (M_r), extensor (M_{ext}) and flexor (M_{flex}) knee moments in N m/kg for the entire gait cycle of the amputated limb, non-amputated limb and control limb. (c) Knee power in W/kg for the entire gait cycle of the three different limbs. The data are from two representative subjects.
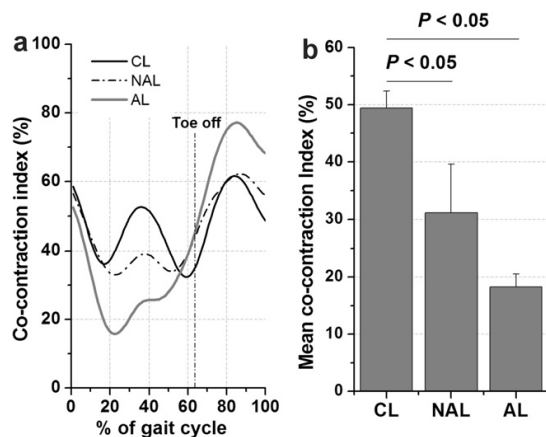
Fig. 2. (a) Co-contraction index for the gait cycle of the amputated limb (AL), non-amputated limb (NAL) and control limb (CL). (b) Mean values of the co-contraction index during the single limb support phase for the three different limbs.

CL (49 (SD 7.3) %) was greater (*P* < 0.05) compared to the NAL (31.1 (SD 20.8) %) and AL (18.2 (SD 5.6) %) (see Fig. 2).

4. Discussion

4.1. Kinematics

As reported by Sanderson and Martin (1997), the present study did not find differences for the spatio-temporal variables (stride length, cadence, speed and percentage of support, and swing phases) for the entire gait cycle.

Considering kinematics, the knee joint reflected considerable similarity between the three limbs for the entire gait cycle as detected previously for amputee gait (Sanderson and Martin, 1997; Lewallen et al., 1986) and for amputee gait obstacle avoidance (Hill et al., 1997). These results reveal at which point the behaviour of children with a TTA is comparable to that of AB children for knee kinematics.

4.2. Muscle strategies

During the stance phase of the gait cycle, maintenance of upright posture and forward propulsion of the body are assured by the lower extremities. These functions can be accomplished with various combinations of moments of force about the three joints of the lower extremity during the entire task (Prilutsky and Zatsiorsky, 2002).

The present study identified differences in knee muscle patterns between AB and children with a TTA during gait. Indeed, at their AL, children with a TTA used their extensor muscle as agonist for all of the support phase compared to their NAL and AB children who had a change of agonist muscle during the stance phase (extensor to flexor). This finding goes along with the observation of Powers et al.

(1998) who noted that children with a TTA had an extensor resultant moment for all of the stance phase of the gait cycle. For their AL, children with a TTA used their extensor muscle to keep the knee in extension compared to the CL where the agonist flexor muscle was deployed eccentrically to slow forward progression of the body. For the NAL, children with a TTA used the same muscle coordination as AB children during the stance phase. By employing muscle redundancy to compensate for their loss of ankle and foot and their knee muscular atrophy (Isakov et al., 2000), children with a TTA can perform the same movement by modifying the efforts of the other muscles. However, this new pattern creates changes on the level of muscular co-contractions.

4.3. Co-contractions

Generally, the results obtained in the present study are in agreement with the experiments of Falconer and Winter (1985) where the greatest value of the CI was during weight acceptance and the swing phase for all children. However, in the current investigation, children with a TTA had less co-contraction during the single limb support phase compared to AB children, especially for the AL where a smaller value with small variability was apparent (see Fig. 2b). With this diminution of co-contraction, children with a TTA could present instability at their knee joint for both the NAL and AL. Knee joint stability is especially important for the single limb support phase because this period of the gait cycle requires high maintenance of balance. Thus, the near zero value of the resultant moment during the first half of the stance phase (0–30% of the gait cycle), observed by Winter and Sienko (1988), could be attributed to a decrease of muscular activity and co-contraction for adults with a TTA.

In regard to articular stability, during knee extension (action by the quadriceps), the hamstring assists the work of the anterior cruciate ligament to maintain knee joint stability and to produce a force opposed to the former translation movement of the tibia (Miller et al., 2000). The observed diminution of co-contraction could then create degenerative diseases, such as osteoarthritis, at the knee of the AL and particularly in the NAL (Burke et al., 1978; Melzer et al., 2001). The fact the NAL was mostly affected could be explained because, during support, children with a TTA have greater vertical, lateral and posterior ground reaction forces on the NAL compared to AL and even the CL (Engsberg et al., 1991; Engsberg et al., 1993; Lewallen et al., 1986), thus creating additional stresses on the structure of the knee joint of the NAL. One of the limit of this study is that we focus principally on joint laxity mechanisms and even if it is a major factor in the development of osteoarthritis (Felson et al., 2000; Issa and Sharma, 2006) others factors like increase contact forces between the tibia and the femur, nutritional factor, bone mineral density, etc. could affect the development of osteoarthritis (Felson et al., 2000).

Finally, this lack of co-contraction during single limb support might reduce the muscular energy expenditure of children with a TTA. Unnithan et al. (1996) suggested that co-contraction is a major factor responsible for the high energy cost of walking by children with cerebral palsy. Children with a TTA would thus choose an energy-saving strategy compared to a joint stability strategy which co-contraction can bring. The absence of difference at the level of co-contraction for the other phases of the gait cycle is also striking. Indeed, children with a TTA have less muscle to carry out these co-contractions; therefore, they demand more activity from the remaining muscles that might change joint constraints.

5. Conclusion

In the present study, children with a TTA used different agonist and antagonist muscle knee patterns during walking but showed consistent kinematic behaviour (angular excursion) compared to AB children. This reorganization, observed at the AL and NAL, occurs to maintain functionality of the gait task for children with a TTA, with some disadvantages. More precisely, changes in muscle patterns matched with kinematic invariance result in a diminution of knee co-contraction, reducing knee stability (or increasing joint laxity), especially during the single limb support period which is the most demanding period of the gait cycle regarding the maintenance of balance. This reduction of stability might be responsible for premature degenerative disease of both the NAL and AL knee joints. Since early modifications are apparent for subjects with a TTA, it is important to quantify the impact of the muscular modifications (atrophy, weakness, etc.) on the components of the musculoskeletal system to avoid the physical problems seen in adults with a TTA.

Acknowledgements

References

Amarantini, A., Martin, L., 2004. A method to combine numerical optimization and EMG data for the estimation of joint moments under dynamic conditions. J. Biomech. 37, 1393–1404.
Arms, S.W., Pope, R.H., Johnson, R.J., Fischer, R.A., Arvidsson, I., Ericksson, E., 1984. The biomechanics of anterior cruciate ligament rehabilitation and reconstruction. Am. J. Sports Med. 12, 8–18.
Boggs, P.T., Tolle, J.W., 1996. Sequential quadratic programming. Acta Numer. 4, 1–52.
Burke, M.J., Roman, V., Wright, V., 1978. Bone and joint changes in lower limb amputees. Ann. Rheum. Dis. 37, 252–254.
De Boor, C., 2004. A Practical Guide to Splines, revised ed. Springer-Verlag, New York.
Engsberg, J.R., Lee, A.G., Patterson, J.L., Harder, J.A., 1991. External loading comparisons between able-bodied and below-knee-amputee children during walking. Arch Phys Med Rehabil. 72, 657–661.
Engsberg, J.R., Lee, A.G., Tedford, K.G., et Harder, J.A., 1993. Normative ground reaction force data for able-bodied and below-knee-amputee children during walking. J. Pediatr. Orthop. 13, 169–173.
Falconer, K., Winter, D.A., 1985. Quantitative assessment of co-contraction at the ankle joint in walking. Electromyogr. Clin. Neurophysiol. 25, 135–149.
Felson, D.T., Lawrence, R.C., Dieppe, P.A., Hirsch, R., Helmick, C.G., Jordan, J.M., Kington, R.S., Lane, N.E., Nevitt, M.C., Zhang, Y., Sowers, M., McAlindon, T., Spector, T.D., Poole, A.R., Yanovski, S.Z., Ateshian, G., Sharma, L., Buckwalter, J.A., Brandt, K.D., Fries, J.F., 2000. Osteoarthritis: new insights. Part 1: the disease and its risk factors. Ann. Intern. Med. 133, 635–646.
Hill, S.W., Patla, A.E., Ishac, M.G., Adkin, A.L., Supan, T.J., Barth, D.G., 1997. Kinematic patterns of participants with a below knee prosthesis stepping over obstacles of various heights during locomotion. Gait Posture 6, 186–192.
Isakov, E., Keren, O., Benjuya, N., 2000. Trans-tibial amputee gait: time-distance parameters and EMG activity. Prosthet. Orthot. Int. 24, 216–220.
Issa, S.N., Sharma, L., 2006. Epidemiology of osteoarthritis: an update. Curr. Rheumatol. Rep. 8, 7–15.
Lewallen, R., Dyck, G., Quanbury, A., Ross, K., Letts, M., 1986. Gait kinematics in below-knee child amputees: a force plate analysis. J. Pediatr. Orthop. 6, 291–298.
Melzer, I., Yekutiel, M., Sukenik, S., 2001. Comparative study of osteoarthritis of the contralateral knee joint of male amputees who do and do not play volleyball. J. Rheumatol. 28, 169–172.
Miller, J.P., Croce, R.V., Hutchins, R., 2000. Reciprocal coactivation patterns of the medial and lateral quadriceps and hamstrings during slow, medium and high speed isokinetic movements. J. Electromyogr. Kinesiol. 10, 233–239.
Powers, C.M., Rao, S., Perry, J., 1998. Knee kinetics in trans-tibial amputee gait. Gait Posture 8, 1–7.
Prilutsky, B.I., Zatsiorsky, V.M., 2002. Optimization-based models of muscle coordination. Exerc. Sport Sci. Rev. 30, 32–38.
Sadeghi, H., Allard, P., Duhaime, M., 2001. Muscle power compensatory mechanisms in below-knee amputee gait. Am. J. Phys. Med. Rehabil. 80, 25–32.
Sanderson, D.J., Martin, P.E., 1997. Lower extremity kinematic and kinetic adaptations in unilateral below-knee amputees during walking. Gait Posture 6, 126–136.
Solomonow, M., Baratta, R., D'Ambrosia, R., 1989. The role of the hamstrings in the rehabilitation of the anterior cruciate ligament-deficient knee in athletes. Sports Med. 7, 42–48.
Unnithan, V.B., Dowling, J.J., Frost, G., Bar-Or, O., 1996. Role of cocontraction in O_2 cost of walking in children with cerebral palsy. Med. Sci. Sports Exerc. 28, 1498–1504.
van Dieen, J.H., Visser, B., 1999. Estimating net lumbar sagittal plane moments from EMG data. The validity of calibration procedures. J. Electromyogr. Kinesiol. 9, 309–315.
Winter, D.A., 1991. The Biomechanics and Motor Control of Human Gait: Normal, Elderly and Pathological, second ed. Waterloo Biomechanics, Waterloo, Ont., Canada.
Winter, D., Sienko, S., 1988. Biomechanics of below-knee amputee gait. J. Biomech. 21, 361–367.
Zajac, F.E., Gordon, M.E., 1989. Determining muscle's force and action in multi-articular movement. Exerc. Sport Sci. Rev. 17, 187–230.

Influence of additional load on the moments of the agonist and antagonist muscle groups at the knee joint during closed chain exercise

Guillaume Rao [a,b,*], David Amarantini [c], Eric Berton [a]

[a] *Movement and Perception Laboratory, UMR CNRS 6152, CNRS, University of the Mediterranean,*
Parc Scientifique et Technologique de Luminy, 163, Avenue de Luminy, 13288 Marseille cedex 09, France
[b] *University of Delaware, Department of Mechanical Engineering, 126 Spencer Laboratory, University of Delaware, Newark, DE, USA*
[c] *Laboratoire Adaptation Perceptivo-Motrice et Apprentissage, UFR APS, Universite Paul Sabatier, Toulouse III, 118,*
Route de Narbonne, 31062 Toulouse cedex 09, France

Abstract

The present study investigated the influence of additional loads on the knee net joint moment, flexor and extensor muscle group moments, and cocontraction index during a closed chain exercise. Loads of 8, 28, or 48 kg (i.e., respectively, $11.1 \pm 1.5\%$, $38.8 \pm 5.3\%$, and $66.4 \pm 9.0\%$ of body mass) were added to subjects during dynamic half squats. The flexor and extensor muscular moments and the amount of cocontraction were estimated at the knee joint using an EMG-and-optimization model that includes kinematics, ground reaction, and EMG measurements as inputs. In general, our results showed a significant influence of the *Load* factor on the net knee joint moment, the extensor muscular moment, and the flexor muscle group moment (all Anova $p < .05$). Hence we confirmed an increase in muscle moments with increasing load and moreover, we also showed an original *''more than proportional''* evolution of the flexor and extensor muscle group moments relative to the knee net joint moment. An influence of the *Phase* (i.e., descent *vs.* ascent) factor was also seen, revealing different activation strategies from the central nervous system depending on the mode of contraction of the agonist muscle group. The results of the present work could find applications in clinical fields, especially for rehabilitation protocols.
© 2007 Elsevier Ltd. All rights reserved.

Keywords: Muscular cocontraction; Numerical optimization; Muscle group moments; Load; Closed chain exercises

1. Introduction

Rehabilitation programs employed for restoring the functional capacity of the joints after ligament injuries include either *open chain* exercises when the distal segment is free to move or *closed chain* exercises when the terminal segment is fixed (Escamilla et al., 1998). Relative to open chain efforts, closed chain exercises may be more adapted to reha-

bilitation programs, especially at the knee joint, because of minimal translation of the tibial plateau and lower forces experienced by the ligaments (Escamilla et al., 1998). For both types of movement, agonist–antagonist muscle cocontractions have been reported (Aagaard et al., 2000; Escamilla, 2001), suggesting contribution of muscular activity to active joint stabilization. Indeed, Basmajian and DeLuca (1985) and Stokes and Gardner-Morse (2003) indicated that co-activation of antagonist muscles about the joints participates in joint stability. Moreover, the cocontraction index (CI) has been reported to be a reliable variable to quantify the co-activation of agonist–antagonist muscle groups during multijoint dynamic exercises (see Kellis et al., 2003, for a comparison of the CI estimation methods).

---
* Corresponding author. Address: Movement and Perception Laboratory, UMR CNRS 6152, CNRS, University of the Mediterranean Parc, Scientifique et Technologique de Luminy, 163, Avenue de Luminy, 13288 Marseille cedex 09, France. Tel.: +33 491 17 04 78.
E-mail address: guillaume.rao@univmed.fr (G. Rao).

Considering open chain exercises and mainly isokinetic movements, the effects of fatigue, injuries, speed or load on co-activation of knee agonist–antagonist muscles have been extensively investigated (Aagaard et al., 2000; Aalbersberg et al., 2005; Kellis, 1998; Kellis and Baltzopoulos, 1998; Kellis and Kellis, 2001; Kingma et al., 2004). First, these studies reported either no evidence of a relationship between the amount of cocontraction and the knee anterior shear force (Aalbersberg et al., 2005; Kingma et al., 2004) or a possible positive correlation (Aagaard et al., 2000). Second, increasing the required agonist moment during open chain exercises (i.e., adding loads) leads to a higher EMG activity of the agonist muscles. The antagonist EMG activity also increases, but this raise is lower than that of the required agonist moment (i.e., a "less than proportional trend" for Kingma et al., 2004).

During closed chain exercises, previous works revealed that relative to healthy subjects, non-coper anterior cruciate ligament (ACL) deficient patients may use different activation patterns of the lower limb muscles to counteract the knee antero-posterior laxity (Alkjaer et al., 2002; Kingma et al., 2006; Rudolph et al., 2001). The use of external loads (e.g., additional weights) is frequent during rehabilitation programs, but few studies investigated the influence of load on the activity of the muscles surrounding the knee joint during a closed chain exercise. McCaw and Melrose (1999) reported an increase activity of the three superficial Quadriceps muscles with increasing load and no effect on the Biceps Femoris activity. These results would suggest a decrease in the amount of cocontraction at the knee joint as load increases.

The methods employed in the above studies on agonist–antagonist co-activation focused on EMG data to study cocontraction and, as noticed by Kellis (1998), EMG data alone could lead to misinterpretations because of normalization issues, possible distortions of the signal (Rainoldi et al., 2000) and the influence of joint kinematics in dynamic conditions (Potvin, 1997). Alternatively, the use of an EMG-and-optimization model may overcome the previous limitations and provide a convenient procedure to obtain the cocontraction index from reliable estimates of the contribution of the agonist and antagonist muscle groups to the net joint moment (Amarantini and Martin, 2004; Doorenbosch and Harlaar, 2003; Kellis and Baltzopoulos, 1997; Kellis et al., 2003).

The present work investigated the influence of load on the knee flexor and extensor muscle group moments during dynamic squats, i.e., a closed chain exercise of lower body. Three levels of external load, corresponding to what is usually encountered in rehabilitation protocols, were applied to the subjects. An updated version of the EMG-to-moment optimization process developed by Amarantini and Martin (2004) provided estimates of the knee agonist and antagonist muscle group moments further used to compute CI. Our working hypothesis is that during closed chain exercises, the CI would increase with load to actively stabilize the knee joint. We also hypothesized differences in the CI as well as in

flexor and extensor muscle group moments depending on the squat cycle phases because each muscle group may have a different role depending on the mode of contraction of the agonist muscle group (i.e., eccentric or concentric).

2. Methods

2.1. Subjects

Eight male students at the Sport Sciences Faculty of Marseilles, novice in weight lifting and free of knee-injury histories participated in this study. Mean (±s.d.) age, height and mass were 20.1 ± 2.8 years, 177.0 ± 3.2 cm and 75.1 ± 11.8 kg, respectively. The project was approved by the University Review Board and all participants gave informed consent in accordance with the Helsinky convention.

2.2. Instrumentation

A six cameras Vicon624 system (Vicon Motion System, Lake Forest, CA) operating at 120 Hz recorded kinematics data from eight markers attached to the fifth metatarsal head, the lateral malleolus, the lateral femoral condyle, the major trochanter, the head of the clavicle, the jaw, the vertex of the head, and the center of the barbell. Cartesian coordinates were smoothed with a cubic spline smoothing procedure (Matlab Spline Toolbox, version 3.2.2).

Ground reactions were sampled at 240 Hz from a forceplate (AMTI, Model LG6-4-CE, Watertown, USA). Raw dynamic data were low-pass filtered using a fourth-order, zero-lag Butterworth filter with a 10 Hz cutoff frequency.

Electromyographic data were recorded at 1000 Hz (Mega ME 3000 P8, Mega Electronics Ltd.; gain = 412, CMRR = 110 dB) using Ag/Ag-Cl bipolar surface electrodes (Skintact model FS 501, Innsbruck, Austria) placed over the bellies of gastrocnemius medialis (ga), biceps femoris (bf), rectus femoris (rf), and vastus medialis (vm) right leg muscles with a 2 cm center-to-center inter-electrodes distance. These muscles were chosen according to Amarantini and Martin (2004) and Olney and Winter (1985) and included mono-articular (vm) as well as bi-articular muscles spanning both the knee joint as well as the hip (bf and rf) and ankle (ga) joints.

2.3. Instructions

Subjects stood with both feet on the forceplate and performed dynamic half squats, beginning in an upright position, bending the knees until thighs were parallel to the floor and returning to the initial posture. After an active warm-up, the subjects performed seven consecutive cycles at self-selected speed randomly loaded by a barbell of 8 (barbell only), 28, or 48 kg with 4 min rest between each condition. The barbell was positioned across the back of the shoulders. These loads corresponded, respectively, to $11.1 \pm 1.5\%$, $38.8 \pm 5.3\%$, and $66.4 \pm 9.0\%$ of body mass. Numerous studies on closed chain exercises have used either loads corresponding to a percentage of one repetition maximum (Ebben and Jensen, 2002; Escamilla et al., 1998; Escamilla, 2001) or no load (Isear et al., 1997). As the results of the present study may find direct applications for rehabilitation, constant loads were used considering first that it may be hazardous to perform a maximum effort just after surgery and second, that rehabilitation equipments usually offer fixed increasing loads.

2.4. Data processing and modeling

Angular displacements of foot, shank, thigh and trunk segments were computed from smoothed Cartesian coordinates and interpolated to 1000 Hz using third-order splines. Joint angular velocities and accelerations were obtained by analytical differentiation. For each subject and load, each cycle was normalized in time from 0% to 100% of the squat cycle duration. The net knee flexion/extension moment was computed for each time instant t by solving inverse dynamics for a planar four bar-linkage system where ankle, knee, hip, and shoulder joints were considered as frictionless hinges (see Cahouët et al., 2002, for the generalized form of equations). Bilateral symmetry was assumed (Escamilla et al., 1998) and net joint moments were computed using body segment parameters data (Zatsiorsky and Seluyanov, 1983). To estimate the contribution of a single leg, the net joint moment was divided by half.

The first and the last cycles were removed from the analysis and one representative cycle per subject and condition was obtained by averaging the kinematics, net joint moment, and EMG data of the five remaining consecutive cycles. The selected number of cycles was sufficient to obtain reliable EMG data (Arsenault et al., 1986).

The estimates of the knee net joint moment, flexor and extensor moments were obtained from an updated version of the Amarantini and Martin (2004) model. The major update consisted of the incorporation of the isometric EMG-to-moment calibration directly into the dynamic procedure by assuming a linear trend between the muscle group moments and the rectified and filtered EMGs (Amarantini and Martin, 2004). Hence, the coefficients for the isometric EMG-to-moment relationship (α_i in Eq. (2)) were estimated during the dynamic session (Centomo et al., 2007a,b). In the model, the force production capacity of each muscle group is attributed to the selected muscles of the corresponding muscle group.

Thus, the flexor and extensor muscle group moments were estimated at the knee joint by solving the following optimization problem:

Find:

$$\alpha_i = \{\alpha_{ga}, \alpha_{bf}, \alpha_{rf}, \alpha_{vm}\}, \; w_i(t) = \{w_{ga}(t), w_{bf}(t), w_{rf}(t), w_{vm}(t)\},$$
$$\beta_j = \{\beta_a, \beta_k, \beta_h\} \text{ and } \delta_j = \{\delta_a, \delta_k, \delta_h\}$$

that minimize : $C = \frac{1}{2} \cdot \sum_t (M_K(t) - \widehat{M}_K(t))^2$ (1)

with : $\widehat{M}_K(t) = \sum_i (\alpha_i \cdot w_i(t) \cdot S_i(t))^T \cdot [1 + E \cdot (\beta_j \cdot \Delta\theta_j) - E \cdot (\delta_j \cdot \dot{\theta}_j)]$ (2)

$i = \{ga, bf, rf, vm\}$ and $j = \{a, k, h\}$

where a refers to the ankle joint, k to the knee, and h to the hip.

$$\text{subject to} : \begin{cases} \alpha_{ga}, \alpha_{bf} < 0; \; \alpha_{rf}, \alpha_{vm} > 0 \\ \beta_j \text{ and } \delta_j > 0 \\ 0 < w_i(t) < 1 \\ \widehat{M}_{ga}, \widehat{M}_{bf} < 0; \widehat{M}_{rf}, \widehat{M}_{vm} > 0 \end{cases} \text{ as inequality constraints}$$
(3)

In (1), $M_K(t)$ represents the knee net joint moment computed by inverse dynamics while $\widehat{M}_K(t)$ is the net joint moment estimated through the optimization procedure using the EMG data as input. In Eq. (2), $M_{Flex}(t)$ corresponds to the sum at each time t of $\widehat{M}_{ga}$ and $\widehat{M}_{bf}$ while $M_{Ext}(t)$ results from the sum of $\widehat{M}_{rf}$ and

$\widehat{M}_{vm}$. $S_i(t)$ contains the full-wave rectified and filtered (fourth-order, zero-lag Butterworth, 2.5 Hz cutoff frequency) EMG data of the four selected muscles. α_i is the matrix establishing the isometric EMG-moment relationship and $w_i(t)$ represents the matrix of individual muscle gains. This matrix defines the contribution of each muscle to the corresponding muscle group moment. The mathematical expression of $\widehat{M}_K(t)$ also includes matrices of biarticularity, stiffness, and viscosity (respectively, E, β_j and δ_j) to take into account the force–length and force–velocity relationships (please refer to Amarantini and Martin, 2004 for more details). According to van Dieen and Visser (1999), $\Delta\theta_j(t)$ was computed relative to the mean value of the angular range covered by the ankle, knee, and hip joints during squats.

For each subject, the optimization procedure was completed after concatenating the averaged cycles of the three conditions of load in a single row to obtain constant isometric EMG-moment coefficients (α_i). Indeed, as a result of the design of the experiment, this subject specific physiologic coefficient (i.e., the EMG-to-moment isometric coefficient) should not vary during the experiment. This non-linear constrained optimization problem was solved using a Sequential Quadratic Programming (Boggs and Tolle, 1995) (Matlab Optimization Toolbox, version 3.0.3).

CI was computed at each time instant t using the expression given in Falconer and Winter (1985):

$$CI(t) = \frac{2 \cdot |M_{Antago}(t)|}{|M_{Ago}(t)| + |M_{Antago}(t)|}$$ (4)

where $M_{Antago}(t)$ and $M_{Ago}(t)$ correspond to $M_{Flex}(t)$ or $M_{Ext}(t)$ relative to the sign of the net joint moment ($\widehat{M}_K(t)$).

2.5. Statistics

Based upon the sign of the vertical velocity of the barbell, the minimum, mean, and peak values of knee angular velocity, net joint moment, flexor and extensor moments, and CI were computed during the descent and the ascent phases of the squat cycle. Two factors (*Load* and *Phase*) ANOVAs with repeated measures on both factors were conducted on each dependent variable. Prior to the test, each variable was normalized by the mean absolute value of the barbell vertical velocity to counterbalance the influence of movement velocity because loaded squats were performed at self-selected speed. Moreover, dependent variables were also normalized by subject's body weight.

Follow-up analyses were conducted using two sets of planned comparisons between the levels of *Load* and *Phase* because we were interested in comparisons between specific conditions rather than an overall condition effect. A first planned comparison examined whether each modality of *Load* was affected by a *Phase* effect. A second set of planned comparisons examined the influence of *Load* within each phase. A significance level of .05 was used for all comparisons.

3. Results

As expected from the design of the objective function in the optimization process, the EMG-and-optimization model provided estimates of the knee net joint moment ($\widehat{M}_K(t)$) with a very high correspondence to $M_K(t)$ and a coefficient of determination between both time series close to 1.0.

3.1. Load effect

The three levels of load supported by the subjects corresponded to significant different percentages of their body mass ($F_{2,42} = 1207.48$; $p < .05$). Statistical analyses showed high consistency in subject behaviors with no influence of *Load* neither on minimum, maximum, nor mean values of the knee angular velocity (respectively: $F_{2,14} = 0.37$; $p > .05$; $F_{2,14} = 0.62$; $p > .05$; $F_{2,14} = 0.76$; $p > .05$).

The presence of higher loads significantly increased the knee net joint moment (Table 1, Fig. 1). The mean values of $\widehat{M}_K(t)$ computed over the entire squat cycle were linearly related to *Load*, with r^2 values close to 1.0 (Fig. 2). Indeed, mean $\widehat{M}_K(t)$ values increased by 7.8% between the 8 and 28 kg conditions and by 8.3% between the 28 and 48 kg conditions. Peak values of the knee net joint moment were also significantly affected by the *Load* factor ($F_{2,42} = 3.28$; $p < .05$). Especially during the descent phase, the peaks of $\widehat{M}_K(t)$ for the condition 48 kg were higher than those obtained for the condition 8 kg. This significant influence of *Load* was also shown ($F_{2,42} = 15.63$; $p < .05$) on the minimum values of the knee net joint moment (Table 1). Indeed, whatever the phase, minimum values of $\widehat{M}_K(t)$ for the condition 8 kg were higher than those of the conditions 28 and 48 kg. Moreover, the results for the condition 28 kg were higher than those obtained when carrying 48 kg.

The extensor and flexor muscular moments estimated through the EMG-to-moment optimization procedure were also dependent on the *Load* factor (Table 1, Figs. 1 and 2). The normalized maximum values of the extensor muscular moments for the condition 48 kg were higher ($F_{2,42} = 4.19$; $p < .05$) than those of the condition 8 kg (Table 1 and Fig. 1). Regarding the normalized mean values of the flexor moment, conditions 8 and 28 kg were similar (overall averages: -21.5 ± 10.3 a.u. and -22.6 ± 7.6 a.u., respectively, for 8 and 28 kg) while the condition 48 kg produced lower values (-32.1 ± 9.3 a.u.; $F_{2,42} = 3.96$; $p < .05$). Similar

results were found with the minimum peaks of the flexor moment as values of the 48 kg condition (-56.1 ± 19.9 a.u.) were statistically lower than those of the 8 and 28 kg conditions (-36.3 ± 16.9 a.u. and -34.9 ± 10.4 a.u. for 8 and 28 kg, respectively; $F_{2,42} = 7.06$; $p < .05$). Mean values of the extensor moments increased by 6.0% between the 8 and 28kg conditions while these means raised by 16.6% between the 28 and 48 kg conditions. A similar trend was seen for the flexor moment mean values with a low (1.9%) decrease between 8 and 28 kg conditions and a sharp drop (33.2%) between the 28 and 48 kg conditions.

Opposite to these results, no main *Load* effect was seen neither on the minimum, mean, nor peak values of CI. However, a clear trend was seen for the knee angles at the time instants of maximal values of cocontraction index (Fig. 3). Indeed, these angles shifted from $24.46 \pm 9.42°$ for 8 kg, to $29.56 \pm 10.58°$ for 28 kg up to $33.17 \pm 14.13°$ for 48 kg.

3.2. Phase effect

The mode of contraction of the agonist muscle group was considered as eccentric during the descent phase and concentric during the ascent phase. Our results showed a significant influence of the *Phase* factor with higher absolute mean values of the flexor muscle group moments during the ascent phase than during the descent (Table 1). Hence, the amount of antagonist (flexor muscle group) moment depends on the type of muscular action of the agonist muscle group with higher levels of antagonist moment while the agonist group act concentrically. Statistical analyses revealed no influence of *Phase* neither on the minimum, maximum, nor mean values of the knee net joint moment and extensor muscle group moments. Regarding the CI, the influence of *Phase* was also not significant whatever the variable studied. On the contrary, a significant influence ($F_{1,42} = 5.68$; $p < .05$) was seen for the absolute mean values of the flexor moment with descent phase (22.97 ± 9.83 a.u.) lower than the ascent (27.80 ± 8.20 a.u.).

Table 1
Averaged ± s.d. values ($n = 8$) of the parameters investigated in this study (minimal, mean and maximal values)

Load (kg)	Phase					
	Descent			Ascent		
	8	28	48	8	28	48
CI_{mean}	48.5 ± 14.3	44.7 ± 14.2	45.2 ± 9.6	52.5 ± 10.1	53.6 ± 10.8	54.2 ± 11.5
CI_{max}	90.9 ± 14.3	93.7 ± 17.2	98.5 ± 3.8	91.9 ± 9.4	98.4 ± 3.4	99.9 ± 0.1
Net^L_{min}	$2.6 \pm 11.9^†$	$-9.1 \pm 14.1^\infty$	$-30.7 \pm 25.4^{†\infty}$	1.2 ± 11.1	$-12.1 \pm 12.6^\infty$	$-27.0 \pm 16.8^\infty$
Net_{mean}	52.3 ± 16.9	61.3 ± 20.8	69.6 ± 24.3	46.7 ± 14.5	46.7 ± 18.1	47.3 ± 21.9
Net^L_{max}	$112.2 \pm 27.7^†$	132.9 ± 31.2	$149.3 \pm 39.7^†$	103.1 ± 28.7	120.6 ± 38.6	133.2 ± 49.8
Ext_{mean}	74.6 ± 21.1	81.2 ± 19.5	96.2 ± 23.6	67.5 ± 13.5	72.0 ± 18.8	83.7 ± 17.5
Ext^L_{max}	$130.7 \pm 26.7^†$	153.7 ± 31.3	$173.7 \pm 37.5^†$	122.4 ± 25.6	141.6 ± 38.6	161.6 ± 45.9
$Flex^{L,P}_{mean}$	-22.3 ± 13.5	-19.9 ± 7.5	$-26.7 \pm 8.5^*$	$-20.7 \pm 7.0^†$	$-25.3 \pm 7.6^\infty$	$-37.4 \pm 10.0^{†\infty*}$
$Flex^L_{min}$	-37.3 ± 24.7	$-32.6 \pm 8.7^\infty$	$-53.4 \pm 21.9^\infty$	$-35.2 \pm 9.0^†$	$-37.1 \pm 11.9^\infty$	$-58.8 \pm 17.8^{†\infty}$

CI corresponds to cocontraction index, Net stands for knee net joint moment, Ext represents the extensor muscular moment, and Flex is the moment of the flexor muscle group. P and L superscripts indicate significant *Phase* and *Load* main effects, respectively. Significant results of planned comparisons are indicated in each cell by *, †, and ∞: * reveals a *Phase* effect for the associated load. Within each phase, † indicates differences between loads 8 and 48 kg, and ∞ indicates differences between loads 28 and 48 kg.
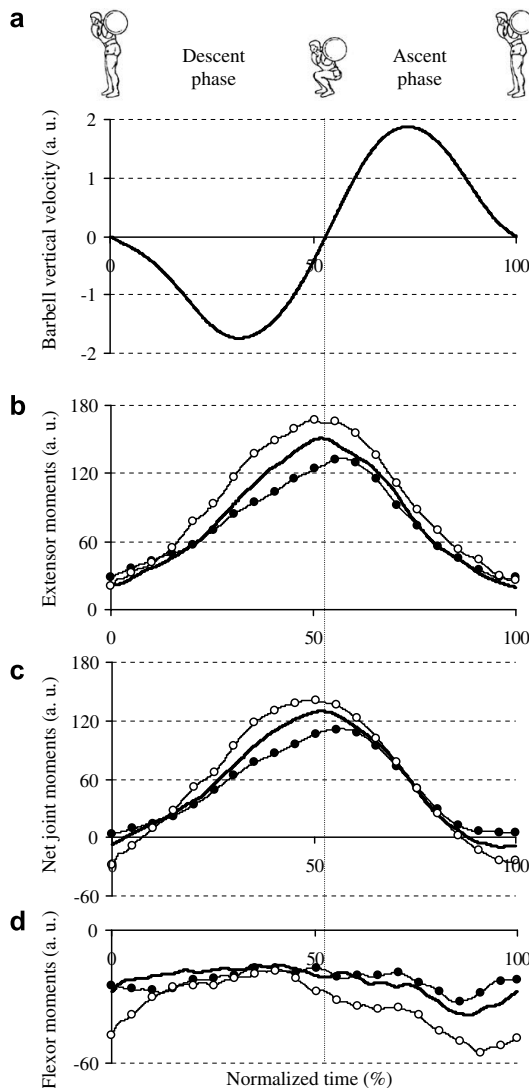
Fig. 1. From top to bottom: (a) Normalized values of the barbell vertical velocity averaged over the three conditions of load, (b) normalized knee extensor muscle group moments, (c) knee net joint moments, and (d) the normalized flexor muscular moments. For each graph, black dots correspond to the 8 kg load, thick black line to 28 kg, and open white dots to 48 kg. All these variables are averaged across subjects ($n = 8$). Please note the influence of *Phase* (descent *vs.* ascent) on the mean values of the flexor muscle group moments.

Fig. 2. Means ($n = 8$) of the normalized net (black triangles), extensor (black squares), and flexor (black dots) moments as a function of the barbell weight. Values were averaged over the squat cycle time. * indicates significant differences ($p < .05$).

Fig. 3. Means (and s.d., $n = 8$) of the knee angles at the time instant of maximal cocontraction as a function of the barbell weight. Please note the general increase in knee angle as the carried load increases.

4. Discussion

Relative to open chain efforts, closed chain exercises are widely used in rehabilitation protocols following knee ACL injuries because first, the functional restoration is more complete and second, the shear stress on the joint is reduced (Ben Kibler and Livingston, 2001). Numerous studies revealed 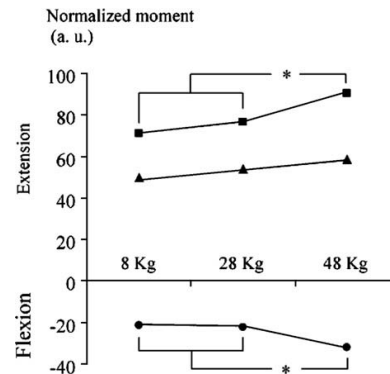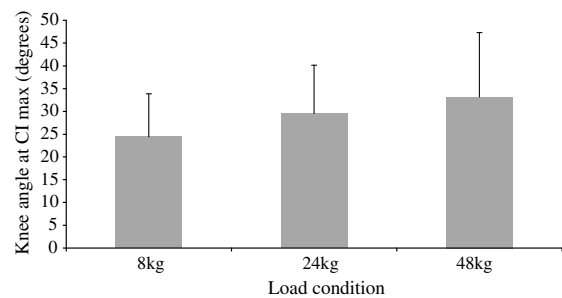that cocontraction of the agonist and antagonist muscle groups surrounding the knee may help in stabilizing the joint. The higher stability resulted from an increased axial compression force due to the antagonist coactivity (Stokes and Gardner-Morse, 2003). However, despite the use of different weights during closed chain exercises for rehabilitation purposes, few studies investigated the influence of load either on the activity of the agonist and antagonist muscle groups, or on the cocontraction level. Hence, the present study analyzed the influence of *Load* on the flexor and extensor muscular moments and on the CI at the knee joint during dynamic half-squat movements. Considering the uncertainties associated to the use of the EMG data solely, the flexor and extensor muscle group moments were evaluated using a reliable EMG-to-moment optimization process. Previous studies reported an increased hamstrings activity during the ascent phase (Escamilla et al., 1998; Isear et al., 1997; McCaw and Melrose, 1999). These authors associated this higher activity of the hamstrings bi-articular muscles to an increase in the hip extensor moment to be generated. While this explanation is certainly convincing, the use of the hamstrings muscles solely is not sufficient to estimate the overall flexor activity at the knee joint. Because the gastrocnemius

muscle is bi-articular, crossing both the knee and the ankle joints, and shows significant activity during squat movements (Escamilla et al., 1998), its influence on the knee joint flexor activity has to be taken into account. The present EMG-to-moment model included EMG data from the gastrocnemius muscle, thus enhancing the accuracy of the estimation of the knee flexor muscle group moment.

As expected, a constant increase in *Load* (20 kg between each condition) led to a linear evolution of the mean knee net joint moments (+7.8% and +8.3% between the 8 and 28 kg, and the 28 and 48 kg, respectively). This linear trend is confirmed by a coefficient of determination close to 1.0 between the mean knee net joint moment and the *Load*. Our results also showed an increase in the net knee joint moments as well as in the flexor and extensor muscle group moments with *Load* as most of the dependent variables for the 48 kg condition are higher than for the 8 kg situation (Table 1). As McCaw and Melrose (1999), our data showed a significant influence of *Load* on knee joint flexor and extensor muscle groups moments. Indeed, the peaks of the extensor and flexor muscle moments increased with *Load* (see Fig. 1 and Table 1). Mean values of flexor muscle group moments were also affected by *Load*, as absolute values of the conditions 8 kg and 28 kg were inferior to those observed for 48 kg (see Fig. 2). These results reflected the higher demand placed on both muscle groups to achieve the required task, especially when supporting a 48 kg load.

During closed chain exercises, our results provide new insights into the mechanisms underlying changes in muscle group moments. Our findings introduce the new idea that different loads may have different roles during rehabilitation exercises. Opposite to Kingma et al. (2004) who reported a ''less than proportional'' evolution of the agonist and antagonist EMG activities relative to the net joint moment during an open chain task, our results showed changes in $M_{Ext}(t)$ and $M_{Flex}(t)$ ''more than proportional'' as *Load* increased (Fig. 2). Statistical analysis of mean antagonist muscle moments showed an initial plateau with no difference between weaker loads (1.9% between 8 and 28 kg), followed by a sharp increase for the higher load (33.2% between 28 and 48 kg). This specific trend could reflect a threshold in the moments developed by the antagonist muscle group under different conditions of loading. For the 48 kg load, the significant increase in the moment developed by the antagonist muscle group may increase joint stability (Granata and Marras, 2000) and actively protect the knee ACL (Aagaard et al., 2000). Rehabilitation protocols could take advantage of this feature by proposing closed chain exercises with low loads to mobilize the knee and exercises with higher loads to train the antagonist muscle group to stabilize actively the joints. Considering the differences in the slopes of the antagonist activities between open and closed chain exercises (i.e., respectively, less and more than proportional relative to the net joint moment), our results would also suggest that fundamental findings from studies focusing on open chain exercises may not be fully applied to rehabilitation protocols.

In our study, no difference was seen in the amount of cocontraction despite modifications of both the extensor and flexor muscle group moments. This result may be explained by the equation that governed the estimation of the cocontraction index (Eq. (4)). Indeed, similar increases in the agonist and antagonist muscle group moments would lead to similar amount of cocontraction. This result emphasizes the fact that investigating the agonist and antagonist activities by themselves is complementary to the analysis of the cocontraction index around a joint. However, a clear trend was seen for the values of the knee angles corresponding to the instants of maximal cocontraction depending on the *Load* (Fig. 3). These knee angles where CI was maximal were 24° for 8 kg, 30° for 28 kg and 33° for 48 kg. Kingma et al. (2004) reported that below a 15–22° knee flexion angle, the hamstrings muscles are ineffective to counteract the anterior shear force produced by the quadriceps. Our results tend to show that with higher loads, requiring a higher stability of the knee joint, the peak of cocontraction is shifted to an angular range where the efficiency of the hamstrings muscles to actively stabilize the knee is maximal. These results confirm the advantageous role of cocontraction because the contribution of active stiffness to joint stability depends both on the knee angle and on the external load. These findings also suggest the ability of the neuromuscular system to appropriately activate the opposing muscle groups to assist the passive elements of stability crossing the knee joint.

Our results provide insights on the specific role of antagonist muscle group during closed chain exercises as the amount of antagonist moment depends on the type of muscular action of the agonist group (i.e., concentric/eccentric). It was previously shown that the control of movements involving eccentric contraction requires a single muscle group and conversely that a concentric activation alone may not result in coordinated motions (Enoka, 1996). Our data showed that the mean flexor muscle group moment is lower during the descent phase (while the knee extensor muscles act eccentrically) than during the ascent phase (i.e., when the extensor muscles contract concentrically). Besides an increased joint stability (Granata and Marras, 2000), modifications in the amount of antagonist cocontraction have been reported depending on the level of expertise (Osu et al., 2002), the required precision of a task (Gribble et al., 2003), or the presence of interaction torques (Gribble and Ostry, 1999). From the design of the present experiment that implied novices, low precision task and little amount of interaction torques, it is likely that most of the antagonist coactivity will be related to a demand of a higher joint stability. Hence during the descent phase, the knee extensor muscles would produce force and control movement velocity while the knee flexors act as joint stabilizers (i.e., by increasing the axial compression force). During the ascent phase and considering the conclusion of Enoka (1996), the extensor muscles would generate motion while the flexor muscles would both stabilize knee joint and regulate movement speed.

To conclude, our results emphasize the influence of *Load* and *Phase* on the knee flexor and extensor muscle group moments during closed chain exercises. Despite no modification in the amount of cocontraction with the increasing *Load*, our results showed that changes in the agonist and antagonist muscle group moments were "more than proportional" relative to the net joint moment. Finally, the simultaneous activation of agonist and antagonist muscles also varied depending on the mode of contraction of the agonist muscle group revealing different roles of antagonist cocontraction. Our findings may extend the use of squat exercises for rehabilitation programs (Kellis, 1998). Indeed, working with weak loads following surgery would develop the capacities of force production in the knee extensor muscles with minimal risk of injuries. Latter, adding load would enhance the efficiency of the neuromuscular system in actively assist joint stability. The differences observed in the agonist and antagonist muscle groups moments between the concentric and the eccentric phases of motion may also improve the efficiency of the closed chain rehabilitation protocols, as both modes of contraction are usually encountered in daily functional activities.

Acknowledgements

References

Aagaard P, Simonsen EB, Andersen JL, Magnusson SP, Bojsen-Moller F, Dyhre-Poulsen P. Antagonist muscle coactivation during isokinetic knee extension. Scand J Med Sci Spor 2000;10:58–67.

Aalbersberg S, Kingma I, Blankevoort L, van Dieen JH. Co-contraction during static and dynamic knee extensions in ACL deficient subjects. J Electromyogr Kines 2005;15:349–57.

Alkjaer T, Simonsen EB, Magnusson SP, Aagaard H, Dyhre-Poulsen P. Differences in the movement pattern of a forward lunge in two types of anterior cruciate ligament deficient patients: copers and non-copers. Clin Biomech (Bristol, Avon) 2002;17:586–93.

Amarantini D, Martin L. A method to combine numerical optimization and EMG data for the estimation of joint moments under dynamic conditions. J Biomech 2004;37:1393–404.

Arsenault AB, Winter DA, Marteniuk RG, Hayes KC. How many strides are required for the analysis of electromyographic data in gait? Scand J Rehabil Med 1986;18:133–5.

Basmajian JV, DeLuca CJ. In: Butler J, editor. Muscles alive. 5th ed. Baltimore: Williams and Wilkins; 1985. p. 223–43.

Ben Kibler W, Livingston B. Closed-chain rehabilitation for upper and lower extremities. J Am Acad Orthop Surgeons 2001;9:412–21.

Boggs PT, Tolle JW. Sequential quadratic programming. Acta Numer 1995;4:1–52.

Cahouët V, Martin L, Amarantini D. Static optimal estimation of joint accelerations for inverse dynamics problem solution. J Biomech 2002;35:1507–13.

Centomo H, Amarantini D, Martin L, Prince F. Muscle adaptation patterns of children with a trans-tibial amputation during walking. Clin Biomech (Bristol, Avon) 2007a;22:457–63.

Centomo H, Amarantini D, Martin L, Prince F. Differences in the coordination of agonist and antagonist muscle groups in below-knee amputee and able-bodied children during dynamic exercise. J Electromyogr Kines 2007. doi:10.1016/j.jelekin.2006.11.008.

Doorenbosch CA, Harlaar J. A clinically applicable EMG-force model to quantify active stabilization of the knee after a lesion of the anterior cruciate ligament. Clin Biomech (Bristol, Avon) 2003;18:142–9.

Ebben WP, Jensen RL. Electromyographic and kinetic analysis of traditional, chain and elastic band squats. J Strength Cond Res 2002;16:547–50.

Enoka RM. Eccentric contractions require unique activation strategies by the nervous system. J Appl Physiol 1996;81:2339–46.

Escamilla RF, Fleisig GS, Zheng N, Barrentine SW, Wilk KE, Andrews JR. Biomechanics of the knee during closed kinetic chain and open kinetic chain exercises. Med Sci Sport Exer 1998;30:556–69.

Escamilla RF. Knee biomechanics of the dynamic squat exercise. Med Sci Sport Exer 2001;33:127–41.

Falconer K, Winter DA. Quantitative assessment of co-contraction at the ankle joint in walking. Electromyogr Clin Neurophysiol 1985;25:135–49.

Granata KP, Marras WS. Cost-benefit of muscle cocontraction in protecting against spinal instability. Spine 2000;25:1398–404.

Gribble PL, Ostry DJ. Compensation for interaction torques during single- and multijoint limb movement. J Neurophysiol 1999;82:2310–26.

Gribble PL, Mullin LI, Cothros N, Mattar A. Role of cocontraction in arm movement accuracy. J Neurophysiol 2003;89:2396–405.

Isear JA, Erickson JC, Worrel TD. EMG analysis of lower extremity recruitment patterns during an unloaded squat. Med Sci Sport Exer 1997;29:532–9.

Kellis E, Baltzopoulos V. The effect of antagonist moment on the resultant knee joint moment during isokinetic testing of the knee extensors. Eur J Appl Physiol Occup Physiol 1997;76:253–9.

Kellis E. Quantification of quadriceps and hamstring antagonist activity. Sports Med 1998;25:37–62.

Kellis E, Baltzopoulos V. Muscle activation differences between eccentric and concentric isokinetic exercise. Med Sci Sports Exer 1998;30:1616–23.

Kellis E, Kellis S. Effects of agonist and antagonist muscle fatigue on muscle coactivation around the knee in pubertal boys. J Electromyogr Kines 2001;11:307–18.

Kellis E, Arabatzi F, Papadopoulos C. Muscle co-activation around the knee in drop jumping using the co-contraction index. J Electromyogr Kines 2003;13:229–38.

Kingma I, Aalbersberg S, van Dieen JH. Are hamstrings activated to counteract shear forces during isometric knee extension efforts in healthy subjects? J Electromyogr Kines 2004;14:307–15.

Kingma I, Aalbersberg S, van Dieen JH. Co-activation during isometric whole leg extensions in ACL deficient subjects. Gait Posture 2006;S4S:S175.

McCaw ST, Melrose DR. Stance width and bar load effects on leg muscle activity during the parallel squat. Med Sci Sports Exer 1999;31:428–36.

Olney SJ, Winter DA. Predictions of knee and ankle moments of force in walking from EMG and kinematic data. J Biomech 1985;18:9–20.

Osu R, Franklin DW, Kato H, Gomi H, Domen K, Yoshioka T, et al. Short- and long-term changes in joint co-contraction associated with motor learning as revealed from surface EMG. J Neurophysiol 2002;88:991–1004.

Potvin JR. Effects of muscle kinematics on surface EMG amplitude and frequency during fatiguing dynamic contractions. J Appl Physiol 1997;82:144–51.

Rainoldi A, Nazzaro M, Merletti R, Farina D, Caruso I, Gaudenti S. Geometrical factors in surface EMG of the vastus medialis and lateralis muscles. J Electromyogr Kines 2000;10:327–36.

Rudolph SK, Axe MJ, Buchanan TS, Scholz JP, Snyder-Mackler L. Dynamic stability in the anterior cruciate ligament deficient knee. Knee Surg, Sports Traumatology, Arthroscopy 2001;9:62–71.

Stokes IAF, Gardner-Morse M. Spinal stiffness increases with axial load: another stabilizing consequence of muscle action. J Electromyogr Kines 2003;13:397–402.

van Dieen JH, Visser B. Estimating net lumbar sagittal plane moments from EMG data. The validity of calibration procedures. J Electromyogr Kines 1999;9:309–15.

Zatsiorsky V, Seluyanov V. The mass and inertial characteristics of main segments of the human body. In: Matsui H, Kobayashi K, editors. Biomechanics VIII-B. Champaign: Human Kinetics Publishers; 1983. p. 1152–9.

Guillaume Rao obtained his Ph.D. degree in Human Movement Sciences (Biomechanics) from the University of the Mediterranean (Marseille, France) in 2007. He is currently a post-doctoral researcher in the Mechanical Engineering Department at the University of Delaware, Newark, USA. His research interests are primarily in the area of musculoskeletal modeling, analysis of muscle fatigue, and signal processing of the electromyographic signal.

David Amarantini obtained his Ph.D. degree in Biomechanics from the Joseph Fourier University (Grenoble, France) in 2003. He is currently employed as an Assistant Professor in biomechanics at the Paul Sabatier University of Toulouse, France. His main research interests are estimation of muscle forces and joint moments, multi-muscle and multi-degrees of freedom coordination, and biomechanical applications of numerical optimization and signal processing.

Eric Berton obtained his Ph.D. degree in Mechanics in 1992. He is currently Professor in Mechanical Engineering at the University of the Mediterranean, Marseilles, France. Eric Berton is head of the Biomechanics of Movement and Modeling Team and is vice-director at the ''Movement and Perception Laboratory'' (CNRS). His main research interests concern Biomechanics and Movement, Biomechanical Models, and Sport Engineering.

« En ma fin est mon commencement »

IV.   **« En ma fin est mon commencement »** [10]

En synthèse, le chapitre précédent est l'exposé du cheminement scientifique que j'ai suivi à la suite de ma thèse, après avoir été recruté comme ATER à la Faculté de Sciences du Sport de Marseille. J'ai été intégré au Laboratoire d'Aérodynamique et de Biomécanique du Mouvement dans un contexte dynamique de structuration d'une équipe de recherche en biomécanique du mouvement sous la responsabilité d'Eric Berton. Dans cette situation, j'ai eu une première expérience d'animation et de direction de recherche avec le co-encadrement de la thèse de Guillaume Rao (Rao, 2006), enrichie par ma participation active au travail de thèse d'Hugo Centomo (Centomo, 2006) dans le cadre d'une collaboration internationale avec le Département de kinésiologie de l'Université de Montréal. Ma démarche a été de poursuivre mes travaux sur la modélisation EMG-assistée du système musculo-squelettique dans les deux directions suivantes :

- D'une part, reformuler le modèle d'estimation des efforts agoniste et antagoniste développé au cours de ma thèse (Amarantini & Martin, 2004) pour en simplifier la procédure expérimentale de calibration des données EMG, afin d'en généraliser l'application dans une perspective d'analyse de la coordination multi-musculaire lors de mouvements pluri-articulaires complexes (Centomo *et al.,* 2007 ; Rao *et al.,* 2009) y compris en situation de fatigue (Rao *et al.,* 2010).

- D'autre part, contribuer à lever le verrou méthodologique relatif à l'estimation des forces musculaires individuelles, en proposant une solution qui prenne directement en compte le niveau de co-contraction agoniste / antagoniste (Amarantini *et al.,* 2010).

Ces travaux ont apporté une meilleure compréhension du rôle fonctionnel de la co-contraction agoniste / antagoniste en matière de stabilité articulaire et de coordination motrice chez le sujet sain et l'enfant amputé trans-tibial. Ils ont également contribué à identifier la co-contraction agoniste / antagoniste comme i) un facteur important de

---

[10] Devise que Marie Stuart, incontournable et fascinante figure de la Renaissance, alors reine déchue, avait brodée en ses années de captivité : « En ma fin est mon commencement ». Reprise, plus récemment, par Catwoman dans le film éponyme (Pitof, de son vrai nom Jean-Christophe Comar, 2004) contournable, lui.

l'apparition de certaines pathologies ostéo-articulaires chez des individus présentant une altération de la fonction motrice (Centomo *et al.,* 2007), et ii) un marqueur d'une forme d'optimisation du contrôle moteur chez des individus experts présentant une plasticité neuro-musculaire consécutivement à un entrainement en force (Amarantini & Bru, 2015).

Mon parcours scientifique a été marqué par deux autres évènements qui ont déterminé l'orientation thématique et disciplinaire des projets de recherche que j'ai développés jusqu'à aujourd'hui et auxquels je souhaite donner priorité à l'avenir.

Le premier de ces évènements a été mon recrutement comme maître de conférences à l'UFR STAPS de Toulouse au sein du Laboratoire Adaptation Perceptivo-Motrice et Apprentissage. En lien direct avec mes travaux sur la redondance musculaire, ma collaboration avec Marieke Longcamp, chercheure spécialiste en neurosciences cognitives, a fait émerger de nouveaux questionnements relatifs aux mécanismes centraux nerveux de contrôle de l'activité musculaire volontaire et involontaire lors de contractions produites ou imaginées. L'ouverture à ces nouvelles problématiques correspond en tous points à la nécessité réciproque d'étudier les mécanismes nerveux sous-jacents la modulation de l'activité musculaire pour comprendre le fonctionnement biomécanique du système musculo-squelettique (Latash, 2016). Le travail réflexif qui en a découlé a rapidement pointé les limites de l'approche biomécanique – pourtant géniale – pour étudier de manière approfondie l'implication de certains processus d'origine corticale, et tout particulièrement du couplage cortico-musculaire (Hari et Salenius, 1999 ; Mima et Hallett, 1999 ; Salenius et Hari, 2003), dans le contrôle de la co-contraction agoniste / antagoniste. EN LA FIN DE MA DÉMARCHE BIOMÉCANIQUE EST LE COMMENCEMENT DE MA DÉMARCHE NEURO-BIOMÉCANIQUE. Cette totale remise en question de ma démarche scientifique a été une réelle prise de risque, que j'ai pu assumer grâce à la complicité de Marieke Longcamp et le soutien d'Eric Berton. La conversion thématique qui a suivi, que j'ai qualifiée d'« extension thématique » en *Introduction*, m'a amené à développer une nouvelle approche méthodologique novatrice pour étudier le contrôle de la redondance musculaire en combinant l'enregistrement du signal électroencéphalographique (EEG) à celui du signal électromyographique (EMG) et de l'effort musculaire résultant lors de contractions musculaires à un fort pourcentage de la force maximale volontaire. Le projet « Neuro-Biomécanique de la cohérence cortico-musculaire » (*NeuroBiomeCo*), co-porté avec Marieke Longcamp auprès de l'Université Paul Sabatier Toulouse 3 dans le cadre du 1er appel d'offre du Conseil Scientifique « opérations scientifiques 2006-2008 » a été

fondateur de cette nouvelle approche neuro-biomécanique de la redondance musculaire, qui n'amine aujourd'hui et qui est au cœur de mes perspectives de recherche. Ce projet a bénéficié d'une allocation doctorale présidentielle pour le travail de thèse de Fabien Dal Maso (Dal Maso, 2012), que j'ai co-dirigé avec Marieke Longcamp sur la modulation des oscillations corticales et des interactions cortico-musculaires chez des participants entrainés en force ou en endurance (Dal Maso *et al.,* 2012, 2017), et d'un soutien financier significatif pour l'achat d'un système EEG 64 canaux, contribuant du point de vue matériel au développement de ces travaux précurseurs avec une grande autonomie. Il a initié la collaboration avec Jérémie Bigot, actuellement Professeur des Universités à l'Institut de Mathématiques de Bordeaux, qui a permis d'une part de lever les verrous associés au calcul et à la quantification de la cohérence dans le domaine temps-fréquence et, d'autre part, de mettre à disposition en accès libre pour la communauté scientifique un package de fonctions MATLAB (MathWorks Inc., Natick, MA, USA) particulièrement approprié pour ce type d'analyse (Bigot *et al.,* 2011). Il a été, finalement, la première pierre des thèses de Sylvain Cremoux (Cremoux, 2013) et de Camille Charissou (Charissou, 2018) dont les contributions les plus significatives sont présentées dans le chapitre suivant.

Le second évènement a été mon intégration en septembre 2013 à l'Unité Inserm 825 « Imagerie cérébrale et handicaps neurologiques » (UMR 825 Inserm / UPS) devenue « Toulouse Neuro Imaging Center » (ToNIC, UMR 1214 Inserm / UPS) » au 1 janvier 2016. Sans doute porté par l'esprit de l'énigmatique Prof. Glloq, dont mon directeur de DEA avait souligné l'influence sur son parcours, ce changement de laboratoire a contribué à faire décoller mes travaux [11] relatifs à la redondance musculaire chez des patients présentant une altération de la fonction motrice. Plus sérieusement, à la suite de la thèse de David Gasq que j'ai co-dirigée sur l'application de l'analyse temps-fréquence à l'évaluation de l'instabilité posturale chez le patient neurologique (Gasq, 2015), ce nouveau rattachement a enrichi mes travaux de recherche fondamentale en me permettant d'étudier les plasticités centrales et périphériques associées à l'altération de la co-contraction agoniste / antagoniste chez des patients cérébro-lésés. Il a également permis de donner une perspective clinique et translationnelle à mes travaux, en étroite collaboration avec les services des Explorations Fonctionnelles Physiologiques (ch. de serv. : Ivan Tack) et de Médecine Physique et de Réadaptation à l'hôpital Rangueil (ch. de serv. : Philippe Marque) du CHU de Toulouse.

---

[11] « Un brin d'humour ne fait jamais de mal », comme le rappelle de manière convaincante Michel, alias Didier Bourdon, dans *Youpi Matin*, sketch parodique de l'émission *Télématin* présenté par William Leymergie (Les Inconnus, 1991).

82

La neuro-biomécanique, c'est magique !

V.   La neuro-biomécanique, c'est magique !

Comme je l'ai mentionné précédemment, mon parcours scientifique m'a conduit à opérer une transition thématique à la suite de ma nomination comme maître de conférences au sein de la Faculté des Sciences du Sport et du Mouvement Humain de l'Université Paul Sabatier. Ce changement ne relève en rien de subtilités géométrico-sportives relatives à un changement de forme du rond vers l'ovale, mais bien à ma volonté d'apporter des éléments de réponses aux hypothèses restées en suspens sur le lien existant entre la plasticité des mécanismes nerveux centraux de contrôle de la motricité et la régulation de la co-contraction agoniste / antagoniste. L'augmentation significative de co-contraction agoniste / antagoniste chez certaines populations de patients (Cremoux *et al.,* 2012 ; Thomas *et al.,* 1998) pourrait en effet résulter d'une diminution du contrôle cortical des mécanismes inhibiteurs spinaux (Knikou, 2012) ou d'une réorganisation des commandes corticales (Muller-Putz *et al.,* 2007). De la même manière, la diminution de co-contraction suite à un entrainement en force (Amarantini & Bru, 2015 ; Carolan & Cafarelli, 1992) semble liée, au moins en partie, aux adaptations induites aux niveaux cortical (Falvo *et al.,* 2010 ; Griffin & Cafarelli, 2005) et du faisceau cortico-spinal (Aagaard *et al.,* 2002 ; Carroll *et al.,* 2002 ; Vila-Chã *et al.,* 2012). Avec ma alors néo-collègue Marieke Longcamp, spécialiste des neurosciences cognitives, nous avons rapidement pris conscience de la nécessité d'initier une nouvelle démarche au croisement de la biomécanique, des neurosciences et du traitement avancé du signal pour relever ce défi. Ce travail réflexif a abouti au projet *NeuroBioméCo* qui m'a permis, tout en poursuivant mes travaux en biomécanique, de co-encadrer la thèse de Fabien Dal Maso (Dal Maso, 2012) sur les corrélats cérébraux de la co-contraction agoniste / antagoniste, précurseur des thèses de Sylvain Cremoux (Cremoux, 2013) et Camille Charissou (Charissou, 2018).

Ces travaux reposent sur un corpus très étendu de publications en neurosciences et en contrôle moteur qui ont tous établi de manière convergente que le contrôle et la régulation des activations musculaires agonistes et antagonistes sont principalement effectués par les structures spinales et corticales. Au niveau spinal, les motoneurones alpha (α) et les

interneurones inhibiteurs permettent de moduler rapidement les activations musculaires en stimulant la contraction des muscles agonistes et en inhibant la contraction des muscles antagonistes (Pierrot-Deseilligny & Burke, 2005). Au niveau cortical, le cortex moteur primaire contrôle et régule le niveau de stimulation et d'inhibition des motoneurones α et des interneurones inhibiteurs (Crone *et al.,* 1994). Lors de la réalisation d'une action motrice, les premières études par EEG ont mis en évidence une modulation caractéristique de l'activité corticale enregistrée au-dessus du cortex moteur (Gastault, 1952 ; Gastault *et al.,* 1952), décrite plus tard comme une diminution de la puissance spectrale comparativement à un état de repos (Pfurtscheller, 1977, 1981 ; Pfurtscheller & Aranibar, 1977, 1979 ; Pfurtscheller *et al.,* 1997 ; Pfurtscheller & Lopes da Silva, 1999). Cette réactivité somatotopique des rythmes électrocorticaux est connue sous le terme de désynchronisation corticale (abrégé ERD pour 'Event-Related Desynchronization'). L'ERD ~20 Hz au-dessus du cortex moteur reflèterait une augmentation de l'excitabilité cortical spécifiquement liée aux processus de préparation et d'exécution du mouvement (Crone *et al.,* 1998 ; Patino *et al.,* 2006 ; Pfurtscheller, 1981 ; Pfurtscheller *et al.,* 2003 ; Riehle *et al.,* 2004 ; Salmelin & Hari, 1994). Si des travaux ont ainsi montré que l'activation de cortex moteur augmente avec le niveau de force (Mima *et al.,* 1999 ; Stancák *et al.,* 1997), il restait à clarifier l'hypothèse d'un codage supra-spinal de l'activation antagoniste en lien avec la modulation de la co-contraction.

Dans ce contexte, l'étude de Dal Maso *et al.* (2012) a été d'une importance majeure pour mon cheminement scientifique. Ce travail visait à comparer la désynchronisation EEG quantifiée ~20 Hz lors de contractions isométriques des extenseurs et des fléchisseurs du genou entre des participants entraînés en force (ST) et des participants entraînés en endurance (ED) (Figure 6). Du point de vue de ma démarche de recherche, ce travail a été à l'origine de l'ensemble des questions de recherche que j'ai développées depuis, et auxquelles je souhaite donner priorité à l'avenir dans le domaine de la neuro-biomécanique (cf. VI.) Il a révélé pour la première fois une augmentation de l'activation du cortex moteur primaire associée à une diminution du niveau d'activation des muscles antagonistes entre ST et ED. Ces résultats ont permis de suggérer un encodage spécifique de l'activation antagoniste à travers les oscillations corticales dans la bande de fréquence β (21-31 Hz), qui pourrait être responsable de l'amélioration de l'efficience énergétique de la contraction musculaire chez les participants entrainés en force à travers une diminution de la co-contraction agoniste / antagoniste (Amarantini & Bru, 2015). En outre, en mettant en évidence pour la première fois que les adaptations induites par un entraînement régulier en force sont

associées à une modulation des oscillations corticales au cours de contractions isométriques sous-maximales, cette étude a également permis d'enrichir les connaissances fondamentales relatives à la plasticité centrale induite par l'entrainement (Falvo *et al.,* 2010 ; Griffin & Cafarelli, 2005).
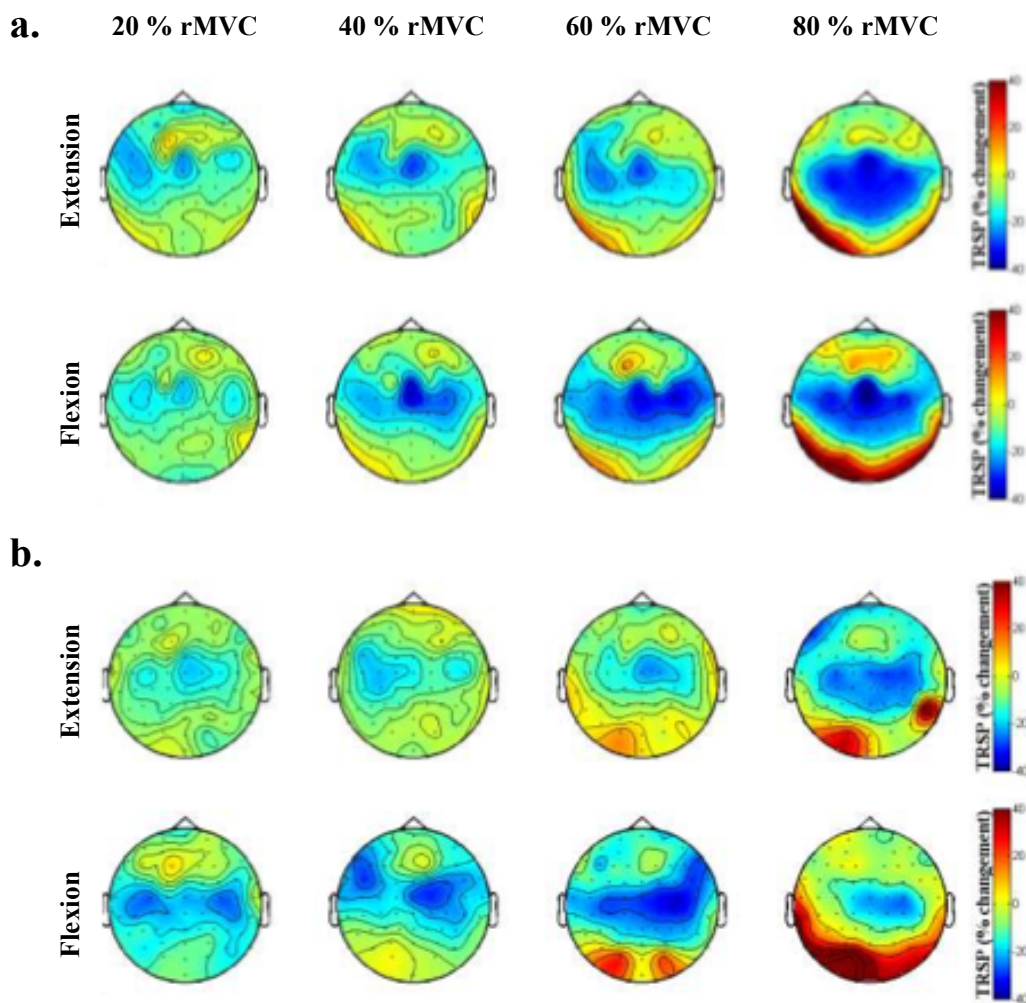
Figure 6, adaptée de Dal Maso (2012) : Représentation topographique de la réactivité des rythmes électrocorticaux dans la bande de fréquences 21-31 Hz (β-haut) chez des participants entrainés en force (**a.**) et en endurance (**b.**) au cours des contractions isométriques en extension et en flexion réalisées à 20, 40, 60 et 80 % de la force maximale volontaire dite « relative » (rMVC) définie comme la force maximale produite sans contamination du signal EEG par des artefacts oculaires, musculaires ou mécaniques liés à la contraction. La désynchronisation EEG, c'est-à-dire la diminution de la puissance spectrale des signaux EEG (en bleu), reflète l'activité corticale liée à la contraction des muscles impliqués dans la production de force.

Ce travail a souligné tout le bien-fondé et la pertinence d'avoir entrepris la conversion thématique de mes activités de recherche de la biomécanique vers la neuro-biomécanique en développant, à partir d'une feuille presque blanche, un paradigme combinant l'analyse EEG à celle de l'EMG et des efforts musculaires. Si cette tâche relevait d'un challenge risqué aussi bien du point de vue méthodologique que de ma démarche scientifique et de sa valorisation, elle est apparue nécessaire et judicieuse pour dépasser les limites d'une approche restreinte à l'analyse biomécanique afin d'étudier de manière approfondie les mécanismes nerveux centraux de contrôle de la redondance musculaire. Les résultats positifs obtenus au début de la thèse de Fabien Dal Maso (Dal Maso, 2012 ; Dal Maso *et al.,* 2012) m'ont encouragé à approfondir l'étude du lien entre la réactivité des rythmes électrocorticaux et la co-contraction agoniste / antagoniste à travers l'étude des interactions cortico-musculaires et intermusculaires. Ces travaux novateurs ont constitué la seconde partie de la thèse de Fabien Dal Maso et se sont poursuivis de manière logique dans le cadre des thèses de Sylvain Cremoux (Cremoux, 2013) et Camille Charissou (Charissou, 2018) que j'ai co-encadrées.

En neurophysiologie et en neurosciences, la notion de cohérence repose sur le constat, aujourd'hui unanimement partagé, que les oscillations cérébrales EEG présentent la particularité d'être couplées avec l'activité EMG (Conway *et al.,* 1995 ; Kilner *et al.,* 1999, 2000 ; Mima *et al.,* 1999 ; Salenius *et al.,* 1997). Même si les premières études étudiant les similarités entre les activités corticale et musculaire remontent aux années 1930 (Adrian & Moruzzi, 1939 ; Jasper & Andrews), ce couplage singulier a été mis en évidence dans le milieu des années 1990 et peut être mesurée par la cohérence cortico-musculaire. Cette dernière correspond à la corrélation entre le signal EEG enregistré au-dessus du cortex moteur et le signal EMG du muscle d'intérêt (Mima & Hallett, 1999), et reflète la communication entre les niveaux central et périphérique. L'étude princeps de Conway *et al.* (1995) a montré que l'activité corticale est significativement corrélée avec l'activité musculaire dans la bande de fréquence ~20 Hz lors d'une contraction musculaire volontaire isométrique. A la lumière de ces résultats, il a été suggéré que la cohérence cortico-musculaire pourrait fournir une information pertinente sur le contrôle supra-spinal de la contraction musculaire (Baker & Baker, 2003 ; Chakarov *et al.,* 2009). De nombreuses études ont enrichi cette première analyse par l'apport de nouvelles connaissances sur les différents facteurs qui interviennent dans la modulation de la cohérence cortico-musculaire. Ces travaux ont établi que, tout en reflétant essentiellement l'implication de commandes

d'origine corticale dans le contrôle direct des muscles impliqués dans la production d'un effort musculaire (Boonstra, 2013 ; Reyes *et al.,* 2017), la cohérence cortico-musculaire peut aussi refléter le contrôle de la circuiterie spinale par les structures corticales et sous-corticales (Hansen *et al.,* 2005 ; Norton & Gorassini, 2006 ; Raethjen *et al.,* 2002 ; Semmler *et al.,* 2013).

Au regard de ces hypothèses, l'analyse des interactions cortico-musculaires m'est apparue particulièrement adaptée pour étudier les stratégies neurales relatives au contrôle de la redondance musculaire et de la co-contraction agoniste / antagoniste. Pour approfondir cette approche, il m'a semblé intéressant de faire appel à l'analyse de cohérence inter-musculaire en complément de celle réalisée par cohérence EEG-EMG (Boonstra *et al.,* 2009). La cohérence intermusculaire, ou cohérence EMG-EMG, mesure la synchronie entre deux signaux EMG issus d'une paire de muscles synergistes (Farmer, 1998 ; Farmer *et al.,* 1993 ; Grosse *et al.,* 2002 ; Rosenberg *et al.,* 1989). D'une part, elle peut être considérée comme un marqueur de la coordination intermusculaire (Jesunathadas *et al.,* 2013 ; Kattla & Lowery, 2010 ; Poston *et al.,* 2010 ; Winges *et al.,* 2008). D'autre part, même si son interprétation peut donner lieu à débat (Dideriksen *et al.,* 2018), sa modulation permet d'émettre des hypothèses quant à l'implication de différentes conductions nerveuses synchrones dans la régulation des activités musculaires (Aumann & Prut, 2015 ; Boonstra, 2013 ; de Vries *et al.,* 2016 ; Erimaki & Christakos, 2008 ; Farmer, 1998 ; Farmer *et al.,* 1993 ; Laine & Valero-Cuevas, 2017 ; Nazarpour *et al.,* 2012 ; Poston *et al.,* 2010).

Dès lors, l'objectif des travaux que j'ai menés sur les cohérences cortico-musculaire et intermusculaires visaient à contribuer à la fois à une meilleure compréhension du contrôle nerveux central de la co-contraction agoniste / antagoniste, et à l'acquisition de connaissances nouvelles sur le rôle fonctionnel encore peu, voire pas connu, de chacune des cohérences EEG-EMG et EMG-EMG. La thèse de Fabien Dal Maso chez des participants entrainés en force *vs* en endurance, puis celle de Sylvain Cremoux chez des participants tétraplégiques, et enfin celle de Camille Charissou sur la préhension se sont inscrites dans cette démarche innovante dont j'ai pu poursuivre le développement grâce à l'étroite collaboration d'Eric Berton et Laurent Vigouroux de l'Institut des Sciences du Mouvement Etienne-Jules Marey à Marseille.

Mais, parce qu'il y a un important « mais » d'ordre méthodologique qui aurait pu compromettre la faisabilité de ces projets, ces travaux n'auraient pas pu aboutir sans remettre en question de manière fondamentale la méthode la plus communément utilisée pour

l'analyse de cohérence. Cette démarche traduit ma volonté, parfois jusqu'au-boutiste, de faire reposer les produits de mes recherches sur des données auxquelles peuvent être accordé le niveau de confiance le plus élevé quelle que soit la complexité des traitements dont elles sont issues. Ce mode de fonctionnement a été au cœur de mon travail de thèse sur l'estimation des moments musculaires, et revêt un caractère absolument essentiel qui conditionne en partie mon cheminement scientifique et ma pratique d'encadrement. Force est de constater que, comme l'ont souligné McClelland *et al.* (2012), une grande partie des travaux sur l'analyse de cohérence en neurosciences perpétuent des méthodes d'analyse inappropriées qui peuvent biaiser les résultats. Non, à mon sens, le débat concernant par exemple la rectification du signal EMG n'a pas lieu d'être (Boonstra & Breakspear, 2012 ; Dakin *et al.,* 2014 ; Farina *et al.,* 2013 ; Farmer & Halliday, 2014 ; Keenan *et al.,* 2012 ; McClelland *et al.,* 2012, 2014a, 2014b ; Myers *et al.,* 2003 ; Neto & Christou, 2010 ; Ward *et al.,* 2013) : l'analyse de cohérence repose sur la modélisation des signaux EEG et/ou EEG comme des processus gaussiens centrés, pré-requis que ne satisfait évidemment pas un signal EMG redressé, même si ce prétraitement permettait d'améliorer la détection de la cohérence (Ward *et al.,* 2013). De la même manière, le fait que la très grande majorité des études fassent appel à une analyse fréquentielle alors que les signaux électrophysiologiques sont fortement non-stationnaires (Allen & MacKinnon, 2010 ; Brittain *et al.,* 2007 ; Cohen & Walden, 2010 ; Mehrkranoon *et al.,* 2011) constitue une limite à la généralisation des résultats.

Ces réflexions ont abouti au développement d'une méthode temps-fréquence novatrice permettant d'évaluer la dépendance entre des processus oscillatoires non stationnaires. Cette importante contribution méthodologique a donné lieu à la publication suivante, présentée de manière détaillée p. 91-105 et illustrée Figure 7 :

- Bigot, J., Longcamp, M., Dal Maso, F., **Amarantini, D.** (2011). A new statistical test based on the wavelet cross-spectrum to detect time-frequency dependence between non-stationary signals: application to the analysis of cortico-muscular interactions. *NeuroImage*. 55(4), 1504-1518.

Cette méthode repose sur la transformation des signaux dans le domaine temps-fréquence par une approche en ondelettes adaptée du package 'cross wavelet and wavelet coherence toolbox for MATLAB' initialement mis à disposition de la communauté scientifique par Grinsted *et al.* (2004) pour des applications dans le domaine de l'océanographie. L'originalité de la méthode développée en collaboration avec Jérémie Bigot, spécialiste en mathématiques et statistiques, est de tester la significativité des

interactions entre les processus oscillatoires sur le spectre croisé des signaux étudiés. Cette approche permet de s'affranchir du problème récurrent de détection de faux positifs sur la cohérence, et présente l'avantage d'être performante même quand le nombre d'essais est faible (Pedrosa *et al.,* 2014). La quantité d'interaction entre les deux signaux est alors quantifiée à partir des valeurs de cohérence retenues sur les régions où le spectre croisé est détecté comme statistiquement significatif. Initialement développée pour l'analyse de la cohérence cortico-musculaire (Bigot *et al.,* 2011 ; Cremoux *et al.,* 2017 ; Dal Maso *et al.,* 2017), cette méthode a été généralisée à la cohérence intermusculaire (Charissou *et al.,* 2016, 2017) puis à la cohérence cortico-corticale (Blais *et al.,* 2018). Elle est ainsi devenue le cadre méthodologique de référence pour l'ensemble des travaux que j'ai menés sur la cohérence et sur la réactivité des rythmes électrocorticaux sur la base d'une analyse temps-fréquence.
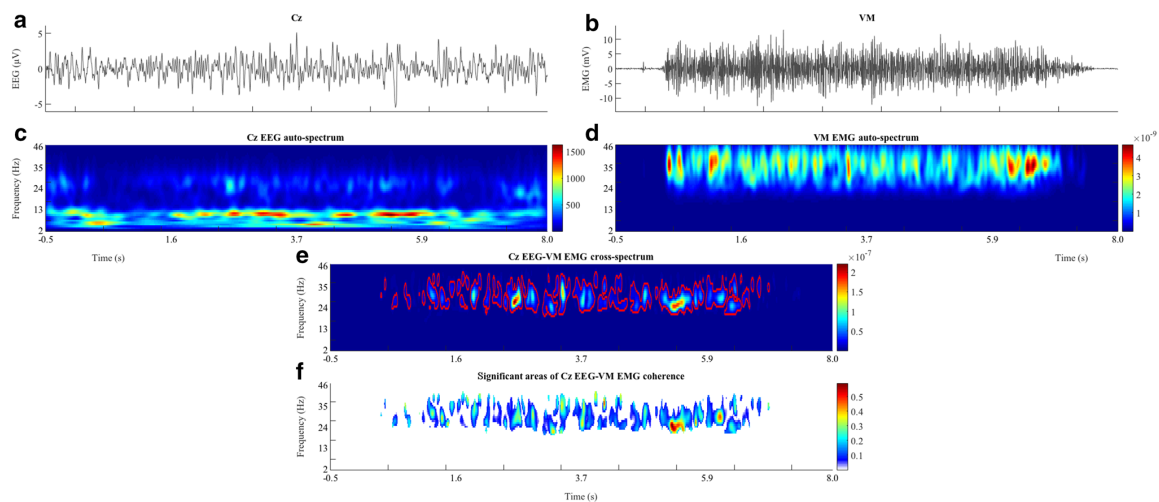
Figure 7, adaptée de Dal Maso *et al.* (2017) : Illustration des étapes recommandées pour le calcul et la quantification de la cohérence cortico-musculaire, ici à partir des données de l'électrode EEG Cz et de l'activité du muscle *vastus medialis* (VM) chez un participant entrainé en force au cours d'une contraction isométrique des extenseurs du genou réalisée à 20 % de la force maximale volontaire « relative ». **a :** Signal moyen de l'électrode Cz EEG. **b :** Signal EMG moyen du muscle VM. **c & d :** Cartes temps-fréquence des auto-spectres du signal EEG de l'électrode Cz (**c**) et du signal EMG du muscle VM (**d**). **e :** Carte temps-fréquence de la densité d'interaction, également appelée « spectre croisé » (c-à-d. : 'cross-spectrum'), entre le signal EEG de l'électrode Cz et le signal EMG du muscle VM. Les contours rouges identifient les régions de la carte temps-fréquence dans lesquelles la corrélation entre les deux signaux est significative. **f :** Carte temps-fréquence des zones significatives de cohérence cortico-musculaire entre le signal EEG de l'électrode Cz et le signal EMG du muscle VM. Dans chaque bande de fréquence d'intérêt (p. ex., bêta (β) : 13-31 Hz), la quantité la cohérence cortico-musculaire est quantifiée comme le volume sous les valeurs de cohérence où une corrélation significative a été détectée sur le spectre croisé entre les séries temporelles EEG et EMG.

En plus des travaux de Sylvain Cremoux sur l'EMG et sur la réactivité des rythmes électrocorticaux (Cremoux *et al.,* 2013a, 2013b, 2016), l'exploration des cohérences cortico-musculaire et intermusculaire a produit de nouvelles connaissances essentielles à une compréhension de la contribution des mécanismes supra-spinaux au contrôle de l'activité musculaire antagoniste et à la régulation de la co-contraction. Ces travaux ont donné lieu à plusieurs publications significatives (Charissou *et al.,* 2017 ; Cremoux *et al.,* 2017 ; Dal Maso *et al.,* 2017), dont les deux suivantes sont présentées de manière détaillée p. 106-127 :

- Cremoux, S., Tallet, J., Dal Maso, F., Berton, E., **Amarantini, D.** (2017). Impaired corticomuscular coherence during isometric elbow flexion contractions in human with cervical Spinal Cord Injury. *European Journal of Neuroscience*, 46(4), 1991-2000.

- Charissou, C., **Amarantini, D.**, Baurès, R., Berton, E., Vigouroux, L. (2017). Effects of hand configuration on muscle force coordination, co-contraction and concomitant intermuscular coupling during maximal isometric flexion of the fingers. *European Journal of Applied Physiology*, 117(11), 2309-2320.

Dans leur ensemble, les résultats de ces études montrent que la modulation de la co-contraction agoniste / antagoniste est associée à celle du couplage entre les niveaux central et périphérique, ainsi qu'entre les muscles eux-mêmes. L'interprétation des mécanismes spinaux et supra-spinaux sous-jacents à ces adaptations doit être conduite avec prudence, mais les connaissances nouvelles apportées par ces études soutiennent l'hypothèse d'un contrôle cortical direct de la co-contraction agoniste / antagoniste lors de tâches isométriques. La contribution des mécanismes impliqués dans cette régulation semble cependant différente selon le rôle fonctionnel qui peut être attribué au groupe musculaire antagoniste et selon l'intégrité du faisceau cortico-spinal. Ces travaux suggèrent également que les couplages cortico-musculaire et intermusculaire ont un rôle fonctionnel important – qui reste à clarifier – dans la régulation de l'activité antagoniste / antagoniste. Ils mettent également en évidence que la modulation de la cohérence constitue un outil particulièrement intéressant pour explorer les mécanismes de contrôle de la contraction musculaire intacte ou altérée, et pour étudier des conséquences d'une plasticité de la voie cortico-spinale sur le contrôle de la redondance musculaire. Les axes prioritaires dans lesquels je souhaite engager mes travaux de recherche permettront d'éclairer ces problématiques sous différentes perspectives dans la continuité de la démarche scientifique que j'ai entreprise en neuro-biomécanique.
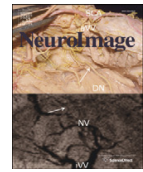
A new statistical test based on the wavelet cross-spectrum to detect time–frequency dependence between non-stationary signals: Application to the analysis of cortico-muscular interactions

Jérémie Bigot [a,b,*], Marieke Longcamp [c,e], Fabien Dal Maso [c], David Amarantini [c,d]

[a] *Institut de Mathématiques de Toulouse et CNRS (UMR 5219), Université de Toulouse, France*
[b] *Center for Mathematical Modelling, Universidad de Chile, Chile*
[c] *LAPMA, Université de Toulouse, France*
[d] *Département de kinésiologie, Centre de réadaptation Marie-Enfant, Université de Montréal, Montreal, Quebec, Canada*
[e] *INCM (UMR 6193), CNRS-Université de la Méditerranée, Marseille, France*

ARTICLE INFO

ABSTRACT

The study of the correlations that may exist between neurophysiological signals is at the heart of modern techniques for data analysis in neuroscience. Wavelet coherence is a popular method to construct a time–frequency map that can be used to analyze the time–frequency correlations between two time series. Coherence is a normalized measure of dependence, for which it is possible to construct confidence intervals, and that is commonly considered as being more interpretable than the wavelet cross-spectrum (WCS). In this paper, we provide empirical and theoretical arguments to show that a significant level of wavelet coherence does not necessarily correspond to a significant level of dependence between random signals, especially when the number of trials is small. In such cases, we demonstrate that the WCS is a much better measure of statistical dependence, and a new statistical test to detect significant values of the cross-spectrum is proposed. This test clearly outperforms the limitations of coherence analysis while still allowing a consistent estimation of the time–frequency correlations between two non-stationary stochastic processes. Simulated data are used to investigate the advantages of this new approach over coherence analysis. The method is also applied to experimental data sets to analyze the time–frequency correlations that may exist between electroencephalogram (EEG) and surface electromyogram (EMG).

© 2011 Elsevier Inc. All rights reserved.

Introduction

In the last decades, the oscillatory behavior of neurophysiological signals has drawn increased attention among neuroscientists Buzsaki and Draguhn (2004), Salenius and Hari (2003), Schnitzler and Gross (2005), Varela et al. (2001). In this framework, the correlations occurring at different frequencies between two or more signals are assumed to indicate oscillatory coupling of neuronal groups. Typically, neurophysiological signals contain noise at different frequency bands and are thus considered as random time series or stochastic processes. Fourier analysis has been widely used for studying the spectral contents of such signals, and the correlations that may exist at different frequencies between electroencephalogram (EEG), electromyogram (EMG) and magnetoencephalogram (MEG) Grosse et al. (2002), Halliday et al. (1995, 1998), Mima and Hallett (1999b), Mima et al. (2000) have been investigated using Fourier coherence. If the investigated signals are assumed to be stationary, then estimates of

the auto and cross-spectra can be calculated to compute an estimation of the coherence at different frequencies. However, signals typically encountered in biomedical applications are non-stationary times series whose frequency behavior changes with time. A powerful alternative to Fourier analysis is the wavelet transform which is a widely developed tool for the study of non-stationary signals as it allows a simultaneous analysis of the content of a signal over time and frequency (see e.g. Mallat (1998) for an introduction to wavelet analysis, and Allen and MacKinnon (2010) for a review and comparison of time–frequency methods for the analysis of EEG signals). In recent years, wavelet coherence has been proposed as an alternative to Fourier coherence for the analysis of time–frequency dependence between two time series. There exists a rich literature on estimating time–frequency dependence between time series using localized transforms, see e.g. Ombao et al. (2001), Sanderson et al. (2010), Whitcher et al. (2005), Whitcher (2000). Applications of time–frequency coherence can be found in neuroscience Lachaux et al. (2002), Ombao and Van Bellegem (2008), Zhan et al. (2006), but also in geophysics Grinsted et al. (2004), Maraun and Kurths (2004), and wind engineering Gurley et al. (2003) to name but a few. The wavelet coherence is a normalized measure (between 0 and 1) of

time–frequency dependence between two time series that is commonly considered as being more interpretable than the wavelet cross-spectrum (WCS). Statistical tests have been proposed in Gish and Cochran (1988), Halliday et al. (1995), Maris et al. (2007) to derive confidence intervals for the Fourier coherence between two time series. A similar statistical test, based on averaging over repeated trials, has been suggested in Zhan et al. (2006) to determine if the time–frequency coherence between neurophysiological signals is significant or not.

The objective of this paper is to discuss the relevance of wavelet coherence as a statistical measure of time–frequency dependence between random time series, and to compare it to the statistical information contained in the WCS. The main contributions are the following: first theoretical and empirical arguments are detailed to show some limitations of wavelet coherence analysis. In particular, we exhibit some drawbacks of the test proposed in Zhan et al. (2006) which may yield an erroneous estimation of time–frequency correlations between two signals.

Second, as an alternative to the limitations of wavelet coherence, a new statistical test to detect significant values of the WCS is proposed. Contrary to the standard test in Gish and Cochran (1988), Halliday et al. (1995), Zhan et al. (2006) to derive confidence intervals for the coherence, our test correctly estimates the areas in the time–frequency plane where the dependence between the time series is truly significant, and does not detect any area where no correlation between the signals exists (an example being the case of two independent Gaussian time series with zero mean). The idea of the test is rather simple. High values of the WCS should correspond to areas in the time–frequency plane where there exists a correlation between the time series. Thus, we first derive a threshold such that, with high probability and under the null hypothesis that the observed signals are independent Gaussian times series, all the values of the WCS fall below this threshold. This means that the values of the WCS that do not correspond to a significant level of time–frequency dependence lie below a certain value with large probability. We show that this probabilistic bound is a threshold that can be easily computed from the data. A standard criticism on the use of the cross-spectrum is that one cannot assess the strength of dependence because this measure does not take into account the variances of the time series contrary to the coherence. To overcome this issue, our method automatically includes an estimation of the variance of the two time series in the computation of the threshold. Therefore, the procedure is fully data-driven, and it is in particular adapted to the case where one pair of time series has a higher magnitude of covariance than the second pair. This new test is also based on averaging over repeated trials as in Zhan et al. (2006). However, the proposed probabilistic bound is non-asymptotic, meaning that it holds for any values of the number of trials and length of the signals. Moreover, the test is valid for any Gaussian processes with zero-mean without assuming stationarity or making parametric assumptions on the covariance functions of the time series. It is therefore very robust in the sense that excellent results can be obtained for a broad class of random signals using very few trials.

Third, a detailed simulation study is proposed to investigate the advantages of this new approach over coherence analysis, and the method is applied to experimental data sets to analyze the time–frequency correlations that may exist between EEG and EMG signals.

Methods

The standard test for detecting significant values of wavelet coherence

First, let us fix the notations and recall the definitions of wavelet transform, WCS and wavelet coherence between stochastic processes. Let $\mathbf{x} = [x(t_k)]_{k=1}^T$ and $\mathbf{y} = [y(t_k)]_{k=1}^T$ denote two random time

series of length T observed at regularly spaced time points t_k. The wavelet transform (WT) of $\mathbf{x}$ (resp. $\mathbf{y}$) at scale $s>0$ and time u is defined as (see e.g. Mallat (1998))

$$W_{\mathbf{x}}(s,u) = \sum_{k=1}^T x(t_k)\overline{\psi_{s,u}(t_k)}$$

where $\bar{z}$ denotes the conjugate of a complex number z,

$$\psi_{s,u}(t_k) = \frac{1}{\sqrt{s}}\psi\left(\frac{t_k-u}{s}\right),$$

and $\psi(\cdot)$ is an oscillating function called wavelet which should satisfy a number of regularity and admissibility conditions (see e.g. Mallat (1998)). The WT can be seen as a time–frequency representation of a signal by converting the scale parameter s to a frequency parameter ω. This correspondence depends on a specific frequency ω_0, which represents the central frequency location of the energy ψ in the Fourier domain, and the relationship between frequency and scale is given by $\omega \approx \frac{\omega_0}{s}$. Thus the WT at frequency ω and time u can be expressed as

$$W_{\mathbf{x}}(\omega,u) = \sum_{k=1}^T x(t_k)\sqrt{\frac{\omega}{\omega_0}}\,\psi\left(\frac{\omega}{\omega_0}(t_k-u)\right).$$

A commonly used wavelet in practice is the Morlet wavelet, which is a complex-valued function, defined as

$$\psi(u) = \pi^{-1/4}e^{i\omega_0 u}e^{-u^2/2}, \tag{2.1}$$

where ω_0 is the central frequency of ψ. A Morlet wavelet is thus a complex sine wave within a Gaussian envelope, and the parameter ω_0 determines the number of oscillations of the wavelet within this envelope. In all the numerical experiments presented in this paper, we took $\omega_0 = 7$ as it is a common choice in wavelet analysis of neurophysiological signals, see e.g. Tallon-Baudry et al. (1996).

The wavelet coherence at frequency ω and time u between the time series $\mathbf{x}$ and $\mathbf{y}$ is then defined by (see e.g. Grinsted et al. (2004), Maraun and Kurths (2004), Zhan et al. (2006))

$$R_{\mathbf{xy}}^2(\omega,u) = \frac{|S_{\mathbf{xy}}(\omega,u)|^2}{S_{\mathbf{x}}(\omega,u)S_{\mathbf{y}}(\omega,u)},$$

where $S_{\mathbf{xy}}(\omega,u)$ is the WCS between $\mathbf{x}$ and $\mathbf{y}$, and $S_{\mathbf{x}}(\omega,u)$ (resp. $S_{\mathbf{y}}(\omega,u)$) is the wavelet auto-spectrum (WAS) of $\mathbf{x}$ (resp. $\mathbf{y}$) defined respectively as

$$S_{\mathbf{xy}}(\omega,u) = \mathbb{E}\left(W_{\mathbf{x}}(\omega,u)\overline{W_{\mathbf{y}}(\omega,u)}\right) \text{ and } S_{\mathbf{x}}(\omega,u) = \mathbb{E}|W_{\mathbf{x}}(\omega,u)|^2,$$

where $\mathbb{E}Z$ denotes the expectation of a random variable Z.

Recall that if one observes n independent realizations $Z_m, m=1,\ldots,n$ of Z then $\mathbb{E}Z = \lim_{n\to+\infty}\frac{1}{n}\sum_{m=1}^n Z_m$ by the law of large numbers. Hence, if one observes data consisting of n repeated trials $(\mathbf{x}_m)_{m=1,\ldots,n} = \left([x_m(t_k)]_{k=1}^T\right)_{m=1,\ldots,n}$ and $(\mathbf{y}_m)_{m=1,\ldots,n} = \left([y_m(t_k)]_{k=1}^T\right)_{m=1,\ldots,n}$ (viewed as n independent realizations of the stochastic processes $\mathbf{x}$ and $\mathbf{y}$, respectively) then the WCS between the two time series is naturally estimated by the following empirical wavelet cross-spectrum

$$\hat{S}_{\mathbf{xy}}(\omega,u) = \frac{1}{n}\sum_{m=1}^n W_{\mathbf{x}_m}(\omega,u)\overline{W_{\mathbf{y}_m}(\omega,u)}$$

and an estimator of the wavelet coherence is given by the following empirical wavelet coherence

$$\hat{R}^2_{\mathbf{xy}}(\omega, u) = \frac{\left| \sum_{m=1}^{n} W_{\mathbf{x}_m}(\omega, u)\overline{W_{\mathbf{y}_m}(\omega, u)} \right|^2}{\left(\sum_{m=1}^{n} |W_{\mathbf{x}_m}(\omega, u)|^2 \right)\left(\sum_{m=1}^{n} |W_{\mathbf{y}_m}(\omega, u)|^2 \right)}.$$

Note that the "true" coherence $R^2_{\mathbf{xy}}(\omega, u)$ is the limit as the number of trials tends to infinity ($n \to +\infty$) of the above empirical coherence $\hat{R}^2_{\mathbf{xy}}(\omega, u)$.

The wavelet coherence is a normalized measure (between 0 and 1) of time–frequency dependence between two time series. Note that if $\mathbf{x}$ and $\mathbf{y}$ are independent zero-mean processes then, at any frequency ω and time u, one has that

$$S_{\mathbf{xy}}(\omega, u) = \mathbb{E}(W_{\mathbf{x}}(\omega, u))\mathbb{E}\left(\overline{W_{\mathbf{y}}(\omega, u)}\right) = 0$$

and thus $R^2_{\mathbf{xy}}(\omega, u) = 0$. To the contrary, if there exists a linear relationship $W_{\mathbf{y}}(\omega, u) = aW_x(\omega, u)$ between $\mathbf{x}$ and $\mathbf{y}$ at some frequency ω and time u with $a \neq 0$, then $S_{\mathbf{xy}}(\omega, u) = \bar{a}S_{\mathbf{x}}(\omega, u)$ and $S_{\mathbf{y}}(\omega, u) = |a|^2 S_{\mathbf{x}}(\omega, u)$ which implies that $R^2_{\mathbf{xy}}(\omega, u) = 1$. Therefore, values of wavelet coherence close to 1 are interpreted as evidence for a significant time–frequency correlation between $\mathbf{x}$ and $\mathbf{y}$. In practice, as a preliminary step, the observed times series can be centered to have zero mean over the n repetitions before computing the empirical wavelet cross-spectrum and coherence.

To derive a threshold to detect automatically significant values of the coherence, most authors in the literature use a procedure proposed in Gish and Cochran (1988) to test the null hypothesis H_0 that the two time series $\mathbf{x}$ and $\mathbf{y}$ are independent Gaussian white noise. Based on repeated observations $(\mathbf{x}_m, \mathbf{y}_m)_{m=1,...,n}$ with $n \geq 2$, it has been shown in Gish and Cochran (1988) that, under H_0, $\hat{R}^2_{\mathbf{xy}}(\omega, u) \leq r_\alpha$ with probability $1 - \alpha$ where the threshold r_α is equal to

$$r_\alpha = 1 - \alpha^{1/(n-1)} \text{ for } 0 \leq \alpha \leq 1.$$

Therefore, at level $\alpha = 5\%$, a detection threshold is $r_\alpha = 1 - 0.05^{1/(n-1)}$ and values of $\hat{R}^2_{\mathbf{xy}}(\omega, u)$ that are above this level are considered as a significant level of coherence.

A new statistical test for detecting significant values of the wavelet cross-spectrum

It is often argued that wavelet coherence is more interpretable than the WCS which is a non-normalized measure of dependence. Indeed, at first glance, it seems difficult to judge if an observed value of the cross-spectrum is significant. Let us recall that the standard method to detect significant values of the coherence is based on a statistical procedure to test the null hypothesis H_0 that the components $x(t_k)$ and $y(t_k)$ of the two time series $\mathbf{x}$ and $\mathbf{y}$ are independent and identically distributed (iid) centered Gaussian variables (that is $x(t_k) \sim_{\text{iid}} N(0, \sigma_x^2)$ and $y(t_k) \sim_{\text{iid}} N(0, \sigma_y^2)$ for $k = 1, ..., T$). We propose to derive a new statistical procedure to test the more general null hypothesis $H_0(\Sigma_x, \Sigma_y)$ that the random time series $\mathbf{x} = [x(t_k)]^T_{k=1}$ and $\mathbf{y} = [y(t_k)]^T_{k=1}$ of length T are independent Gaussian vectors with zero mean and covariance matrix Σ_x and Σ_y respectively, namely

$$H_0\left(\Sigma_x, \Sigma_y\right) : \mathbf{x} \text{ and } \mathbf{y} \text{ are independent vectors of length T with}$$
$$\mathbf{x} \sim N(0, \Sigma_x) \text{ and } \mathbf{y} \sim N\left(0, \Sigma_y\right),$$

where $N(0, \Sigma)$ denotes a Gaussian random vector of length T with zero mean and covariance matrix Σ. Note that $H_0(\Sigma_x, \Sigma_y)$ includes the case where the components of the two time series $\mathbf{x}$ and $\mathbf{y}$ are iid centered Gaussian variables with variance σ_x^2 and σ_y^2 which corresponds to the

choice $\Sigma_x = \sigma_x^2 I_T$ and $\Sigma_y = \sigma_y^2 I_T$ where I_T denotes the identity matrix of size $T \times T$.

Theoretical arguments developed in the Appendix show that under $H_0(\Sigma_x, \Sigma_y)$, $|\hat{S}_{\mathbf{xy}}(\omega, u)| \leq \hat{\lambda}_\alpha$ with probability larger than $1 - \alpha$ where the threshold $\hat{\lambda}_\alpha$ is equal to

$$\hat{\lambda}_\alpha = \frac{\hat{\rho}_x \hat{\rho}_y}{\left(1 + \sqrt{\frac{T}{n}}\right)^2} \left(-\frac{log(\alpha/2)}{n} + \sqrt{-\frac{2log(\alpha/2)}{n}} \right),$$

with $\hat{\rho}_x^2$ (resp. $\hat{\rho}_y^2$) being the largest eigenvalue of the empirical covariance matrix of the time series $\mathbf{x}$ (resp. $\mathbf{y}$). We refer the Appendix for a precise definition, and for the computation of $\hat{\lambda}_\alpha$ in practice. Using such a procedure, the values of the empirical cross-spectrum that are lower than the threshold $\hat{\lambda}_\alpha$ (with e.g. $\alpha = 5\%$) are considered as not significant, whereas the values $|\hat{S}_{\mathbf{xy}}(\omega, u)|$ that are above the threshold $\hat{\lambda}_\alpha$ can be considered as being a truly significant level of time–frequency dependence at frequency ω and time u. Note that this test does not make any parametric assumption on the covariance matrices Σ_x and Σ_y.

As explained previously, coherence is a normalized measure of dependence that is usually considered as being more interpretable than the cross-spectrum which does not take into account the variance of the time series to assess the strength of dependence. Hence, if one pair of time series has a very large auto-spectrum this may cause the cross-spectrum to be very large even in the absence of dependence between two time series. In the computation of the threshold $\hat{\lambda}_\alpha$, the term $\frac{\hat{\rho}_x \hat{\rho}_y}{\left(1 + \sqrt{\frac{T}{n}}\right)^2}$ corresponds to a data-based upper bound of the amplitude of the auto-spectra of the time series.

Indeed, consider first the null hypothesis $H_0(\sigma_x^2 I_T, \sigma_y^2 I_T)$. Under such an assumption, the test is based on the properties that

— with probability larger than $1 - \alpha$: $\left| \hat{S}_{\mathbf{xy}}(\omega, u) \right|^2 \leq \sigma_x^2 \sigma_y^2 * C(n, \alpha)$ where $C(n, \alpha) = \left(-\frac{log(\alpha/2)}{n} + \sqrt{-\frac{2log(\alpha/2)}{n}} \right)^2$ is a constant depending only on n and the level of the test α.
— with large probability: $\hat{\lambda}_\alpha^2 \approx \sigma_x^2 \sigma_y^2 * C(n, \alpha)$.

Hence, the computation of the threshold $\hat{\lambda}_\alpha$ includes an estimation of the variance σ_x^2 and σ_y^2 of each time series.

In the more general case where $\Sigma_x \neq \sigma_x^2 I_T$ or $\Sigma_y \neq \sigma_y^2 I_T$, the test uses the properties that

— with probability larger than $1 - \alpha$: $\left| \hat{S}_{\mathbf{xy}}(\omega, u) \right|^2 \leq S_{\mathbf{x}}(\omega, u)S_{\mathbf{y}}(\omega, u) * C(n, \alpha)$ where $S_{\mathbf{x}}(\omega, u)$ (resp. $S_{\mathbf{y}}(\omega, u)$) is the wavelet auto-spectrum of $\mathbf{x}$ (resp. $\mathbf{y}$).
— with large probability: $\hat{\lambda}_\alpha^2 \geq S_{\mathbf{x}}(\omega, u)S_{\mathbf{y}}(\omega, u) * C(n, \alpha)$, which corresponds to a data-based upper bound for the product of the wavelet auto-spectra of the two time series.

Thus, the above arguments show that the test automatically adapts to the case where one pair of time series has a large wavelet auto-spectra (which results in a large wavelet cross-spectrum) while still controlling the level of dependence between the two time series. Such a test is also non-asymptotic in the sense that it holds for any value of number of trials n and length of the signals T.

Results

Simulated data

Let us first consider some simulated examples to illustrate the differences between the test based on wavelet coherence (using the threshold r_α), and the test based on the WCS (using the data-based

threshold $\hat{\lambda}_\alpha$) for the detection of time–frequency correlations between random signals.

Analysis of time–frequency dependent Gaussian processes

Example 1. We simulate n independent realizations (trials) of the following two Gaussian times series with zero mean of length T = 1000 ms generated with sampling rate 1 kHz:

$$x(t_k) = Z(sin(2\pi\omega_1 t_k)\mathbb{1}_{[0,u_1[}(t_k) + sin(2\pi\omega_2 t_k)\mathbb{1}_{[u_1,u_2[}(t_k)) + \sigma_x\epsilon_{1,k}$$

$$y(t_k) = Z(a_1 sin(2\pi\omega_1 t_k)\mathbb{1}_{[0,u_1[}(t_k) + a_2 sin(2\pi\omega_2 t_k)\mathbb{1}_{[u_1,u_2[}(t_k)) + \sigma_y\epsilon_{2,k},$$
(3.1)

where $Z \sim N(0,1)$, with $t_k = 1,...,T$, $\omega_1 = 10Hz$, $\omega_2 = 30Hz$, $u_1 = 300$ ms, $u_2 = 700$ ms, $a_1 = 1.2$, $a_2 = 1.5$, and where the $\epsilon_{.,k}$'s are independent Gaussian variables with zero mean and variance 1. The parameters σ_x, σ_y are levels of noise that can be adjusted according to the desired signal-to-noise ratio (SNR). For two reals a and b, $\mathbb{1}_{[a,b[}(t_k)$ denotes the function which is equal to 0 if $t_k < a$ or $t_k \geq b$ and to 1 otherwise. Note that for the signal **x**, the SNR is defined as $20 log_{10}(1/\sigma_x)$, and for the signal **y**, the SNR is $20 log_{10}(a_2/\sigma_y)$. The two times series are thus two sine waves with random amplitude of different frequency and time localization with additive Gaussian white noise. It should be noted that the amplitude of the two time series are correlated on the time intervals [0, 300 ms] and [300 ms, 700 ms] at frequency $\omega_1 = 10Hz$ and $\omega_2 = 30Hz$ respectively. Thus **x** and **y** are time–frequency dependent Gaussian processes.

An example of realization for each time series with a SNR equal to −5 dB is given in Fig. 1(a). The wavelet coherence $R_{xy}^2(\omega,u)$ and the "true" WCS $S_{xy}(\omega,u)$ are displayed in Fig. 1(d, e). The empirical coherence $\hat{R}_{xy}^2(\omega,u)$ computed with $n = 10$ trials is displayed in Fig. 2(c) together with a time–frequency map showing (in red) the values of the empirical coherence that are above the threshold r_α with $\alpha = 5\%$.

First, remark the wavelet coherence $R_{xy}^2(\omega,u)$ and the "true" WCS $S_{xy}(\omega,u)$ do not contain the same information. Large value of the cross-spectrum are mainly observed in narrow frequency bands centered at the frequencies $\omega = 10Hz$ and $\omega = 30Hz$ and on the time intervals [0, 300] ms and [300, 700] ms which is consistent with model (2). To the contrary, the large values of wavelet coherence are much more spread in the time–frequency plane, and are found for example around the point $(\omega, u) = 20$ Hz, 300 ms which is somewhat unexpected in the sense that there does not exist such a time–frequency correlation between the two time series in model (3.1).

Secondly, it can be seen from Fig. 2(d) that the statistical test using the threshold r_α finds significant values for the coherence in the time–frequency plane around the points $(\omega, u) = 10$ Hz, 200 ms and $(a, u) = 30$ Hz, 500 ms which is consistent with model (3.1) used to simulate the data. However, the test also detects areas in the time–frequency plane which do not correspond to significant values of the true coherence displayed in Fig. 1(d), or to an expected time–frequency dependence for such data. Now, let us consider the new statistical test suggested in Section 2.2 that is based on the thresholding of the empirical WCS with the data-based threshold $\hat{\lambda}_\alpha$. In Fig. 2(f) we display the result of this thresholding procedure for data from model (3.1), i.e., Example 1 with $n = 10$ trials. One can see that the results are much better than those obtained by thresholding the empirical wavelet coherence with r_α. This new test correctly estimates the areas in the time–frequency plane where the dependence between the time series is truly significant, and does not detect any area where no correlation between the signals exists.

Results obtained using only $n = 2$ trials are displayed in Fig. 3. It can be seen that the results using the threshold r_α to detect significant values of the wavelet coherence are worse. Indeed, most of the truly significant values of the coherence found previously with $n = 10$ trials (around the points $(\omega,u) = (10Hz, 200ms)$ and $(\omega,u) = (30Hz, 500ms)$) fall below the threshold r_α when using $n = 2$ trials. To the contrary, the results displayed in Fig. 3(f) show that our procedure using the threshold $\hat{\lambda}_\alpha$ to detect significant values of the wavelet cross-spectrum performs very well with only $n = 2$ trials.

Coherence detection in the absence of time–frequency dependence between signals

Let us now compare the behavior of the two tests when there is a priori no time–frequency dependence between the signals. A simple example being the case of two independent Gaussian time series with zero mean. For this consider the following simulated experiments:

Example 2. We simulate n independent realizations (trials) of the following two times series of length T = 1000 ms generated with sampling rate 1 kHz:

$$x(t_k) = Z(sin(2\pi\omega_1 t_k)\mathbb{1}_{[0,u_1[}(t_k) + sin(2\pi\omega_2 t_k)\mathbb{1}_{[u_1,u_2[}(t_k)) + \sigma_x\epsilon_{1,k}$$

$$y(t_k) = \sigma_y\epsilon_{2,k},$$
(3.2)

where $Z \sim N(0,1)$, with $t_k = 1,...,T$, $\omega_1 = 10$ Hz, $\omega_2 = 30$ Hz, $u_1 = 300$ ms, $u_2 = 700$ ms, and where the $\epsilon_{j, k}$'s are independent Gaussian variables with zero mean and variance 1. The second signal **y** is therefore a purely Gaussian white noise (we took $\sigma_y = \sigma_x$ in this numerical example), and therefore the coherence between **x** and **y** is expected to be zero. An example of coherence estimation using model (3.2) with $n = 10$ is given in Fig. 4. It can be seen that the test finds many significant values for the wavelet coherence which is clearly not consistent with the data from model (3.2). Consider now the results of our test on Examples 2. One can see from Fig. 4 that all the values of the empirical WCS fall below the data-based threshold $\hat{\lambda}_\alpha$. Therefore, contrary to the test based on the empirical wavelet coherence, our test does not find significant values for the WCS which is consistent with model (3.2).

Example 3. Let us simulate again n independent realizations (trials) $(\mathbf{x}_m)_{m=1,...,n}$ and $(\mathbf{y}_m)_{m=1,...,n}$ of the two times series **x** and **y** from model (3.1) with a SNR equal to −5dB. Then, we apply data shuffling to the trials from the second time series to artificially create independence across samples. More precisely, we propose to compare the detection of time–frequency dependence when computing the wavelet coherence and the WCS either from the raw data $(\mathbf{x}_m)_{m=1,...,n}$ and $(\mathbf{y}_m)_{m=1,...,n}$ or from the shuffled trials $(\mathbf{x}_m)_{m=1,...,n}$ and $(\tilde{\mathbf{y}}_m)_{m=1,...,n}$ where $\tilde{\mathbf{y}}_m = \mathbf{y}_{m+1}$ (see Fig. 5 for an example with $n = 30$). By data shuffling, the time series $\mathbf{x}_m$ and $\mathbf{y}_m$ are independent samples, and it is thus expected there is no coherence between such signals. It can be seen in Fig. 5(f) that the test on coherence detection finds many significant values for the wavelet coherence using the shuffled data which is clearly not satisfactory. To the contrary, Fig. 5(h) shows that our procedure does not find significant values for the WCS when using the shuffled data while still performing a consistent estimation of the WCS when using the raw data, see Fig. 5(d). When the number of trials is small (see Fig. 6(h) with $n = 10$), the results of the data shuffling show remaining significant values of the WCS which are due to large values of the auto-spectrum of **x** and **y**, but with much smaller areas than without data shuffling, see Fig. 6(d).

Robustness to Gaussianity

The derivation of the threshold $\hat{\lambda}_\alpha$ relies on the assumption that the time series are Gaussian processes. Therefore, one may wonder if the test is robust to such an hypothesis.
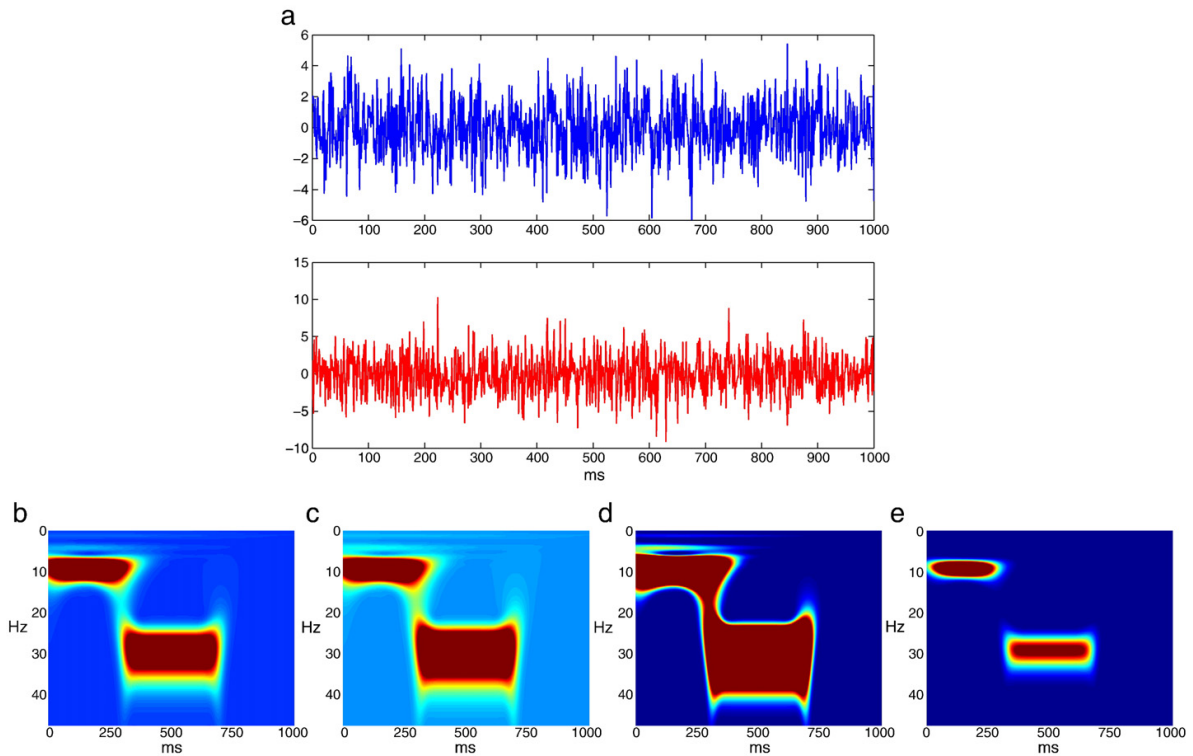
Fig. 1. Example 1 (a) An example of time series $\mathbf{x}_1$ and $\mathbf{y}_1$ generated from model (3.1) with SNR $= -5dB$. (b) Wavelet auto-spectrum $S_{\mathbf{x}}(\omega, u)$. (c) Wavelet auto-spectum $S_{\mathbf{y}}(\omega, u)$. (d) Wavelet coherence $R^2_{\mathbf{xy}}(\omega, u)$. (e) Wavelet cross-spectrum $|S_{\mathbf{xy}}(\omega, u)|^2$. The two time series have a common sine wave of 10 Hz from 1 ms to 300 ms and another common sine wave of 30Hz from 300 ms to 700 ms in each trial.

Example 4. To study robustness to Gaussianity, we simulate n independent realizations (trials) of the following times series of length $T = 1000$ ms with sampling rate 1 kHz.

$$x(t_k) = Z(sin(2\pi\omega_1 t_k)\mathbb{1}_{[0,u_1[}(t_k) + sin(2\pi\omega_2 t_k)\mathbb{1}_{[u_1,u_2[}(t_k)) + \sigma_x \epsilon_{1,k}$$

$$y(t_k) = Z(a_1 sin(2\pi\omega_1 t_k)\mathbb{1}_{[0,u_1[}(t_k) + a_2 sin(2\pi\omega_2 t_k)\mathbb{1}_{[u_1,u_2[}(t_k)) + \sigma_y \epsilon_{2,k},$$
$$(3.3)$$

where Z~Laplace (0,1) and $\epsilon_{1,k}$~iid Laplace (0,1) $\epsilon_{2,k}$~iid Laplace (0,1) with $u_1, u_2, \omega_1, \omega_2, a_1, a_2, \sigma_x, \sigma_y$ chosen as in model (3.1), and where Laplace (0,1) denotes a random variable following a Laplace distribution with zero mean and variance one. The time series in model (3.3) thus follows a Laplace distribution, and are such that they have the same wavelet coherence and WCS than the Gaussian time series from model (3.1) which are displayed in Fig. 1(d, e).

An example of realization from model (3.3) with a SNR equal to -5 dB is displayed in Fig. 7(a). It can be seen that time series following such a Laplace distribution are signals which contains isolated peaks. Hence, when compared to the Gaussian signals from model (3.1) in Fig. 1(a), they are more appropriate to model spiky processes. The results of our testing procedure displayed in Fig. 7(g) are very satisfactory. The test correctly estimates the areas in the time–frequency plane where the dependence between the time series is truly significant. Moreover, it does not detect any area where no correlation between the signals exists. Again, the results using the standard test to detect significant values of the wavelet coherence are not so satisfactory, see Fig. 7(e).

Evaluation of type I and type II errors: effects of n and SNR

To test the performances of this new procedure to detect significant values of time–frequency dependence between random signals, we propose to generate time series from model (3.1) using different values for the SNR and the number of trials, and to compare the results with those given by the standard test in Gish and Cochran (1988); Zhan et al. (2006) to detect significant values of wavelet coherence. Recall that the quality of a statistical test is expressed in terms of its type I and type II error rate. The type I error rate is the probability of a false positive, rejecting the null hypothesis at frequency-time point (w, u) when it is true. The type II error rate is the probability of a false negative i.e. accepting the null hypothesis at frequency-time point (w, u) when there is a truly significant level of time–frequency dependence at (ω, u) between the two-time series. The goal of this simulation study is to evaluate the type I and type II errors of the two tests at various points (w, u) in the time–frequency plane.

The different values for the factors in the simulations are SNR $= -10, -20$ dB and $n = 10, 100$ trials. For each combination of these two factors, we compare the two tests on $M = 100$ repetitions from model (3.1). For $m = 1,... M$, each repetition m consists in simulating n trials from model (3.1) for a given level of SNR. Then, based on these n trials, one constructs two time–frequency testing maps $T_m(\omega, u)$ (one for each test) containing the result of each statistical test with $T_m(\omega, u) = 0$ if the test accepts the null hypothesis H_0, and $T_m(\omega, u) = 1$ if the test rejects H_0. For some repetition m, it is possible that the two (or only one) tests perform poorly or very good. It is therefore important to quantify the behavior of such tests on average, and not to draw conclusions from a single set of n trials.
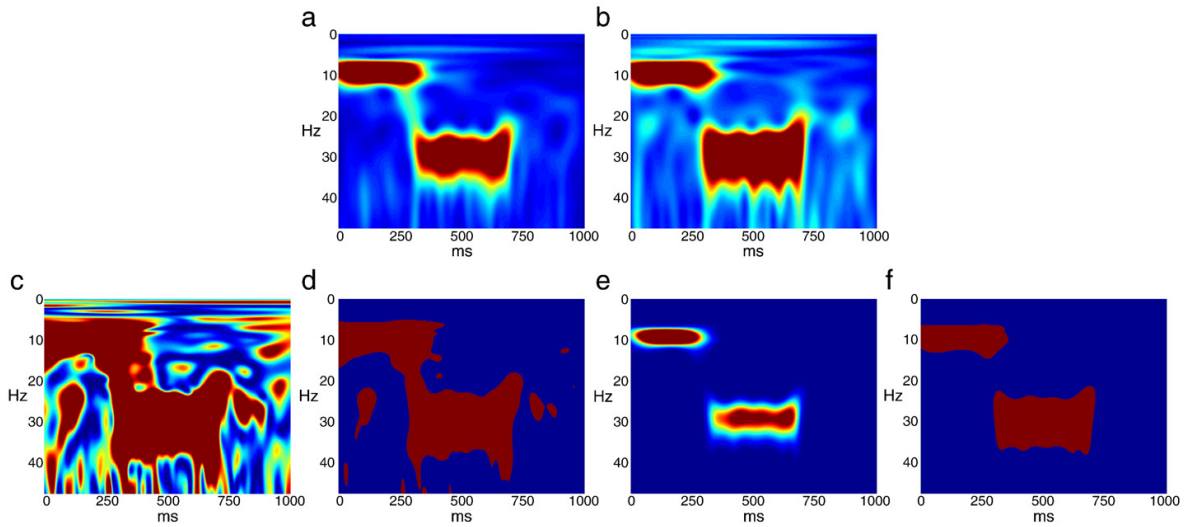
Fig. 2. Example 1—Automatic detection of time–frequency dependence using $n = 10$ trials with SNR $= -5dB$. (a) Empirical wavelet auto-spectum $\hat{S}_{\mathbf{x}}(\omega, u)$. (b) Empirical wavelet auto-spectum $\hat{S}_{\mathbf{y}}(\omega, u)$. (c) Empirical wavelet coherence $\hat{R}^2_{\mathbf{xy}}(\omega, u)$. (d) Significant values (in red) of the empirical wavelet coherence that are above the threshold r_α. (e) Empirical WCS $|\hat{S}_{\mathbf{xy}}(\omega, u)|^2$. (f) Significant values (in red) of the empirical WCS that are above the threshold $\hat{\lambda}_\alpha$. The value of α is 5% for both thresholds.

For this purpose, the performances of each test, over the $M = 100$ repetitions, can be visualized from the following averaged time–frequency testing map:

$$\overline{T}(\omega, u) = \frac{1}{M} \sum_{m=1}^{M} T_m(\omega, u).$$

Note that $\overline{T}(\omega, u)$ is a value between 0 and 1 that can be interpreted as the probability that the test rejects the null hypothesis H_0 at frequency-time point (w, u). Values close to 1 indicate that (on average) the test rejects H_0 at frequency ω and time u, while values close to 0 indicate that (on average) the test accepts H_0. Therefore,

comparing the values $\overline{T}(\omega, u)$ to the true WCS and the true wavelet coherence is way to evaluate the type I and type II errors of each test. Results are displayed in Figs. 8 and 9, and the main comments that can be made are the following:

— as the SNR decreases the time–frequency maps given by the true wavelet coherence $R^2_{\mathbf{xy}}(\omega, u)$ and the true WCS $|S_{\mathbf{xy}}(\omega, u)|^2$ are more and more similar, compare Figs. 1(a), (b) with Figs. 8, 9(a), (d).
— the number of false positives using our test is extremely low. This means that a value of the empirical WCS that is above the threshold $\hat{\lambda}_\alpha$ can be considered as being a truly significant level of
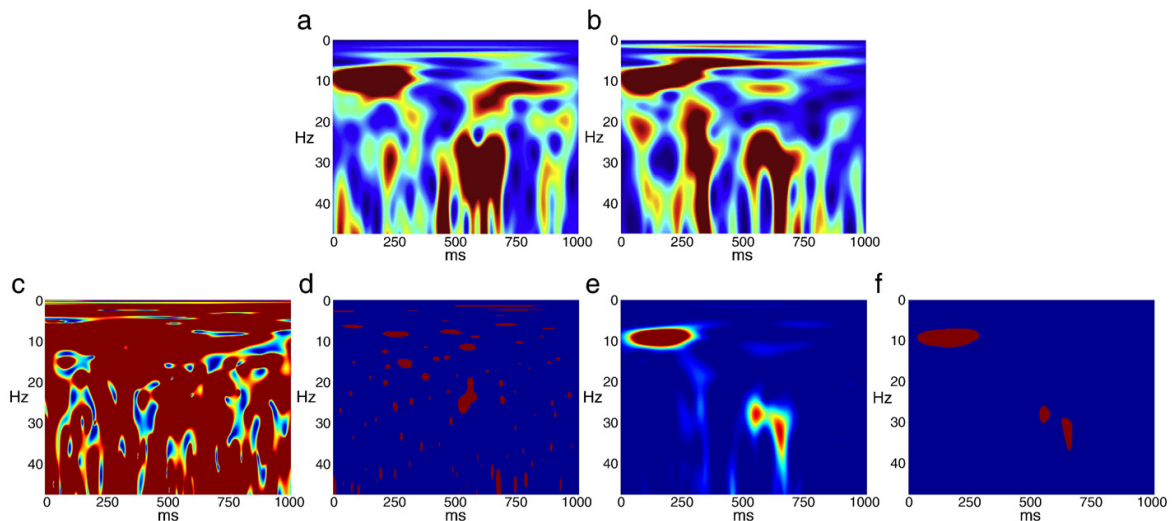
Fig. 3. Example 1—Automatic detection of time–frequency dependence using $n = 2$ trials with SNR $= -5dB$. (a) Empirical wavelet auto-spectum $\hat{S}_{\mathbf{x}}(\omega, u)$. (b) Empirical wavelet auto-spectum $\hat{S}_{\mathbf{y}}(\omega, u)$. (c) Empirical wavelet coherence $\hat{R}^2_{\mathbf{xy}}(\omega, u)$. (d) Significant values (in red) of the empirical wavelet coherence that are above the threshold r_α. (e) Empirical WCS $|\hat{S}_{\mathbf{xy}}(\omega, u)|^2$. (f) Significant values (in red) of the empirical WCS that are above the threshold $\hat{\lambda}_\alpha$ - The value of α is 5% for both thresholds.
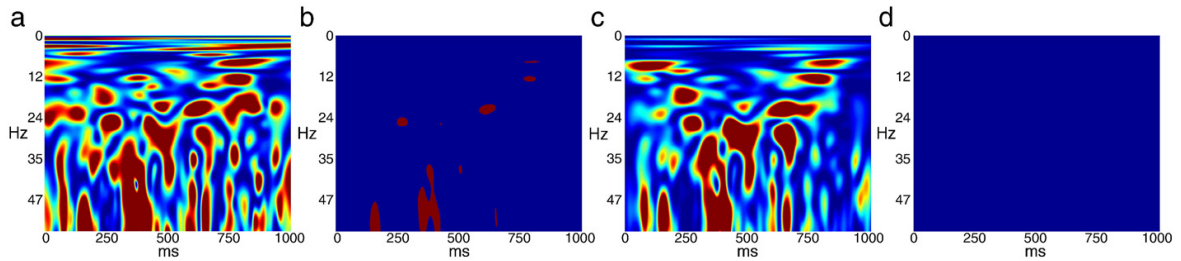
Fig. 4. Example 2—Automatic detection of time–frequency dependence using $n = 10$ trials with SNR $= -10dB$. (a) Empirical wavelet coherence $\hat{R}^2_{\mathbf{xy}}(\omega, u)$. (b) Significant values (in red) of the empirical wavelet coherence that are above the threshold r_α. (c) Empirical WCS $|\hat{S}_{\mathbf{xy}}(\omega, u)|^2$. (d) No significant values are found for the empirical WCS using the threshold $\hat{\lambda}_\alpha$. The value of α is 5% for both thresholds.

time–frequency dependence with a high confidence. To the contrary, the test on empirical wavelet coherence using the threshold r_α yields many false positive.

— when the signal-to-noise ratio is high (SNR $= -10$ db), our test performs very well with few trials ($n = 10$). For a higher SNR, the performances of our test are still very satisfactory when using more trials.

*Application to the analysis of corticomuscular interactions*

To assess the usefulness of the proposed approach with an experimental example, we compare the results of the two tests when applied to neurophysiological signals. Data were collected from a single healthy adult male volunteer, as part of a study on the effects of force level on corticomuscular interactions during submaximal voluntary isometric contractions. The participant was secured in a seated position with the right knee 60° flexed on a calibrated dynamometer (System 4 Pro, Biodex Medical Systems, Shirley, NY, USA) used to record the net joint torque around the knee at 1000 Hz. He was asked to perform blocks of isometric contractions of the right knee extensors at either 10% or 20% of previously determined maximal voluntary contraction (MVC), in a randomized order. Each contraction level was performed 10 times per block for 6 seconds, and

was followed by a 6-second rest interval. Each block was followed by 3 minutes of rest, and overall, 10 blocks were performed leading to a total of 100 contractions per MVC level. The required MVC level was controlled through a visual torque feedback displayed on a screen placed 1 m in front of the participant. The participant had to exert the required torque level as soon as torque feedback was provided, and to maintain it as accurately as possible through the duration of the contraction until disappearance of the torque feedback. During the contractions, he was required to keep its upper body and left lower limb muscles relaxed and its arms rested on each tight.

Electroencephalographic signal (EEG) was recorded reference-free at 1024 Hz using a 64-channel ActiveTwo system (BioSemi, Amsterdam, Netherlands; electrode impedances below 5 k), with electrodes arranged according to the International 10-20 system. The continuous EEG signal was high-pass filtered at 0.5 Hz (zero-lag, 4th order Butterworth filter) and referenced to the FCz electrode. The Cz electrode was selected for further analysis as the electrode optimally located to record cerebral activity directly linked to right lower limb muscles contraction Masakado and Nielsen (2008); Perez et al. (2006). Following suitable skin preparation Hermens et al. (2000), surface electromyographic signal (EMG) was recorded from Vastus Medialis (VM) at 1000 Hz using a Bagnoli-8 system (DE-2.1, Delsys, Inc., Boston, MA, USA) with the reference electrode on the left radial
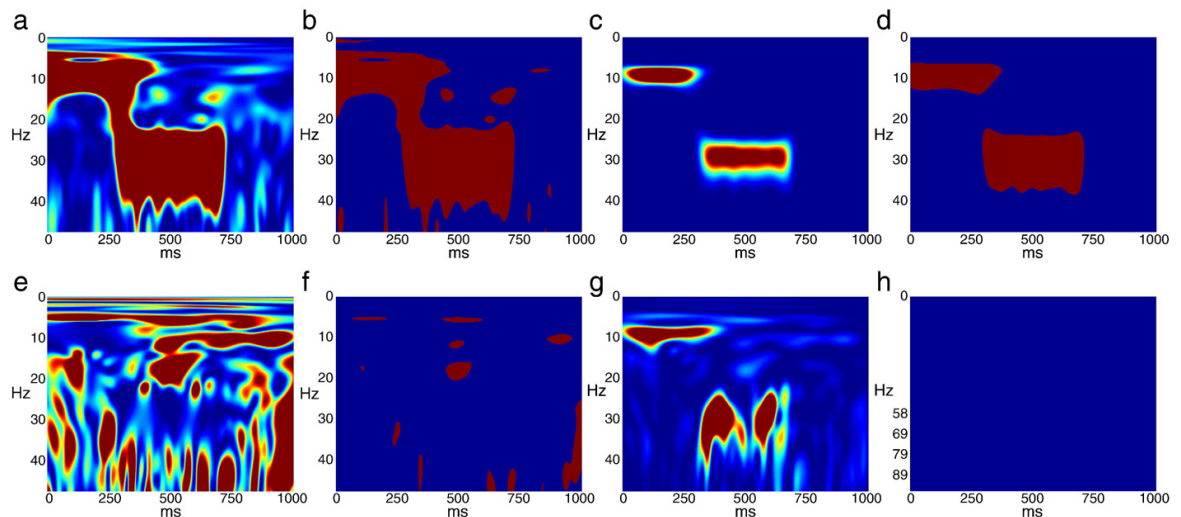

Fig. 5. Example 3—Automatic detection of time–frequency dependence using $n = 30$ trials using either the raw data (first line) or the shuffled data (second line) (a, e) Empirical wavelet coherence $\hat{R}^2_{\mathbf{xy}}(\omega, u)$. (b, f) Significant values (in red) of the empirical wavelet coherence that are above the threshold r_α. (c, g) Empirical WCS $|\hat{S}_{\mathbf{xy}}(\omega, u)|^2$. (d, h) Significant values (in red) of the empirical WCS that are above the threshold $\hat{\lambda}_\alpha$. The value of α is 5% for both thresholds.
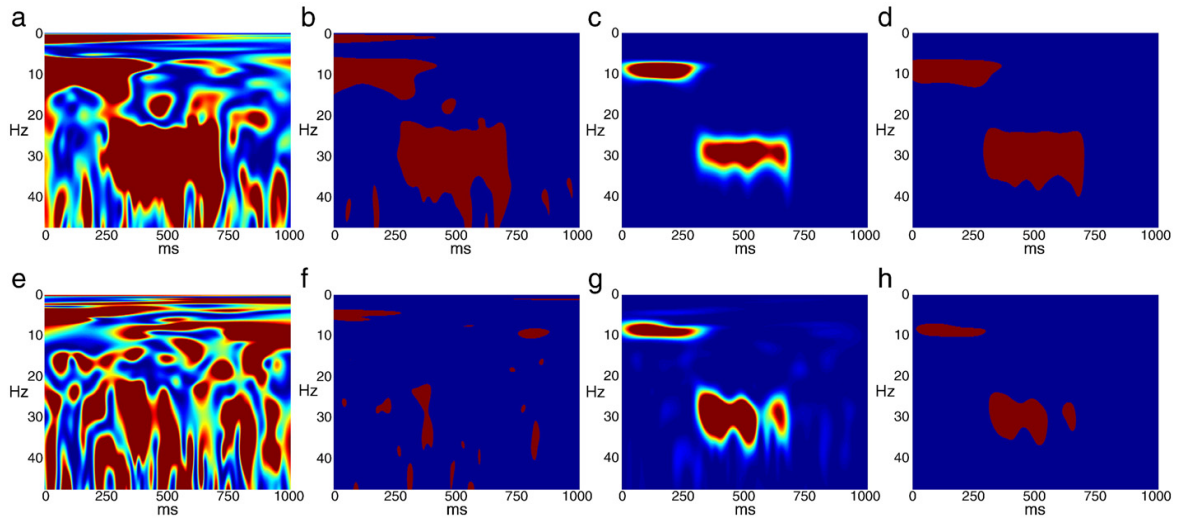
Fig. 6. Example 3—Automatic detection of time–frequency dependence using $n = 10$ trials using either the raw data (first line) or the shuffled data (second line) (a, e) Empirical wavelet coherence $\hat{R}^2_{\mathbf{xy}}(\omega, u)$. (b, f) Significant values (in red) of the empirical wavelet coherence that are above the threshold r_α. (c, g) Empirical WCS $|\hat{S}_{\mathbf{xy}}(\omega, u)|^2$. (d, h) Significant values (in red) of the empirical WCS that are above the threshold $\hat{\lambda}_\alpha$. The value of α is 5% for both thresholds.

styloid. The continuous EMG was resampled to 1024 Hz by third-order spline interpolation and high-pass filtered at 3 Hz (zero-lag, 4th order Butterworth filter).

Continuous data were then epoched from -1000 ms to $+7000$ ms after the onset of the torque feedback, i.e., $T = 8192$ for each contraction. After rejection of the trials contaminated by EEG and/or
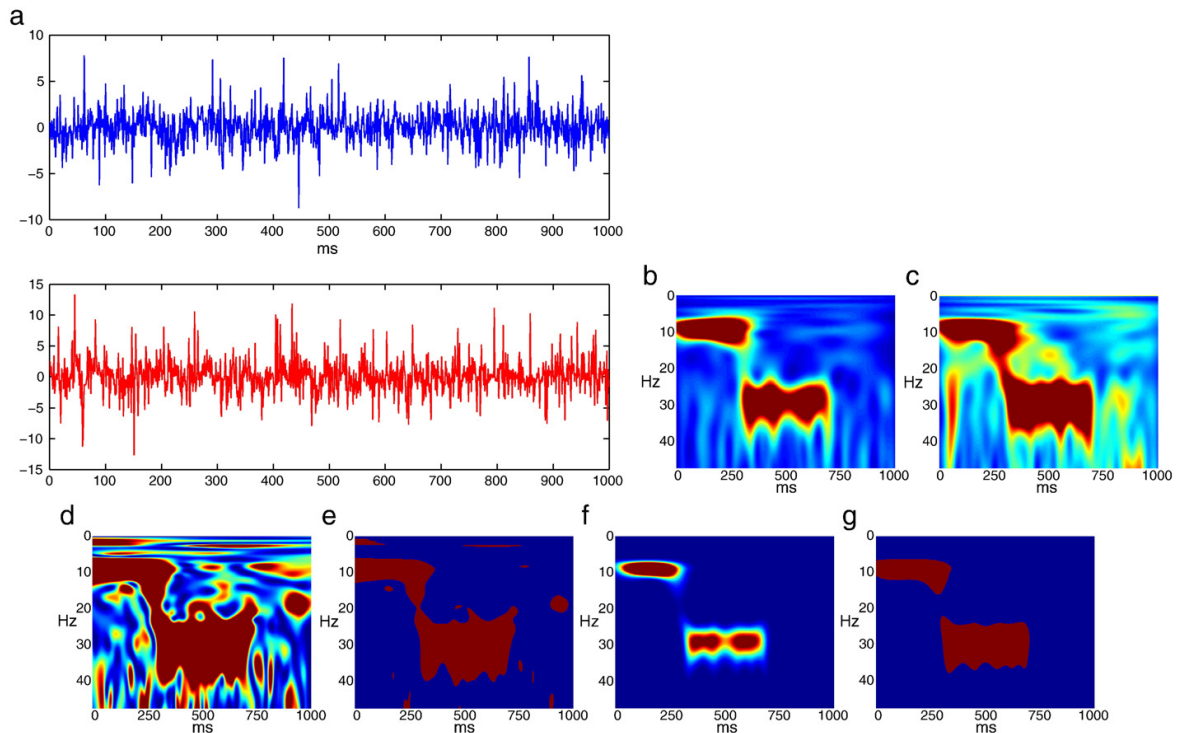

Fig. 7. Example 4—Robustness to Gaussianity using $n = 10$ trials with SNR $= -5dB$. (a) An example of time series $\mathbf{x}_1$ and $\mathbf{y}_1$ generated from model (4). (b) Empirical wavelet auto-spectum $\hat{S}_{\mathbf{x}}(\omega, u)$. (c) Empirical wavelet auto-spectum $\hat{S}_{\mathbf{y}}(\omega, u)$. (d) Empirical wavelet coherence $\hat{R}^2_{\mathbf{xy}}(\omega, u)$. (e) Significant values (in red) of the empirical wavelet coherence that are above the threshold r_α. (f) Empirical WCS $|\hat{S}_{\mathbf{xy}}(\omega, u)|^2$. (g) Significant values (in red) of the empirical WCS that are above the threshold $\hat{\lambda}_\alpha$. The value of α is 5% for both thresholds.
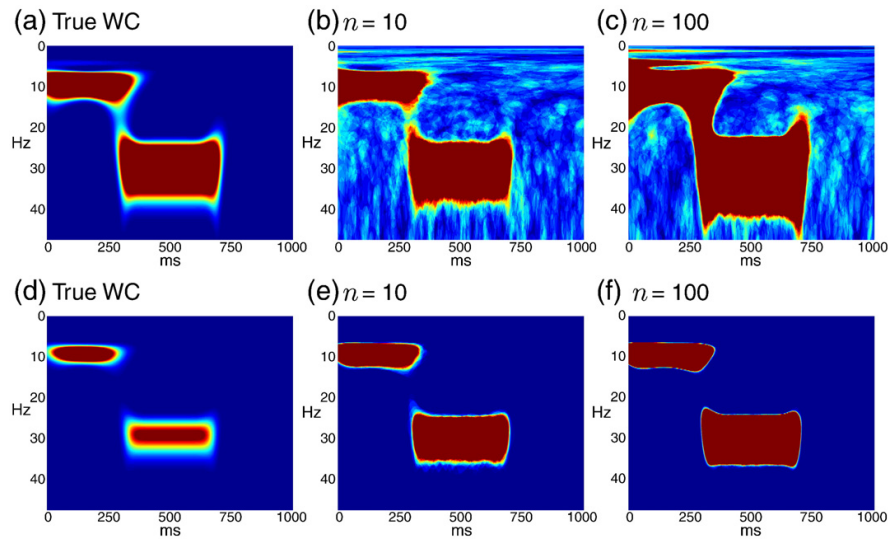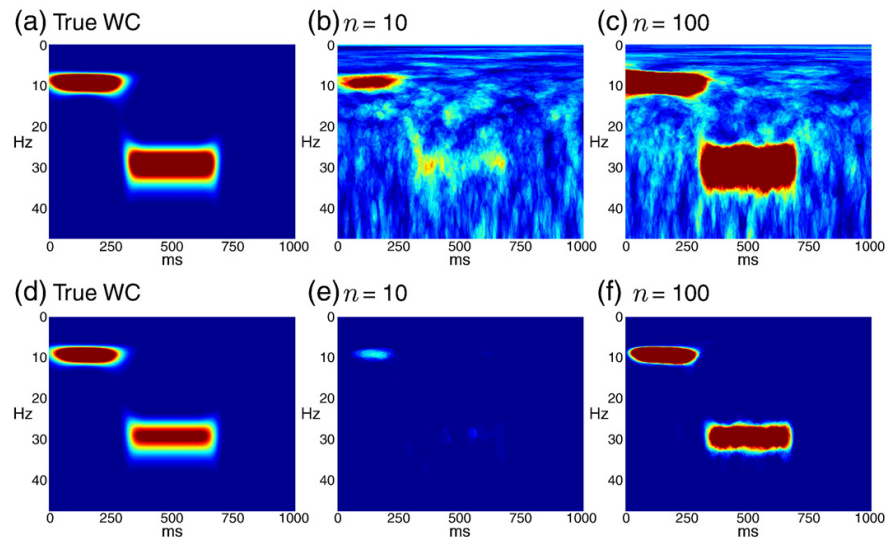
Fig. 8. Simulations with SNR $= -10dB$. (a) True wavelet coherence $R^2_{xy}(\omega, u)$. (d) True WCS $|S_{xy}(\omega, u)|^2$. First row: averaged testing map for the detection of significant values of the wavelet coherence with (b) $n = 10$ and (c) $n = 100$. Second row: averaged testing map for the detection of significant values of the WCS with (e) $n = 10$ and (f) $n = 100$ (red indicates values close to 1 and blue indicates values close to 0).

EMG artefacts, the number of remaining contraction was $n = 70$ for each MVC level. Thus, the value of the ratio T/n is in agreement with the conditions discussed in the Appendix in the sense that T is much larger than n.

Experimental results

Fig. 10 (third to fifth row) present the values of the WCS and the wavelet coherence between EEG and EMG, and their corresponding significant values, for a large number of trials ($n = 70$). First, the

results show that WCS and wavelet coherence contain different information. Large values of wavelet coherence are widely spread in the time–frequency plane whatever the MVC level, without clear difference in the correlation between EEG and EMG during the rest and contraction periods. To the contrary, large values of WCS are observed for non-null MVC levels in frequency bands centered at 10 Hz and 20 Hz, specifically on the time interval of muscular contraction (knee extension). Secondly, the statistical test using the threshold r_α finds isolated significant values of the wavelet coherence, dispersed both in time and frequency, whatever the MVC level. The

Fig. 9. Simulations with SNR $= -20dB$. (a) True wavelet coherence (WC) $R^2_{xy}(\omega, u)$. (b) True WCS $|S_{xy}(\omega, u)|^2$. First row: averaged testing map for the detection of significant values of the wavelet coherence with (b) $n = 10$ and (c) $n = 100$. Second row: averaged testing map for the detection of significant values of the WCS with (e) $n = 10$ and (f) $n = 100$ (red indicates values close to 1 and blue indicates values close to 0).
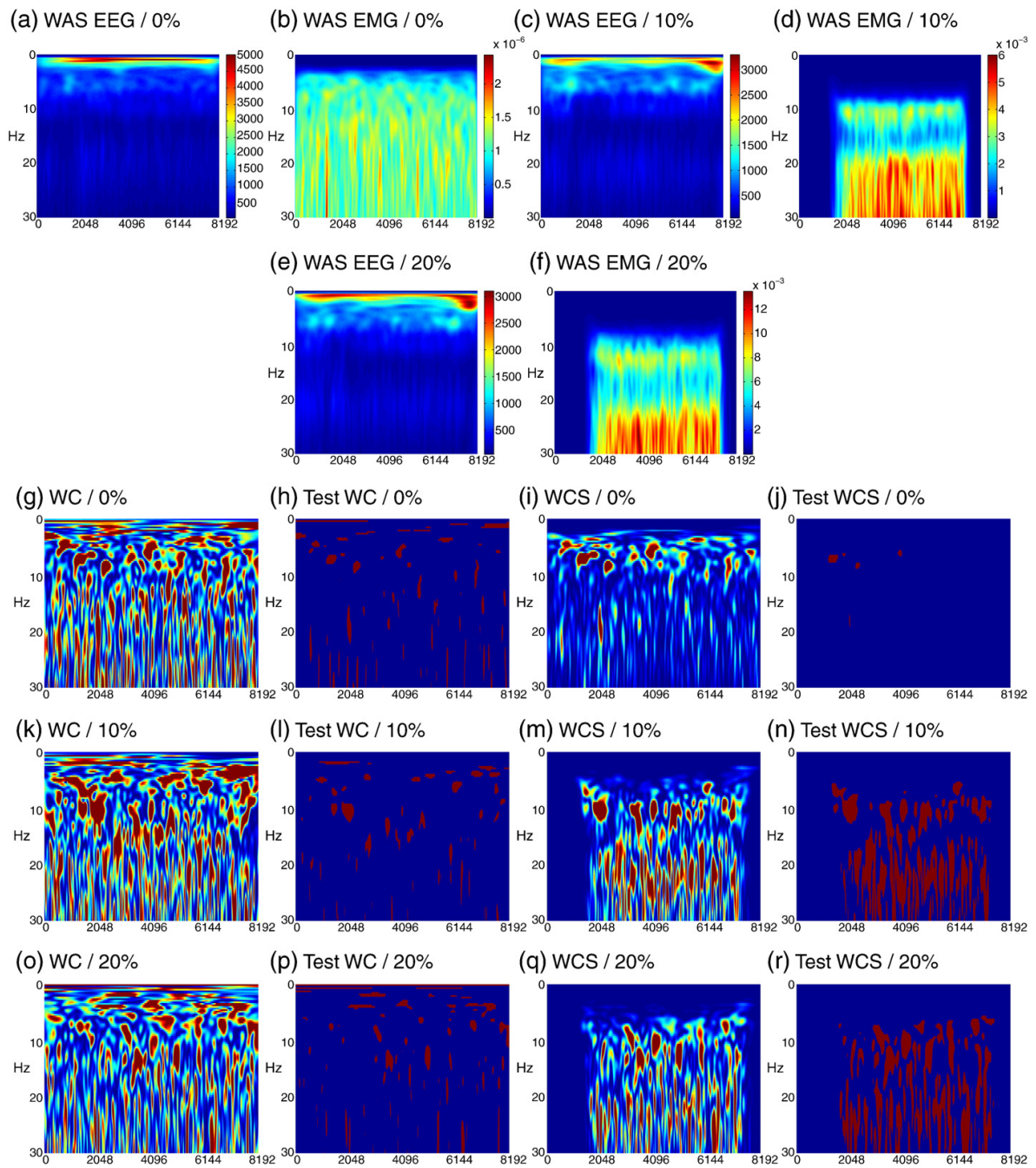
Fig. 10. Analysis of wavelet coherence and WCS on EEG and EMG during isometric contractions of the knee extensors using $n = 70$ trials. First row : empirical wavelet auto-spectra (WAS) of EEG and EMG for MVC = 0%, (no efforts) and MVC = 10%. Second row: WAS of EEG and EMG for MVC = 20%. Third row : data MVC = 0%, (no efforts), fourth row: data for MVC = 10%, fifth row data for MVC = 20%. First column: empirical wavelet coherence $\hat{R}_{\mathbf{xy}}^2(\omega, u)$. Second column: significant values (in red) of the empirical wavelet coherence that are above the threshold r_α. Third column: empirical WCS $|\hat{S}_{\mathbf{xy}}(\omega, u)|^2$. Fourth column: significant values (in red) of the empirical WCS that are above the threshold $\hat{\lambda}_\alpha$.

test detects significant areas in the time–frequency plane during rest periods and does not display a clear correlation between EEG and EMG during maintained knee extension. Opposite to these results, the proposed test using the threshold $\hat{\lambda}_\alpha$ reveals absence of correlation

between EEG and EMG during rest periods and for 0% MVC, and finds bands of significant correlation centered at 10 Hz and 20 Hz during knee extension for 10% and 20% MVC. In addition to these highlighted features, the statistical test based on the thresholding of the WCS

indicates clearer differences in the correlation between EEG and EMG with increased MVC level.

Another benefit of our approach is that it gives good results with very few trials. To illustrate this fact, we display the results obtained when using only $n = 10$ trials (randomly chosen from the 70 trials) in Fig. 11. Using a smaller number of trials ($n = 10$, see Fig. 11), similar

differences are observed between the WCS and the wavelet coherence, and a similar trend is found between the two tests. Apart from this general result, the significant values of the wavelet coherence (threshold r_α) indicate increased dispersion of the correlation between EEG and EMG in the time–frequency plane with $n = 10$ than with n = 70. When thresholding the WCS with $\hat{\lambda}_\alpha$, it
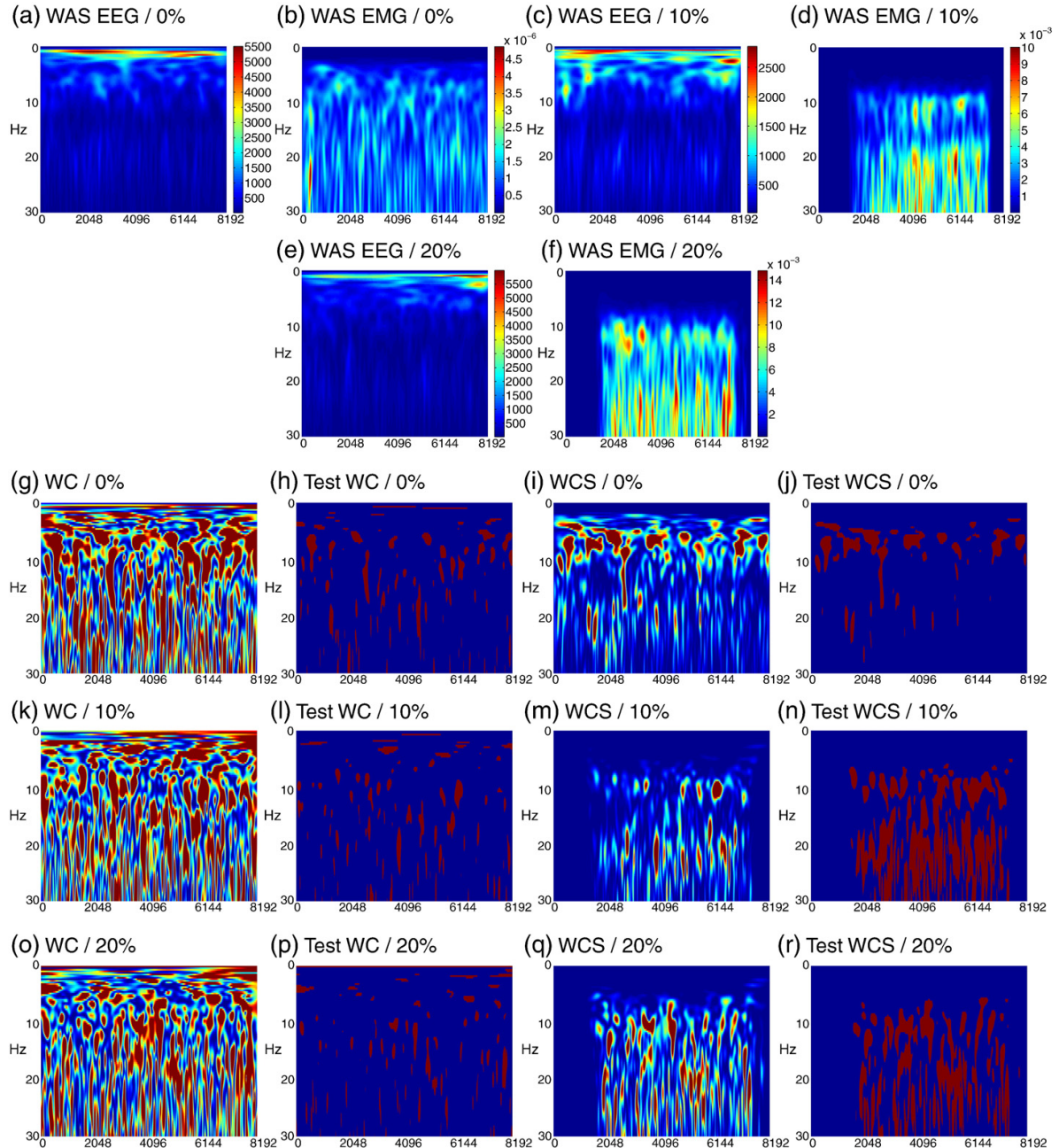
Fig. 11. Analysis of wavelet coherence and WCS on EEG and EMG during isometric contractions of the knee extensors using only $n = 10$ trials. First row : empirical wavelet auto-spectra (WAS) of EEG and EMG for MVC = 0%, (no efforts) and MVC = 10%. Second row: WAS of EEG and EMG for MVC = 20%. Third row : data MVC = 0%, (no efforts), fourth row: data for MVC = 10%, fifth row data for MVC = 20%. First column: empirical wavelet coherence (WC) $\hat{R}^2_{\mathbf{xy}}(\omega, u)$. Second column: significant values (in red) of the empirical wavelet coherence that are above the threshold r_α. Third column: empirical WCS $|\hat{S}_{\mathbf{xy}}(\omega, u)|^2$. Fourth column: significant values (in red) of the empirical WCS that are above the threshold $\hat{\lambda}_\alpha$.

can be seen from Fig. 11(n) and (r) c results i) in broader bands centered at 10 Hz and 20 Hz of significant correlation between EEG and EMG, and ii) in the detection of significant areas centered at 7 Hz during periods of rest, see Fig. 11(j).

Data shuffling

For MVC = 10% and MVC = 20%, Fig. 10(c, e) show large variations of the EEG WAS power specifically in the frequency bands of interest centered at 10 Hz and 20 Hz (i.e., alpha and beta bands, respectively), when compared to the case MVC = 0%, Fig. 10(a). This marked variation in the autospectra causes variation in the WCS, and one may wonder if our test automatically adapts to the change in magnitude of the WCS while still allowing a consistent detection of the significant values of the WCS. To illustrate this point, we used data shuffling as follows. We have compared the results of our test when computing either a WCS using the EEG trials at MVC = 0% and the EMG trials at MVC = 0% or a WCS using the EEG trials at MVC = 20% and the EMG trials at MVC = 0%. In both cases our test detects very few significant values in the WCS (see Fig. 12(d) and compare with Fig. 10(j)).

Discussion

Theoretical comparison of the two statistical procedures

Our method has been analyzed from the point of view of statistical hypothesis testing. With small probability, the procedure rejects the null hypothesis that the repeated trials come from two independent Gaussian time series. The method is thus valid for the analysis of any Gaussian processes with zero mean, in particular for those that are not stationary. Its use is therefore more general than the standard test for significant wavelet coherence detection which is mainly valid for the null hypothesis that the two time series are independent white noise.

Comparison using simulated data

First, if the level of noise in the measurements is high, then the "true" wavelet coherence and the "true" WCS tend to carry the same kind of information on time–frequency dependence between two time series. However, the testing procedures using either the empirical wavelet coherence or the empirical WCS clearly yield to very different conclusions on the nature of the correlations between two times series.

The numerical experiments show that the use of the standard test using wavelet coherence yields erroneous coherence detection (type I error in statistical hypothesis testing), and can miss truly significant values (type II error in statistical hypothesis testing). In particular, this test detects areas the time–frequency plane where no correlation between the signals exists. Indeed, for all values of SNR and numbers

of trials, the test using the wavelet coherence yields many false positive, which clearly questions the interpretability of this test and its level of confidence. To the contrary, our procedure correctly estimates the areas in the time–frequency plane where the dependence between the time series is truly significant. Moreover, our test does not detect any area where no correlation between the signals exists, meaning that our test is more conservative.

These results using data shuffling support the argument that our test is adapted to the case where the auto-spectrum of each time series can be very large. Hence, a value of the WCS above the threshold $\hat{\lambda}_\alpha$ can generally be considered as being due to time–frequency dependence between the signals.

With very few trials, the results obtained using the test on wavelet coherence detection are extremely unsatisfactory. To the contrary, our procedure to detect significant values of the cross-spectrum performs very well with few repeated observations. Indeed, the results obtained with only $n = 2$ trials clearly show that our test correctly estimates the areas in the time–frequency plane where the dependence between the time series is truly significant, and does not detect any area where no correlation between the signals exists.

The numerical examples also demonstrate some robustness of the test to the assumption that the time series should be Gaussian.

To the best of our knowledge, this testing procedure to detect significant values of the cross-spectrum is new, and we believe that it represents a powerful alternative to some limitations of wavelet coherence analysis.

Discussion on the analysis of corticomuscular interactions

Our results on the analysis of the correlation between EEG and EMG, i.e. the corticomuscular interactions, emphasize those obtained from simulated data and illustrate the potential of the proposed test to effectively detect time–frequency dependence between non-stationary signals. Thresholding the WCS with the data-based threshold $\hat{\lambda}_\alpha$ overcomes the effects of both time and frequency scaling observed when thresholding the wavelet coherence with r_α. In agreement with previous findings on corticomuscular synchronization (for review, see Mima and Hallett (1999a); Salenius and Hari (2003)), the proposed statistical test improves the detection of the significant areas of correlation at 10 Hz and 20 Hz between EEG and EMG in the time–frequency plane. Significant corticomuscular interactions were found around 20 Hz in agreement with the literature (see Conway et al. (1995); Kilner et al. (2000); Salenius et al. (1997)) but also around 10 Hz, a finding that is less common but nonetheless reported in several studies in healthy subjects (see Feige et al. (2000); Marsden et al. (2001)) and in Parkinson's patients (see (Raethjen et al. (2009)).

Using our method, corticomuscular interaction was not significant during the rest periods and during 0% MVC trials. This feature is clearly an advantage of the proposed test for application to the analysis of
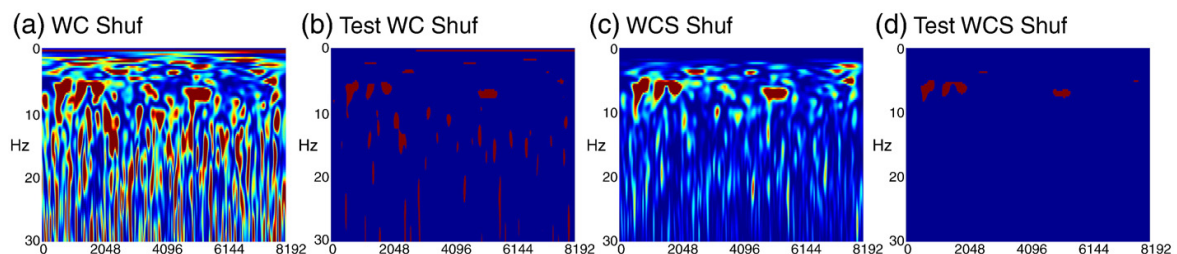
Fig. 12. Analysis of wavelet coherence and WCS on EEG and EMG during isometric contractions of the knee extensors using $n = 70$ trials and data shuffling. First row: data shuffling (EEG − MVC = 20%/EMG − MVC = 0%). First column: empirical wavelet coherence $\hat{R}^2_{xy}(\omega, u)$. Second column: significant values (in red) of the empirical wavelet coherence that are above the threshold r_α. Third column: empirical WCS $|\hat{S}_{xy}(\omega, u)|^2$. Fourth column: significant values (in red) of the empirical WCS that are above the threshold $\hat{\lambda}_\alpha$.

corticomuscular interactions, because it does not detect significant area where no correlation exists between the non-stationary signals. For non-null MVC levels, the statistical test on the WCS with $\hat{\lambda}_\alpha$ does not find significant peaks of coherence dispersed in the time–frequency plane. To the contrary, when the number of trials is high ($n = 70$), the proposed test detects accurate bands of correlation centered at 10 Hz and 20 Hz during the time interval of muscular contraction. With regards to the results from simulated data, one can suggest that the proposed test estimates more correctly the areas in the time–frequency plane where the dependence between EEG and EMG is truly significant, and that it offers the major advantage to reduce the detection of false positive when compared with the test on the wavelet coherence with r_α.

Another benefit of our approach for application to the analysis of corticomuscular interactions is that the improvement of the detection of corticomuscular interactions is maintained with a small number of trials. Despite an observed increased dispersion in frequency with few trials ($n = 10$), the results obtained using the proposed test conserve similar general features to those observed with a large number of trials, which illustrates the practical advantage of our approach when the clinical conditions limit the possible number of experimental trials.

Finally, using data shuffling, we have shown that our method automatically includes an estimation of the variance of the two time series in the computation of the threshold used to detect significant value of the WCS. Indeed, although in the case EEG − MVC = 0%/EMG − MVC = 0% the magnitude of the WCS increases, our test does not detect more significant time–frequency dependence which is consistent with the fact that connectivity does not change when compared to the case EEG − MVC = 20%/EMG − MVC = 0%.

Advantages of WCS in contrast with wavelet coherence

Although the cross-spectrum is a non-normalized measure of dependence, our testing procedure can be used to detect significant values of the empirical WCS since it automatically estimates the amplitude of the auto-spectra of the time series. Coherence is often considered as being more interpretable since it is a normalized measure. However, results in this paper clearly show that a significant value of wavelet coherence (above the detecting threshold r_α) does not necessarily correspond to a significance level of time–frequency dependence. Hence, the use of the standard test on wavelet coherence may lead to erroneous conclusions. To the contrary, in many situations, the use of the WCS combined with our testing procedure is a much more reliable way to detect areas in the time–frequency plane where the dependence between two time series is truly significant. Although we have demonstrated some robustness to Gaussianity, a limitation of our approach is that the derivation of the threshold <mbda$_\alpha$ relies on the assumption that the time series are Gaussian.

Conclusion

We have proposed a new statistical test to detect significant values of the wavelet cross-spectrum between two time series using repeated trials. These values correspond to a truly significant level of time–frequency dependence between the two time series. The test is a fully data-driven procedure based a simple thresholding of the wavelet cross-spectrum. Throughout the paper, this method has been compared with the standard test described in the literature to detect significant values of wavelet coherence between two time series. Comparisons have been made using both theoretical arguments and numerical experiments.

In usual experiments in neuroscience, one often wants to know if a WCS is statistically different from another WCS. This corresponds to the null hypothesis that the difference between two WCS computed

from two data sets consisting of pair of time series is zero. A natural procedure to test such an hypothesis would be to compute the difference between two empirical WCS, and then to use an appropriate threshold to detect significant values of the resulting time–frequency map. We believe that the theoretical arguments developed in this paper could be used to derive such a threshold, which represents an interesting topic for future work.

Appendix

Derivation of the threshold $\hat{\lambda}_\alpha$

The following proposition shows that it is possible to derive under $H_0(\Sigma_x, \Sigma_y)$ a probabilistic upper bound for the empirical WCS (the proof is given in Section 5.2). The key quantities to control such an upper bound are the maximal eigenvalues ρ_x^2 and ρ_y^2 of the covariance matrices Σ_x and Σ_y defined as $\rho_x^2 = max_{v \in \mathbb{R}^T} \frac{v' \Sigma_x v}{v' v}$ and $\rho_y^2 = max_{v \in \mathbb{R}^T} \frac{v' \Sigma_y v}{v' v}$. Note that in the case where $\Sigma_x = \sigma_x^2 I_T$ and $\Sigma_y = \sigma_y^2 I_T$ then $\rho_x^2 = \sigma_x^2$ and $\rho_y^2 = \sigma_y^2$.

Proposition 5.1. Suppose that the hypothesis $H_0(\Sigma_x, \Sigma_y)$ is true. Let $0 < \alpha < 1$. Assume that ψ is the Morlet wavelet defined in (2.1). For any frequency ω and time u, define the threshold

$$\lambda_\alpha = \frac{\rho_x \rho_y}{n} \|\psi_{\omega,u}\|^2 \left(-log(\alpha/2) + \sqrt{-2nlog(\alpha/2)} \right),$$

where $\|\psi_{\omega,u}\|^2 = \sum_{k=1}^{T} |\psi_{\omega,u}(t_k)|^2$ and $\psi_{\omega,u}(t_k) = \sqrt{\frac{\omega}{\omega_0}} \psi\left(\frac{\omega}{\omega_0}(t_k - u)\right)$. Then, for any $n \geq 1$

$$\mathbb{P}\left(|\hat{S}_{\mathbf{xy}}(\omega, u)| > \lambda_\alpha\right) \leq \alpha,$$

where for a random variable Z and a real $t > 0$, the notation $\mathbb{P}(|Z| > t)$ denotes the probability of the event that the modulus of Z is greater than t.

In all the numerical experiments of the paper, *the energy (or L^2 norm) of the wavelet ψ is normalized to be one at all scales (meaning that* $\|\psi_{\omega, u}\|^2 = 1$*)*. Under such an assumption, the threshold λ_α does not depend on the frequency ω and time u, and one can take the simplified threshold

$$\lambda_\alpha = \frac{\rho_x \rho_y}{n} \left(-log(\alpha/2) + \sqrt{-2nlog(\alpha/2)} \right).$$

Note also that Proposition 5.1 can be applied with any mother wavelet ψ that is a real-valued function. However, this procedure is obviously not directly applicable to real data, as the covariance matrices Σ_x and Σ_y and thus the eigenvalues ρ_x^2 and ρ_y^2 are typically unknown in practice. Nevertheless, data-based values for these parameters can be given. Indeed, if one observes n repeated trials $(\mathbf{x}_m)_{m=1,...,n}$ and $(\mathbf{y}_m)_{m=1,...,n}$ (viewed as n independent realizations of the stochastic processes $\mathbf{x}$ and $\mathbf{y}$ respectively) then one can define

unbiased estimators of Σ_x and Σ_y by taking the following empirical covariance matrices

$$\hat{\Sigma}_x = \frac{1}{n}\sum_{m=1}^{n} \mathbf{x}_m\mathbf{x}'_m \text{ and } \hat{\Sigma}_y = \frac{1}{n}\sum_{m=1}^{n} \mathbf{y}_m\mathbf{y}'_m.$$

It is then tempting to estimate ρ_x^2 and ρ_y^2 by the maximal eigenvalues $\hat{\rho}_x^2$ and $\hat{\rho}_y^2$ of the empirical covariance matrices $\hat{\Sigma}_x$ and $\hat{\Sigma}_y$ defined as

$$\hat{\rho}_x^2 = \max_{v\in\mathbb{R}^T}\frac{v'\hat{\Sigma}_x v}{v'v} \text{ and } \hat{\rho}_y^2 = \max_{v\in\mathbb{R}^T}\frac{v'\hat{\Sigma}_y v}{v'v}.$$

Note that the quantities $\hat{\rho}_x^2$ and $\hat{\rho}_y^2$ are not difficult to compute numerically using standard software such as the MATLAB programming environment. However, results from random matrix theory (see El Karoui (2007) and references therein) show that $\hat{\rho}_x^2$ and $\hat{\rho}_y^2$ are not consistent estimators of ρ_x^2 and ρ_y^2. Indeed, in the case where $\Sigma_x = \sigma_x^2 I_T$ and $\Sigma_y = \sigma_y^2 I_T$ then

$$\lim_{n\to+\infty,T\to+\infty} \hat{\rho}_x = \sigma_x(1+\sqrt{\gamma}) \text{ and } \lim_{n\to+\infty,T\to+\infty} \hat{\rho}_y = \sigma_y(1+\sqrt{\gamma})$$

where $\gamma = \lim_{n\to+\infty,T\to+\infty}\frac{T}{n}$. Therefore if $\gamma>0$ then $\hat{\rho}_x$ does not converge to σ_x. The coefficient γ reflects the ratio between the length T of the time series and the number of trials n. Typically, T is much larger than n and in practice, the ratio $\frac{T}{n}$ can be larger than 10 or 100, meaning that the ratio $\frac{\hat{\rho}_x}{\sigma_x}\approx(1+\sqrt{\gamma})$ is not close to one. This phenomena is a well known problem for the statistical estimation of large covariance matrices (see e.g. Bickel and Levina (2008) and references therein) in the high-dimensional data setting when the size of the data (here the number of time points T) is much larger than the number of repeated observations n.

In the more general case where $\Sigma_x \neq \sigma_x^2 I_T$ or $\Sigma_y \neq \sigma_y^2 I_T$, using Theorem II.13 in Davidson and Szarek (2001) it can be shown that for any value of $0<\beta\leq 1$ and any fixed $n\geq 1$ and $T\geq 1$ then

$$\mathbb{P}\left(\hat{\rho}_x\geq\rho_x\left(1+\sqrt{\frac{T}{n}}+\sqrt{\frac{-2\log(\beta)}{n}}\right)\right)\leq\beta.$$

These results therefore suggest to estimate ρ_x and ρ_y by $\hat{\rho}_x\left/\left(1+\sqrt{\frac{T}{n}}\right)\right.$ and $\hat{\rho}_y\left/\left(1+\sqrt{\frac{T}{n}}\right)\right.$ which leads to the use of the following data-based threshold $\hat{\lambda}_\alpha$ (in the case where the energy of the wavelet ψ is normalized to be one)

$$\hat{\lambda}_\alpha = \frac{\hat{\rho}_x\hat{\rho}_y}{\left(1+\sqrt{\frac{T}{n}}\right)^2}\left(-\frac{\log(\alpha/2)}{n}+\sqrt{-\frac{2\log(\alpha/2)}{n}}\right).$$

Proof of Proposition 5.1

Let $Z = \hat{S}_{\mathbf{xy}}(\omega,u)$ and remark that under H_0 the random variable Z can be written as

$$Z = \frac{1}{n}\sum_{m=1}^{n} X'_{m,1}\Sigma_x^{1/2}a\overline{a}'\Sigma_y^{1/2}X_{m,2},$$

where $X_{m,1}$ and $X_{m,2}$ are independent centered Gaussian vector in $\mathbb{R}^T$ with covariance matrix the identity, and a is the deterministic vector in $\mathbb{C}^T$ with entries

$$a = \left[\psi_{\omega,u}(t_k)\right]_{k=1}^T \text{ where } \psi_{\omega,u}(t_k) = \sqrt{\frac{\omega}{\omega_0}}\psi\left(\frac{\omega}{\omega_0}(t_k-u)\right).$$

Then, define the following vector $X\in\mathbb{R}^{n2T}$ by concatenation of the vectors $X_{m,1}$ and $X_{m,2}$ in the following way:

$$X = \begin{pmatrix}X_{m,1}\\X_{m,2}\end{pmatrix}_{m=1,\ldots,n}\in\mathbb{R}^{n2T}.$$

Note that X is a centered Gaussian vector with covariance matrix the identity. Then, define the $2T\times 2T$ matrix with complex entries

$$A_{xy} = \frac{1}{2n}\begin{pmatrix}\Sigma_x^{1/2} & 0\\0 & \Sigma_x^{1/2}\end{pmatrix}\begin{pmatrix}0 & a\overline{a}'\\\overline{a}a' & 0\end{pmatrix}\begin{pmatrix}\Sigma_y^{1/2} & 0\\0 & \Sigma_y^{1/2}\end{pmatrix}$$

and introduce the following $n2T\times n2T$ block-diagonal matrix

$$A = \begin{pmatrix}A_{xy} & 0 & \ldots & 0\\0 & A_{xy} & 0 & 0\\\vdots & 0 & \ldots & 0\\0 & 0 & 0 & A_{xy}\end{pmatrix}.$$

Given the definition (2.1) of the Morlet wavelet ψ, one can check that the matrix $a\overline{a}'$ is Hermitian which implies that the matrices A_{xy} and A are Hermitian. Then, one can remark that the random variable mphZ can be written in the form of a χ^2 variable as

$$Z = X'AX.$$

Now, the result of Proposition 5.1 follows from the lemma below (its proof follows from standard arguments on the concentration of χ^2 variables, see e.g. Proposition 3 in Comte (2001) and Lemma 1 in Laurent and Massart (2000)):

Lemma 5.2. Let $X\in\mathbb{R}^p$ be a centered Gaussian vector with covariance matrix the identity. Let Γ be a $p\times p$ Hermitian matrix (with complex entries). Let $\gamma_1, \ldots, \gamma_p$ be the eigenvalues of Γ. Define

$$\gamma = \max_{1\leq i\leq p}\{|\gamma_i|\} \text{ and } s^2 = \sum_{i=1}^p |\gamma_i|^2.$$

Then, for any $\eta>0$ one has that

$$\mathbb{P}\left(|X'\Gamma X - tr(\Gamma)|\geq 2\gamma\eta + 2\sqrt{s^2\eta}\right)\leq 2exp(-\eta),$$

where $tr(\Gamma)$ is the trace of the matrix Γ.

Then, remark that the eigenvalues of the $2T\times 2T$ Hermitian matrix A_{xy} are smallest than $\frac{\rho_x\rho_y}{2n}\|a\|^2$, where $\|z\|$ denotes the standard Euclidean norm of a vector z in C^T. Therefore, if one denotes by $\gamma_1, \ldots, \gamma_p$ the eigenvalues of A with $p=2nT$, it follows that

$$\max_{1\leq i\leq p}\{|\gamma_i|\}\leq\frac{\rho_x\rho_y}{2n}\|a\|^2.$$

Remark also that A_{xy}^2 is of rank 2 with eigenvalues bounded by $\left(\frac{\rho_x\rho_y}{2n}\|a\|^2\right)^2$ and therefore

$$\sum_{i=1}^p |\gamma_i|^2 = tr(A^2) = ntr(A_{xy}^2)\leq 2n\left(\frac{\rho_x\rho_y}{2n}\|a\|^2\right)^2 = \frac{\rho_x^2\rho_y^2}{2n}\|a\|^4.$$

Finally, note that

$$\|a\|^2 = \|\psi_{\omega,u}\|^2 \text{ where } \|\psi_{\omega,u}\|^2 = \sum_{k=1}^T |\psi_{\omega,u}(t_k)|^2.$$

Therefore, using that $tr(A) = 0$ and by applying Lemma 5.2 with $p = 2nT, \Gamma = A, \gamma = \frac{1}{2n}\rho_x\rho_y\|\psi_{\omega,u}\|^2$ and $s^2 = \frac{1}{2n}\rho_x^2\rho_y^2\|\psi_{\omega,u}\|^4$, it follows that for any $\eta > 0$

$$\mathbb{P}\left(|Z| \geq \frac{\rho_x\rho_y}{n}\|\psi_{\omega,u}\|^2\left(\eta + \sqrt{2m\eta}\right)\right) \leq 2exp(-\eta).$$

Thus, the result of Proposition 5.1 follows by taking $\eta = -log(\alpha/2)$ which completes the proof. □

References

Allen, D., MacKinnon, C.D., 2010. Time–frequency analysis of movement-related spectral power in eeg during repetitive movements: a comparison of methods. J. Neurosci. Meth. 186, 107–115.

Bickel, P., Levina, E., 2008. Covariance regularization by thresholding. Ann. Stat. 36, 2577–2604.

Buzsaki, G., Draguhn, A., 2004. Neuronal oscillations in cortical networks. Science 304, 1926–1929.

Comte, F., 2001. Adaptative estimation of the spectrum of a stationary gaussian sequence. Bernoulli 7, 267–298.

Conway, B., Halliday, D., Farmer, S., Shahani, U., Maas, P., Weir, A.I., et al., 1995. Synchronization between motor cortex and spinal motoneuronal pool during the performance of a maintained motor task in man. J. Physiol. 489, 917–924.

Davidson, K.R., Szarek, S.J., 2001. Local operator theory, random matrices and Banach spaces. Handbook of the geometry of Banach spaces, Vol. I. North-Holland, Amsterdam, pp. 317–366.

El Karoui, N., 2007. Tracy–Widom limit for the largest eigenvalue of a large class of complex sample covariance matrices. Ann. Probab. 35, 663–714.

Feige, B., Aertsen, A., Kristeva-Feige, R., 2000. Dynamic synchronization between multiple cortical motor areas and muscle activity in phasic voluntary movements. J. Neurophysiol. 84, 2622–2629.

Gish, H., Cochran, D., 1988. Generalized coherence. International Conference on Acoustics, Speech, and Signal Processing, pp. 2745–2748.

Grinsted, A., Moore, J.C., Jevrejeva, S., 2004. Application of the cross wavelet transform and wavelet coherence to geophysical time series. Nonlinear Processes Geophys. 11, 561–566.

Grosse, P., Cassidy, M., Brown, P., 2002. Eeg–emg, meg–emg and emg–emg frequency analysis: physiological principles and clinical applications. Clin. Neurophysiol. 113, 1523–1531.

Gurley, G., Kijewski, T., Kareem, A., 2003. First- and higher-order correlation detection using wavelet transforms. J. Neurosci. Meth. 129, 188–201.

Halliday, D., Conway, B., Farmer, S., Rosenberg, J., 1998. Using electroencephalography to study functional coupling between cortical activity and electromyograms during voluntary contractions in humans. Neurosci. Lett. 241, 5–8.

Halliday, D.M., Rosenberg, J.R., Amjad, A.M., Breeze, P., Conway, B.A., Farmer, S.F., 1995. A framework for the analysis of mixed time series/point process data—theory and application to the study of physiological tremor, single motor unit discharges and electromyograms. Progr. Biophys. Mol. Biol. 64, 237–278.

Hermens, H., Freriks, B., Disselhorst-Klug, C., Rau, G., 2000. Development of recommendations for semg sensors and sensor placement procedures. J. Electromyogr. Kinesiol. 10, 361–374.

Kilner, J., Baker, S., Salenius, S., Hari, R., Lemon, R., 2000. Human cortical muscle coherence is directly related to specific motor parameters. J. Neurosci. 20, 8838–8845.

Lachaux, J.P., Lutz, A., Rudrauf, D., Cosmelli, D., Le Van Quyen, M., Martinerie, J., Varela, F., 2002. Estimating the time-course of coherence between single-trial brain signals: an introduction to wavelet coherence. Neurophysiol. Clin. 32, 157–174.

Laurent, B., Massart, P., 2000. Adaptive estimation of a quadratic functional by model selection. Ann. Stat. 28, 1302–1338.

Mallat, S., 1998. A Wavelet Tour of Signal Processing. Academic Press, New York.

Maraun, D., Kurths, J., 2004. Cross wavelet analysis: significance testing and pitfalls. Nonlinear Processes Geophys. 11, 505–514.

Maris, E., Schoffelen, J.M., Fries, P., 2007. Nonparametric statistical testing of coherence differences. J. Neurosci. Meth. 163, 161–175.

Marsden, J., Brown, P., Salenius, S., 2001. Involvement of the sensorimotor cortex in physiological force and action tremor. NeuroReport 12, 1937–1941.

Masakado, Y., Nielsen, J., 2008. Task-and phase-related changes in cortico-muscular coherence. Keio J. Med. 57, 50–56.

Mima, T., Hallett, M., 1999a. Corticomuscular coherence: a review. J. Clin. Neurophysiol. 16, 501–511.

Mima, T., Hallett, M., 1999b. Electroencephalographic analysis of cortico-muscular coherence: reference effect, conduction and generator. Clin. Neurophysiol. 110, 1892–1899.

Mima, T., Steger, J., Gerlo, C., Hallett, M., 2000. Electroencephalographic measurement of motor cortex control of muscle activity in humans. Clin. Neurophysiol. 111, 326–337.

Ombao, H.C., Raz, J.A., von Sachs, R., Malow, B.A., 2001. Automatic statistical analysis of bivariate nonstationary time series. J. Am. Stat. Assoc. 96, 543–560.

Ombao, H., Van Bellegem, S., 2008. Evolutionary coherence of nonstationary signals. IEEE Trans. Signal Process. 56, 2259–2266.

Perez, M., Lundbye-Jensen, J., Nielsen, J., 2006. Changes in corticospinal drive to spinal motoneurones following visuo-motor skill learning in humans. J. Physiol. 573, 843–855.

Raethjen, J., Govindan, R., Muthuraman, M., Kopper, F., Volkmann, J., Deuschl, G., 2009. Cortical correlates of the basic and first harmonic frequency of parkinsonian tremor. Clin. Neurophysiol. 120, 1866–1872.

Salenius, S., Hari, R., 2003. Synchronous cortical oscillatory activity during motor action. Curr. Opin. Neurobiol. 13, 678–684.

Salenius, S., Portin, K., Kajola, M., Salmelin, R., Hari, R., 1997. Cortical control of human motoneuron firing during isometric contraction. J. Neurophysiol. 77, 3401–3405.

Sanderson, J., Fryzlewicz, P., Jones, M.W., 2010. Estimating linear dependence between nonstationary time series using the locally stationary wavelet model. Biometrika 97, 435–446.

Schnitzler, A., Gross, J., 2005. Normal and pathological oscillatory communication in the brain. Nat. Rev. Neurosci. 6, 285–296.

Tallon-Baudry, C., Bertrand, O., Delpuech, C., Pernier, J., 1996. Stimulus specificity of phase-locked and non-phase-locked 40*hz* visual responses in human. J. Neurosci. 16, 4240–4249.

Varela, F., Lachaux, J.P., Rodriguez, E., Martinerie, J., 2001. The brainweb: phase synchronization and large-scale integration. Nat. Rev. Neurosci. 2, 229–239.

Whitcher, B., 2000. Wavelet analysis of covariance with application to atmospheric time series. J. Geophys. Res. 105, 200.

Whitcher, B., Craigmile, P.F., Brown, P., 2005. Time-varying spectral analysis in neurophysiological time series using hilbert wavelet pairs. Signal Process. 85, 2065–2081.

Zhan, Y., Halliday, D., Jiang, P., Liu, X., Feng, J., 2006. Detecting the time-dependent coherence between non-stationary electrophysiological signals—a combined statistical and time–frequency approach. J. Neurosci. Meth. 156, 322–332.

CLINICAL AND TRANSLATIONAL NEUROSCIENCE

Impaired corticomuscular coherence during isometric elbow flexion contractions in humans with cervical spinal cord injury

Sylvain Cremoux,[1] [iD] Jessica Tallet,[2] Fabien Dal Maso,[3,4] Eric Berton[5] and David Amarantini[2]

[1]LAMIH, UMR CNRS 8201, Université de Valenciennes et du Hainaut-Cambrésis, F-59313, Valenciennes, France
[2]Toulouse NeuroImaging Center, Université de Toulouse, Inserm, UPS, Toulouse, France
[3]Département de Kinésiologie, Université de Montréal, Montréal, QC, Canada
[4]School of Physical and Occupational Therapy, McGill University, Montréal, QC, Canada
[5]Aix-Marseille Université, CNRS, ISM UMR 7287, Marseille Cedex 09, France

Abstract

After spinal cord injury (SCI), the reorganization of the neuromuscular system leads to increased antagonist muscles' co-activation—that is, increased antagonist vs. agonist muscles activation ratio—during voluntary contractions. Increased muscle co-activation is supposed to result from reduced cortical influences on spinal mechanisms inhibiting antagonist muscles. The assessment of the residual interactions between cortical and muscles activity with corticomuscular coherence (CMC) in participants with SCI producing different force levels may shed new lights on the regulation of muscle co-activation. To achieve this aim, we compared the net joint torque, the muscle co-activation and the CMC ~ 10 and ~ 20 Hz with both agonist and antagonist muscles in participants with SCI and healthy participants performing actual isometric elbow flexion contractions at three force levels. For all participants, overall CMC and muscle co-activation decreased with the increase in the net joint torque, but only CMC ~ 10 Hz was correlated with muscle co-activation. Participants with SCI had greater muscle co-activation and lower CMC ~ 10 Hz, at the highest force levels. These results emphasize the importance of CMC as a mechanism that could take part in the modulation of muscle co-activation to maintain a specific force level. Lower CMC ~ 10 Hz in SCI participants may reflect the decreased cortical influence on spinal mechanisms, leading to increased muscle co-activation, although plasticity of the corticomuscular coupling seems to be preserved after SCI to modulate the force level. Clinically, the CMC may efficiently evaluate the residual integrity of the neuromuscular system after SCI and the effects of rehabilitation.

Introduction

After spinal cord injury (SCI), the intensive reorganization of the neuromuscular system leads to increased antagonist muscles co-activation (Thomas *et al.*, 1998; Cremoux *et al.*, 2016). Muscle co-activation refers to the simultaneous activation of agonist and antagonist muscles, respectively, acting in and against the direction of the net joint torque (Kellis *et al.*, 2003). It takes an active part in joint stabilization according to the exerted force level (Baratta *et al.*, 1988; Solomonow *et al.*, 1988; Gribble *et al.*, 2003; Rao *et al.*, 2009; Amarantini & Bru, 2015). After SCI, increased muscle co-activation may be caused by reduced influence of the cortical structures on the spinal mechanisms inhibiting antagonist muscles (Boorman *et al.*, 1996; Xia & Rymer, 2005), and especially altered reciprocal inhibition (Cremoux *et al.*, 2016). Therefore, the residual interactions

between cortical and muscles' activities may play a major role in the regulation of muscle co-activation.

Interestingly, the corticomuscular coherence (CMC) can be taken to investigate motor cortex-to-muscle interactions. CMC is the spectral relationship between the electroencephalographic activity (EEG) recorded over the primary motor cortex (M1) and the electromyographic (EMG) activity of the muscles involved in the motor performance (Salenius & Hari, 2003). Significant CMC is found in the frequency band ~ 10 and ~ 20 Hz (Mima & Hallett, 1999). The CMC ~ 20 Hz is supposed to reflect the direct implication of the M1 neurons in muscle activations (Conway *et al.*, 1995). The modulation of the magnitude of the CMC ~ 20 Hz is thought to be specifically related to the task performance (Kristeva-Feige *et al.*, 2002) and has functional relevance for the modulation of the net joint torque (Chakarov *et al.*, 2009; Ushiyama *et al.*, 2010, 2012). The neurophysiological processes underlying CMC ~ 10 Hz are still object of debates in the literature. On the one side, some authors

Correspondence: Sylvain Cremoux, as above.
E-mail: sylvain.cremoux@univ-valenciennes.fr

1992   S. Cremoux *et al.*

proposed that CMC ~ 10 Hz could reflect some integrative cortical processing of sensory afferent inputs (Vecchio *et al.*, 2008; Budini *et al.*, 2014). For example, Budini *et al.* (2014) revealed CMC between EEG channels over the sensorimotor cortex and the EMG from biceps brachii (BB) muscle in healthy individuals performing sustained elbow contractions against a spring load and in isometric conditions. CMC ~ 10 Hz was found in some participants during isometric contractions and in all but one participants during contractions against the spring load. These results were interpreted as enhanced afferent activity from muscle spindles during contractions against the spring load. On the other side, based on the systematic phase difference between cortex and muscles activation, Raethjen *et al.* (2002) interpreted CMC ~ 10 Hz as a transmission of information from the supraspinal structures to the muscles. Both of these interpretations are supported by Williams & Baker (2009a,b) who modeled that a reduction in CMC ~ 10 Hz can be understood by spinal inhibitory mechanisms, enhanced by sensory afferent inputs. It is well known that reciprocal inhibition mechanism, inhibiting antagonist muscles activation, is under the influence of both sensory and cortical information (Schomburg, 1990; Jankowska, 1992). A modulation of the CMC ~ 10 Hz with antagonist muscles could thus reflect an alteration of the cortical control on spinal reciprocal inhibition after SCI.

This study aimed to test whether the CMC ~ 10 and ~ 20 Hz are linked to the level of co-activation in healthy people and following SCI. All participants performed elbow flexion contractions at different force levels. We hypothesized differences in the magnitude of CMC with both agonist and antagonist muscles with the modulation of force level between participants. An alteration of CMC ~ 10 Hz especially with antagonist muscles, correlated with the level of muscle co-activation, was expected in participants with cervical SCI. Such an alteration could reflect the reduced cortical influences on spinal inhibitory mechanisms controlling muscle co-activation.

Materials and methods

Participants

Eighteen volunteers participated in this study. Prior to any procedure, all participants signed informed consent to participate after receiving explicit information about the experimental design. The study protocol followed the local ethic guidelines from the Faculty of Sport Sciences and Human Movement, Paul Sabatier University (Toulouse 3) in Toulouse, France. All participants were right-handed as assessed by the Edinburgh handedness inventory (mean laterality quotient: 69.3 ± 23.8%; Oldfield, 1971). Two groups of participants, matched for age, mass and height (*t*-tests; all $P > 0.05$), were distinguished. The SCI group included eight participants (age: 32.5 ± 6.2 years; mass: 61.5 ± 13.3 kg; height: 174.7 + 9.7 cm). Seven participants (one female) had a complete SCI located from C5-C6 to C8-T1 vertebrae, and one participant had an incomplete SCI located at the C5-C6 vertebrae (graded D on the American Spinal Injury Association Impairment Scale). The able-bodied (AB) group included 10 healthy participants with no neuromusculoskeletal or sensory disorders (27.0 ± 4.0 years; 69.6 ± 8.0 kg; 175.3 ± 4.5 cm).

Materials

The net moment was recorded around the right elbow joint at 1 kHz using a calibrated dynamometer (System 4 Pro, Biodex Medical Systems, Shirley, NY, USA).

Electromyographic was recorded from four muscles of the right upper limb at 1000 Hz with Ag-AgCl EL503 surface electrodes connected to MP 150 amplifiers (Biopac Systems Inc., Goleta, USA). Electrodes were placed with a 2-cm inter-electrode distance on the belly of each muscle following suitable skin preparation (Hermens *et al.*, 2000). The BB and brachioradialis (BR) were chosen as representative of elbow flexors, and the long and lateral heads of the triceps brachii (TBlh and TBlt, respectively) were chosen as representative of elbow extensors (Bouisset *et al.*, 1976; Buchanan *et al.*, 1989). The reference electrode was placed on the left ulna styloid process.

Electroencephalography was recorded at 1024 Hz from 64 electrodes mounted on a 10–20 system cap (Active II, Biosemi Inc., Amsterdam, the Netherlands). Electro-oculogram was recorded from the left eye to detect any eye movements or blinks.

Time synchronization of data acquisitions was achieved offline using a TTL pulse.

Experimental setup

Participants were seated on the chair of the dynamometer with their trunk firmly strapped to the back of the chair. The right arm was positioned along the trunk, and the right forearm was supinated and 90° flexed relative to the arm before being strapped to the limb support of the dynamometer. Participants were asked to place the left arm at rest on the left thigh.

Protocol

Prior the experimental session, participants performed 3 so-called relative Maximum Voluntary Contractions (rMVC) around the right elbow joint in flexion. The rMVC was determined as the highest net moment reached while keeping at rest all the muscles not involved in the task, especially face and neck muscles, to avoid muscles artifact in EEG recordings (Dal Maso *et al.*, 2012; Cremoux *et al.*, 2013a,b). The experimental protocol consisted of 21 elbow isometric flexion contractions at 25, 50 and 75% rMVC randomized in seven sets of contractions. Each contraction lasted 6 s and was followed by a 6 s rest. Each set of contractions was followed by a 3-min rest period. The required force level was presented with a visual feedback (Presentation program, NeuroBehavioral Systems Inc. Albany, USA) appearing on a screen located 1 m in front of the participants. A full description of the experimental protocol is given in Cremoux *et al.* (2013a).

Data analysis

The continuous data were reduced into [-0.5 + 8] s trials from the appearance of the visual feedback. Each trial was visually inspected through the EEGLAB Matlab toolbox (Delorme & Makeig, 2004) to remove trials where EEG signals were contaminated by muscle artifacts. Whatever the force level, the number of trials used for further analysis was similar for all participants (18.01 ± 2.29; $P > 0.05$).

All filters mentioned below were fourth-order, zero-lag Butterworth-type filters.

Net torque production

The net torque signal was low-pass filtered at 10 Hz (Nordez *et al.*, 2008). For each trial, the net torque production was averaged over a [+3 + 6] s period, considered as a relevant period of interest.

Muscle co-activation

Raw EMG data were [10–400] Hz band-pass filtered, full-wave rectified and 9 Hz low-pass filtered to obtain the linear envelope (Shiavi *et al.*, 1998). As recommended by Kellis *et al.* (2003), the muscle co-activation between elbow agonist/antagonist muscle pairs, expressed as a percentage, was calculated over the [+3 + 6] s period of interest from MVC-normalized linear envelopes of antagonist (TBlt and Tblh) and agonist (BB and BR) muscles (Falconer & Winter, 1985; Winter, 2005; Amarantini & Bru, 2015).

$$\text{Muscle Co-activation} = \frac{2 \times \text{EMG}_{\text{ANTAGO}}}{\text{EMG}_{\text{AGO}} + \text{EMG}_{\text{ANTAGO}}} \times 100\% \quad (1)$$

Corticomuscular coherence

Corticomuscular coherence was calculated in the time-frequency domain using the *WaveCrossSpec* software for wavelet coherence analysis (Bigot *et al.*, 2011; http://www.math.u-bordeaux1.fr/~jbigot/Site/Software_files/WavCrossSpec.zip) between the signal from the C3 EEG electrode and each of the four EMG signals. Previous methodological studies revealed that time-frequency transformation was most suitable to conventional frequency domain analysis for analyzing coherence in non-stationary electrophysiological signals (Zhan *et al.*, 2006; Allen & MacKinnon, 2010; Bigot *et al.*, 2011), even though the quantification of corticomuscular interactions is subsequently quantified over a specified time period of interest. C3 EEG electrode was taken as the optimal location for studying cortical activity dedicated to right elbow muscle contractions, in accordance with previous investigations (Siemionow *et al.*, 2000; Caviness *et al.*, 2006; Tuncel *et al.*, 2010; Cremoux *et al.*, 2013a,b).

For CMC calculation, the following steps were used. The EEG and EMG data were first band-pass filtered at [3–100] Hz and notched at [45–55] Hz (Sabri & Campbell, 2002; Baker & Baker, 2012; Dal Maso *et al.*, 2012; Cremoux *et al.*, 2013b). Channels visually identified as 'bad' channels were removed, and EEG signals were average referenced (Delorme *et al.*, 2007; note that the C3 EEG channel has never been identified as 'bad' channel during this step; see Fig. 1A and B after these processing steps). The wavelet power spectrum of centered C3 EEG signal (Fig. 1C) and each unrectified EMG signals (Fig. 1D) was then obtained with parameters 'nvoice' (scale resolution of the wavelet), 'J1' (number of scales) and 'wavenumber' (Morlet mother wavelet parameter) set, respectively, to 0.125, 871 and 7 to yield accurate identification of oscillatory activity from 0.13 Hz to 114.39 Hz in 1.07 Hz step. EMG signals were not rectified to properly model EMG time series as centered Gaussian processes (Bigot *et al.*, 2011; Charissou *et al.*, 2016) and not to lose important information contained in the EMG signal spectrum (Neto & Christou, 2010; McClelland *et al.*, 2012; Yang *et al.*, 2016). The wavelet cross-spectrum (Fig. 1E), that is, the common power spectrum between the centered C3 EEG signal and each unrectified EMG signal, was calculated using the following equation.

$$S_{\text{EMG,EEG}}(\omega, u) = \mathbb{E}\left(W_{\text{EMG}}(\omega, u)\overline{W_{\text{EEG}}(\omega, u)}\right) \quad (2)$$

where $S_{\text{EMG}}(\omega, u)$ and $S_{\text{EEG}}(\omega, u)$ are the wavelet auto-spectrum of each **EMG** and **EEG** signal, respectively, which are defined as

$$S_{\text{EMG}}(\omega, u) = \mathbb{E}|W_{\text{EMG}}(\omega, u)|^2 \quad (3)$$

$$S_{\text{EEG}}(\omega, u) = \mathbb{E}|W_{\text{EEG}}(\omega, u)|^2 \quad (4)$$

The values of the wavelet cross-spectrum between EEG and EMG signals that were above the significant threshold $\hat{\lambda}_{\alpha}$ (with

$\alpha = 0.05$) were considered as significant interactions (Bigot *et al.*, 2011). The significance threshold was calculated using the following equation.

$$\hat{\lambda}_{\alpha} = \frac{\hat{\rho}\mathbf{EMG}\hat{\rho}\mathbf{EEG}}{\left(1 + \sqrt{\frac{\mathbf{T}}{\mathbf{n}}}\right)^2} \left(-\frac{\log(\alpha/2)}{\mathbf{n}} + \sqrt{-\frac{2\log(\alpha/2)}{\mathbf{n}}}\right) \quad (5)$$

With $\hat{\rho}_{\text{EMG}}$ and $\hat{\rho}_{\text{EEG}}$ being the largest eigenvalue of the empirical covariance matrix of the EMG and the EEG signal, respectively. The computation of the threshold is thus data-based as it includes an estimation of the variance of the two time series. This procedure is particularly adapted for signals having different magnitude of covariance.

Finally, the wavelet magnitude-squared coherence (Fig. 1F), that is, the cross-spectrum normalized by the power spectrum of each signal, was calculated using the following equations.

$$R^2_{\text{EMGEEG}}(\omega, u) = \frac{|S_{\text{EMG,EEG}(\omega,u)}|^2}{S_{\text{EMG}}(\omega, u)S_{\text{EEG}}(\omega, u)}, \quad (6)$$

where $S_{\text{EEG, EEG}}(\omega, u)$ is the wavelet cross-spectrum between **EMG** and **EEG** signals (Eqn 2), and $S_{\text{EMG}}(\omega, u)$ and $S_{\text{EEG}}(\omega, u)$ are the wavelet auto-spectrum of each **EMG** and **EEG** signal (Eqns 3 and 4).

The magnitude of the CMC was calculated from 0 to 1 bounded corticomuscular values as the volume under the time-frequency map of magnitude-squared coherence only where the wavelet cross-spectrum between the EEG and EMG signals was detected as significant (Charissou *et al.*, 2016; Yoshida *et al.*, 2017). Over the [+3 + 6] s period of interest, the magnitude of the CMC was computed in two frequency bands of interest: [8–13] Hz (CMC_{8-13}) (Christou *et al.*, 2007) and [13–31] Hz (CMC_{13-31}) (Mima *et al.*, 1999). For each frequency band, the magnitude of the CMC was finally averaged for two elbow flexor muscles, BB and BR, and for two elbow extensor muscles, TBlh and TBlt.

Figure 2 illustrates more precisely the modulation of the magnitude of the CMC depicted in Fig 1E over frequency in the period of interest (left panel) and time in the frequency bands of interest (bottom panel).

Statistical analysis

A two-factor group (between-subjects factor: AB vs. SCI) × force level (within-subjects factor: 25% vs. 50% vs. 75%) mixed analysis of variance (ANOVA) was conducted on the mean net torque, muscle co-activation and magnitude of CMC. For the latter, independent ANOVA was performed for CMC_{8-13} and CMC_{13-31} magnitude with elbow flexors and extensors with η_p^2 reported to represent effect size. Huynh & Feldt (1976) correction for degrees of freedom was used where applicable. For each force level, Spearman's correlation coefficients were calculated to test the strength of correlation between muscle co-activation and CMC_{8-13} and CMC_{13-31} magnitude with elbow flexors and extensors. For all statistical tests, the level of significance was set at $P < 0.05$.

Results

Net torque

The ANOVA performed on the mean net torque revealed only a main force level effect ($F_{2,32} = 208.77$; $P < 0.01$; $\eta_p^2 = 0.93$). For
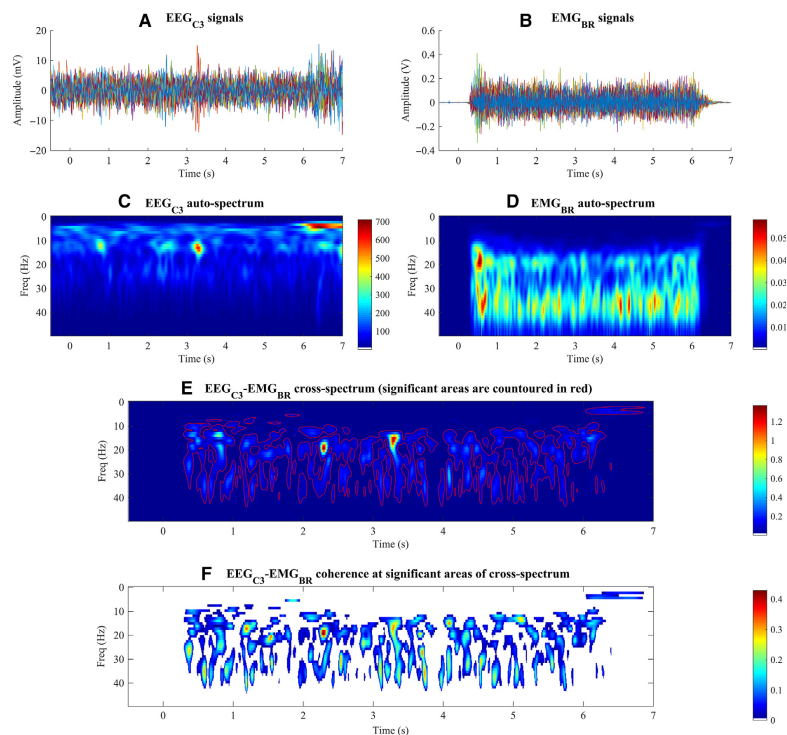
1994   S. Cremoux *et al.*

FIG. 1. Illustration of the processing steps used for time-frequency analysis of corticomuscular coherence from one representative able-bodied participant. First row: typical recordings of C3 electroencephalography (EEG) signals (A) and brachioradialis (BR) electromyographic (EMG) signals (B) obtained during contractions at 25% relative Maximum Voluntary Contraction after filtering and C3 EEG signals normalization. Second row: auto-spectra of the C3 EEG (C) and BR EMG (D) time series. Third row (E): wavelet cross-spectrum between the C3 EEG and the BR EMG time series; the red contours identify the time-frequency areas where the correlation between the C3 EEG and BR EMG time series is significant. Fourth row (F): significant wavelet magnitude-squared coherence between the C3 EEG and BR EMG signals in the time-frequency domain. All non-significant values are whitened. [Colour figure can be viewed at wileyonlinelibrary.com].
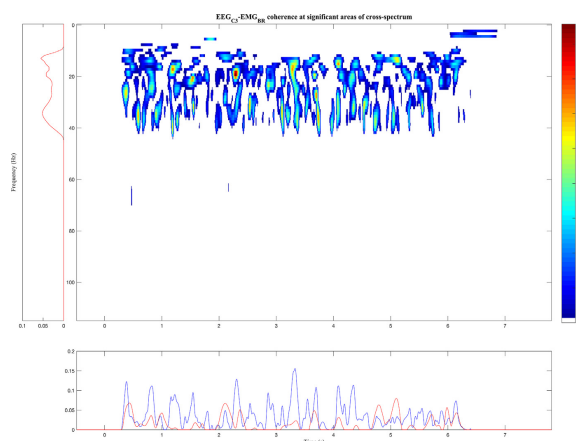
FIG. 2. Significant wavelet magnitude-squared coherence between the C3 electroencephalography and brachioradialis electromyographic signals in the time-frequency domain (also depicted in Fig. 1F). All non-significant values are whitened. Left panel: average corticomuscular coherence in the period of interest. Bottom panel: average corticomuscular coherence in the 8–13 Hz (red line) and 13–31 Hz (blue line) frequency bands of interest over time. [Colour figure can be viewed at wileyonlinelibrary.com].

all participants, the mean net torque increased from 10.63 ± 3.25 Nm at 25% rMVC to 30.89 ± 8.59 Nm at 75% rMVC (Fig. 3A).

Muscle co-activation

The ANOVA performed on the muscle co-activation revealed a force level effect ($F_{2,32} = 14.94$; $P < 0.01$; $\eta_p^2 = 0.48$) and a group effect

FIG. 3. Net joint torque (A) and muscle co-activation (B) for the participants with spinal cord injury (orange triangle) and healthy participants (blue square). * next to a curly bracket represents a significant group effect; * above an arrow represents significant force level effect. [Colour figure can be viewed at wileyonlinelibrary.com].

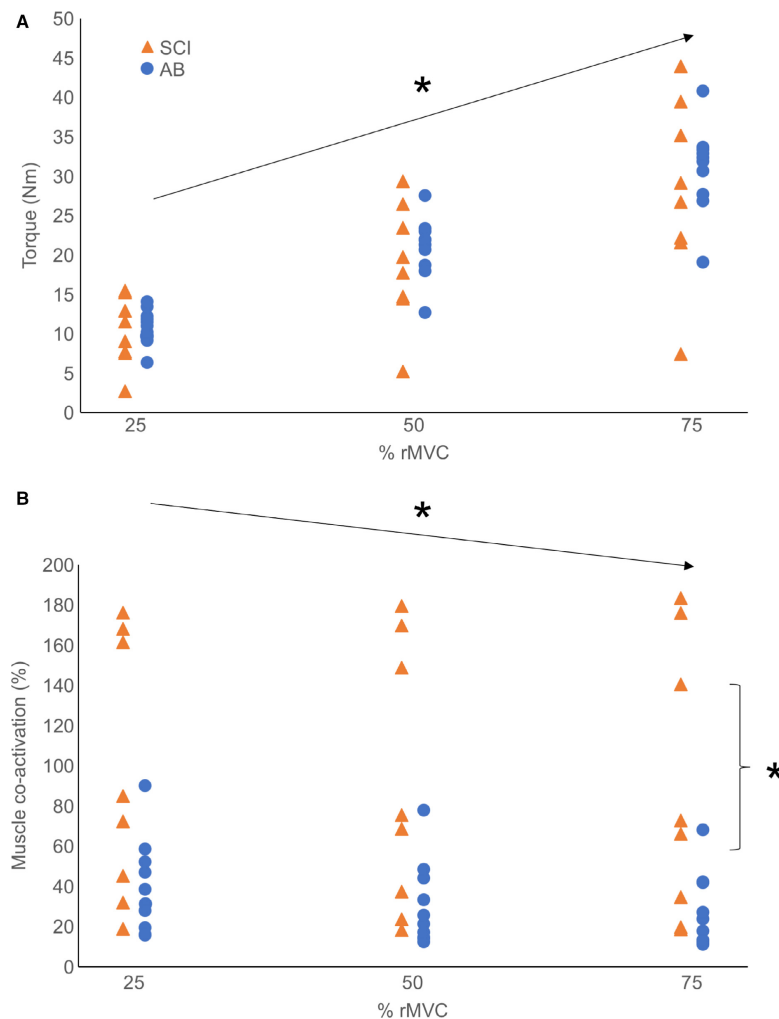($F_{1,16} = 7.12$; $P = 0.02$; $\eta_p^2 = 0.31$). For all participants, the muscle co-activation decreased from $64.11 \pm 52.93\%$ at 25% rMVC to $54.44 \pm 55.72\%$ at 75% rMVC. All force levels combined, and the muscle co-activation was higher for the SCI group ($91.23 \pm 63.53\%$) in comparison with that of the AB group ($32.40 \pm 20.94\%$) (Fig. 3B).

Magnitude of CMC$_{8-13}$

The ANOVA performed on the magnitude of the CMC$_{8-13}$ with elbow flexors only revealed a force level effect ($F_{2,32} = 21.98$; $P < 0.01$; $\eta_p^2 = 0.58$). For all participants, the magnitude of the CMC$_{8-13}$ with elbow flexors decreased by $72.25 \pm 29.43\%$ from 25% rMVC to 75% rMVC (Fig. 4A).

Concerning the magnitude of the CMC$_{8-13}$ with elbow extensors, the ANOVA revealed a force level ($F_{2,32} = 21.29$; $P < 0.01$; $\eta_p^2 = 0.57$) and a group effect ($F_{1,16} = 124.38$; $P = 0.04$; $\eta_p^2 = 0.24$). For all participants, the magnitude of the CMC$_{8-13}$ with

elbow extensors decreased by $46.94 \pm 27.06\%$ from 25% rMVC to 75% rMVC (Fig. 4A). All force levels combined, and the magnitude of the CMC$_{8-13}$ with elbow extensors was smaller for the SCI group in comparison with that of the AB group (Fig. 4B).

Magnitude of CMC$_{13-31}$

The ANOVA performed on the magnitude of the CMC$_{13-31}$ with elbow flexors only revealed a force level effect ($F_{2,32} = 8.69$; $P < 0.01$; $\eta_p^2 = 0.35$). For all participants, the magnitude of the CMC$_{13-31}$ with elbow flexors decreased by $22.20 \pm 27.19\%$ from 25% rMVC to 75% rMVC (Fig. 5A).

Concerning the magnitude of the CMC$_{13-31}$ with elbow extensors, the ANOVA only revealed a force level ($F_{2,32} = 5.54$; $P < 0.01$; $\eta_p^2 = 0.26$). For all participants, the magnitude of the CMC$_{13-31}$ with elbow extensors decreased by $5.34 \pm 53.97\%$ from 25% rMVC to 75% rMVC (Fig. 5B).
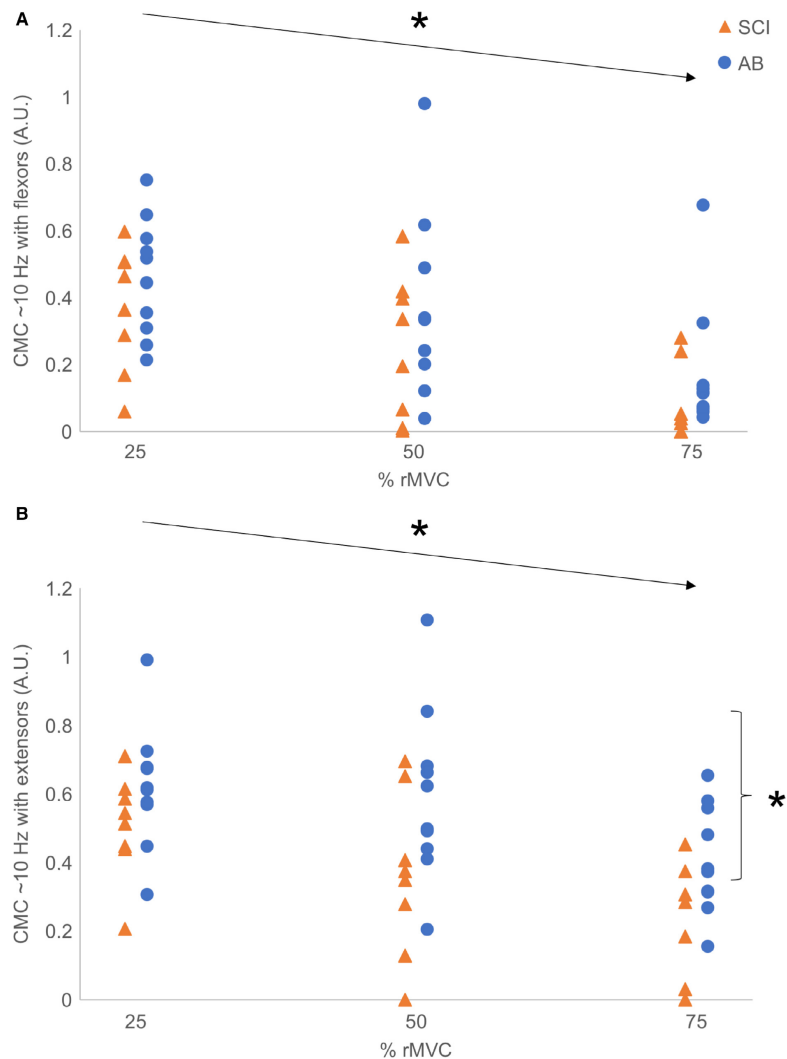
1996   S. Cremoux *et al.*

FIG. 4. Corticomuscular coherence ~ 10 Hz with elbow flexors (A) and elbow extensors (B) for the participants with spinal cord injury (orange triangle) and healthy participants (blue square). * next to a curly bracket represents a significant group effect; * above an arrow represents significant force level effect. [Colour figure can be viewed at wileyonlinelibrary.com].

Correlation between muscle co-activation and CMC

The modulation of muscle co-activation was significantly negatively correlated with the levels of CMC_{8-13} with both elbow flexors and extensors at 50% rMVC (r_s = -0.42, P = 0.04 and r_s = -0.57, P = 0.01, respectively) and 75% rMVC (r_s = -0.46, P = 0.03 and r_s = -0.58, P = 0.01, respectively).

Discussion

This study aimed to evaluate the modulation of muscle co-activation in people with cervical SCI compared to healthy participants by evaluating the corticomuscular coupling with agonist and antagonist muscles. All participants were able to perform voluntary isometric elbow flexion contractions at different submaximal force levels. For all participants, CMC ~ 10 Hz was significantly correlated with

muscle co-activation level, and participants with cervical SCI presented increased muscle co-activation and decreased CMC ~ 10 Hz with elbow extensors in comparison with healthy participants. The increase in the force level was associated with a decrease in the magnitude of the CMC ~ 10 and ~ 20 Hz with both elbow flexors and extensors.

Decreased CMC ~ 10 Hz is correlated with increased muscle co-activation

Even though all participants exerted comparable net joint torque, our results revealed increased muscle co-activation in the SCI group. This increase in muscle co-activation mainly arises from increased antagonist muscles activation, as previously shown in participants with SCI during both electrically evoked and voluntary contractions
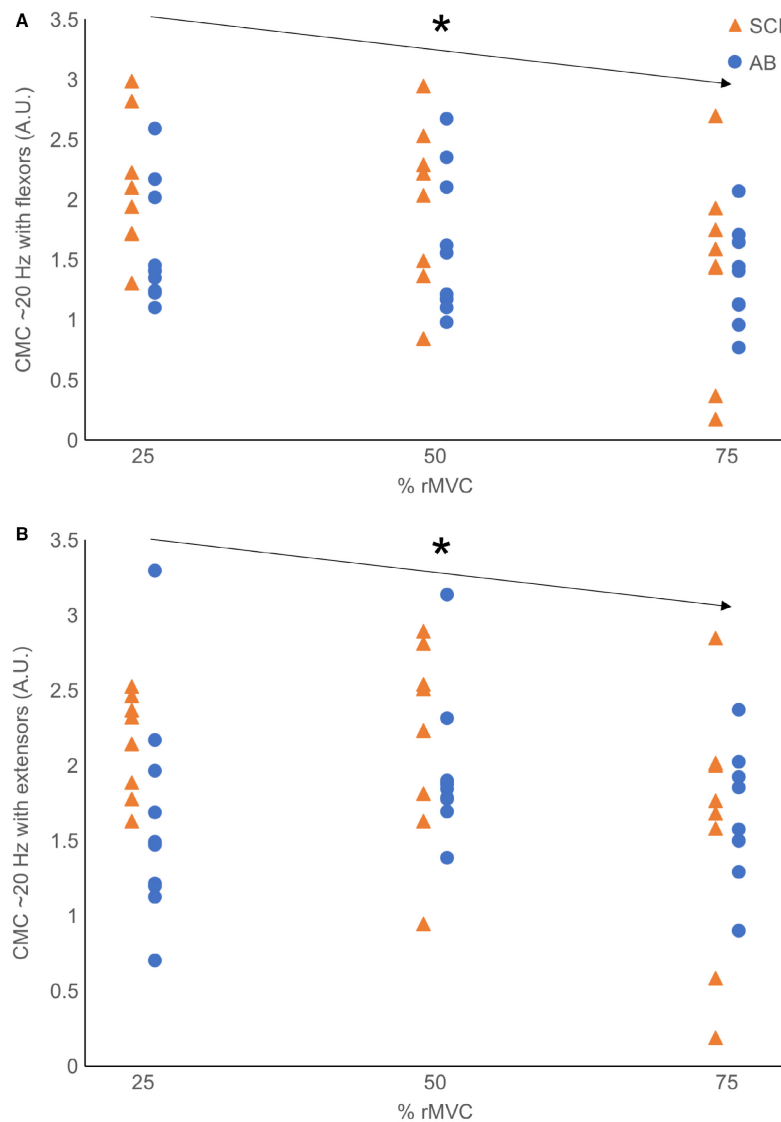
FIG. 5. Corticomuscular coherence ~ 20 Hz with elbow flexors (A) and elbow extensors (B) for the participants with spinal cord injury (orange triangle) and healthy participants (blue square). * above an arrow represents significant force level effect. [Colour figure can be viewed at wileyonlinelibrary.com].

(Thomas *et al.*, 1998; Cremoux *et al.*, 2016). Although necessary for data comparison, the normalization of EMG data revealed a supramaximal activation of elbow extensors when used as antagonist muscles (Cremoux *et al.*, 2012). Increased antagonist muscles activation is supposed to be due to the disruption of the descending pathways regulating spinal reciprocal inhibition mechanisms (Boorman *et al.*, 1996; Xia & Rymer, 2005; Knikou & Mummidisetty, 2011).

In the SCI group, CMC ~ 10 Hz with elbow extensors was lower in comparison with healthy participants. Higher CMC ~ 10 Hz was unexpected in healthy people given that CMC ~ 10 Hz is supposed

to be either reduced or absent because of efficient spinal inhibitory mechanisms (Williams & Baker, 2009a,b). The detection of significant CMC ~ 10 Hz has been improved using a novel statistical procedure based on the EEG-EMG cross-spectrum (Bigot *et al.*, 2011). This statistical procedure is particularly relevant to detect truly significant corticomuscular interactions when the number of contractions is small (Lu *et al.*, 2013; Pedrosa *et al.*, 2014). In healthy people, CMC ~ 10 Hz is supposed to reflect complex two-way communication between cortical and muscles structures (Raethjen *et al.*, 2002, 2007; Budini *et al.*, 2014). The specific decrease in CMC ~ 10 Hz with antagonist muscles revealed in people with SCI may

1998 S. Cremoux *et al.*

highlight both concomitant decreased cortical integration of somatosensory afferent inputs and the decreased influence of cortical structures on spinal reciprocal inhibition mechanisms modulating antagonist muscles activation. Previous results also revealed altered EEG-EMG and EMG-EMG coherence ~ 10 Hz after SCI (Babiloni *et al.*, 2004; Hansen *et al.*, 2005). All of these results can be understood by the neurophysiological mechanisms underlying motor recovery following SCI. CMC ~ 10 Hz may efficiently evaluate the residual integrity of the neuromuscular system after SCI and the effects of rehabilitation.

An interesting finding is that for all participants, the increase in muscle co-activation was significantly correlated with the decrease in the magnitude of the CMC ~ 10 Hz with both elbow flexors and extensors. Even if further work is needed to reach a definitive conclusion, CMC ~ 10 Hz could then reflect a more general central mechanism controlling muscle co-activation through spinal inhibitory mechanisms. This would be in line with previous studies that inferred that the modulation of neurophysiological oscillations ~ 10 Hz could reflect complex corticospinal mechanisms modulating both agonist and antagonist muscles co-activation (Vallbo & Wessberg, 1993; Wessberg & Vallbo, 1996; Wessberg & Kakuda, 1999).

Both CMC ~ 10 and ~ 20 Hz decrease with the increase in the force level

For all participants, the increase in the force level was associated with a decrease in the muscle co-activation and in the magnitude of both CMC ~ 10 and ~ 20 Hz with elbow flexors and extensors. Previous studies indicated that the magnitude of the CMC ~ 20 Hz is modulated with the task performance (Kristeva-Feige *et al.*, 2002) and the force level (Mima *et al.*, 1999; Chakarov *et al.*, 2009; Ushiyama *et al.*, 2012). The scope of the aforementioned studies was, however, limited to the modulation of the CMC ~ 20 Hz with agonist muscles. Dal Maso *et al.* (2012) suggested that the cortical oscillations ~ 20 Hz recorded over the M1 might have a critical role in the modulation of antagonist muscle activations. The decrease in the magnitude of the CMC ~ 10 and ~ 20 Hz with the force level could thus reflect a functional neurophysiological mechanism that would take part in the control of the exerted force by modulating agonist and antagonist muscle activations. The overall decrease in the magnitude of the CMC with the increase in the force level and the specific decrease in the magnitude of the CMC ~ 10 Hz with the increase in muscles co-activation may thus shed new light on the 'common drive' principle (De Luca & Mambrito, 1987; Miles, 1987; De Luca & Erim, 1994, 2002; Mullany *et al.*, 2002). This principle supposes that the modulation of one master-driving cortical signal influences multiple antagonistic muscle activations. In such a context, the CMC ~ 10 Hz could represent the common drive influencing spinal inhibitory mechanisms that are degraded after cervical SCI, while CMC ~ 20 Hz could represent neurophysiological pathways exciting directly the motoneurons involved in the activation of both agonist and antagonist muscles during voluntary contractions. Both 10 Hz and 20 Hz frequency bands would be modulated in amplitude to adapt the level of agonist and antagonist muscles to the requested task. This interpretation would be in line with the influence of the cortical descending pathways on the spinal network as described in Duchateau & Baudry (2014). Despite the care taken to ensure the comparison across the conditions, results revealed in this study cannot rule out the implication of the other physiological systems that may influence motor output differently depending on the produced force level (Heroux & Gandevia, 2013; Farina *et al.*, 2014). To further investigate this interpretation about the neurophysiological mechanisms underlying CMC, it would be interesting to assess the relationship between the CMC and agonist and antagonist muscles activation using transcranial magnetic stimulation, which has direct access to the neuronal circuitry of the motor cortex (Hansen & Nielsen, 2004) in healthy and SCI participants.

Conclusion

Our results revealed that both force level and SCI modulate the muscle co-activation and the magnitude of the CMC during isometric elbow flexion contractions. On the one hand, the magnitude of the CMC ~ 10 and ~ 20 Hz, and muscle co-activation decreased with the increase in the force level for the two groups but only CMC ~ 10 Hz was correlated with muscle co-activation. These results emphasize the importance of corticomuscular coupling as a mechanism that could take part in the modulation of the muscle co-activation to maintain a specific force level. They also suggest a preserved plasticity of the corticospinal drive allowing to modulate force in participants with SCI. On the other hand, participants with cervical SCI had an increased muscle co-activation associated with a decreased magnitude of the CMC ~ 10 Hz with antagonist muscles. This result suggests that CMC ~ 10 Hz may reflect the alteration of the cortical mechanisms controlling muscle co-activation after a cervical SCI, especially through spinal reciprocal inhibition. Although further investigations are needed to complement these results, corticomuscular coupling appears to be a promising tool to explore the cortical mechanisms involved in the modulation of muscle co-activation. In a clinical environment, these results may have potential relevance to assess the integrity of the neurophysiological pathways of voluntary motor functions after SCI and its plasticity with rehabilitation.

Acknowledgements

Conflict of interest

The authors of the manuscript declare no conflict of interest, including any financial, personal or other relationships with other people or organization.

Author contributions

Each author has been involved in the design of the study, collection, analysis and interpretation of data and writing of the manuscript.

Data accessibility

Raw data supporting this article can be received by e-mail upon request.

Abbreviations

AB, able-bodied; ANOVA, analysis of variance; BB, biceps brachii; BR, brachioradialis; CMC, corticomuscular coherence; EEG, electroencephalography; EMG, electromyography; M1, primary motor cortex; rMVC, relative Maximum Voluntary Contraction; SCI, spinal cord injury; TBlh, triceps brachii long head; TBlt, triceps brachii lateral head; TTL, transistor-transistor logic.

References

Allen, D.P. & MacKinnon, C.D. (2010) Time–frequency analysis of movement-related spectral power in EEG during repetitive movements: a comparison of methods. *J. Neurosci. Meth.*, **186**, 107–115.

Amarantini, D. & Bru, B. (2015) Training-related changes in the EMG–moment relationship during isometric contractions: further evidence of improved control of muscle activation in strength-trained men? *J. Electromyogr. Kines.*, **25**, 697–702.

Babiloni, C., Vecchio, F., Babiloni, F., Brunelli, G.A., Carducci, F., Cincotti, F., Pizzella, V., Romani, G.L. *et al.* (2004) Coupling between "hand" primary sensorimotor cortex and lower limb muscles after ulnar nerve surgical transfer in paraplegia. *Behav. Neurosci.*, **118**, 214–222.

Baker, M.R. & Baker, S.N. (2012) Beta-adrenergic modulation of tremor and corticomuscular coherence in humans. *PLoS One*, **7**, e49088.

Baratta, R., Solomonow, M., Zhou, B., Letson, D., Chuinard, R. & D'ambrosia, R. (1988) Muscular coactivation the role of the antagonist musculature in maintaining knee stability. *Am. J. Sport. Med.*, **16**, 113–122.

Bigot, J., Longcamp, M., Dal Maso, F. & Amarantini, D. (2011) A new statistical test based on the wavelet cross-spectrum to detect time–frequency dependence between non-stationary signals: application to the analysis of cortico-muscular interactions. *NeuroImage*, **55**, 1504–1518.

Boorman, G.I., Lee, R.G., Becker, W.J. & Windhorst, U.R. (1996) Impaired "natural reciprocal inhibition" in patients with spasticity due to incomplete spinal cord injury. *Electromyo. Clin. Neur.*, **101**, 84–92.

Bouisset, S., Lestienne, F. & Maton, B. (1976) The stability of synergy in agonists during the execution of a simple voluntary movement. *Electromyo. Clin. Neur.*, **42**, 543–551.

Buchanan, T.S., Rovai, G.P. & Rymer, W.Z. (1989) Strategies for muscle activation during isometric torque generation at the human elbow. *J. Neurophysiol.*, **62**, 1201–1212.

Budini, F., McManus, L.M., Berchicci, M., Menotti, F., Macaluso, A., Di Russo, F., Lowery, M.M. & De Vito, G. (2014) Alpha band corticomuscular coherence occurs in healthy individuals during mechanically-induced tremor. *PLoS One*, **9**, e115012.

Caviness, J.N., Shill, H.A., Sabbagh, M.N., Evidente, V.G., Hernandez, J.L. & Adler, C.H. (2006) Corticomuscular coherence is increased in the small postural tremor of Parkinson's disease. *Movement Disord.*, **21**, 492–499.

Chakarov, V., Naranjo, J.R., Schulte-Mönting, J., Omlor, W., Huethe, F. & Kristeva, R. (2009) Beta-range EEG-EMG coherence with isometric compensation for increasing modulated low-level forces. *J. Neurophysiol.*, **102**, 1115–1120.

Charissou, C., Vigouroux, L., Berton, E. & Amarantini, D. (2016) Fatigue- and training-related changes in 'beta' intermuscular interactions between agonist muscles. *J. Electromyogr. Kines.*, **27**, 52–59.

Christou, E.A., Rudroff, T., Enoka, J.A., Meyer, F. & Enoka, R.M. (2007) Discharge rate during low-force isometric contractions influences motor unit coherence below 15 Hz but not motor unit synchronization. *Exp. Brain Res.*, **178**, 285–295.

Conway, B.A., Halliday, D.M., Farmer, S.F., Shahani, U., Maas, P., Weir, A.I. & Rosenberg, J.R. (1995) Synchronization between motor cortex and spinal motoneuronal pool during the performance of a maintained motor task in man. *J. Physiol.*, **489**(Pt 3), 917.

Cremoux, S., Tallet, J., Berton, E., Dal Maso, F. & Amarantini, D. (2012) Atypical EMG activation patterns of the elbow extensors after complete C6 tetraplegia during isometric contractions: a case report. *Comput. Method. Biomec.*, **15**(sup1), 266–268.

Cremoux, S., Tallet, J., Berton, E., Dal Maso, F. & Amarantini, D. (2013a) Does the force level modulate the cortical activity during isometric contractions after a cervical spinal cord injury? *Clin. Neurophysiol.*, **124**, 1005–1012.

Cremoux, S., Tallet, J., Berton, E., Dal Maso, F. & Amarantini, D. (2013b) Motor-related cortical activity after cervical spinal cord injury: multifaceted EEG analysis of isometric elbow flexion contractions. *Brain Res.*, **1533**, 44–51.

Cremoux, S., Amarantini, D., Tallet, J., Dal Maso, F. & Berton, E. (2016) Increased antagonist muscle activity in cervical SCI patients suggests altered reciprocal inhibition during elbow contractions. *Clin. Neurophysiol.*, **127**, 629–634.

Dal Maso, F., Longcamp, M. & Amarantini, D. (2012) Training-related decrease in antagonist muscles activation is associated with increased motor cortex activation: evidence for central mechanisms for control of antagonist muscles. *Exp. Brain Res.*, **220**, 287–295.

De Luca, C.J. & Erim, Z. (1994) Common drive of motor units in regulation of muscle force. *Trends Neurosci.*, **17**, 299–305.

De Luca, C.J. & Erim, Z. (2002) Common drive in motor units of a synergistic muscle pair. *J. Neurophysiol.*, **87**, 2200–2204.

De Luca, C.J. & Mambrito, B. (1987) Voluntary control of motor units in human antagonist muscles: coactivation and reciprocal activation. *J. Neurophysiol.*, **58**, 525–542.

Delorme, A. & Makeig, S. (2004) EEGLAB: an open source toolbox for analysis of single-trial EEG dynamics including independent component analysis. *J. Neurosci. Meth.*, **134**, 9–21.

Delorme, A., Sejnowski, T. & Makeig, S. (2007) Enhanced detection of artifacts in EEG data using higher-order statistics and independent component analysis. *NeuroImage*, **34**, 1443–1449.

Duchateau, J. & Baudry, S. (2014) The neural control of coactivation during fatiguing contractions revisited. *J. Electromyogr. Kines.*, **24**, 780–788.

Falconer, K. & Winter, D.A. (1985) Quantitative assessment of co-contraction at the ankle joint in walking. *Electromyo. Clin. Neur.*, **25**(2–3), 135.

Farina, D., Merletti, R. & Enoka, R.M. (2014) The extraction of neural strategies from the surface EMG: an update. *J. Appl. Physiol.*, **117**(11), 1215–1230.

Gribble, P.L., Mullin, L.I., Cothros, N. & Mattar, A. (2003) Role of cocontraction in arm movement accuracy. *J. Neurophysiol.*, **89**, 2396–2405.

Hansen, N. & Nielsen, J. (2004) The effect of transcranial magnetic stimulation and peripheral nerve stimulation on corticomuscular coherence in humans. *J. Physiol.*, **561**, 295–306.

Hansen, N.L., Conway, B.A., Halliday, D.M., Hansen, S., Pyndt, H.S., Biering-Sørensen, F. & Nielsen, J.B. (2005) Reduction of common synaptic drive to ankle dorsiflexor motoneurons during walking in patients with spinal cord lesion. *J. Neurophysiol.*, **94**, 934–942.

Hermens, H.J., Freriks, B., Disselhorst-Klug, C. & Rau, G. (2000) Development of recommendations for SEMG sensors and sensor placement procedures. *J. Electromyogr. Kines.*, **10**, 361–374.

Heroux, M.E. & Gandevia, S.C. (2013) Human muscle fatigue, eccentric damage and coherence in the EMG. *Acta Physiol.*, **208**, 294–295.

Huynh, H. & Feldt, L.S. (1976) Estimation of the Box correction for degrees of freedom from sample data in randomized block and split-plot designs. *J. Educ. Behav. Stat.*, **1**, 69–82.

Jankowska, E. (1992) Interneuronal relay in spinal pathways from proprioceptors. *Prog. Neurobiol.*, **38**, 335–378.

Kellis, E., Arabatzi, F. & Papadopoulos, C. (2003) Muscle co-activation around the knee in drop jumping using the co-contraction index. *J. Electromyogr. Kines.*, **13**, 229–238.

Knikou, M. & Mummidisetty, C.K. (2011) Reduced reciprocal inhibition during assisted stepping in human spinal cord injury. *Exp. Neurol.*, **231**, 104–112.

Kristeva-Feige, R., Fritsch, C., Timmer, J. & Lücking, C.H. (2002) Effects of attention and precision of exerted force on beta range EEG-EMG synchronization during a maintained motor contraction task. *Clin. Neurophysiol.*, **113**, 124–131.

Lu, Q., Wang, Y., Luo, G., Li, H. & Yao, Z. (2013) Dynamic connectivity laterality of the amygdala under negative stimulus in depression: a MEG study. *Neurosci. Lett.*, **547**, 42–47.

McClelland, V.M., Cvetkovic, Z. & Mills, K.R. (2012) Rectification of the EMG is an unnecessary and inappropriate step in the calculation of corticomuscular coherence. *J. Neurosci. Meth.*, **205**, 190–201.

Miles, T.S. (1987) The cortical control of motor neurones: some principles of operation. *Med. Hypotheses*, **23**, 43–50.

Mima, T. & Hallett, M. (1999) Corticomuscular coherence: a review. *J. Clin. Neurophysiol.*, **16**, 501.

Mima, T., Simpkins, N., Oluwatimilehin, T. & Hallett, M. (1999) Force level modulates human cortical oscillatory activities. *Neurosci. Lett.*, **275**, 77–80.

Mullany, H., O'Malley, M., Gibson, A.S.C. & Vaughan, C. (2002) Agonist–antagonist common drive during fatiguing knee extension efforts using surface electromyography. *J. Electromyogr. Kines.*, **12**, 375–384.

Neto, O.P. & Christou, E.A. (2010) Rectification of the EMG signal impairs the identification of oscillatory input to the muscle. *J. Neurophysiol.*, **103**, 1093–1103.

Nordez, A., Casari, P. & Cornu, C. (2008) Accuracy of Biodex system 3 pro computerized dynamometer in passive mode. *Med. Eng. Phys.*, **30**, 880–887.

Oldfield, R.C. (1971) The assessment and analysis of handedness: the Edinburgh inventory. *Neuropsychologia*, **9**, 97–113.

Pedrosa, D.J., Quatuor, E.L., Reck, C., Pauls, K.A.M., Huber, C.A., Visser-Vandewalle, V. & Timmermann, L. (2014) Thalamomuscular coherence in essential tremor: hen or egg in the emergence of tremor? *J. Neurosci.*, **34**, 14475–14483.

Raethjen, J., Lindemann, M., Dümpelmann, M., Wenzelburger, R., Stolze, H., Pfister, G., Elger, C.E., Timmer, J. *et al.* (2002) Corticomuscular coherence in the 6–15 Hz band: is the cortex involved in the generation of physiologic tremor?. *Exp. Brain Res.*, **142**, 32–40.

Raethjen, J., Govindan, R.B., Kopper, F., Muthuraman, M. & Deuschl, G. (2007) Cortical involvement in the generation of essential tremor. *J. Neurophysiol.*, **97**, 3219–3228.

2000   S. Cremoux *et al.*

Rao, G., Amarantini, D. & Berton, E. (2009) Influence of additional load on the moments of the agonist and antagonist muscle groups at the knee joint during closed chain exercise. *J. Electromyogr. Kines.*, **19**, 459–466.

Sabri, M. & Campbell, K.B. (2002) The effects of digital filtering on mismatch negativity in wakefulness and slow-wave sleep. *J. Sleep Res.*, **11**, 123–127.

Salenius, S. & Hari, R. (2003) Synchronous cortical oscillatory activity during motor action. *Curr. Opin. Neurobiol.*, **13**, 678–684.

Schomburg, E.D. (1990) Spinal sensorimotor systems and their supraspinal control. *Neurosci. Res.*, **7**, 265–340.

Shiavi, R., Frigo, C. & Pedotti, A. (1998) Electromyographic signals during gait: criteria for envelope filtering and number of strides. *Med. Biol. Eng. Comput.*, **36**, 171–178.

Siemionow, V., Yue, G.H., Ranganathan, V.K., Liu, J.Z. & Sahgal, V. (2000) Relationship between motor activity-related cortical potential and voluntary muscle activation. *Exp. Brain Res.*, **133**, 303–311.

Solomonow, M., Baratta, R., Zhou, B.H. & d'Ambrosia, R. (1988) Electromyogram coactivation patterns of the elbow antagonist muscles during slow isokinetic movement. *Exp. Neurol.*, **100**, 470–477.

Thomas, C.K., Tucker, M.E. & Bigland-Ritchie, B. (1998) Voluntary muscle weakness and co-activation after chronic cervical spinal cord injury. *J. Neurotraum.*, **15**, 149–161.

Tuncel, D., Dizibuyuk, A. & Kiymik, M.K. (2010) Time frequency based coherence analysis between EEG and EMG activities in fatigue duration. *J. Med. Syst.*, **34**, 131–138.

Ushiyama, J., Takahashi, Y. & Ushiba, J. (2010) Muscle dependency of corticomuscular coherence in upper and lower limb muscles and training-related alterations in ballet dancers and weightlifters. *J. Appl. Physiol.*, **109**, 1086–1095.

Ushiyama, J., Masakado, Y., Fujiwara, T., Tsuji, T., Hase, K., Kimura, A., Liu, M., & Ushiba, J. (2012) Contraction level-related modulation of corticomuscular coherence differs between the tibialis anterior and soleus muscles in humans. *J. Appl. Physiol.*, **112**, 1258–1267.

Vallbo, A.B. & Wessberg, J. (1993) Organization of motor output in slow finger movements in man. *J. Physiol.*, **469**, 673.

Vecchio, F., Del Percio, C., Marzano, N., Fiore, A., Toran, G., Aschieri, P., Gallamini, M., Cabras, J. *et al.* (2008) Functional cortico-muscular coupling during upright standing in athletes and nonathletes: a coherence electroencephalographic-electromyographic study. *Behav. Neurosci.*, **122**, 917–927.

Wessberg, J. & Kakuda, N. (1999) Single motor unit activity in relation to pulsatile motor output in human finger movements. *J. Physiol.*, **517**, 273–285.

Wessberg, J. & Vallbo, A.B. (1996) Pulsatile motor output in human finger movements is not dependent on the stretch reflex. *J. Physiol.*, **493**(Pt 3), 895.

Williams, E.R. & Baker, S.N. (2009a) Circuits generating corticomuscular coherence investigated using a biophysically based computational model. I. Descending systems. *J. Neurophysiol.*, **101**, 31–41.

Williams, E.R. & Baker, S.N. (2009b) Renshaw cell recurrent inhibition improves physiological tremor by reducing corticomuscular coupling at 10 Hz. *J. Neurosci.*, **29**, 6616–6624.

Winter, D.A. (2005). *Biomechanics and motor control of human movement*, 3rd edn. Wiley, New York, NY.

Xia, R. & Rymer, W.Z. (2005) Reflex reciprocal facilitation of antagonist muscles in spinal cord injury. *Spinal Cord*, **43**, 14–21.

Yang, Y., Solis-Escalante, T., van de Ruit, M., van der Helm, F.C. & Schouten, A.C. (2016) Nonlinear coupling between cortical oscillations and muscle activity during isotonic Wrist Flexion. *Front. Comput. Neurosc.*, **10**, 126.

Yoshida, T., Masani, K., Zabjek, K., Chen, R. & Popovic, M.R. (2017) Dynamic increase in corticomuscular coherence during bilateral, cyclical ankle movements. *Front. Hum. Neurosci.*, **11**, 155.

Zhan, Y., Halliday, D., Jiang, P., Liu, X. & Feng, J. (2006) Detecting time-dependent coherence between non-stationary electrophysiological signals—a combined statistical and time–frequency approach. *J. Neurosci. Meth.*, **156**, 322–332.

115

CrossMark

ORIGINAL ARTICLE

Effects of hand configuration on muscle force coordination, co-contraction and concomitant intermuscular coupling during maximal isometric flexion of the fingers

Camille Charissou[1,2,4] · David Amarantini[2] · Robin Baurès[3] · Eric Berton[1] · Laurent Vigouroux[1]

Abstract

Purpose　The mechanisms governing the control of musculoskeletal redundancy remain to be fully understood. The hand is highly redundant, and shows different functional role of extensors according to its configuration for a same functional task of finger flexion. Through intermuscular coherence analysis combined with hand musculoskeletal modelling during maximal isometric hand contractions, our aim was to better understand the neural mechanisms underlying the control of muscle force coordination and agonist–antagonist co-contraction.

Methods　Thirteen participants performed maximal isometric flexions of the fingers in two configurations: power grip (*Power*) and finger-pressing on a surface (*Press*). Hand kinematics and force/moment measurements were used as inputs in a musculoskeletal model of the hand to determine muscular tensions and co-contraction. EMG–EMG coherence analysis was performed between wrist and finger flexors and extensor muscle pairs in alpha, beta and gamma frequency bands.

Results　Concomitantly with tailored muscle force coordination and increased co-contraction between *Press* and *Power* (mean difference: 48.08%; $p < 0.05$), our results showed muscle-pair-specific modulation of intermuscular coupling, characterized by pair-specific modulation of EMG–EMG coherence between *Power* and *Press* ($p < 0.05$), and a negative linear association between co-contraction and intermuscular coupling for the ECR/FCR agonist–antagonist muscle pair ($r = -0.65$; $p < 0.05$).

Conclusions　This study brings new evidence that pair-specific modulation of EMG–EMG coherence is related to modulation of muscle force coordination during hand contractions. Our results highlight the functional importance of intermuscular coupling as a mechanism contributing to the control of muscle force synergies and agonist–antagonist co-contraction.

Communicated by Toshio Moritani.

Electronic supplementary material　The online version of this article (doi:10.1007/s00421-017-3718-6) contains supplementary material, which is available to authorized users.

✉ Camille Charissou
　camille.charissou@univ-amu.fr

　David Amarantini
　david.amarantini@inserm.fr

　Robin Baurès
　robin.baures@cnrs.fr

　Eric Berton
　eric.berton@univ-amu.fr

　Laurent Vigouroux
　laurent.vigouroux@univ-amu.fr

[1]　CNRS, ISM UMR 7287, Aix-Marseille Université, Marseille, France

[2]　ToNIC, Toulouse NeuroImaging Center, INSERM, UPS, Université de Toulouse, Toulouse, France

[3]　CerCo, Université de Toulouse, CNRS, UPS, Toulouse, France

[4]　Institut des Sciences du Mouvement-Etienne-Jules Marey, CP 910, 163 av. de Luminy, 13288 Marseille Cedex 9, France

Keywords　Redundancy control · Wavelet-based intermuscular coherence · Hand modelling · Muscle tensions · Neural control

Abbreviations
ANCOVA　Analysis of covariance
ANOVA　　Analysis of variance

⌂ Springer

| CNS | Central nervous system |
DoF	Degree of freedom
ECR	Extensor carpi radialis
EDC	Extensor digitorium commonis
EMG	Electromyography
FCR	Flexor carpi radialis
FDS	Flexor digitorum superficialis
FE	Extrinsic finger extensor muscle group
FF	Extrinsic finger flexor muscle group
INT	Intrinsic muscles
N	Number of participants or sample size
SE	Standard error
WE	Extrinsic wrist extensor muscle group
WF	Extrinsic wrist flexor muscle group

Introduction

A fundamental feature of the musculoskeletal system is the high degree of redundancy, i.e., a greater number of muscles than articular degrees of freedom (DoF). As a consequence, muscle force combinations are infinite to achieve most isometric and dynamic motor actions, providing a large flexibility but making the control extremely complex (D'Avella et al. 2003). Understanding which mechanisms govern muscle force coordination and co-contraction of synergistic agonist and antagonist muscles is a central theme of research. As emphasized in recent studies (e.g., Hirashima and Oya 2016), a crucial question yet to be answered is how the central nervous system (CNS) solve such redundancy.

Regarding the control of muscle activation in voluntary contractions, it has been suggested that motoneurons of synergistic muscles share common corticospinal drives (Farmer et al. 2007) resulting in intermuscular coupling (Kattla and Lowery 2010). This coupling is traduced by the oscillatory synchronicity of electromyographic (EMG) activity in synergistic muscle pairs, often called 'EMG–EMG coherence' (e.g., Danna-Dos-Santos et al. 2010). Previous studies reached a broad consensus that EMG–EMG coherence provides a comprehensive index of intermuscular coordination (Charissou et al. 2016; De Marchis et al. 2015). Through this approach, it was demonstrated that intermuscular coupling takes part to the regulation of muscle activities (Farmer et al. 2007; Siemionow et al. 2010) and the importance of such coupling was emphasized as a mechanism responsible for the maintenance of the neuromuscular performance (Charissou et al. 2016; Danna-Dos Santos et al. 2010). In addition, even though it is a highly debated issue (Farina et al. 2014), coherence between pairs of EMG signals would reflect common central drive to muscle pairs (Boonstra 2013; Farmer et al. 1998, 2007) and can thus be taken as a sensitive tool to explore common neural inputs implicated in the control of synergistic muscle activation during voluntary contractions

(Lee et al. 2014; Power et al. 2006; Winges et al. 2006). Associated with different neural processes, coordinated intermuscular coupling can arise from divergent descending oscillatory pathways (Heroux and Gandevia 2013; Nazarpour et al. 2012). Typically, the modulation of EMG–EMG coherence in the 'alpha' (α) frequency band impacts postural muscles and involuntary contractions (Boonstra et al. 2008; Kattla and Lowery 2010). There is every possibility that some of the α band coherence is of subcortical origin (Hansen et al. 2005; Poston et al. 2010) but it is also thought to be mediated by spinal sources (Budini et al. 2014; Norton and Gorassini 2006). Coherence in the 'beta' (β) frequency band has been linked with voluntary isometric contractions and is likely to reflect oscillatory drives from the corticospinal pathway (Chang et al. 2012; Gwin and Ferris 2012). Changes in the 'gamma' (γ) frequency band have been associated with efferent drives to muscles during very strong tonic contractions and cognitive processes, such as focused attention, resulting from cortical-originating signals (Mima et al. 2000). In light of previous studies on intermuscular synchronization (Poston et al. 2010; Winges et al. 2008), it may be proposed that, for a given task, modification of intermuscular coherence could represent a mechanism that contributes to the coordination of muscular forces according to the functional roles attributed to the muscles. Thus, the modulation of EMG–EMG coherence in the α, β and γ frequency bands could reflect mechanisms that solve synergistic muscle coordination—specifically reflecting a way of controlling agonist–antagonist co-contraction.

The hand and fingers are one of the most complex musculoskeletal systems and its fine control allows extremely diverse and complex movements. With 23 DoF and over 40 muscles, mostly polyarticular each mobilizing several DoF, the regulation of hand muscle coordination is extremely specific. The hand, thus, represents a reliable model that could bring further knowledge to current understanding of the mechanisms participating in the control of muscle force coordination between synergistic muscles, especially at the co-contraction level. Previous studies on hand musculoskeletal modelling demonstrated that muscle coordination patterns and force distribution are task specific (Valero-Cuevas et al. 2009). Especially, muscle force coordination and the functional role of the hand extensors can differ depending on whether hand contractions involve gripping objects or finger pressing on a plane surface, though in both configurations the same functional task is required which is to perform voluntary flexion of the fingers (Goislard de Monsabert et al. 2012; Snijders et al. 1987). During finger-pressing (see Fig. 1a), hand extensors are weakly mobilized, at a lower level than flexors, and are engaged in the hand joint postural stabilisation. Conversely, during power grip (see Fig. 1b), extensors are highly employed, approximately at the same
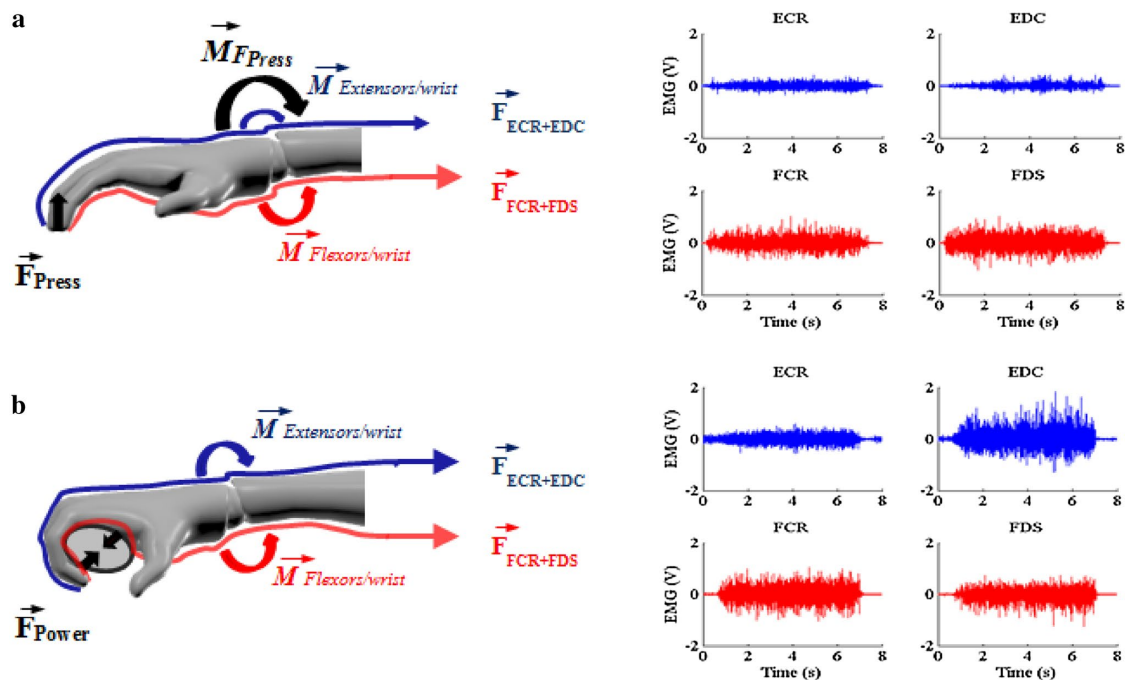
Fig. 1 Schematic representation of the two different configurations of finger force application in which participants performed maximal voluntary finger isometric flexion contractions: **a** "Finger pressing" (*Press*) and **b** "Power grip" (*Power*). F_{Power} and F_{Press} represent the force produced in the direction normal to the contact surface in *Power* and *Press*, respectively. $M_{Flexors/wrist}$, $M_{Extensors/wrist}$ and M_{FPress} represent the moments of force about the wrist joint. In each hand configuration, $F_{ECR+EDC}$ and $F_{FCR+FDS}$ represent the tension of extensor and flexor muscles, respectively. The right panels show high-pass-filtered (3 Hz, 4th-order zero-lag Butterworth) EMG activity of ECR, EDC, FCR and FDS muscles in *Press* (upper panels) and in *Power* (lower panels). Note that with *Press*, the grip force generates a wrist moment (curved black arrow) leading to a low requirement of extensor mechanical action. With *Power*, no wrist moment is generated by the grip forces (black arrows) since the latter are balanced inside the hand-object mechanical system, this mechanical aspect, thus, explaining the higher wrist extensor muscle tensions required to balance the mechanical action of finger flexors at the wrist level. Such mechanical phenomenon leads to different muscle coordination which can be identified on the corresponding EMG patterns

level than flexors, and play a major functional role for system equilibrium. These observations suggest that muscle coordination strategies, co-contraction and consequently concomitant intermuscular coupling, differ between these two configurations of hand force application for a same functional task of finger flexion.

The aim of the present study was to better understand the neural mechanisms underlying the control of musculoskeletal redundancy. We harness the unique opportunity offered by hand contractions to clarify the functional significance of EMG–EMG coherence, reflecting tailored neural drive to hand muscles, in the control of muscle force coordination and in the regulation of co-contraction between synergistic agonist and antagonist muscles. The proposed approach thus combines hand/wrist musculoskeletal modelling (Goislard de Monsabert 2012)—used to quantify mechanical outcomes in terms of hand muscle

tensions and agonist–antagonist co-contraction—and time–frequency wavelet-based EMG–EMG coherence (Bigot et al. 2011; Charissou et al. 2016)—used to quantify intermuscular coupling in the alpha-, beta- and gamma range. Power grip and finger pressing were studied with the aim of changing the functional role of wrist and finger muscles for a same functional maximal isometric finger flexion. Based on previous research (Johnston et al. 2005; Poston et al. 2010), we hypothesized pair-specific differences in EMG–EMG coherence values between power grip and finger pressing, related to modulation of muscle force coordination. A correlation between intramuscular coherence, especially in the beta-range, and the level of agonist–antagonist co-contraction was expected. Such a linear association could reflect the functional importance of intermuscular coupling as a mechanism that contributes to the control of co-contraction.

Methods

Participants

Thirteen right-handed males (age: 24.8 ± 3.7 years; height: 176.8 ± 6.8 cm; weight: 74.2 ± 10.7 kg, hand length: 19.1 ± 1.2 cm; hand width: 8.7 ± 0.5 cm; mean $\pm$ SD), free of known neuromuscular disorders or musculoskeletal hand injuries on their dominant side, were recruited in the study. All participants were physically active university students not involved in any specific training program. Written informed consent was obtained from all of them according to the Declaration of Helsinki. The study followed institutional ethics board guidelines for research on humans.

Protocol

Participants were seated in a comfortable position with their right arm placed on a rigid support so that the shoulder was flexed at 0° and abducted at 45°. The elbow was flexed at 90° and the forearm and wrist held in a neutral position. Participants were asked to perform maximal voluntary flexion contractions of the fingers in two different configurations of force application presented in random order (Fig. 1). During "power grip" contractions (*Power*), participants held a 3.5-cm custom-made hand dynamometer between the bottom of the palm of the hand and middle phalange of the fingers, excluding the thumb to avoid its influence on finger force coordination (Vigouroux et al. 2011). During "finger-pressing" contractions (*Press*), participants kept their hand horizontal and pressed vertically on the support with the index, major, ring and little fingers (Li et al. 1998). In each hand configuration, they performed five 6-s maximal contractions with strong verbal encouragements. They were allowed 2-min rest between contractions and 5-min rest between configurations to prevent muscle fatigue. Three participants were excluded from analysis because they failed to comply with the instruction to not overstretch the fingers in *Press*.

Recordings

The experimental setup was largely inspired by the work of Goislard de Monsabert et al. 2012. In brief:

- Forces and moments produced by the fingers were recorded by a 6-axis force/torque sensor (Nano25-E, ATI Industrial Automation, Apex, NC, USA) at 1 kHz. In *Press*, the force sensor was fixed on the support; in *Power* it was enclosed by two steel plates to apply the required mechanical effort.
- 3-D positions of the fingers, hand and forearm segments and of the dynamometer (in *Power*) or the surface (in *Press*) were recorded at 125 Hz by an 8-camera system (MX T40, Vicon, Oxford, UK) with 33 spherical reflective markers of 6-mm diameter (Suppl. Figure 1a).
- After suitable skin preparation (Hermens et al. 2000), muscle activities were collected at 2 kHz using a surface EMG system (MP150; Biopac Systems Inc., Goleta, CA, USA) with Ag-AgCl 11-mm bipolar electrodes (2 cm spacing). *Flexor digitorum superficialis* (FDS), *flexor carpi radialis* (FCR), *extensor digitorum communis* (EDC), and *extensor carpi radialis* (ECR) were taken to represent finger flexors (FF), wrist flexors (WF), finger extensors (FE) and wrist extensors (WE), respectively. Using the recommendations in Vigouroux et al. (2015), pairs of surface electrodes were placed along the direction of muscle fascicles of right FDS, FCR, EDC and ECR muscles (Suppl. Figure 1b) from anatomical description, palpation and a series of functional tests including finger and wrist flexion and extension contractions. Moreover, the quality of the electrical signal was inspected through a visual feedback using the software AcqKnowledge (BIOPAC, Systems Inc., Goleta, CA, USA), before the beginning of voluntary isometric contractions to assess correct EMG sensor location in the desired target muscle.

Data processing

All computations were performed using MATLAB (Mathworks, Natick, MA, USA).

Maximal net force After calibration matrix application of the force/torque sensor and low-pass filtering (10 Hz, fourth-order, zero-lag Butterworth), maximal net force was calculated as mean normal force computed on the 0.5-s time interval of interest of highest force production.

Muscular tensions A musculoskeletal model of the entire hand including wrist and fingers (Goislard de Monsabert et al. 2012) was used to estimate muscular forces over the time period of interest in the two configurations of force application. This model considered bones as rigid bodies articulated around 16 articulations with 23 DoF and mobilized by 42 muscles. The muscle moment arms of muscle tendons across each joint were estimated from the finger joint angles computed using 3D hand kinematics and the data of Chao et al. (1989) and Lemay and Crago (1999). The underdetermined set of static moment equilibrium equations stating that the external force moments are counterbalanced by the muscle force moments at each DoF was solved using nonlinear constrained optimization to determine the muscle tensions which minimize the following muscle stress criterion:

$$\min \sum_m \left(\frac{t_m}{\text{PCSA}_m} \right)^4$$

where t_m and PCSA$_m$ are respectively the muscle tensions and the physiological cross-sectional area of muscle m.

For the nine participants for whom the optimization process converged to a global minimum of the cost function in less than 1000 iterations, tension of finger and wrist flexor muscle group was then obtained by summing FF and WF tensions, while that of the finger and wrist extensor muscle group was quantified by summing FE and WE tensions, (Vigouroux et al. 2015). Noteworthy is that INT was not considered in the analysis as EMG was not collected from these muscles and they do not cross the wrist joint. Finally, muscle group tensions were used to compute co-contraction between finger and wrist flexors and extensors according to the expression given by Falconer and Winter (1985).

EMG–EMG coherence Given strong a priori evidence from the literature that *Press* and *Power* functionally differ by the specific role of the wrist extensors (Snijders et al. 1987), this work focused on ECR/FCR, ECR/FDS and ECR/EDC muscle pairs. For each muscle pair, intermuscular coherence analysis was performed using the approach described by Charissou et al. (2016; see 'Intermuscular interactions' in "Methods" and Online Appendix A), which:

- takes advantage of time–frequency analysis to account for how the oscillatory patterns of EMG change with time;
- presents the crucial advantage to assess coherence with values corresponding to a truly significant level of dependence between the EMG time series, particularly when the number of trials is small (Bigot et al. 2011).

First, EMG–EMG coherence was calculated in the time–frequency domain using the *WavCrossSpec* software (Bigot et al. 2011; available for download at: http://www.math.u-bordeaux1.fr/~jbigot/Site/Software_files/WavCrossSpec.zip). In *WavCrossSpec*, the parameter 'nvoice' (i.e., the scale resolution of the wavelet), 'J1' (i.e., the number of scales used in the wavelet analysis) and 'wavenumber' (i.e., the Morlet mother wavelet parameter) optimally set respectively to 7, 50 and 10 based on the processing of simulated data, to provide a satisfactory compromise between time and frequency resolution for the identification of oscillatory activity on the $[0.32 \times 10^{-2}:0.23:79.97]$ Hz frequency range. To meet the theoretical and practical recommendations of previous studies (e.g., Bigot et al. 2011; McClelland et al. 2014), magnitude-squared coherence (Fig. 2, fourth row) was computed from unrectified high-pass filtered (3 Hz, 4th-order zero-lag Butterworth) EMG time series (Fig. 2, first row) as follows:

$$R^2_{\text{EMG1/EMG2}}(\omega,\ u) = \left| S_{\text{EMG1/EMG2}}(\omega,\ u) \right|^2 / $$
$$\left(S_{\text{EMG1}}(\omega,\ u)\ S_{\text{EMG2}}(\omega,\ u)' \right)$$

where $S_{\text{EMG1/EMG2}}(\omega,\ u)$ is the wavelet cross-spectrum between the two EMG time series at frequency ω and time u (Fig. 2, third row); $S_{\text{EMG1}}(\omega,\ u)$ and $S_{\text{EMG2}}(\omega,\ u)$ are wavelet auto-spectra of EMG time series at frequency ω and time u. (Fig. 2, second row). Refer to Bigot et al. (2011) for detailed equations.

Then, EMG–EMG coherence was quantified in 'alpha' (α), 'beta' (β) and 'gamma' (γ) frequency bands. In agreement with previous intermuscular coherence studies (Danna Dos Santos et al. 2010; Kattla and Lowery 2010), boundaries were respectively set as follows: α, 8–12 Hz; β, 15–35 Hz; γ, 35–60 Hz. In each frequency band, EMG–EMG coherence value was calculated as the volume under magnitude-squared coherence values in the time window of interest where the correlation between the EMG time series was detected significant on the wavelet cross-spectrum (Fig. 2, fifth row).

Statistics

All kinetic variables met normality (Shapiro–Wilk test, $\alpha = 0.05$) and homogeneity of variance (Levene's test, all $p > 0.05$) assumptions. Student's t-tests were used to assess between-*Configuration* effects (*Press* vs. *Power*) on maximal net force ($N = 10$), predicted muscular tensions and co-contraction ($N = 9$). A 2 *Configuration* (*Press* vs. *Power*) × 2 *Muscle Function* (*Flexors* vs. *Extensors*) repeated measures ANOVA was performed on muscle group tensions ($N = 9$).

For each muscle pair and frequency band, an ANCOVA was first performed on EMG–EMG coherence ($N = 10$) with *Configuration* as a within-participant factor and maximal net force as a co-variable, to check if EMG–EMG coherence was influenced by the *Configuration* while controlling for the exerted net force. Indeed, it is yet unclear how exerted net force may (1) affect EMG–EMG coherence (Farina et al. 2014; Heroux and Gandevia 2013; Semmler et al. 2003; Witte et al. 2007), and (2) have a different influence on EMG–EMG coherence depending on the *Configuration*. Importantly, this analysis failed to show any significant interaction between *Configuration* and the maximal net force (all $p > 0.05$), showing a lack of correlation between EMG–EMG coherence and maximal net force for each *Configuration*. However, EMG–EMG coherence values failed to meet both normality and homogeneity of variance assumptions. As used in other studies in the presence of skewed distribution (e.g., Vrána et al. 2005), permutation tests with bootstrapping technique (Efron and Tibshirani 1993) with 10,000 replications were, thus, conducted for each muscle pair and frequency band to test between-*Configuration* differences on EMG–EMG coherence irrespective of the maximal net force. A significant effect of *Configuration* was declared significant if the observed difference between *Power* and *Press* was outside the 95% confidence interval of the newly built 10,000 mean difference distributions under the null hypothesis.
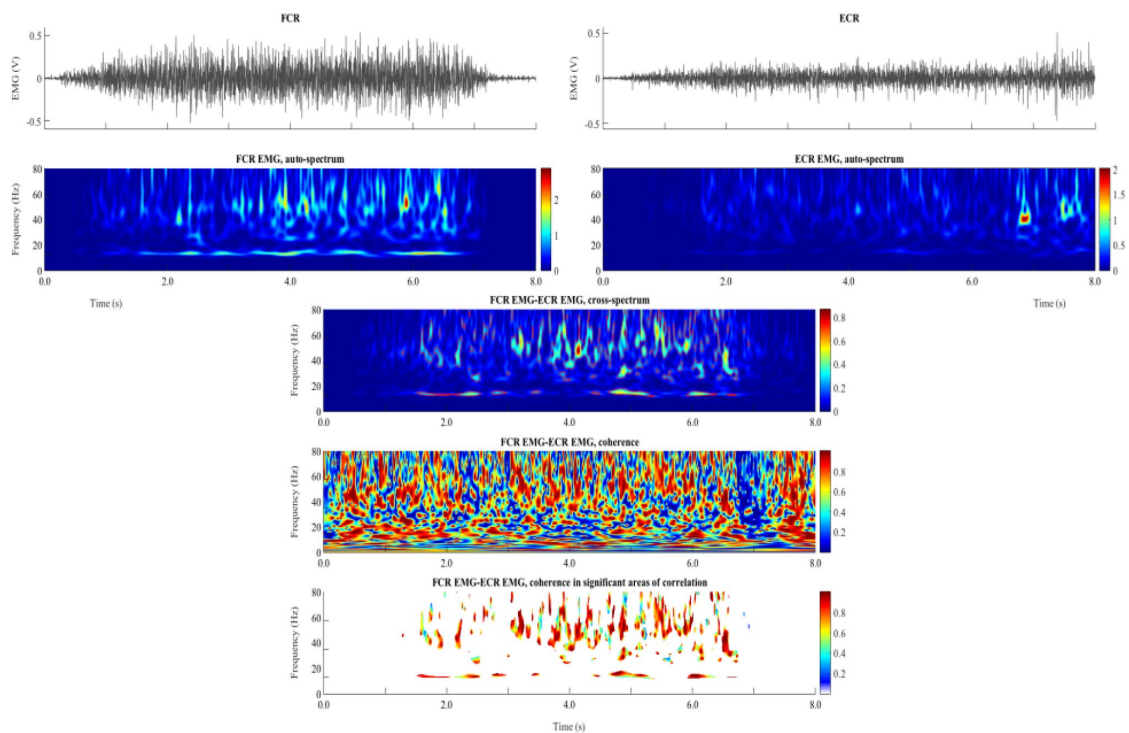
Fig. 2 Illustration of the different steps involved in the calculation of time–frequency wavelet-based EMG–EMG coherence (muscle pair: ECR/FCR; configuration: *Press*). First row: mean EMG signals from FCR (left) and ECR (right) muscles. Second row: wavelet auto-spectra of EMG time series from FCR (left) and ECR muscles (right). Third row: wavelet cross-spectrum between the two EMG time series; the red contours identify the areas in the time–frequency plane where the correlation between the EMG signals is significant. Fourth row: wavelet magnitude-squared coherence between the two EMG time series. Fifth row: wavelet magnitude-squared coherence between the two EMG time series where the correlation between the EMG signals is significant. In each frequency band (α: 8–12 Hz; β: 15–35 Hz; γ: 35–60 Hz), EMG–EMG coherence value was defined as the volume under magnitude-squared coherence values in the 0.5-s time window of interest where the correlation between the EMG time series was detected significant on the wavelet cross-spectrum

Finally, Pearson's correlations were tested between co-contraction and EMG–EMG coherence for each muscle pair and frequency band ($N = 9$).

Data are reported as mean with 95% CI within the text and Figs. 3 and 4. The level of significance was set at $p < 0.05$ for all tests.
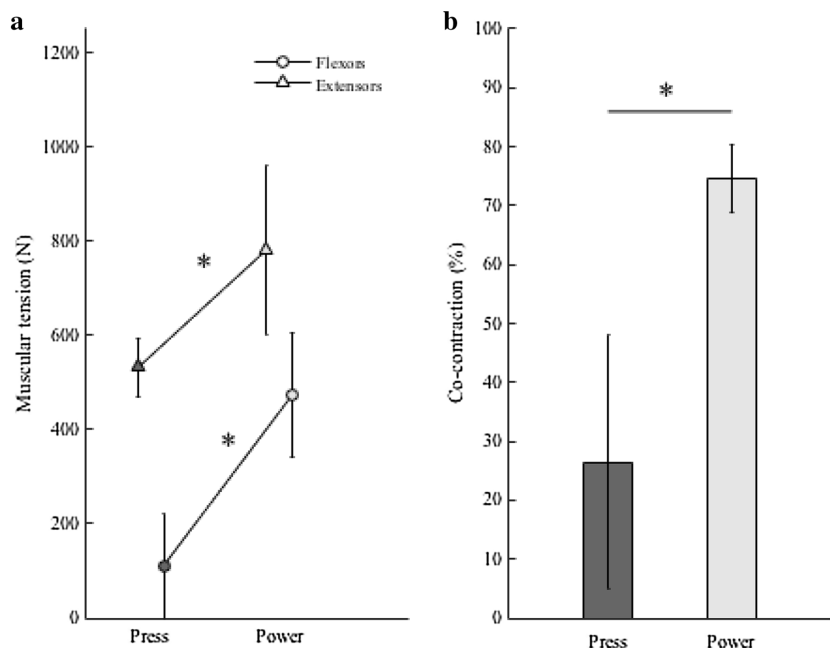
Results

Maximal net force and muscular tensions

Statistical analysis revealed greater maximal net force in *Power* than in *Press* [232.14 N, 95% CI (188.59:275.68) vs. 76.13 N, 95% CI (66.55:85.70); $t_8 = 7.59$, $p < 0.05$], in association with significant differences in all estimated muscular tensions (all $t_8 > 2.13$, $p < 0.05$): between *Press* and *Power* the tensions developed by WE, FE and FF increased in mean respectively by $\times 1.40$, $\times 0.92$ and $\times 3.04$ the corresponding difference of maximal net force, whereas WF tension decreased in mean by $\times 1.44$. These differences resulted in significantly increased tensions developed by the finger and wrist flexors and extensors between *Press* and *Power* ($F_{1,32} = 29.34$, $p < 0.05$; Fig. 3a), with a significant main *Muscle Function* effect ($F_{1,32} = 41.61$, $p < 0.05$) but no significant interaction between *Configuration* and *Muscle Function* ($F_{1,32} = 0.98$, $p > 0.05$).

As a consequence, co-contraction between finger and wrist flexors and extensors was significantly higher in *Power* than in *Press* [mean difference = 48.08%, 95% CI (24.57:71.60); $t_8 = 4.62$, $p < 0.05$; Fig. 3b].

Fig. 3 ($N=9$) **a** Tensions of finger and wrist flexors and extensors during maximal isometric contractions in *Press* and *Power*. **b** Corresponding co-contraction levels in *Press* and *Power*. Asterisk: indicates a significant *Configuration* effect

EMG–EMG coherence

Figure 4a show typical profiles of the normal force exerted by the fingers and typical time–frequency maps of EMG–EMG coherence between ECR and FCR muscles in *Press* (left) and *Power* (right).

A first important qualitative result was that the detection of significant areas of intermuscular interactions in the time–frequency plane differed depending on the muscle pair (i.e., ECR/FCR, ECR/FDS or ECR/EDC) and the *Configuration* level (i.e., *Power* or *Press*). For example, significant areas of correlation between EMG time series were detected for all participants in all muscles pairs in *Press* and in *Power* in the γ (35–60 Hz) frequency band. A similar finding was observed in terms of detection for, e.g., ECR/EDC muscle pair in *Press* in the β (15–35 Hz) frequency band, whereas, on the contrary, no significant area of correlation between EMG time-series were found for, e.g., ECR/FCR muscle pair in *Power* in the α (8–12 Hz) frequency band.

Noteworthy is that the proposed ANCOVA pre-analysis performed on EMG–EMG coherence (see "Statistics" section) showed that the lack of correlation between EMG–EMG coherence and maximal net force was true for all *Configuration* levels, whatever the frequency band. These findings allow one to compare EMG–EMG coherence results between *Power* and *Press* irrespective of the exerted maximal net force.

Statistical analysis revealed that β EMG–EMG coherence was significantly lower in *Power* than in *Press* for both ECR/FCR [mean difference = 0.191, 95% CI (0.05:0.241); $p < 0.05$] and ECR/EDC [mean difference = 0.494, 95% CI (-0.047:0.941); $p < 0.05$] muscle pairs, with no significant difference for ECR/FDS (Fig. 4b, middle). In the gamma-range (γ), statistical analysis showed lower EMG–EMG coherence in *Power* than in *Press* for ECR/EDC muscle pair [mean difference = 1.003, 95% CI (0.439:1.567); $p < 0.05$], with no significant difference for both ECR/FCR and ECR/FDS (Fig. 4b, right). Permutation tests disclosed significant difference of α EMG–EMG coherence between *Press* and *Power* for all muscle pairs (all $p > 0.05$) (Fig. 4b, left).

Correlations between co-contraction and EMG–EMG coherence

Pearson's correlation analysis between co-contraction and EMG–EMG coherence showed significant negative correlation between levels of co-contraction and β EMG–EMG coherence for ECR/FCR muscle pair [$r = -0.65$, 95% CI (-0.86:-0.26); $t_{16} = 3.42$, $p = 0.003$] and ECR/EDC muscle pair [$r = -0.47$, 95% CI (-0.77:-0.01); $t_{16} = 2.15$, $p = 0.04$]. For both muscle pairs (see Fig. 5 for ECR/FCR), the lower was β EMG–EMG coherence, the higher was agonist–antagonist co-contraction between finger and wrist flexors and extensors. For all other frequency bands and muscles
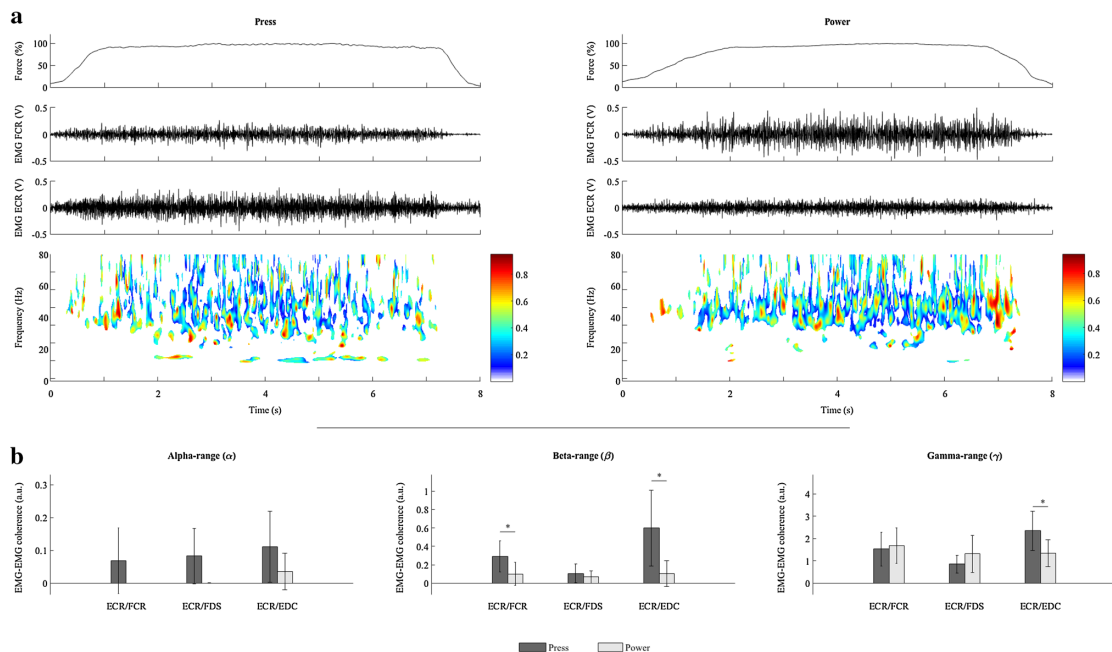
Fig. 4 a Typical net force (first row), EMG signal from ECR and FCR (second and third rows, respectively), and maps of EMG–EMG coherence between ECR and FCR muscles where intermuscular interactions were significant on the wavelet cross-spectrum (forth row) in *Press* (left panels) and *Power* (right panels) for a representative participant. **b** EMG–EMG coherence values in the alpha-range (8–12 Hz, α; left column), the beta-range (15–35 Hz, β; middle column) and the gamma-range (35–60 Hz, γ; right column) for ECR/FCR, ECR/FDS and ECR/EDC muscle pairs during maximal voluntary isometric flexion contraction of the fingers in *Press* and *Power* ($N = 10$). Asterisk: indicates a significant *Configuration* effect
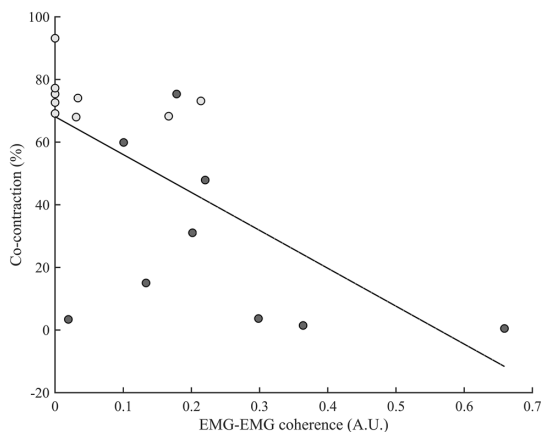
Fig. 5 Correlation between co-contraction of finger and wrist flexors and extensors and β (15–35 Hz) EMG–EMG coherence for ECR/FCR muscle pair ($N = 9$). The light grey and dark grey dots represent observations in *Power* and in *Press*, respectively; the black line shows the best fit linear regression. The Pearson product-moment correlation coefficient is -0.65 [95% CI = $(-0.86 : -0.26)$], with significant negative linear association between co-contraction and EMG–EMG coherence ($p = 0.003$)

pairs (including EDC/FCR, EDC/FDS and FCR/FDS, not presented here) the analysis did not reveal any significant correlation between co-contraction and EMG–EMG coherence (all $t_{16} < 0.89$, $p > 0.05$).

Discussion

Based on an original approach, which combines for the first time musculoskeletal biomechanical modelling and intermuscular coherence analysis, this study compares muscular tensions, co-contraction and intermuscular coupling between finger and wrist flexors and extensors during two different configurations of maximal finger force application. Our key results demonstrated first, that the modulation of muscle force coordination and intermuscular coherence are strongly related to the task constraints, and second, that a linear association exists between agonist–antagonist co-contraction and beta-range intermuscular coupling for the primary agonist–antagonist muscle pair.

Maximal net force and muscular tensions

As expected, *Power* and *Press* differed greatly in muscle force coordination. Greater maximum net force was obtained in *Power* than in *Press* in association with (1) higher tensions developed by WE, FE and FF, and (2) lower tension developed by WF. These results showed that *Configuration*-related changes in maximal net force were not accompanied by a trivial or a proportional modulation of muscle tensions. Each muscle tension demonstrated a specific pattern of change between *Press* and *Power*, suggesting that muscle-synergy patterns used to perform maximal voluntary flexion contractions of the fingers are highly dependent on the configuration of finger force application. During *Press*, the extensors were weakly solicited and coupled with a classical role of joint stabilisation, resulting in low-level of co-contraction. Conversely, during *Power*, the extensors were highly mobilized to serve the functional role of system equilibrium, culminating in high level of co-contraction. These results were comparable to those reported for both configurations in the literature (Goislard de Monsabert et al. 2012) and demonstrated task-related changes in muscle force coordination (Nazarpour et al. 2012; Valero-Cuevas et al. 2009). Consequently, co-contraction level was different between the two configurations. The higher co-contraction observed in *Power* has been explained previously (Snijders et al. 1987) by specific mechanical configuration in which the contribution of extensors was needed to equilibrate unintended flexion moments caused by finger flexors at the wrist joint level. Our data thus demonstrated that muscle coordination patterns differed according to the configuration of finger force application, although the functional demand to exert maximal voluntary flexion was similar between *Power* and *Press*.

Together with the possibility to discuss between-*Configuration* differences on EMG–EMG coherence irrespective of the maximal net force, these findings confirm that the proposed comparison between *Power* and *Press* is relevant to investigate the modulation of EMG–EMG coherence according to different muscle coordination and functional role of muscles for a similar given task.

EMG–EMG coherence

Concomitantly with the above changes in muscle forces, our results revealed significant differences in the magnitude of EMG–EMG coherence, with different modulation patterns in both the frequency band (α, β or γ) and the muscle pair (ECR/FCR, ECR/FDS or ECR/EDC) according to the configuration (*Press* vs. *Power*). One cannot exclude the possibility that a part of EMG–EMG coherence may result from cross-talk artifacts inherent to surface EMG recordings, especially among the forearm muscles (Kong et al.

2010). Nevertheless, our experimental design devoted particular attention to EMG sensor placement (see "Recordings" section) and the same electrode placement was maintained during all the experiment. We thus are confident in the fact that cross-talk artifacts or electrode placement (Keenan et al. 2011) cannot explain the differences observed on EMG–EMG coherence between the two *Configurations*.

The statistical pre-test revealed that the difference observed between *Press* and *Power* in the absolute maximal net force did not influence the magnitude of EMG–EMG coherence. This result contributes to the open debate on the influence of net-exerted muscle force/torque on the strength of intermuscular coupling (Farina et al. 2014; Heroux and Gandevia 2013). In agreement with Poston et al. (2010), this finding provides direct support for a net force-independent modulation of intermuscular coherence during voluntary maximal flexion contraction of the wrist and fingers muscles. It suggests an involvement of force-independent mechanisms constraining the concurrent activation of multiple hand muscles according to the configuration of finger force application. Importantly for the purpose of the present study, the observed lack of significant correlation between EMG–EMG coherence and maximal net force for each *Configuration* allows discussing for differences in EMG–EMG coherence values depending only on the *Configuration*.

Beta-range (β) intermuscular coupling

The main findings of our study concern beta-range (β) intermuscular coupling. In the β (15–35 Hz) frequency band, significant EMG–EMG coherence was detected for all muscle pairs in both configurations. This first result is consistent with the identification of β intermuscular synchronization between synergistic muscles (Boonstra et al. 2008; Poston et al. 2010). In addition, the magnitude of EMG–EMG coherence was different between *Power* and *Press* only for ECR/EDC and ECR/FCR. For these two muscle pairs, the strength of beta-range intermuscular coupling was lower in *Power* than in *Press*, while no significant difference was found for ECR/FDS. This finding is in line with Winges et al. (2008) indicating that the modulation of β EMG–EMG coherence is muscle pair specific. In view of the results obtained from hand modelling, it is particularly relevant to note that the lower strength of intermuscular coupling observed in *Power* than in *Press* was concomitant with the increased tension developed by wrist extensors identified with the musculoskeletal model outputs. Our results are thus consistent with the hypothesis that beta-range intermuscular coupling is a mechanism that may take part in the regulation of muscle force coordination (Charissou et al. 2016; De Marchis et al. 2015). Moreover, we extend the evidence provided by Winges et al. (2006) that β EMG–EMG coherence

differs according to muscle functional role determined by task constraints.

Furthermore, our study is the first to the best of our knowledge, to show a direct link between agonist–antagonist co-contraction and β EMG–EMG coherence. Our results from hand modelling indeed showed that *Configuration*-related changes in muscle tensions led to greater agonist–antagonist co-contraction in *Power* than in *Press*. Interestingly, correlation analysis revealed significant negative correlations between the level of co-contraction and beta-range intermuscular coupling for ECR/FCR and ECR/EDC, that is for the two muscle pairs specifically associated with a significant effect of *Configuration* on β EMG–EMG coherence. Especially, with a r value of -0.65 ($p = 0.003$) the correlation between the level co-contraction and EMG–EMG coherence for ECR/FCR muscle pair indicates linear association between co-contraction and intramuscular coupling for the primary agonist–antagonist muscle pair. For ECR/EDC muscle pair, although the correlation is significant ($p = 0.04$), it becomes more difficult with a weak *r* value of -0.45 to find support for a linear relationship between co-contraction and intermuscular coupling. In line with Pizzamiglio et al. (2017), who recently suggested that ~ 40–100 Hz intermuscular coupling could take part in regulating the co-contraction of arm muscles, these novel findings suggest that the modulation of β EMG–EMG coherence may reflect a mechanism contributing to muscle pair-specific regulation of co-contraction between synergistic agonist and antagonist muscles. Our results thus highlight that muscle pair-specific modulation of intermuscular coupling could take part in the "tuning of muscle activations" (von Tscharner et al. 2011) and in the mechanisms underlying the regulation of agonist–antagonist co-contraction. Even if the conclusions should be considered in regards to the reliability and the limitations of coherence analysis between electrophysiological signals (e.g., Farina et al. 2014), β-band coherence is generally considered to be of cortical origin and it is likely "that the primary motor cortex is involved in the generation of EMG–EMG coherence between hand muscles in the β-band during grip tasks" (Lee et al. 2014). In this view, our findings strengthen the idea formulated by Poston et al. (2010) that the relative contribution of spinal and supraspinal mechanisms is modulated according to task constraints and beyond muscle contribution and functional role. Furthermore, our results on tailored modulation of beta-range intermuscular coupling between *Press* and *Power* provides additional arguments sustaining a muscle pair-specific distribution of common neural inputs to the hand muscles (Johnston et al. 2005) during maximal voluntary isometric flexion contraction of the fingers. These results support the view that central

mechanisms are directly involved in the regulation of agonist–antagonist muscle co-contraction (Dal Maso et al. 2012; Mullany et al. 2002). Our study thus provides new evidence that muscle pair-specific beta-range intermuscular coupling would take part in the regulation of muscle redundancy around hand joints, especially at the level of agonist–antagonist co-contraction.

Alpha-range (α) intermuscular coupling

In the α (8–12 Hz) frequency band, statistical analysis showed no significant effect of *Configuration* on intermuscular coupling, whatever the studied muscle pair. This finding is not consistent with previous studies that showed that hand postural function was associated with modulation of α EMG–EMG (Poston et al. 2010). However, from a more qualitative point of view, our results showed that the presence of EMG–EMG coherence in the α (8–12 Hz) frequency band was different according to both the muscle pair and the hand configuration. Especially, an absence of α EMG–EMG coherence was identified for all subjects only in *Power* and only for the ECR/FCR muscle pair. This finding was concomitant with the modulation of the level of co-contraction between *Press* and *Power*, associated with the postural functional role of ECR during *Press*. One could thus suggest that α EMG–EMG coherence was specifically required between synergistic agonist and antagonist muscles acting around the wrist when the extensors were specifically involved as joint stabilisers. Our results may thus support the importance of alpha-range intermuscular coupling between agonist and antagonist muscles as a key mechanism in the control of joint stabilisation. Even if previous studies have reported that α-band coherence may be mediated by spinal sources (Budini et al. 2014; Norton and Gorassini 2006), further work is needed to investigate the involvement of spinal mechanisms in the regulation of agonist–antagonist co-contraction when the task needs particular heeding requisites for joint stability.

Gamma-range (γ) intermuscular coupling

In the γ (35–60 Hz) frequency band, significant intermuscular coherence was found for all studied muscle pairs in both *Press* and *Power* configurations. This finding is consistent with the relation previously established between γ EMG–EMG coherence and strong contractions (Gwin and Ferris 2012). However, significant modulation of γ EMG–EMG coherence was found for ECR/EDC muscle pair only, with higher strength of intermuscular coherence in *Press* than in *Power*. Although it is difficult to arrive at a definitive conclusion with regards to the literature, we can suggest that the observed pair-specific modulation of gamma-range (γ) intermuscular coherence between

synergistic antagonist muscles may reflect the implication of efferent drives involved in very strong tonic contractions and of cognitive processes, such as focused attention (Mima et al. 2000). Brown et al. (1998) suggested that gamma-range oscillations may reflect binding of functionally associated cortical elements. Thus, non-intuitively in view that power grip was seen only in humans and highly-developed monkeys (Marzke et al. 2015), our findings may suggest that attentional resources and complex integration of sensory information are used during hand contractions in both configurations, with greater involvement during finger pressing.

Conclusion

The present work harness the opportunity offered by hand contractions and combined musculoskeletal and time–frequency coherence analysis to better understand the neural mechanisms underlying the control of muscle force coordination and co-contraction between agonist and antagonist synergistic muscles. Although further studies are needed to test whether our conclusions can be extended to other muscles than those acting around finger and wrist joints selected is the present study, our findings emphasized the functional importance of intermuscular coupling as a mechanism that could take part in the control of muscle force synergies and agonist–antagonist co-contraction. These findings contribute to a better fundamental understanding of neural hand motor control mechanisms, which could help in the development of diagnostic procedures and clinical rehabilitation (Boonstra 2013).

Compliance with ethical standards

Conflict of interest The authors declare that there are no conflicts of interest.

References

Bigot J, Longcamp M, Dal Maso F, Amarantini D (2011) A new statistical test based on the wavelet cross-spectrum to detect time–frequency dependence between nonstationary signals: application to the analysis of cortico-muscular interactions. Neuroimage 55:1504–1518

Boonstra TW (2013) The potential of corticomuscular and intermuscular coherence for research on human motor control. Front Hum Neurosci 7:855

Boonstra TW, Daffertshofer A, van Ditshuizen JC, van den Heuvel MR, Hofman C, Willigenburg NW, Beek PJ (2008) Fatigue-related changes in motor-unit synchronization of quadriceps muscles within and across legs. J Electromyogr Kinesiol 18:717–731

Brown P, Salenius S, Rothwell JC, Hari R (1998) Cortical correlate of the Piper rhythm in humans. J Neurophysiol 80:2911–2917

Budini F, Lowery M, Durbaba R, De Vito G (2014) Effect of mental fatigue on induced tremor in human knee extensors. J Electromyogr Kinesiol 24:412–418

Chang YJ, Chou CC, Chan HL, Hsu MJ, Yeh MY, Fang CY, Chuang YF, Wei SH, Lien HY (2012) Increases of quadriceps inter-muscular cross-correlation and coherence during exhausting stepping exercise. Sensors 26:16353–16367

Chao EY, An KN, Cooney WP III, Linscheid RL (1989) Biomechanics of the hand: a basic research study. World Scientific, Singapore

Charissou C, Vigouroux L, Berton E, Amarantini D (2016) Fatigue- and training-related changes in 'beta' intermuscular interactions between agonist muscles. J Electromyogr Kinesiol 27:52–59

d'Avella A, Saltiel P, Bizzi E (2003) Combinations of muscle synergies in the construction of a natural motor behavior. Nat Neurosci 6:300–308

Dal Maso F, Longcamp M, Amarantini D (2012) Training-related decrease in antagonist muscles activation is associated with increased motor cortex activation: evidence of central mechanisms for control of antagonist muscles. Exp Brain Res 220:287 – 95

Danna-Dos-Santos A, Poston B, Jesunathadas M, Bobich LR, Hamm TM, Santello M (2010) Influence of fatigue on hand muscle coordination and EMG–EMG coherence during three-digit grasping. J Neurophysiol 104:3576–3587

De Marchis C, Severini G, Margherita Castronovo A, Schmid M, Conforto S (2015) Intermuscular coherence contributions in synergistic muscles during pedaling. Exp Brain Res 233:1907–1919

Efron B, Tibshirani RJ (1993) An introduction to the bootstrap. Chapman & Hall

Falconer K, Winter DA (1985) Quantitative assessment of co-contraction at the ankle joint in walking. Electromyogr Clin Neurophysiol 25:135–149

Farina D, Negro F, Dideriksen JL (2014) The effective neural drive to muscles is the common synaptic input to motor neurons. J Physiol 592:3427–3441

Farmer SF (1998) Rhythmicity, synchronization and binding in human and primate motor systems. J Physiol 1:3–14

Farmer SF, Gibbs J, Halliday DM, Harrison LM, James LM, Mayston MJ, Stephens JA (2007) Changes in EMG coherence between long and short thumb abductor muscles during human development. J Physiol 579:389–402

Goislard de Monsabert B, Rossi J, Berton E, Vigouroux L (2012) Quantification of hand and forearm muscle forces during a maximal power grip task. Med Sci Sports Exerc 44:1906–1916

Gwin JT, Ferris DP (2012) Beta- and gamma-range human lower limb corticomuscular coherence. Front Hum Neurosci 6:258

Hansen NL, Conway BA, Halliday DM, Hansen S, Pyndt HS, Biering-Sorensen F, Nielsen JB (2005) Reduction of common synaptic drive to ankle dorsiflexor motoneurons during walking in patients with spinal cord lesion. J Neurophysiol 94:934–942

Hermens HJ, Freriks B, Disselhorst-Klug C, Rau G (2000) Development of recommendations for SEMG sensors and sensor placement procedures. J Electromyogr Kinesiol 10:361–74

Heroux ME, Gandevia SC (2013) Human muscle fatigue, eccentric damage and coherence in the EMG. Acta Physiol 208:294–295

Hirashima M, Oya T (2016) How does the brain solve muscle redundancy? Filling the gap between optimization and muscle synergy hypotheses. Neurosci Res 104:80–87

Johnston JA, Winges SA, Santello M (2005) Periodic modulation of motor-unit activity in extrinsic hand muscles during multidigit grasping. J Neurophysiol 94:206–218

Kattla S, Lowery MM (2010) Fatigue related changes in electromyographic coherence between synergistic hand muscles. Exp Brain Res 202:89–99

Keenan KG, Collins JD, Massey WV, Walters TJ, Gruszka HD (2011) Coherence between surface electromyograms is influenced by electrode placement in hand muscles. J Neurosci Methods 195:10–14

Kong YK, Hallbeck MS, Jung MC (2010) Crosstalk effect on surface electromyogram of the forearm flexors during a static grip task. J Electromyogr Kinesiol 20:1223–1229

Ⓐ Springer

Lee SW, Landers K, Harris-Love ML (2014) Activation and intermuscular coherence of distal arm muscles during proximal muscle contraction. Exp Brain Res 232:739–752

Lemay MA, Crago PE (1999) A dynamic model for simulating movements of the elbow, forearm, and wrist. J Biomech 29:1319–1330

Li ZM, Latash ML, Zatsiorsky VM (1998) Force sharing among fingers as a model of the redundancy problem. Exp Brain Res 119:276–286

Marzke MW, Marchant LF, McGrew WC, Reece SP (2015) Grips and hand movements of chimpanzees during feeding in Mahale Mountains National Park. Am J Phys Anthropol 156:317–326

McClelland VM, Cvetkovic Z, Mills KR (2014) Inconsistent effects of EMG rectification on coherence analysis. J Physiol 592: 249–250

Mima T, Steger J, Schulman AE, Gerloff C, Hallett M (2000) Electro-encephalographic measurement of motor cortex control of muscle activity in humans. Clin Neurophysiol 111: 326–337

Mullany H, O'Malley M, St Clair Gibson A, Vaughan C (2002) Agonist–antagonist common drive during fatiguing knee extension efforts using surface electromyography. J Electromyogr Kinesiol 12:375–384

Nazarpour K, Barnard A, Jackson A (2012) Flexible cortical control of task-specific muscle synergies. J Neurosci 32:12349–12360

Norton JA, Gorassini MA (2006) Changes in cortically related intermuscular coherence accompanying improvements in locomotor skills in incomplete spinal cord injury. J Neurophysiol 95:2580–2589

Pizzamiglio S, De Lillo M, Naeem U, Abdalla H, Turner DL (2017) High-frequency intermuscular coherence between arm muscles during robot-mediated motor adaptation. Front Physiol 7:668

Poston B, Danna-Dos Santos A, Jesunathadas M, Hamm TM, Santello M (2010) Force-independent distribution of correlated neural inputs to hand muscles during three-digit Graspin. J Neurophysiol 104:1141–1154

Power HA, Norton JA, Porter CL, Doyle Z, Hui I, Chan KM (2006) Transcranial direct current stimulation of the primary motor cortex affects cortical drive to human musculature as assessed by intermuscular coherence. J Physiol 577:795–803

Semmler JG, Kornatz KW, Enoka RM (2003) Motor-unit coherence during isometric contractions is greater in a hand muscle of older adults. J Neurophysiol 90:1346–1349

Siemionow V, Yao W, Sahgal V, Yue GH, Yang Q (2010) Single-trial EEG-EMG coherence analysis reveals muscle fatigue-related progressive alterations in corticomuscular coupling. IEEE Trans Neural Syst Rehabil Eng 18:97–106

Snijders CJ, Volkers AC, Melchelse K, Vleeming A (1987) Provocation of epicondylalgia lateralis (tennis elbow) by comparing power grip and pinching. Med Sci Sports Exc 19:518–523

Valero-Cuevas FJ, Venkadesan M, Todorov E (2009) Structured variability of muscle activations supports the minimal intervention principle of motor control. J Neurophysiol 102:59–68

Vigouroux L, Domalain M, Berton E (2011) Effect of object width on muscle and joint forces during thumb–index finger graspin. J Appl Biomech 27:173–180

Vigouroux L, Goislard de Monsabert B, Berton E (2015) Estimation of hand and wrist muscle capacities in rock climbers. Eur J App Physiol 115:947–957

von Tscharner V, Barandun M, Stirling LM (2011) Piper rhythm of the electromyograms of the abductor pollicis brevis muscle during isometric contractions. J Electromyogr Kinesiol 21:184–189

Vrána J, Poláček H, Stančák A (2005) Somatosensory-evoked potentials are influenced differently by isometric muscle contraction of stimulated and non-stimulated hand in humans. Neurosci Lett 386:170–175

Winges SA, Johnston JA, Santello M (2006) Muscle-pair specific distribution and grip-type modulation of neural common input to extrinsic digit flexors. J Neurophysiol 96:1258–1266

Winges SA, Kornatz KW, Santello M (2008) Common input to motor units of intrinsic and extrinsic hand muscles during two-digit object hold. J Neurophysiol 99:1119–1126

Witte M, Patino L, Andrykiewicz A, Hepp-Reymond MC, Kristeva R (2007) Modulation of human corticomuscular beta-range coherence with low-level static forces. Eur J Neurosci 26:3564–3570

Perspectives scientifiques

VI.   Perspectives scientifiques

Les axes de recherche qui structurent mon projet scientifique et auxquels je souhaite donner priorité à l'avenir sont dans la continuité directe de la conversion thématique que j'ai opérée du domaine de la biomécanique vers celui de la neuro-biomécanique avec le projet *NeuroBioméCo*, fondateur des travaux sur les cohérences « (EEG-[EEG]-{EMG}-EMG} » qui m'animent aujourd'hui. En poursuivant la démarche originale réellement interdisciplinaire dans laquelle je m'inscris au croisement de la biomécanique, du contrôle moteur et des neurosciences, soutenue par le traitement avancé du signal, ces travaux approfondiront l'analyse de la redondance musculaire et de la co-contraction à travers une définition élargie de cette dernière. Ces projets sont un marqueur de ma volonté assumée de diversifier mes problématiques de recherche avec l'apport de collaborations variées dans de nouveaux champs scientifiques, en cohérence avec les compétences que j'ai acquises et les connaissances que j'ai produites depuis ma thèse. Ils témoignent également de l'ouverture de mes travaux de recherche fondamentale à des problématiques cliniques et translationnelles depuis mon intégration en septembre 2013 à l'équipe iDREAM « Plasticité Neuromotrice, Médecine Régénérative et Médicaments innovants post-AVC » de l'UMR 1214 ToNIC, avec de fortes perspectives en matière d'innovations thérapeutiques promouvant la récupération de la fonction motrice chez le patient cérébro-lésé.

Si ces perspectives scientifiques sont à un niveau d'avancement différent et traitent de problématiques variées, elles reposent toutes sur la démarche originale que j'ai eu cœur à initier et développer dans le domaine de la neuro-biomécanique pour établir un cadre d'analyse de référence à mes travaux de recherche. Ces différents projets font également tous appel, pour tout ou partie, à l'analyse de cohérence entre les signaux électrophysiologiques. Je suis pleinement convaincu du potentiel de cette approche pour étudier de manière originale et pertinente les mécanismes nerveux centraux de contrôle de l'activité musculaire agoniste et antagoniste lors de contractions volontaires et involontaires chez l'homme (Boonstra, 2013), à l'image des conclusions apportées par les travaux récents les plus significatifs auxquels j'ai contribué sur ce sujet (Blais *et al.,* 2018 ; Charissou *et al.,* 2016, 2017 ; Cremoux *et al.,* 2017 ; Dal Maso *et al.,* 2017).

VI.1.   Contractions miroirs chez le sujet sain et les patients post-AVC

Cette première perspective correspond au projet de thèse de Joseph Tisseyre, que je co-encadre au sein de l'UMR 1214 ToNIC avec Jessica Tallet. Même s'il est déjà bien avancé, il trouve toute sa place au titre de perspective dans ce mémoire de synthèse, car il initie une nouvelle problématique qui ouvre mes travaux sur la co-contraction agoniste / antagoniste à de nouvelles techniques comme la stimulation magnétique transcrânienne (TMS) ainsi qu'à une définition élargie de la co-contraction entre les muscles homologues controlatéraux lors de contractions unimanuelles chez l'homme. Ce travail porte sur l'étude des mouvements miroirs, de leur asymétrie comportementale et cérébrale chez le sujet sain et de leurs liens avec les fonctions attentionnelles et exécutives chez le sujet sain et les patients post-AVC. Il a déjà fait l'objet des deux publications les plus significatives suivantes, dont la première est présentée de manière détaillée en annexes (cf. Annexes, p. 153-163) :

- Tisseyre, J., Amarantini, D., Chalard, A., Marque, P., Gasq, D., Tallet, J. (2018). Mirror movements are linked to executive control in healthy and brain-injured adults. *Neuroscience*, 379, 246-256.
- Tisseyre, J., Marquet-Doléac, J., Barral, J., Amarantini, D.*, Tallet, J.* (* co-derniers auteurs) (2019). Lateralized inhibition of symmetric contractions is associated with motor, attentional and executive processes. *Behavioural Brain Research*, 361, 65-73.

Ce projet repose sur le fait bien établi que l'exécution de tâches motrices unimanuelles nécessite un réseau neuronal capable de limiter l'activité neuronale du cortex moteur primaire controlatéral au mouvement volontaire en contrecarrant la propension par défaut à produire des mouvements bimanuels symétriques en miroir (Carson, 2005 ; Cincotta & Ziemann, 2008). Une altération ou un dysfonctionnement transitoire des circuits neuronaux sous-jacents à la latéralisation du mouvement peut conduire à l'apparition de mouvements miroirs (MM) involontaires (Hoy *et al.,* 2004). Ces derniers peuvent être définis comme des mouvements ou des contractions involontaires se produisant simultanément dans les muscles homologues controlatéraux à ceux du mouvement volontaire (Armatas *et al.,* 1994 ; Cernacek, 1961). Selon la théorie d'activation bilatérale (Cernacek, 1961), le mécanisme qui sous-tend les MM chez les adultes sains est la facilitation transcalleuse. Ainsi, l'activation des zones motrices contrôlant l'hémicorps actif

facilite l'activation des mêmes zones motrices dans l'hémisphère controlatéral par l'intermédiaire de fibres transcalleuses, engendrant alors la production de MM dans l'hémicorps opposé censé être inactif. Les MM peuvent alors être considérées comme un défaut des processus inhibiteurs interhémisphériques (Hübers *et al.,* 2008).

Dans la population générale, les MM sont généralement observés pendant l'enfance (avant 10 ans) puis disparaissent progressivement au cours de la maturation du système nerveux central (Addamo *et al.,* 2007 ; Mayston *et al.,* 1999). Cependant, une activité électromyographique (EMG) miroir peut encore être enregistrée chez des adultes sains au cours de tâches rythmiques complexes (Ridderikhoff *et al.,* 2005 ; Vardy *et al.,* 2007) ou nécessitant des niveaux de force faibles ou élevés (Arányi & Rösler, 2002 ; Armatas *et al.,* 1996b). Enfin, les MM semblent réapparaitre progressivement chez les personnes âgées au cours du vieillissement (Baliz *et al.,* 2005 ; Bodwell *et al.,* 2003 ; Koerte *et al.,* 2010 ; Shinohara *et al.,* 2003).

Chez l'adulte sains droitiers, la plupart des études indiquent une occurrence plus importante des MM sur la main dominante lors de mouvements volontaires de la main non dominante (Armatas *et al.,* 1994, 1996a, 1996b ; Leocani *et al.,* 2000 ; Liederman & Foley, 1987 ; Todor & Lazarus, 1986 ; Uttner *et al.,* 2007 ; Wolff *et al.,* 1983). Comme le proposent Todor et Lazarus (Todor & Lazarus, 1986), une telle asymétrie des MM entre la main droite et gauche chez les sujets droitiers pourrait être liée à des différences dans le contrôle hémisphérique de chaque main. Cette hypothèse est en accord avec des études en imagerie par résonance magnétique fonctionnelle (IRMf) réalisées lors de mouvements unimanuels chez des sujets droitiers et qui retrouvent une asymétrie cérébrale avec une activation bilatérale des zones sensorimotrices lors des mouvements de la main gauche et une activation quasi exclusivement controlatérale lors des mouvements de la main droite (Haaland *et al.,* 2004 ; Kim *et al.,* 1993 ; Newton *et al.,* 2005 ; Singh *et al.,* 1998 ; Theorin & Johansson, 2007 ; Verstynen, 2004). Ces travaux corroborent l'idée de la supériorité de l'hémisphère gauche dans le contrôle de la motricité chez les sujets droitiers avec notamment une inhibition interhémisphérique plus importante de l'hémisphère gauche dominant sur l'hémisphère droit non dominant que le contraire (Bäumer *et al.,* 2007 ; Netz *et al.,* 1995).

Par ailleurs, certains travaux suggèrent que les MM pourraient être modulés par des processus cognitifs tels que les fonctions attentionnelles et inhibitrices (Addamo *et al.,* 2007). Ainsi, une exacerbation des MM a été retrouvée chez des participants jeunes et des personnes âgées en bonne santé lorsqu'un détournement de l'attention était effectué (Baliz *et al.,* 2005 ; Bodwell *et al.,* 2003). Une inhibition volontaire des MM est également possible

chez des enfants ainsi que des adultes jeunes et âgés en bonne santé (Addamo *et al.,* 2010 ; Lazarus & Todor, 1991). De plus, des déficits d'attention, d'inhibition ou de communication interhémisphérique sont fréquemment retrouvés dans des pathologies connues pour leur fréquence anormalement élevée de MM telles que le trouble déficitaire de l'attention avec ou sans hyperactivité, le trouble d'acquisition de la coordination, la schizophrénie, la maladie de Parkinson ou encore l'accident vasculaire cérébral (Addamo *et al.,* 2007 ; Cincotta & Ziemann, 2008 ; Hoy *et al.,* 2004 ; Licari *et al.,* 2015 ; MacNeil *et al.,* 2011).

Un paradigme pertinent pour explorer les MM est une tâche d'arrêt sélectif, exigeant l'arrêt d'un mouvement rythmique bimanuel symétrique pour ne continuer qu'un mouvement rythmique unimanuel (Deiber *et al.,* 2001 ; Sallard *et al.,* 2014 ; Tallet *et al.,* 2009, 2013). Cette tâche permet d'évaluer les MM du fait de l'implication de processus excitateurs lors de mouvements bimanuels symétriques (Serrien *et al.,* 2003) par opposition aux processus inhibiteurs engagés lors de mouvements unimanuels en vue de supprimer les MM sur le membre controlatéral (Cincotta & Ziemann, 2008).

La proposition centrale du travail de thèse mené par Joseph Tisseyre est donc d'utiliser ce paradigme pour quantifier les MM ainsi qu'explorer leurs corrélats cérébraux des MM chez des adultes sains droitiers et des patients cérébro-lésés. A travers trois études combinant mesures de force, EMG, EEG et TMS, les objectifs de cette thèse sont d'une part de rechercher l'asymétrie comportementale des MM chez des adultes sains droitiers ainsi que les corrélats cérébraux associés et, d'autre part, d'investiguer le lien entre les MM et les fonctions attentionnelles et exécutives ainsi que l'inhibition interhémisphérique chez des adultes sains et des patients cérébro-lésés.

Les premiers résultats clés de ce travail mettent en évidence une quantité exacerbée de mouvements miroirs sur le membre dominant droit des participants lors d'un mouvement unimanuel gauche par rapport au cas contraire. Comme illustré Figure 8, la condition d'arrêt de la main droite se caractérise par des activations cérébrales motrices plus bilatérales (électrodes C3 et C4) que la condition d'arrêt de la main gauche où les activations motrices concernant la main qui continue (main droite en lien avec l'activité de l'électrode gauche C3) sont supérieures à celles concernant la main arrêtée (main gauche en lien avec l'activité de l'électrode droite C4). De plus, ces MM à droite sont corrélés à l'activité cérébrale controlatérale au niveau du cortex moteur gauche. Il semblerait donc qu'il existe une asymétrie dans l'inhibition des régions motrices. Par ailleurs, l'activation globale et non spécifique au côté d'arrêt retrouvée dans la bande de fréquence alpha (α) au niveau des zones

pariétales pourrait refléter le coût attentionnel global nécessaire pour la réalisation de la tâche. Enfin, l'augmentation rapide et transitoire de l'activité cérébrale dans la bande de fréquence thêta au niveau de la région fronto-centrale à la suite de la transition refléterait les processus inhibiteurs impliqués dans l'arrêt de la réponse motrice. Finalement, l'asymétrie des MM pourrait rendre compte de l'asymétrie hémisphérique en lien avec la dominance motrice chez les sujets sains.
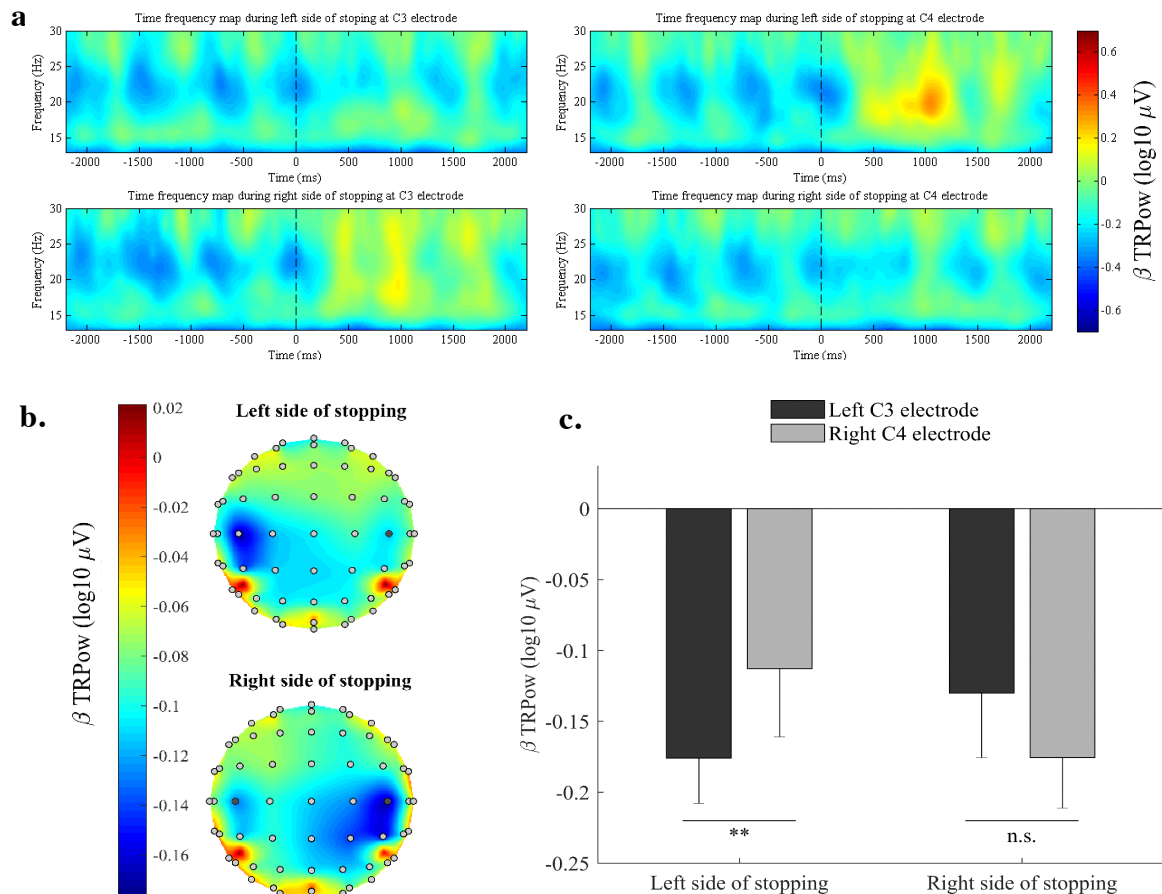
Figure 8, adaptée de Tisseyre *et al.* (2019). a. Cartes temps-fréquence du TRPow (task-related power) dans la bande β (13-30 Hz) avant et après la transition au niveau de l'électrode gauche C3 (cartes de gauche) et de l'électrode droite C4 (cartes de droite) pendant la condition d'arrêt de la main gauche (cartes du haut) et celle de la main droite (cartes du bas). Les lignes pointillées à t = 0 représentent la transition. **b.** Scalps du TRPow (μVolt) moyen (pré et post-transition) dans la bande β lors de la condition d'arrêt de la main gauche et celle de la main droite (panneaux du haut et du bas, respectivement). Les cercles représentent les électrodes ; les cercles pleins et gras représentent les électrodes d'intérêt : C3 (à gauche) et C4 (à droite). Les diminutions du TRPow (zone d'activation) sont représentées en bleu et les augmentations du TRPow sont codées en rouge. **c.** Histogramme du TRPow (μVolt) moyenne dans la bande β au niveau de l'électrode gauche C3 et droite C4 (histogrammes noirs et gris respectivement) lors de la condition d'arrêt de la main gauche et celle de la main droite. * indique une différence significative (p < .05) ; 'n.s.' indique l'absence de différence significative. Les barres verticales représentent l'erreur-type.

VI.2.   Effets de la toxine botulique et de la plasticité neuro-musculaire induite sur la facilitation des mouvements du membre supérieur en post-AVC

Cette seconde perspective scientifique correspond à la thèse CIFRE d'Alexandre Chalard, dirigée par David Gasq et Philippe Marque au sein de l'UMR 1214 ToNIC. Comme en témoigne les productions déjà associées à ce travail (Chalard *et al.,* 2018a, 2018b, 2018c, 2019), je contribue activement à ce travail tentaculaire dans la continuité du stage de Master 2 d'Alexandre Chalard que j'ai co-encadré avec David Gasq. Ma participation active à ce projet de recherche translationnelle extrêmement ambitieux [12] marque l'ouverture de mes travaux à des perspectives cliniques en matière d'innovations thérapeutiques chez le patient post-AVC. Ce projet porte sur les effets l'injection intramusculaire de toxine botulique A (TBA) sur la réduction de la co-contraction spastique en post-AVC, à partir de la caractérisation de la plasticité périphérique et centrale induite par les injections de TBA. Il a déjà fait l'objet de plusieurs productions, dont la publication la plus significative suivante est présentée de manière détaillée en annexes (cf. Annexes, p. 164-168) :

- Chalard, A., Amarantini, D., Tisseyre, J., Marque, P., Tallet, J., Gasq, D. (epub ahead of print). Spastic co-contraction, rather than spasticity, is associated with impaired active function in adults with acquired brain injury: A pilot study. *Journal of Rehabilitation Medicine.*

Ce projet part du constat que, consécutivement à un accident vasculaire cérébral (AVC), 80 % des patients ont une atteinte des voies pyramidales se traduisant par un déficit moteur hémicorporel significatif. Ce dernier est caractérisé d'une part par une altération de la motricité volontaire (parésie) due à une incapacité à activer et synchroniser le recrutement des motoneurones alpha (α) de manière optimale et, d'autre part, par une hypertonie spastique, correspondant à la persistance d'une contraction musculaire alors que le muscle devrait être relâché. L'expression clinique de l'hypertonie spastique comprend plusieurs entités (Gracies, 2005), dont la présence d'une co-contraction exacerbée du muscle

---

[12] Je profite de l'occasion que me donne la rédaction de ce mémoire de synthèse pour souligner, et remercier de manière particulièrement appuyée le travail titanesque que réalise David Gasq depuis des mois pour coordonner, avec une persévérance digne d'éloges, les démarches très excessivement lourdes nécessaires à l'obtention des autorisations éthiques requises pour mener à bien ce projet relevant de la recherche interventionnelle dite de catégorie 1. D'autres se seraient découragés en arpentant, vent juridico-administratif en rafales de face, l'interminable parcours dans les méandres des services de « soutien » aux démarches règlementaires en application de la Loi Jardé du 5 mars 2012. En espérant, sans rire (ou jaune), que la certification de la conformité éthique de ce projet sera obtenue avant que le financement CIFRE d'Alexandre Chalard arrive à échéance…

antagoniste lors de mouvements actifs réalisés par le patient. Même si les mécanismes physiopathologiques des différentes expressions de l'hypertonie spastique ne sont pas encore totalement élucidés chez l'homme, la co-contraction spastique pourrait être favorisée par une diminution de l'inhibition de l'antagoniste lors de la contraction volontaire de l'agoniste. Cette inhibition médiée par des interneurones médullaires serait diminuée en raison de la diminution de l'influx des afférences sensitives Ia provenant de l'agoniste parétique (Morita *et al.,* 2001). Ce défaut d'inhibition du muscle antagoniste au début de la contraction de l'agoniste pourrait aggraver les conséquences d'une commande motrice volontaire altérée et moins sélective chez le patient parétique (Dewald *et al.,* 1995 ; Weidner *et al.,* 2001).

Alors qu'un des enjeux de la rééducation dans les suites d'un AVC est la récupération du membre supérieur parétique, la co-contraction spastique engendre une résistance active lors de la production de mouvement et est actuellement décrite comme une composante majeure de la parésie spastique impliquée dans la limitation du mouvement actif (Gracies *et al.,* 2015 ; Vinti *et al.,* 2013). De manière intéressante, de nombreux travaux ont montré l'efficacité de l'injection intramusculaire de TBA sur la diminution de la spasticité (Ashford *et al.,* 2008 ; Gracies *et al.,* 2015 ; Jahangir *et al.,* 2007 ; McIntyre *et al.,* 2012 ; Yelnik *et al.,* 2009), améliorant la fonction passive notamment au niveau du membre supérieur est également améliorée (Ashford *et al.,* 2008). En revanche, même si Gracies *et al.* (2015) ont montré qu'une injection de TBA dans le muscle biceps brachial permettait une amélioration de l'extension active de coude, il n'y a qu'un faible niveau de preuve concernant les effets de la TBA sur l'amélioration de la fonction active (Foley *et al.,* 2013).

Dès lors, ce projet a pour objectif principal d'évaluer l'effet de l'injection intramusculaire de TBA dans les fléchisseurs du coude sur la réduction de la co-contraction spastique au cours d'un mouvement d'extension active du membre supérieur chez des patients hémiplégiques vasculaires chroniques. Il fait appel à une approche multimodale combinant mesures cinématique tridimensionnelle, EEG et EMG à une évaluation clinique exhaustive du membre supérieur, auxquelles s'ajoutent l'évaluation de l'excitabilité cortico-spinale par TMS et l'évaluation de l'intégrité des voies motrices encéphaliques par IRM sans produit de contraste. Les bénéfices attendus sont de montrer que les injections de TBA permettent de diminuer la co-contraction spastique lors du mouvement, avec pour conséquence d'augmenter l'angle d'extension du coude, considéré comme un élément majeur pour améliorer les capacités fonctionnelles de préhension. Sur un plan plus fondamental, les résultats permettront d'améliorer la compréhension des mécanismes

d'action de la TBA sur la réduction de la co-contraction spastique, à partir de la caractérisation de la plasticité périphérique mais également centrale induite par les injections de TBA (Bergfeldt *et al.,* 2015 ; Huynh *et al.,* 2013 ; Molteni *et al.,* 2015 ; Simpson *et al.,* 2009). Dans une perspective à long terme, ce projet vise également à favoriser le développement des neuroprothèses du membre supérieur chez les patients cérébro-lésés, actuellement limité par le phénomène de co-contraction spastique et par les problématiques d'interface cerveau-machine (Chae *et al.,* 2002).

Les premiers résultats obtenus à partir des données recueillies lors de mouvements d'extension du coude réalisés à vitesse spontanée par dix sujets contrôles et dix patients hémiparétiques avant injection de TBA ont été récemment publiés (Chalard *et al.,* 2019). Ils révèlent un indice de co-contraction plus élevé chez les sujets hémiparétiques comparativement aux contrôles ($w_{19} = 3,4$; $p < 0,01$), avec une différence moyenne de 7,6 % entre les deux groupes. Ils ont également permis de mettre en évidence de manière précurseur une forte association entre l'indice de co-contraction et i) la limitation d'extension active du coude ($p < 0,01$), ii) la cotation de la sélectivité motrice par le score de Fugl-Meyer pour le membre supérieur ($p < 0,01$), et iii) le score ARAT (Action Research Arm Test) utilisé pour évaluer la fonction du membre supérieur et notamment sa récupération après une lésion cérébrale ($p < 0,05$). A l'inverse, aucune corrélation significative n'a été trouvée avec la spasticité. Ces résultats sont donc les premiers à montrer que la co-contraction spastique contribue de manière principale au déficit d'extension active du coude chez l'adulte présentant une lésion cérébrale, même en l'absence de spasticité. Ils soulignent également l'importance de l'altération de la sélectivité motrice comme un mécanisme contribuant à une plus grande co-contraction. Pris ensemble, ces résultats montrent l'impact néfaste de la co-contraction spastique sur la fonction motrice du membre supérieur, avec pour conséquence une restriction anormale du mouvement du bras, en particulier chez les sujets présentant un niveau de déficience motrice élevé. Les enregistrements réalisés après injection intramusculaire de TBA permettront de vérifier l'hypothèse d'une diminution de la co-contraction spastique des fléchisseurs du coude du bras parétique associé à une amélioration de l'angle d'extension active du coude.

Les premiers résultats issus des enregistrements EEG réalisés avant injection de BTA montrent que la désynchronisation corticale observée au cours du mouvement d'extension actif du coude est différente entre les sujets contrôles (CONTROL) et les patients hémiparétiques (STROKE), avec un déficit de désynchronisation chez les sujets

hémiparétiques comparativement aux contrôles (Figure 9). Les analyses de corrélation réalisées à titre préliminaire en regroupant l'ensemble des participants CONTROL et STROKE dans un même échantillon montrent une association significative entre la désynchronisation corticale dans la bande de fréquence β et les paramètres du mouvement : plus la désynchronisation est importante en β, meilleure est la performance motrice aussi bien en matière d'amplitude, de vitesse, de fluidité que de co-contraction (Figure 10). Ces résultats sont particulièrement prometteurs dans la perspective de réduire la co-contraction spastique au cours du mouvement et d'améliorer la fonction motrice active chez les patients hémiparétiques par injection intramusculaire de TBA dans les fléchisseurs du coude. Ils suggèrent en effet que la plasticité induite au niveau central par les injections de TBA pourrait, en complément des effets attendus au niveau périphérique, contribuer à une évolution du recouvrement de la fonction motrice vers le retour à une performance considérée comme « normale » chez les patients hémiparétiques.
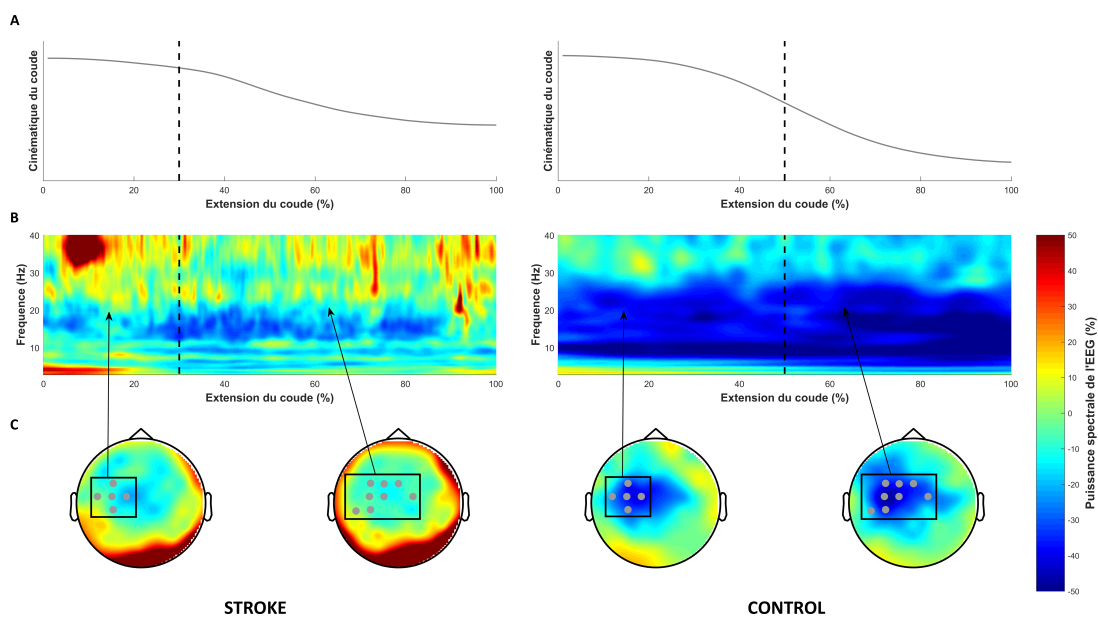
Figure 9. A. Profil angulaire moyen d'extension du coude chez les patients hémiparétiques avant injection de TBA (STROKE) et les sujets contrôles (CONTROL). Le trait noir pointillé représente l'instant de transition entre la phase d'accélération et la phase de décélération du mouvement actif d'extension. **B.** Carte temps-fréquence de la désynchronisation corticale calculée par analyse de masse univariée au niveau topographique à partir des signaux EEG de surface recueillis au cours des phases d'accélération et de décélération du mouvement actif d'extension du coude chez les patients hémiparétiques avant injection de TBA (STROKE) et les sujets contrôles (CONTROL). **C.** Illustration topographique des sites d'électrodes EEG présentant une différence significative de désynchronisation corticale entre les sujets contrôles (CONTROL) les patients hémiparétiques avant injection de TBA (STROKE) au cours des phases d'accélération et de décélération du mouvement actif d'extension du coude.
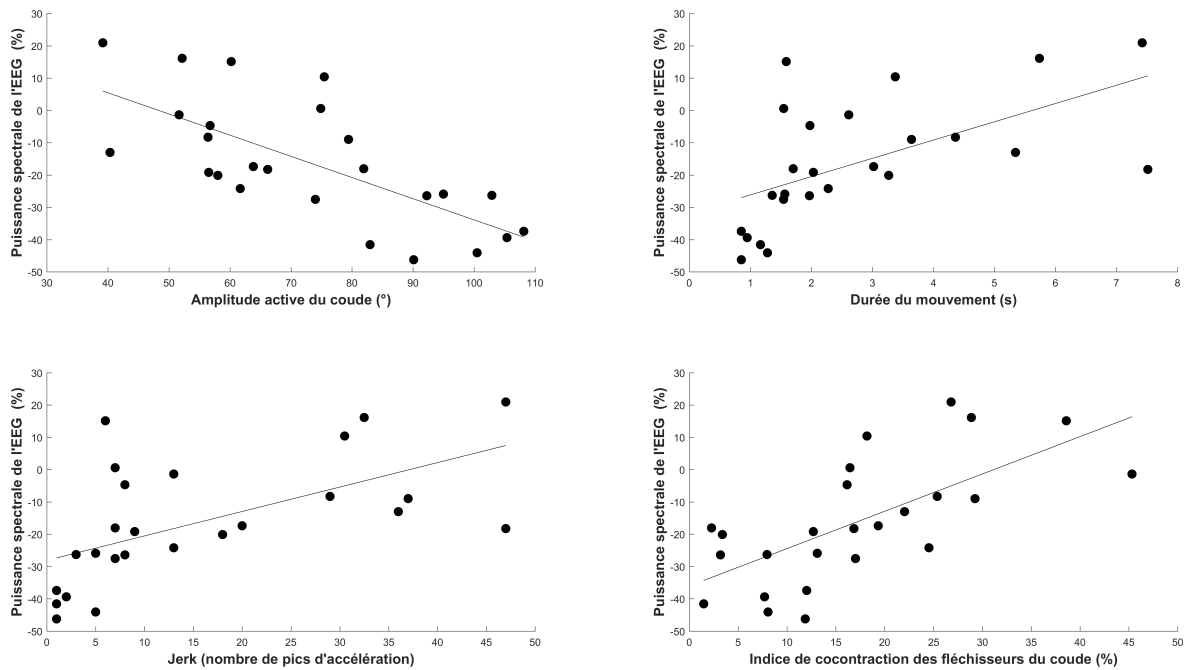
Figure 10. Corrélations entre la désynchronisation corticale observée au cours du mouvement d'extension active du coude et les paramètres cinématiques du mouvement chez l'ensemble des sujets contrôles et des patients hémiparétiques avant injection de TBA. Sur le panneau en bas à gauche, un jerk faible est un indicateur de fluidité du mouvement.

VI.3.   Dynamique des cohérences EEG-EEG, EEG-EMG et EMG-EMG

Ce projet correspond à la thèse de Maxime Fauvet, débutée à la rentrée universitaire 2018-2019 au sein de l'UMR 1214 ToNIC sous la direction de Philipe Marque, que j'aurai plaisir à rejoindre pour co-encadrer ce travail quand j'aurai, je l'espère, l'honneur de me voir décerné le diplôme d'Habilitation à Diriger des Recherches. Porté par les travaux en cours ou déjà aboutis sur les cohérences EEG-EEG, EEG-EMG et EMG-EMG, cette perspective de recherche vise à étudier, de manière novatrice, la modulation des communications interhémisphérique, cortico-musculaire et intermusculaire envisagées comme des processus dynamiques au cours de contractions isométriques ou de mouvements volontaires chez des participants présentant une altération ou au contraire une forme d'optimisation de la fonction motrice. Ce projet amitieux a l'avantage de bénéficier des bases de données déjà constituées dans le cadre des travaux de Fabien Dal Maso (Dal Maso, 2012), Sylvain Cremoux (Cremoux, 2013), Joseph Tisseyre et Alexandre Chalard lors de contractions isométriques ou dynamiques uni- ou bilatérales réalisées par des sujets experts dans des spécialités sportives de force ou d'endurance, des patient cérébro-lésés en phase chronique ou des participants atteints d'une lésion de la moelle épinière. Ce travail nécessite de lever des

verrous importants du point de vue méthodologique, concernant l'analyse de phase de la cohérence, dont la quantification précise permettra d'étudier le sens des interactions entre le système nerveux central et les muscles, et la généralisation du calcul de cohérence à des situations expérimentales marquées par une forte variabilité inter-essais de la durée de la tâche. Sur ce dernier point, le travail mené par Maxime Fauvet dans le cadre de son stage de Master 2 a déjà fait l'objet d'une publication présentée de manière détaillée en annexes (cf. Annexes, p. 169-172) :

- Fauvet, M., Cremoux, S., Chalard, A., Tisseyre, J., Gasq, D.*, Amarantini, D.* (* co-derniers auteurs) (accepted for publication). A novel method to generalize time-frequency coherence analysis between EEG or EMG signals during repetitive trials of different durations. In *2019 9th International IEEE/EMBS Conference on Neural Engineering (NER)*.

Ce projet repose sur l'idée que les mécanismes de contrôle nerveux centraux d'activité musculaire agoniste et antagoniste relèvent de processus dynamiques dont la contribution pourra être étudiée à travers la modulation instantanée de la force du couplage fonctionnel entre les structures centrales et périphériques impliquées dans la contraction musculaire. Ce travail a donc pour objectif, dans une double perspective fondamentale et clinique, de contribuer à une meilleure compréhension des mécanismes de contrôle de la motricité saine et altérée. En faisant appel à l'analyse de cohérence (Boonstra, 2013) entre les signaux électroencéphalographiques (EEG) émanant du cerveau et les signaux électromyographiques (EMG) émanant du muscle, ce travail étudiera la contribution des différents mécanismes nerveux centraux à la régulation de l'activité musculaire lors de contractions isométriques et de mouvements volontaires réalisés par des participants sains et experts dans certains activités sportives et des patients cérébro-lésés présentant une altération des capacités motrices (notamment : accidentés vasculaires cérébraux, tétraplégiques). L'analyse du niveau de cohérence entre les signaux EEG et EMG permettra d'étudier le couplage fonctionnel aux niveaux cortico-musculaire entre les muscles et le cortex moteur, intermusculaire entre les muscles synergistes agonistes et antagonistes et cortico-cortical entre les différentes structures cérébrales impliquées dans le contrôle musculaire, et renseignera sur l'implication respective des mécanismes corticaux et spinaux dans le contrôle moteur (Boonstra & Breakspear, 2012 ; Buzsaki & Draghun, 2004 ; Fries, 2005). S'il est aujourd'hui admis que la ou les cohérences ont un rôle fonctionnel et pourraient encoder une information nécessaire à la production du mouvement et au maintien

des capacités de force lors d'une contraction volontaire, la modulation de ces couplages au cours du temps reste inexplorée alors que cela pourrait être un élément déterminant de la capacité des individus à produire et maintenir une motricité non-altérée quelles que soient les conditions environnementales.

Ainsi, le but de ce travail est d'étudier en détail les mécanismes nerveux centraux de régulation de l'activité musculaire chez différentes populations de sujets en analysant au cours du temps le couplage entre le cortex et les muscles, entre les muscles et au sein du cortex via la mesure des cohérences cortico-musculaire, intermusculaire et cortico-corticales lors de contractions isométriques et de mouvements volontaires. Ces résultats permettront de mieux comprendre les liens fonctionnels entre les différentes structures centrales impliquées dans le contrôle du mouvement et leur dynamique au cours de l'action motrice. L'intégration de sujets sains « normaux », de sujets devenus experts suite à un entraînement et de patients présentant des altérations de la commande centrale permettra, dans une perspective fondamentale, d'analyser la dynamique de l'implication des mécanismes de contrôle moteur et de contribuer au développement d'un modèle de « pilotage » de l'activité musculaire en termes de couplage par le système nerveux central au cours du temps. Dans une perspective clinique, cette démarche permettra de favoriser la prise en charge des patients présentant une altération de la motricité. Une meilleure compréhension de la dynamique de la communication à l'origine du contrôle du mouvement pourra en effet permettre une optimisation des traitements pour les patients souffrant d'une altération de ce contrôle via par exemple une injection de toxine botulique ciblée ou une interface cerveau / machine de stimulation.

Comme indiqué précédemment, une étape préalable à la bonne réalisation de ce projet est la « généralisation du calcul de cohérence à des situations expérimentales marquées par une forte variabilité inter-essais de la durée de la tâche ». En effet, une des limitations majeures à l'utilisation des méthodes d'analyse de cohérence, y compris celle que nous avons développée dans le domaine temps-fréquence (Bigot *et al.*, 2011), est l'absence de régularité inter ou intra-individuelle de la durée des actions motrices, ce qui restreint l'analyse du contrôle moteur à des protocoles impliquant des contractions musculaires isométriques ou des tâches dynamiques très standardisées. Dans ce travail, une technique de normalisation temporelle des signaux EEG ou EMG a été proposée pour permettre un calcul de la cohérence entre des signaux de durée différente tout en respectant les prérequis mathématiques à une analyse de cohérence rigoureuse. Cette technique a été

testée à la fois sur des signaux simulés de durées différentes et contrôlées, et sur des enregistrements EEG et EMG obtenus chez des sujets sains et des patients post-AVC lors de la réalisation d'une extension active du coude. Les résultats montrent que la technique proposée améliore à la fois la précision et la confiance du calcul de la cohérence, que ce soit pour les signaux simulés ou les données réelles des sujets (Figure 11). La technique proposée permet donc de passer outre une des limites majeures à l'analyse de cohérence et sera appliquée dans la suite de travaux menés notamment dans le cadre de cette perspective de recherche ambitieuse, afin de construire un modèle du contrôle moteur basé sur l'analyse dynamique de la cohérence, qu'elle soit cortico-musculaire ou intermusculaire.
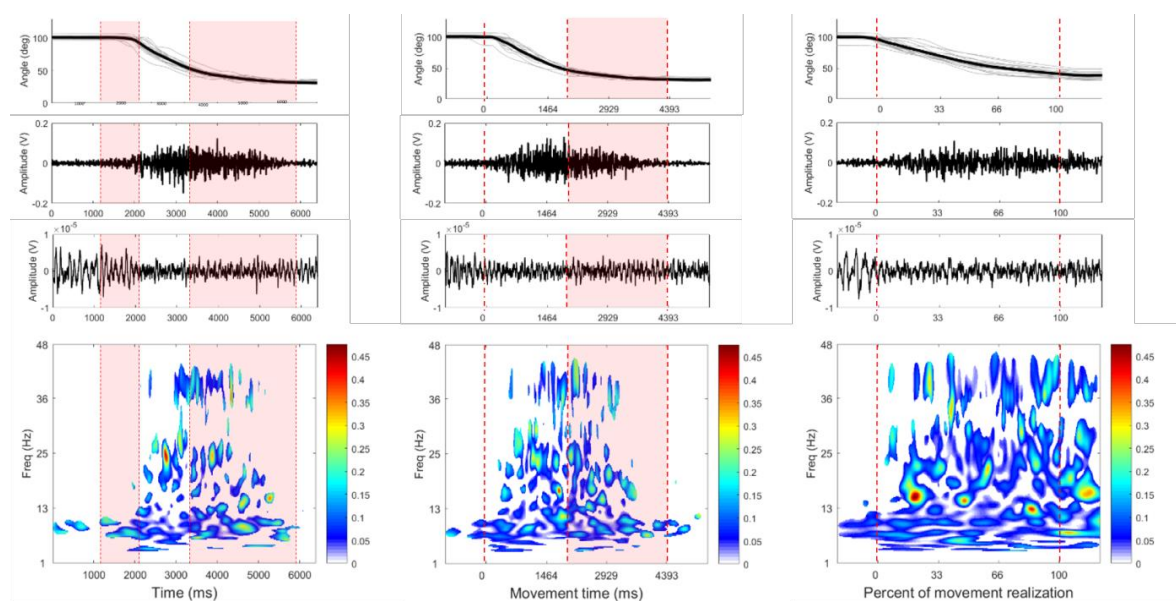
Figure 11, adaptée de Fauvet *et al.* (2019). Illustration des étapes de calcul de cohérence EEG-EMG réalisé à partir des données d'un patient post-AVC sur un total de dix-sept mouvements d'extension du coude réalisés à vitesse spontanée. Les panneaux de la colonne de gauche représentent l'ensemble de données brutes alignées sur le signal sonore indiquant au patient d'initier son mouvement, ceux du milieu représentent l'ensemble de données alignées sur le début du mouvement d'extension et ceux de droite représentent l'ensemble de données de signaux normalisés sans altération de leurs propriétés oscillatoires. La rangée supérieure correspond à la cinématique de mouvement (profil moyen en noir ; essais individuels en gris), la deuxième rangée correspond au signal EMG moyen, la troisième rangée au signal EEG moyen et la rangée inférieure aux cartes temps-fréquence de cohérence là où les interactions entre le cortex moteur et le muscle étudié sont significatives. Sur la colonne de gauche (signaux bruts), la première et la seconde zones ombrées en rouge correspondent respectivement à l'étendue temporelle sur laquelle le patient débute ou termine son mouvement ; sur la colonne du milieu (signaux alignés), le trait rouge pointillé et la zone ombrée en rouge correspondent respectivement au début de mouvement et à l'étendue temporelle sur laquelle le patient termine son mouvement ; sur la colonne de droite (signaux normalisés), le premier et le second traits rouges pointillés correspondent respectivement au début et à la fin du mouvement réalisé par le patient.

## VI.4.   Déclinaison de la cohérence dans tous ses états

Trois autres projets, dont les travaux viennent d'être amorcés, complètent les directions de recherche prioritaires que je souhaite développer à l'avenir en collaboration avec des spécialistes de champs disciplinaires complémentaires aux compétences que j'ai pu acquérir depuis ma thèse : Philippe Pudlo (LAMIH, UMR 8201 CNRS / UPHF, Valenciennes) dans le domaine de la robotique, Julien Duclay (ToNIC, UMR 1214 Inserm / UPS, Toulouse) dans les domaines de la neurophysiologie et de la plasticité neuromusculaire, et Lilian Fautrelle (ToNIC, UMR 1214 Inserm / UPS, Toulouse) dans les domaines du contrôle moteur et de la psychologie cognitive.

Cohérence intermusculaire & modélisation musculo-squelettique

Le premier projet correspond à la thèse que réalisera Emilie Mathieu au sein du Laboratoire d'Automatique, de Mécanique et d'Informatique industrielles et Humaines (LAMIH, UMR CNRS 8201) de l'Université polytechnique des Hauts-de-France sous la direction de Philippe Pudlo. Ce projet marque un retour à la problématique que j'avais développée au cours de ma thèse concernant la modélisation musculo-squelettique et l'estimation des efforts musculaires, envisagés ici en matière de tensions musculaires individuelles développées par les muscles autour de l'articulation du coude lors de mouvements de flexion-extension réalisés à vitesse spontanée et à vitesse maximale par des sujets sains et des patients neurologiques. La base de données sera constituée à partir de l'enregistrement de la cinématique tridimensionnelle de marqueurs passifs positionnés sur le membre supérieur, et des signaux électromyographiques des principaux muscles extenseurs et fléchisseurs du coude. Ces mesures seront réalisées dans le cadre du projet « Effets de la toxine botulique et de la plasticité neuro-musculaire induite sur la facilitation des mouvements du membre supérieur en post-AVC » (*ULAFBoT-Stroke* ; investigateur coordonnateur : David Gasq) à Toulouse et à Valenciennes.

Comme l'ont soutenu les travaux que j'ai réalisés en biomécanique (Amarantini & Martin, 2004 ; Amarantini *et al.,* 2010 ; Vigouroux *et al.,* 2007), un consensus semblait émerger sur la nécessité d'utiliser l'EMG comme une donnée d'entrée pour tenir compte de la « commande neurale » dans les modèles musculo-squelettiques permettant d'estimer les forces musculo-tendineuses (Besier *et al.,* 2009 ; Bogey & Barnes, 2017 ; Buchanan *et al.,* 2004, 2005 ; Cholewicki *et al.,* 1995 ; Gagnon *et al.,* 2011 ; Granata & Marras, 1993 ; Lloyd *et al.,* 2005 ; Olney & Winter, 1985 ; Sartori *et al.,* 2010, 2012 ; Shao *et al.,* 2009). Cette

approche (p. ex., Sartori *et al.,* 2010 ; Figure 12), comme celle de la dynamique directe dite « assistée » (McLean *et al.,* 2003 ; Neptune *et al.,* 2000) est apparue pertinente pour améliorer l'estimation des efforts musculaires (Gagnon *et al.,* 2001), en prenant en compte de manière appropriée la co-contraction agoniste / antagoniste dans l'estimation des forces musculo-tendineuses (Amarantini *et al.,* 2010 ; Nikooyan *et al.,* 2012) ainsi que des forces de contact articulaire (Hoang *et al.,* 2018, 2019). La priorité semble cependant être donnée à l'utilisation de modèles analytiques personnalisés en approche inverse ou pseudo-inverse (p. ex., Moissenet *et al.,* 2016), dont le temps de calcul et la plus grande simplicité de la procédure expérimentale présentent un avantage certain pour leur mise en application en évaluation clinique de la fonction motrice.
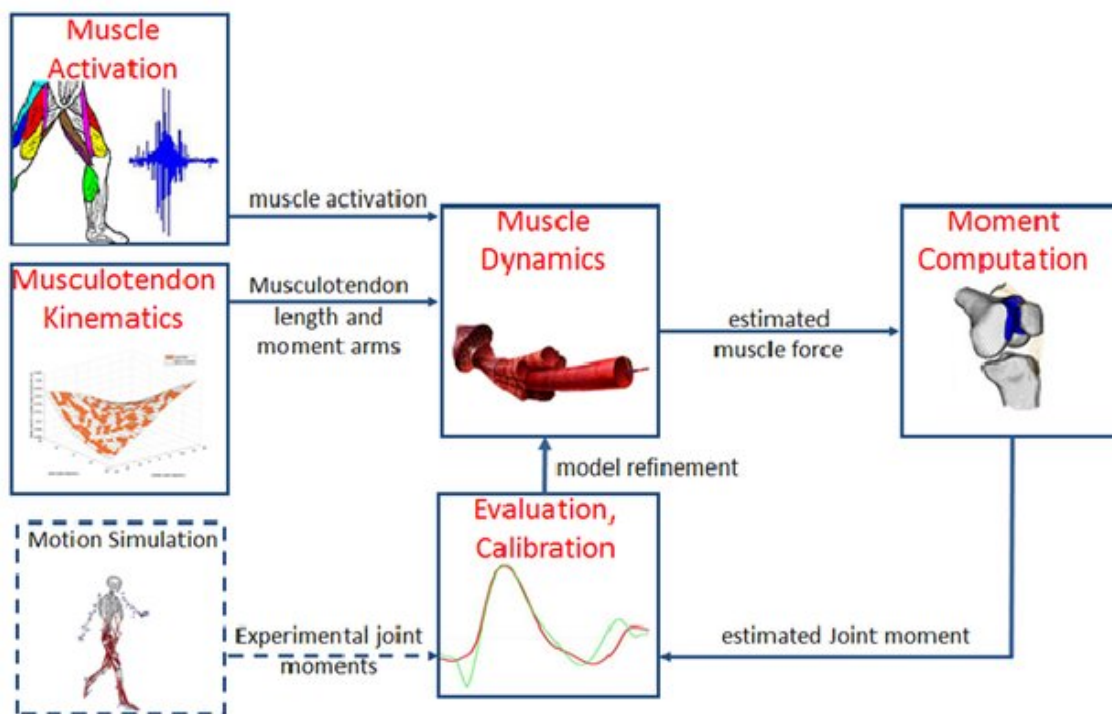
Figure 12, adaptée de Sartori *et al.* (2010). Représentation schématique d'un modèle piloté par EMG permettant l'estimation des forces musculaires et du moment musculaire résultant lors de tâches dynamiques comme la marche ou la course (Sartori *et al.,* 2010, 2012). Pour une application au calcul des forces musculaires et des moments résultants autour de cinq degrés de liberté des articulations de la cheville (flexion-extension), du genou (flexion-extension) et de la hanche (flexion-extension, adduction-abduction et rotation interne-externe), l'activité EMG de seize muscles est utilisée comme donnée d'entrée principale dans le modèle pour calculer les activations de trente-quatre muscles. Le bloc intitulé « Motion Simulation » permet d'estimer les angles et moments articulaires par approche inverse à l'aide d'*OpenSim* (Delp *et al.,* 2007 ; Seth *et al.,* 2018).

La démarche consistant à exploiter la redondance d'informations périphériques ayant déjà fait ses preuves pour estimer le moment résultant de manière fiable (Cahouët *et al.,* 2002), je suis toutefois persuadé que l'introduction de données renseignant sur les synergies musculaires (d'Avella *et al.,* 2003) ou les « stratégies neurales » est indispensable pour estimer les tensions développées par les muscles synergistes de manière plus réaliste. Le couplage intermusculaire, quantifié par la cohérence EMG-EMG dans la bande de fréquence bêta (β) « beta » (Kattla & Lowery, 2010) peut être considéré comme un indice de coordination entre les muscles synergistes (Charissou *et al.,* 2016 ; De Marchis *et al.,* 2015). Récemment, de Vries et al. (2016) et Reyes et al. (2017) ont suggéré qu'il serait également le reflet d'une stratégie de contrôle qui pourrait coder la distribution des activations musculaires. Par conséquent, l'objectif ambitieux de ce projet est d'aboutir à la proposition d'un modèle neuro-musculo-squelettique synthétique, en testant l'hypothèse que l'introduction de la cohérence intermusculaire comme donnée d'entrée ou comme contrainte permettra d'améliorer l'estimation des efforts musculaires en reflétant de manière adaptée la co-contraction agoniste / antagoniste même dans des conditions où la fonction motrice est altérée. La première étape, en cours, est de réaliser une revue de littérature exhaustive des modèles « neuro-assistés » déjà disponibles pour la communauté scientifique en biomécanique du mouvement.

Cohérence cortico-musculaire & contrôle nerveux de la contraction volontaire excentrique

Le second projet a été initié à la rentrée universitaire 2018-2019 par deux Master 2 Recherche réalisés au sein de l'UMR 1214 ToNIC par Dorian Glories et Mathias Soulhol. Je co-encadre ces deux stages avec Julien Duclay, spécialiste s'il en est du contrôle nerveux de la contraction volontaire excentrique élevé au rang de Grand Maître ès *circuiterie* (Barrué-Belou *et al.,* 2016, 2018 ; Duclay & Martin, 2005 ; Duclay *et al.,* 2008, 2009, 2011, 2014). Ces travaux portent sur les effets du mode de contraction (c.-à-d. isométrique *vs* concentrique *vs* excentrique) et du niveau de force sur i) la réactivité des rythmes électrocorticaux et ii) la cohérence cortico-musculaire lors de contractions sous-maximales des fléchisseurs plantaires. Ces deux grandeurs seront quantifiées à partir d'une analyse temps-fréquence par, respectivement, la désynchronisation EEG liée à la contraction (Graimann *et al.,* 2002 ; Makeig, 1993 ; Pfurtscheller, 1992, 2001 ; Pfurtscheller & Aranibar, 1977 ; Pfurtscheller & Lopes da Silva, 1999) et la cohérence EEG-EMG calculée en faisant

appel à la méthode robuste établie au cours de la thèse de Fabien Dal Maso (Bigot *et al.,* 2011 ; Cremoux *et al.,* 2017 ; Dal Maso, 2012 ; Dal Maso *et al.,* 2017). Du point de vue expérimental, ce projet combine la mesure du moment résultant produit autour de la cheville sur un ergomètre isocinétique à des enregistrements EEG, EEG et du réflexe de Hoffman (réflexe H). Ce dernier provient de l'activation directe des motoneurones α via les afférences Ia issues des fuseaux neuromusculaires lors de la contraction volontaire ou au repos ; il est utilisé pour évaluer l'excitabilité spinale (Schieppati, 1987).

De manière intéressante, il a été montré que la contraction excentrique, au cours de laquelle le moment résultant est opposée à celle du mouvement, présente une stratégie propre d'activation musculaire utilisée par le système nerveux (Duchateau & Enoka, 2008, 2016 ; Enoka, 1996). Comparativement aux modes isométrique et concentrique, l'activité corticale est majorée en excentrique (Duclay *et al.,* 2011 ; Fang *et al.,* 2001 ; Gruber *et al.,* 2009). A l'inverse, l'étude de l'activation nerveuse volontaire à travers l'activité EMG, le niveau d'activation volontaire ou encore les potentiels évoqués transcrâniens a mis en évidence une diminution de l'excitabilité cortico-spinale propre à la contraction excentrique (Aagaard *et al.,* 2000 ; Amiridis *et al.,* 1996 ; Duclay *et al.,* 2011 ; Gruber *et al.,* 2009 ; Westing *et al.,* 1991) (Figure 13). Ces modulations semblent s'expliquer par des mécanismes nerveux inhibiteurs qui agissent au niveau spinal et qui se traduisent par une réduction de l'excitabilité spinale lors de contractions excentriques (Abbruzzese *et al.,* 1994 ; Duclay & Martin, 2005 ; Duclay *et al.,* 2009, 2011 ; Nordlund *et al.,* 2002 ; Romano & Schieppati, 1987) elle-même liée, au moins en partie, à la contribution de la voie d'inhibition récurrente (Barrué-Belou *et al.,* 2018).

Dans ce contexte, l'objectif central de ce projet est double :

- D'une part, contribuer à une meilleure compréhension du rôle fonctionnel du couplage cortico-musculaire lors de contractions sous-maximales anisométriques, en testant la spécificité de la modulation de la cohérence EEG-EMG dans le mode excentrique comparativement aux modes isométrique et concentrique. Ces travaux pourront permettre de mieux comprendre les plasticités centrales induites après une sollicitation de type excentrique aiguë ou chronique, dans une double perspective d'optimisation de la performance dans le domaine de l'entrainement et/ou de réadaptation dans le domaine clinique.

- D'autre part, clarifier la contribution des mécanismes nerveux centraux associés à la modulation de la cohérence EEG-EMG. Si certains auteurs ont montré que la cohérence cortico-musculaire pourrait refléter l'implication direct du cortex moteur

primaire dans la génération de la contraction musculaire (Conway *et al.*, 1995 ; Chakarov *et al.*, 2009 ; Ushiyama *et al.*, 2010, 2012), d'autres auteurs ont proposé qu'elle pourrait refléter le contrôle de certains mécanismes spinaux par les structures corticales et sous-corticales (Hansen *et al.*, 2005 ; Norton *et al.*, 2006 ; Raethjen *et al.*, 2002 ; Semmler *et al.*, 2013). Compte tenu du pilotage spécifique de la contraction excentrique, les différences attendues sur la cohérence EEG-EMG entre les modes isométrique, concentrique et excentrique permettront de conclure sur la contribution des mécanismes spinaux et supra-spinaux à la modulation de la communication cortico-musculaire.
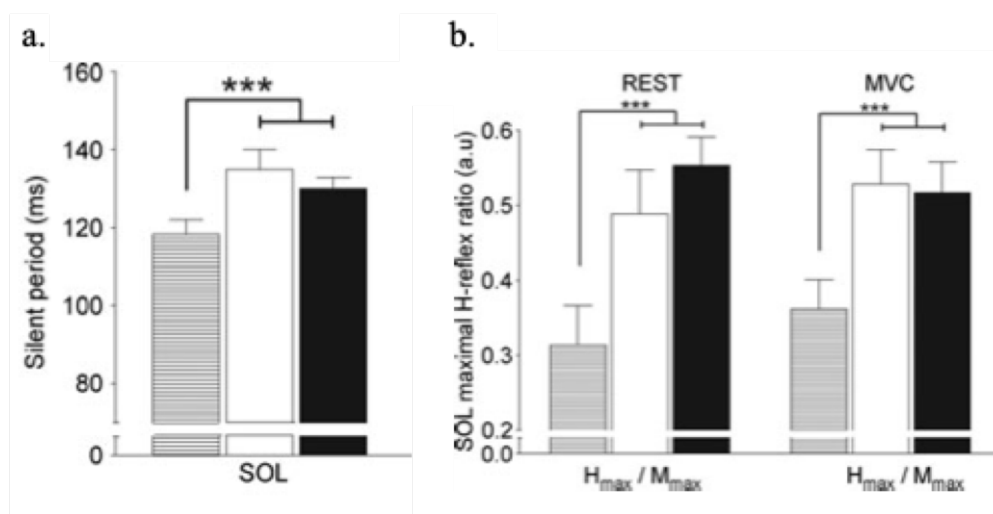
Figure 13, adaptée de Duclay *et al.* (2011). a. Période de silence du muscle soléaire étudiée par TMS. **b.** Réflexe H mesuré au repos et lors de contractions maximales volontaires. Les contractions excentriques sont représentées par la barre rayée horizontalement, les contractions isométriques par la barre blanche, et les contractions concentriques par la barre noire. *** indique une différence significative avec $p < 0.001$.

Cohérence intermusculaire & contexte émotionnel

Finalement, un autre Master 2 Recherche initié à la rentrée universitaire 2018-2019 ouvre une nouvelle perspective à mes activités de recherche. Il s'agit du projet mené au sein de sein de l'UMR 1214 ToNIC par Emeline Pierrieau, que je co-dirige avec Lilian Fautrelle (Institut National Universitaire Champollion, Rodez), spécialiste au croisement des neurosciences, du contrôle moteur et de la psychologie cognitive.

Ce travail, qui fait le lien avec ceux de Mathieu Lajante auxquels j'ai participé dans le domaine du neuromarketing (Lajante *et al.*, 2012 ; Lajante *et al.*, 2017), se place dans une

problématique de compréhension des mécanismes sous-jacents à l'influence d'une expérience émotionnelle sur le comportement moteur. Il repose sur l'hypothèse de la direction motivationnelle (Lang, 1995, 2000), selon laquelle les dimensions de valence et d'activation des stimuli émotionnels seraient intimement liées à l'engagement des circuits neuronaux appétitif et défensif, et donc des motivations à l'approche ou à l'évitement. De nombreuses études démontrent que les émotions appétitives facilitent les mouvements d'approche tandis que les émotions négatives optimisent les comportements de fuite et d'évitement (Elliot, 2006). Naugle et *al.* (2010) ont ainsi observé une longueur de pas rétrécie et une vitesse ralentie lors de l'avancée vers une image déplaisante par rapport à une image plaisante. D'autres études ont montré également une facilitation de l'initiation de la marche vers un stimulus plaisant par une diminution du temps de réaction par rapport aux stimuli déplaisants (Gélat *et al.,* 2011 ; Vernazza-Martin *et al.,* 2017). Le simple fait de visionner des images plaisantes ou déplaisantes modifie également significativement les performances d'endurance et de génération de force musculaire lors d'un effort sur ergocycle (Jaafar *et al.,* 2015). Cependant, les structures et processus neurophysiologiques impliqués dans cette flexibilité restent trop peu connus.

L'enjeu est donc de déterminer les processus du contrôle moteur modulés par le contexte émotionnel. Quelques études par TMS récentes suggèrent une hausse de l'excitabilité corticale en présence d'un stimulus plaisant (Blakemore *et al.,* 2018 ; Hajcak *et al.,* 2007 ; Mirabella, 2018), mais les résultats sont souvent contradictoires. L'analyse de cohérence intermusculaire, qui mesure la synchronie entre deux signaux EMG (Farmer, 1998 ; Farmer *et al.,* 1993 ; Grosse *et al.,* 2002 ; Rosenberg *et al.,* 1989), semble particulièrement pertinente pour répondre à ce nouveau questionnement de recherche. Dans la continuité des travaux de thèse de Camille Charissou (Charissou, 2018 ; Charissou *et al.,* 2016, 2017), l'objectif sera d'étudier l'influence de la valence émotionnelle sur l'implication de différentes commandes centrales communes d'origines spinales et supraspinales reflétées par la cohérence intermusculaire (Dai *et al.,* 2017 ; de Vries *et al.,* 2016 ; Laine & Valero-Cuevas, 2017 ; Nazarpour *et al.,* 2012). Comme illustrée Figure 14, la manipulation du contexte émotionnel sera effectuée au moyen de l'outil IAPS (International Affective Picture System), contrôlé pour chaque participant au moyen du SAM (Self Assessment Manikin). La procédure expérimentale impliquera la réalisation d'une tâche de pointage vers une cible visuelle réalisée dans deux conditions de distance différentes, paradigme particulièrement adapté pour étudier les mécanismes liés à la coordination motrice dans un contexte contrôlé (Fautrelle *et al.,* 2010a, 2010b, 2011).

A long terme, ce projet pourra trouver diverses applications dans lesquelles l'adaptation et la manipulation du contexte émotionnel au service de la performance motrice et/ou cognitive revêt un grand intérêt. L'étude se veut ainsi ouverte sur des questionnements dans les domaines sportif (Coudrat *et al.,* 2014) et clinique, en particulier pour la prise en compte du contexte émotionnel dans le cadre du développement de stratégies adaptées de rééducation motrice des patients post-AVC.
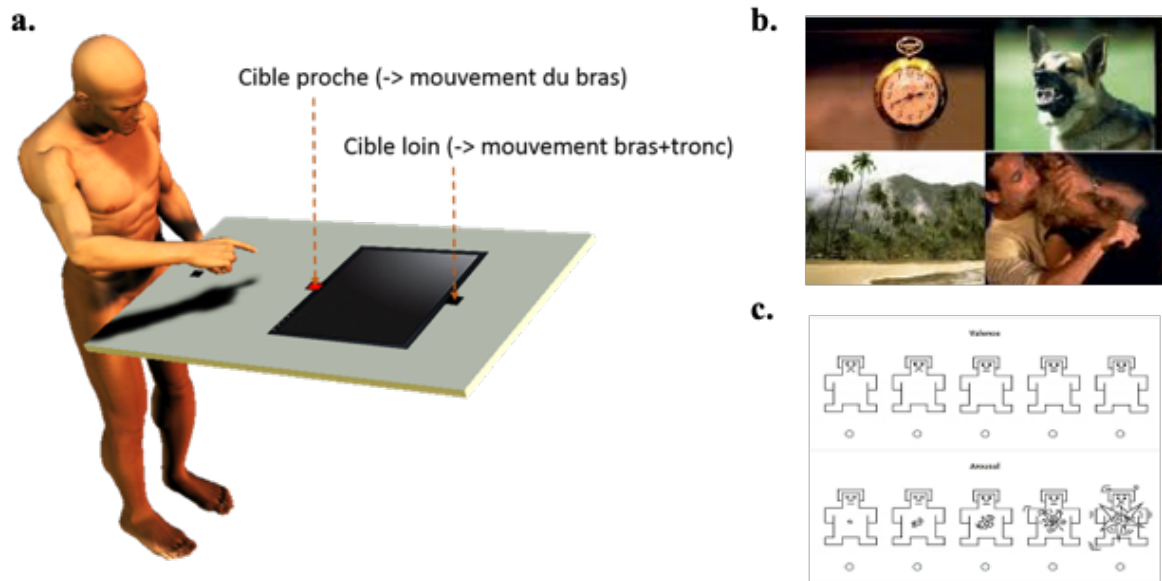
Figure 14. Illustration du protocole utilisé dans le projet « cohérence intermusculaire & contexte émotionnel » pour étudier les mécanismes sous-jacents la flexibilité motrice en fonction du stimulus émotionnel. **a.** Le paradigme expérimental repose sur une tâche de pointage vers une cible visuelle dans deux conditions de distance (c.-à-d. proche *vs* loin), au cours de laquelle sont enregistrées i) la cinématique tridimensionnelle du membre supérieur et ii) l'activité électromyographique de seize muscles des membres supérieurs et inférieurs gauche et droit. **b.** Le contexte émotionnel est manipulé en faisant apparaître, sur un écran placé face au sujet au-dessous de la trajectoire du pointage, des images présentant différentes valences émotionnelles (positive *vs* neutre *vs* négative). Les images présentées sont issues de la base de données IAPS (International Affectives Picture System), outil validé qui catégorise une batterie d'images émotionnelles standardisées selon leur valence et leur activation. **c.** De façon à éviter le biais provoqué par la variabilité interindividuelle de l'expérience émotionnelle induite par l'image, chaque image sélectionnée a été évaluée au préalable pour chaque sujet par l'échelle du Self-Assessment Manikin. Seules les images présentant les niveaux de valence les plus extrêmes et d'activation les plus élevés sont présentées lors de l'étude.

Conclusion

VII.   Conclusion

Au-delà des aspects bibliométriques et des considérations relatives à la gestion de carrière, l'exercice – un peu douloureux – de travail réflexif sur « ma vie, mon œuvre » que m'a imposé la rédaction de ce mémoire de synthèse pour la candidature au diplôme d'Habilitation à Diriger des Recherches aura eu le mérite de me faire mesurer ma chance. La chance d'avoir bénéficié, à la suite immédiate de mon travail de thèse encadré par un savant atypique et passionnant, du soutien inconditionnel d'Eric Berton pour développer, en toute autonomie, les axes de recherches qui ont structuré l'ensemble de mon parcours scientifique résumé dans ce manuscrit. Je ne pouvais avoir meilleur parrain au moment de regarder dans le rétroviseur et de me projeter dans l'avenir. La chance, après avoir été recruté comme maître de conférences à Toulouse, d'avoir rencontré Marieke Longcamp, complice de m'avoir fait bifurquer du domaine – génial – de la biomécanique à celui – magique – de la neuro-biomécanique. A mes questionnements sur les mystères du muscle se sont ainsi ajoutés ceux du cerveau et du couplage qui, à en croire une partie de mes travaux, les associe. La chance d'avoir pu bénéficier, tout au long de mon parcours, de la confiance des étudiant·e·s que j'ai (co-)encadré·e·s. Si j'espère que ce mémoire convaincra du niveau scientifique des produits de mes activités de recherche, du caractère original de la démarche que j'ai suivie pour mener à bien mes projets, et de ma capacité à encadrer de jeunes chercheurs [13], ma plus grande fierté est leurs parcours. La chance, encore, d'avoir pu établir avec de nombreux·ses collègues des relations de collaboration désintéressées, constructives et productives qui participent directement au développement de mes travaux et à leur ouverture à des perspectives fondamentales, cliniques et translationnelles. La chance, enfin, de continuer à explorer l'inexploré [14] dans l'univers fabuleux des mécanismes nerveux centraux de contrôle de l'activité synergique musculaire chez l'homme !

---

[13] Au moment de conclure par une anaphore emplie d'émotion sincère, il n'est pas inutile de rappeler que l'arrêté du 23 novembre 1988, modifié par les arrêtés des 13 février 1992 et 13 juillet 1995, interprété par les circulaires des 5 janvier 1989 et 16 novembre 1992, spécifie que le diplôme d'HDR « sanctionne la reconnaissance d'un haut niveau scientifique, le caractère original d'une démarche, la maîtrise d'une stratégie de recherche dans un domaine large et la capacité à encadrer de jeunes chercheurs ». Dont acte.

[14] Adapté de la devise « Explorons l'inexploré ! » de Russel, membre de la tribu des Wapitis, section 54 (Peterson & Docter, 2009).

Annexes

VIII.   Annexes

Mirror Movements are Linked to Executive Control in Healthy and Brain-injured Adults

Joseph Tisseyre, [a] David Amarantini, [a] Alexandre Chalard, [a,b] Philippe Marque, [a,c] David Gasq [a,d] and Jessica Tallet [a]*

[a] *ToNIC, Toulouse NeuroImaging Center, Université de Toulouse, Inserm, UPS, France*

[b] *Ipsen Innovation, Les Ulis, France*

[c] *Médecine physique et réadaptation fonctionnelle, CHU Toulouse Rangueil, Toulouse, France*

[d] *Explorations Fonctionnelles Physiologiques, CHU Toulouse Rangueil, Toulouse, France*

Abstract—It has been shown that brain-injured patients (BIP) have exacerbated mirror movements (MM). MM are involuntary contractions occurring in homologous muscles contralateral to voluntary movements, particularly in distal upper limb muscles. Attentional and inhibitory processes have been proposed as key factors to explain the level of MM. However, the link between MM and attentional/inhibitory processes has never been formally tested. The present study aims to test this link in 24 right-handed healthy adults and eight chronic BIP. We investigated the link between the amount/intensity of MM and attentional/inhibitory functions. For each participant, MM produced on each limb were assessed with two tasks, and the attentional and inhibitory functions were assessed with six neuropsychological tests. Our results showed (1) a greater amount and intensity of MM and (2) a selective deficit in sustained attention in BIP compared to healthy adults. Moreover, (3) in all participants – independent of the type of task used to evaluate MM – the amount and intensity of MM was predicted by the level of executive control, assessed by the Trail Making Test. High level of MM was associated with weak executive control abilities. This study is the first to highlight the link between MM and executive functioning, which may have implications for rehabilitation in BIP. © 2018 IBRO. Published by Elsevier Ltd. All rights reserved.

Key words: divided attention, stroke, neuropsychological assessment, switching, MVC, sEMG.

INTRODUCTION

Mirror movements (MM) refer to the involuntary contractions occurring in homologous muscles contralateral to voluntary movements, particularly in distal upper limb muscles (Hoy et al., 2004). Such contractions can interfere with the ability to perform hand tasks, especially those requiring inter-manual coordination (Swinnen, 2002). MM are normally present during childhood and disappear gradually as the central nervous system matures (Mayston et al., 1999; Addamo et al., 2007). They become inconspicuous in healthy adults, even though mirrored surface electromyographic (sEMG) activity can still be observed in certain conditions such as complex rhythmic tasks (Ridderikhoff et al., 2005; Vardy et al., 2007) or tasks requiring either low or high force levels (Armatas et al., 1996; Arányi and Rösler, 2002). MM reappear more obviously in elderly people compared to younger adults (Bodwell et al., 2003; Shinohara et al., 2003; Baliz et al., 2005; Addamo et al., 2009a, 2010; Koerte et al., 2010).

The age-related evolution of MM can be explained by the maturation and degeneration of the corpus callosum – a white matter structure that connects both hemispheres. According to the bilateral activation theory proposed by Cernacek (1961), the mechanism underlying MM is transcallosal facilitation, whereby activation in one hemisphere during voluntary movement facilitates activation of the same neural area in the opposite hemisphere, via the connections in the corpus callosum. According to this theory, exacerbated MM can be considered the result of altered interhemispheric inhibitory processes (Hübers et al., 2008). Persistent MM are observed in adults with pathological conditions – particularly in hemiplegic patients following a stroke or brain injury – who have unbalanced interhemispheric inhibitory processes (Cernacek, 1961; Chaco and Blank, 1974; Hopf et al., 1974; Lazarus, 1992; Weiller et al., 1993; Netz et al., 1997; Nelles et al., 1998; Hwang et al., 2005; Nowak

et al., 2009; Chang et al., 2013; Seo, 2013; Kim et al., 2015). However, some authors suggest the pathological presence of MM in brain-injured patients (BIP) is not systematic and consider this symptom to be very heterogeneous (Uttner et al., 2005). Although present in both limbs, most studies show that MM are more important in the non-paretic limb when patients execute unilateral movement with their paretic limb (Lazarus, 1992; Nelles et al., 1998; Chang et al., 2013; Seo, 2013). As proposed by Nelles et al. (1998), the amount of MM in the non-paretic and paretic limb are associated with different degrees of motor deficit after stroke as measured by the Fugl Meyer Assessment of the Upper Extremity (FMA-UE) (Fugl-Meyer et al., 1974). More precisely, high level of MM in the non-paretic limb was related to greater motor deficit in post-stroke patients, whereas the absence of MM in the non-paretic limb was related to better motor abilities (Nelles et al., 1998). In contrast, patients with high level of MM in the paretic limb had better motor function than patients without MM in the paretic limb (Nelles et al., 1998). However, studies failed to find any correlation between the amount of MM and the characteristics of the lesions, and the patient's sex or age (Uttner et al., 2005).

The present study aims to test the link between attentional and inhibitory functions and MM in BIP compared to healthy controls. This study is based on results of previous studies in healthy young and older adults showing that attentional and inhibitory processes are involved in the production of MM (Baliz et al., 2005; Addamo et al., 2009b, 2010). With regard to attentional processes, Baliz et al. (2005) showed that – during a finger force task – the number of MM was significantly greater when attention was diverted. Bodwell et al. (2003) also showed a significant increase in MM intensity in healthy young and elderly adults when a cognitive distraction was applied during a unilateral finger-tapping task. With regard to inhibitory functions, Addamo et al. (2010) showed that both young and older adults were equally able to voluntarily inhibit MM during a finger-pressing task when requested to do so. The authors concluded that MM can be modulated by higher order cognitive control, such as directed attention and inhibition. In this context, BIP may exhibit a large amount of MM due to attentional and/or inhibitory deficits that impair inhibition of MM. Many studies have found attentional and inhibition deficits in BIP (Mathias and Wheaton, 2007; Leśniak et al., 2008; Cumming et al., 2013). These cognitive disturbances are known to limit the patients' functional recovery (Hyndman and Ashburn, 2003) and especially their motor recovery (Mullick et al., 2015). Attentional processes have been proposed as key factors to explain the level of MM in BIP (Uttner et al., 2005). However, the authors did not test this hypothesis experimentally.

In order to determine whether there is a formal link between the level of MM and the level of attentional/inhibitory functions in healthy adults and BIP, we assessed the amount and the intensity of MM in each participant during two tasks: (1) unimanual Maximal Voluntary Contractions (MVC) task and (2) a switching motor task that requires switching from bimanual to unimanual rhythmic contractions (Tallet et al., 2009, 2013). For each limb (right and left), MM was quantified by the residual sEMG activation peaks in the stopping hand. For each participant, we also assessed a wide range of cognitive processes including different types of attention and inhibitory functions. To this purpose, we evaluated different specific functions of attention such as "alertness", "sustained attention", "focused attention" and "divided attention" (in accordance with the Van Zomeren and Brouwer model (Zomeren and Brouwer, 1994)), and also evaluated inhibitory functions with verbal and motor tasks (Stroop task and Go/No Go task respectively). We hypothesized that the level of MM (amount and intensity) is positively correlated to the attentional and inhibitory deficits of participants (healthy and brain-injured adults). Participants with the greatest attentional and inhibitory deficits should have more MM.

EXPERIMENTAL PROCEDURES

Participants

Twenty-four right-handed control volunteers (CTL; 15 men and nine women; mean age: 31 ± 17 years) and eight brain-injured patients (BIP; seven men and one woman; mean age: 54 ± 13 years; mean time since brain injury: 64 ± 49 months, mean FMA-UE score (max. 66): 52 ± 6, mean Action Research Arm Test (ARAT, max. 57): 41 ± 13, mean Erasmus modified Nottingham Sensory Assessment (EmNSA, max. 64): 56 ± 15) participated in the study. The patient characteristics are shown in Table 1. Patients were included if they had suffered a unilateral brain injury of vascular ($n = 7$) or traumatic origin ($n = 1$), and had the ability to perform hand-grip contractions. Exclusion criteria were subjects with spatial neglect, musculoskeletal or neurological disorders in addition to brain injury, or subjects with severe language impairment or psychiatric disorders that could interfere with the ability to follow simple verbal instructions. No participant was excluded from the study. All participants gave informed consent according to the Declaration of Helsinki recommendations for investigations with human participants, and all procedures were approved by local ethics committee and conformed to the standards set by the Declaration of Helsinki.

Neuropsychological assessment

Participants sat comfortably in a chair in front of a table and performed six neuropsychological tests in a randomized order to assess attentional and inhibitory functions in accordance with the Van Zomeren and Brouwer model (Zomeren and Brouwer, 1994). For tests requiring the use of only one hand, the controls and BIP were asked to perform the task with their current dominant hand. This corresponded to the non-paretic hand in seven patients and the paretic hand in one. The aim was to make the patients' performance comparable to each other and to the controls, using their preferred hand for activities of daily living. Testing lasted approximately one hour and included the following tests:

Table 1. Detailed characteristics of the study participants. For control volunteers, values are mean ± standard deviation (SD)

	Number	Sex	Age (years)	Laterality quotient	Lesion side	Disease course (month)	FMA-UE (/66)	ARAT (/57)	EmNSA (/64)
CTL	n = 24	15 M/9F	31 ± 17	83 ± 34	–	–	–	–	–
BIP	1	F	47	−10	Left	48	55	39	62
	2	M	66	−20	Left	14	51	36	57
	3	M	59	+100	Left	27	59	55	62
	4	M	52	−100	Left	43	48	–	60
	5	M	64	−100	Left	39	60	57	60
	6	M	71	+100	Right	60	44	23	19
	7	M	33	+50	Right	146	54	51	64
	8	M	41	−80	Left	132	46	29	64

Focused attention was evaluated with the d2 test of attention (D2; Brickenkamp, 1962). This test involves simultaneous presentation of visually similar stimuli. The task involves crossing out all target characters (a ''d'' with a total of two dashes placed above and/or below), which are interspersed with non-target characters (a ''d'' with more or less than two dashes, and ''p'' characters with any number of dashes), in 14 successive timed trials (20 s for each trial).

Divided attention and flexibility (labeled "executive control" in this paper) were evaluated with the Trail Making Test (TMT, versions A and B; Reitan, 1958).

Preparatory attention was evaluated with a task adapted from the phasic alert test (Zimmermann and Fimm, 2002) under two conditions in which the participants had to respond by pressing the space bar of the keyboard as quickly as possible when a central cross appeared on a computer screen. In the "intrinsic" condition, the stimulus appeared on the screen without warning, while in the ''phasic'' condition, a warning tone preceded the appearance of the stimulus. The time span between the stimuli was random.

Sustained attention was evaluated with the Continuous Performance Test (CPT; Conners, 1994). Participants were required to press the space bar as quickly as possible whenever any letter except the letter 'X' appeared on the computer screen. The interstimulus intervals were 1, 2 and 4 s with a display time of 250 ms.

Motor inhibition was evaluated with an auditory go/no-go task. The participants fixed a center cross on the screen while 100 beeps sounded (25% high-pitched (No Go condition), 75% low-pitched (Go condition)). Beginning with the index finger of the dominant hand pressing the left mouse button, the participants had to press the right button as quickly as possible only when the low-pitched sound was generated. The order of stimuli was randomized and the duration between two stimuli was variable.

Verbal inhibition was evaluated with the Stroop task (Stroop, 1935).

Experimental protocol

Two isometric dynamometers (model TSD121C; Biopac System, Inc., Goleta, CA, USA) were used to record the power grip force in the right and left hands.

Following appropriate skin preparation (Hermens et al., 2000), surface EMG was recorded on both sides with Biopac MP150 system (EMG-100C amplifiers, EL503 Ag–AgCl 11-mm bipolar electrodes with a maximum 2-cm spacing; Biopac System, Inc., Goleta, CA, USA) from two representative superficial anterior and posterior forearm muscles: *flexor carpi radialis* and *extensor digitorum communis*. The reference electrode was placed on the bone area of the right elbow.

Force and sEMG data were automatically synchronized in the MP150 unit, recorded at 1000 Hz with AcqKnowledge software (Biopac System, Inc., Goleta, CA, USA) and analyzed offline.

The protocol consisted of two consecutive tasks.

MVC task: the participants were instructed to perform three maximal power grip isometric voluntary contractions in both left and right *unimanual* conditions and in a *bimanual* condition presented in a random order. In each condition, each contraction lasted 4 s, with 10-s rest between each contraction; each condition was separated by at least 1-min rest. After low-pass filtering at 20 Hz (fourth-order, zero-lag Butterworth filter), MVC force value in each condition was the average force during a 2 s window in which the force of the three maximum voluntary contractions was highest.

Switching motor task: The participants sat comfortably in front of a computer screen with their hands continuously on the dynamometers to perform power grip contractions at 25% MVC in synchronization with an auditory metronome with a period of 700 ms. Inspired by the selective stop task in Tallet et al. (2009, 2013), two sides of stopping conditions were required. In the *left* hand stopping condition, the participants had to switch from bimanual to unimanual power grip contractions by stopping the left hand when the metronome changed from low-pitched tones (500 Hz) to high-pitched tones (4000 Hz), while continuing contractions with the right hand in synchrony with the metronome. In the *right* hand stopping condition, they had to perform exactly the opposite task when the metronome changed from low-pitched tones (500 Hz) to high-pitched tones (4000 Hz). The participants were provided with visual feedback on the computer screen of current force and force target on each hand dynamometer. This feedback allowed participants to control their contractions to 25% of their MVC. Each trial included 20 tones and lasted 14 s. The metronome's

tonality changed randomly after either 6 or 10 low-pitched tones. Five blocks, each consisting in two trials for each side of stopping, were undertaken by the participants with 10-s rest between trials and 2-min rest between blocks. A one-trial familiarization phase was provided for each stopping condition.

Data processing

For neuropsychological data, the following six variables were calculated to identify the participants' neuropsychological profile:

Qualitative performance index (*F*% score) for D2 was used to evaluate focused attention with: *F*% score = $100 \times$ (total number of errors/total number of signs treated);

The difference between the completion time for part A and part B of the TMT was used to assess divided attention and flexibility;

The difference between the "intrinsic" and the "phasic" reaction time for the phasic alert task was used to assess preparatory attention;

Reaction time variability on the CPT was reported to evaluate sustained attention;

The total number of errors in the auditory go/no-go task was used to assess motor inhibition;

Interference score during the Stroop task was used to evaluate verbal inhibition.

For force and sEMG data processing, all computations were done using Matlab (MathWorks, Natick, MA, USA). All filters were fourth-order zero-lag Butterworth type.

Data preprocessing: Raw isometric force data recorded with hand dynamometers were low-pass filtered at 20 Hz. Raw sEMG signals were band-pass filtered in 10–400-Hz band for denoising, and full-wave rectified by computing the absolute value. Then, the rectified sEMG signal was smoothed into a linear envelope using low-pass filtering at 3 Hz, which is within the range of appropriate cutoff frequencies to match the sEMG envelope with the net mechanical effort pattern (Potvin et al., 1996; Amarantini and Martin, 2004). Finally, for the switching motor task, the sEMG activity of each muscle was normalized to the maximal sEMG activity production during *bimanual* MVC for each respective muscle.

Detection of MM: For the *unimanual* MVC task, the "intensity" of MM in the resting hand was assessed for each participant with the amplitude of sEMG activity expressed as the percentage of the sEMG root mean square (RMS) activity calculated in the respective hand when it was active during unimanual MVC. For the switching motor task, the "amount" and the "intensity" of MM of the stopping hand were assessed for each participant as the average number and the average amplitude of post-switching sEMG peaks in the stopping hand, respectively. Peak detection was done using the "peakdet" Matlab function (http://www.billauer.co.il/peakdet.html) in which "a point is considered a maximum peak if it has the maximal value, and was preceded by a value lower by DELTA." For sEMG

peaks, DELTA was set at 1% of the corresponding maximal sEMG activity recorded during MVC. An example of the method used to detect peaks on force and sEMG data during the switching motor task is given in Fig. 1.

Kinetic manifestation of mirror movements: For the *unimanual* MVC task, the involuntary force in the resting hand was quantified as the percentage of the maximum force produced in the respective hand during *unimanual* MVC. For the switching motor task, the involuntary force in the stopping hand was quantified with the average amplitude of post-switching force peaks. For force, peak detection was performed with DELTA set at 2% MVC.

During the switching motor task, the above-described MM assessment was performed over a 2.1 s period from the second to the fourth contraction following motor switching. The first contraction following switching was excluded from the analysis to account for the time required for the participant to apply the "stop" command.

Statistical analyses

All values were normally distributed (Kolmogorov–Smirnov test; $p > 0.05$). Variables expressed as a proportion were arcsine square root transformed before analysis (McDonald, 2009). This applied to the amplitude of sEMG activity and force production in the resting hand during *unimanual* MVC task and the average amplitude of the post-switching sEMG and force peaks in the stopping hand during the switching motor task. For the statistical analysis, the paretic and non-paretic limbs of BIP corresponded to the "weak" and "strong" limbs, respectively. For CTL, the "strong" limb was the one that produced the highest force during bimanual MVC.

A multivariate analysis of covariance (MANCOVA) with age as a covariate was performed on the six neuropsychological scores to test the differences between CTL and BIP while controlling for age.

To test whether force production and amplitude of sEMG activity in the resting hand were influenced by Limb and Group while controlling for age during *unimanual* MVC, analyses of covariance (ANCOVAs) with Limb (strong vs. weak) as a within-participant factor, Group (CTL vs. BIP) as a between-participant factor and Age as covariate were conducted on (1) the force production in the resting hand and (2) the sEMG activity amplitude in the resting hand.

To test whether the post-switching sEMG and force peaks in the stopping hand were influenced by Limb and Group while controlling for age during the switching motor task, ANCOVAs with Limb (strong vs. weak) as a within-participant factor, Group (CTL vs. BIP) as a between-participant factor and age as covariate were conducted on (1) the average amplitude of the post-switching force peaks, (2) the average number of the post-switching sEMG peaks and (3) the average amplitude of the post-switching sEMG peaks. Moreover, one-sample tests were performed to compare the amplitude of force peaks in the stopping hand to the 2% MVC threshold, corresponding to the reference value for peak force detection in this study.
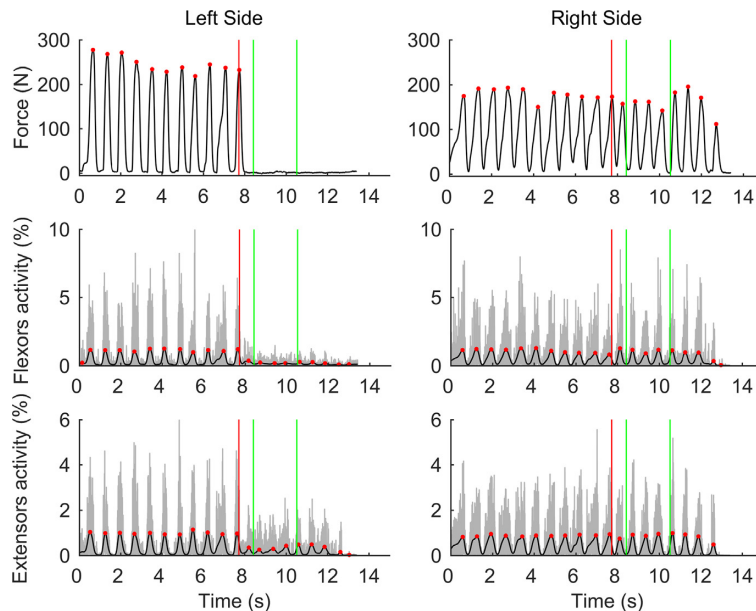
Fig. 1. Illustration of force (upper panels) and sEMG (middle and lower panels) peak detection on left and right side (left and right panels, respectively) during a representative trial of the left hand stopping condition in a brain-injured patient. On the sEMG graphs, the gray plot corresponds to denoised, full-wave rectified sEMG. The vertical red lines indicate the transition i.e. the instant when the metronome changed from low- to high-pitched tones; the red points represent detected force and sEMG peaks; the vertical green lines delimit the period of interest for MM quantification. (For interpretation of the references to color in this figure legend, the reader is referred to the web version of this article.)

Finally, the relationship between the neuropsychological profile of participants and (i) average amplitude of sEMG activity in the resting hand during the *unimanual* MVC task, (ii) average number and (iii) average amplitude of post-switching total sEMG peaks in the stopping hand during the switching motor task was studied with three stepwise regression models with backward elimination. To interpret the results irrespective of age, regressions were performed on residuals only of the significant single regression between each variable and age.

For all tests, the level of significance was set at $p < 0.05$.

RESULTS

Neuropsychological variables

The MANCOVA with age as covariate revealed a significant multivariate Group effect on reaction time variability in the CPT ($F_{1,29} = 8.942$; $p = 0.005$; partial $\eta^2 = 0.235$; f effect size: 0.555). Regardless of age, BIP had a more variable reaction time than CTL (Table 2). The age covariate was significantly related to reaction time variability in the CPT ($F_{1,29} = 8.194$; $p = 0.007$; partial $\eta^2 = 0.220$; f effect size: 0.531) and to $F\%$ score on D2 ($F_{1,29} = 10.393$; $p = 0.003$; partial $\eta^2 = 0.263$; f effect size: 0.598).

MM during MVC task

Force production in the resting hand. The ANCOVA Limb × Group with age as a covariate revealed a significant Group effect on the force production in the resting hand during the *unimanual* MVC task ($F_{1,29} = 21.376$; $p < 0.001$; partial $\eta^2 = 0.424$, f effect size: 0.858). Moreover, the Limb × Group interaction was significant for force production ($F_{1,29} = 5.966$; $p = 0.02$; partial $\eta^2 = 0.170$, f effect size: 0.453). Involuntary force production in the resting hand was higher in BIP than in CTL only in the weak limb (BIP = 14.78 ± 15.95%; CTL = 1.20 ± 1.18%).

Amplitude of sEMG activity in the resting hand. The ANCOVA Limb × Group with age as a covariate revealed a significant Group effect in the amplitude of sEMG activity in the resting hand during the *unimanual* MVC task ($F_{1,29} = 8.984$; $p = 0.005$; partial $\eta^2 = 0.236$, f effect size: 0.556). Moreover, the Limb × Group interaction was significant for the amplitude of sEMG activity ($F_{1,29} = 7.571$; $p = 0.01$; partial $\eta^2 = 0.207$, f effect size: 0.511). The amplitude of sEMG activity was higher in BIP than in CTL only in the weak limb (BIP = 41.51 ± 39.68%; CTL = 6.27 ± 5.34%; Fig. 2).

MM during the switching motor task
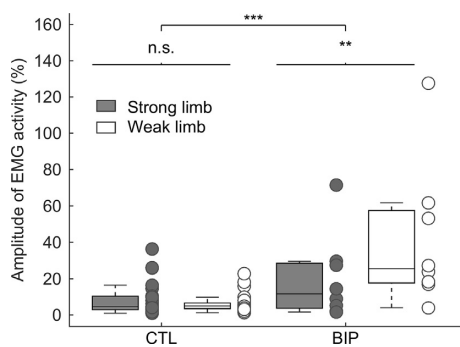
Average amplitude of post-switching force peaks in the stopping hand. The ANCOVA Limb × Group with age as a covariate revealed a significant Group effect in the average amplitude of post-switching force peaks in the stopping hand ($F_{1,29} = 22.016$; $p < 0.001$; partial $\eta^2 = 0.431$, f effect size: 0.871). Regardless of Limb (weak vs. strong), the average amplitude of post-switching force peaks was higher in BIP than in CTL (16.97 ± 10.13% MVC vs. 2.28 ± 4.71% MVC). The age covariate was not significantly related to the average amplitude of post-switching force peaks ($F_{1,29} = 2.725$; $p = 0.109$).

One-sample t-test performed on BIP revealed a significant difference between the amplitude of the force peaks in the stopping hand and the 2% reference value ($t_7 = 4.177$; $p = 0.004$). In contrast, the same one-sample t-test was not significant in CTL ($t_{23} = 0.299$; $p > 0.05$).

Average number of post-switching sEMG peaks in the stopping hand. The ANCOVA Limb × Group with age as

Table 2. MANCOVA summary table of population differences in neuropsychological tests in healthy adults (CTL) and brain-injured patients (BIP). [*]Indicates significant difference between CTL and BIP ($p < 0.05$); df corresponds to the degrees of freedom (effect, error).

Dependent variables	Mean ($\pm$SD)		Univariate		
	CTL	BIP	df	F	p
D2	3.61 ($\pm$2.61)	4.76 ($\pm$3.48)	1,29	0.57	0.453
TMT	36.88 ($\pm$15.50)	156.75 ($\pm$196.74)	1,29	3.50	0.071
PHASIC ALERT	-3.37 ($\pm$21.02)	-18.23 ($\pm$49.47)	1,29	<0.01	0.994
CPT	73.10 ($\pm$21.31)	132.34 ($\pm$47.42)	1,29	8.94	0.005[*]
GO/NO GO	5.36 ($\pm$3.35)	6 ($\pm$2.44)	1,29	0.46	0.499
STROOP	27.12 ($\pm$7.47)	26.87 ($\pm$11.93)	1,29	<0.01	0.992

Fig. 2. Boxplots and stripcharts showing the amplitude of sEMG activity in the resting hand during the unimanual MVC task in the strong and weak limbs in healthy adults (CTL) and brain-injured patients (BIP). [***]Indicates significant difference between CTL and BIP ($p < 0.001$); [**]indicates significant difference between the strong and weak limbs in BIP ($p < 0.01$).

a covariate revealed a significant Group effect in the average number of post-switching sEMG peaks in the stopping hand ($F_{1,29} = 32.028$; $p < 0.001$; partial $\eta^2 = 0.524$, f effect size: 1.050). Regardless of Limb (weak vs. strong), the average number of post-switching sEMG peaks was higher in BIP than CTL (2.554 ± 1.010 vs. 0.879 ± 0.589; Fig. 3, left panel). The age covariate was significantly related to the average number of post-switching sEMG peaks ($F_{1,29} = 8.521$; $p < 0.006$; partial $\eta^2 = 0.227$, f effect size: 0.879).

Average amplitude of post-switching sEMG peaks in the stopping hand. The ANCOVA Limb $\times$ Group with age as a covariate revealed a significant Group effect in the average amplitude of post-switching sEMG peaks in the stopping hand ($F_{1,29} = 13.332$; $p = 0.001$; partial $\eta^2 = 0.314$, f effect size: 0.678). Regardless of Limb (weak vs. strong), the average amplitude of post-switching sEMG peaks was higher in BIP than in CTL ($17.578 \pm 11.589\%$ vs. $5.252 \pm 5.932\%$; Fig. 3, right panel). The age covariate was significantly related to the average amplitude of post-switching sEMG peaks ($F_{1,29} = 10.252$; $p = 0.003$; partial $\eta^2 = 0.261$, f effect size: 0.594).

Relationship between MM and neuropsychological scores

The first stepwise regression model with backward elimination between mean amplitude of sEMG activity in the resting hand during the *unimanual* MVC task and the six neuropsychological variables identified only the TMT score as a significant predictor, regardless of age ($t_{30} = 8.200$; $p < 0.05$; see Table 3).

Similarly, the two stepwise regression models with backward elimination between average number or average amplitude of post-switching sEMG peaks on the stopping hand during the switching motor task and the six neuropsychological variables identified only the TMT score as a significant predictor, regardless of age ($t_{30} = 3.182$ and $t_{30} = 3.430$, respectively; $p < 0.05$; see Table 3).

DISCUSSION

The current study investigated the formal link between the amount and intensity of MM and cognitive functions. To this aim, MM were assessed and correlated with the attentional and inhibitory functions of healthy and BIP adults. Although the BIP cohort was rather small, our findings suggest that BIPs have more MM compared to healthy controls no matter which task used to assess MM (MVC or switching task), and have a selective deficit in sustained attention. Independent of which task was used to assess MM (MVC or switching task), we found a significant relationship between MM and executive control, assessed by the TMT. Our findings are discussed in terms of factors that can modulate the occurrence of MM with possible implications for rehabilitation of BIP.

Selective deficit in sustained attention in BIP

Among all the attentional and inhibitory tests, we found only a deficit in sustained attention in chronic BIP compared to healthy adults, even after controlling for the effect of age. Sustained attention refers to the ability to maintain stable, efficient attention during a long-term task and is part of the "intensity" dimension in the Van Zomeren and Brouwer (1994) model. Our results are partly consistent with previous published studies on the neuropsychological profile of chronic BIP. This selective deficit in sustained attention is surprising given that previous studies found more general deficits in both attention and executive functions (including inhibitory functions)
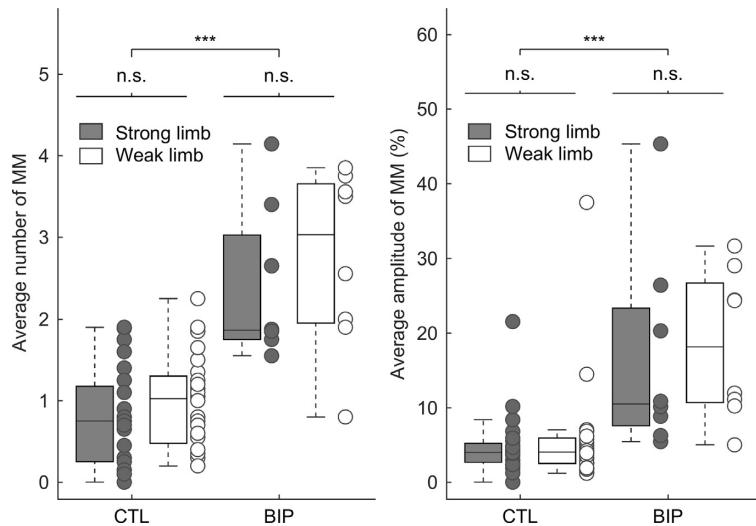
Fig. 3. Boxplots and stripcharts showing the average number and amplitude (left and right panels, respectively) of post-switching sEMG peaks in the stopping hand in the strong and weak limbs in healthy adults (CTL) and brain-injured patients (BIP). ***Indicates significant difference between CTL and BIP (*p* < 0.001).

stroke (Ballard et al., 2003; Sachdev et al., 2004; Roussel et al., 2016) or the post-acute stage (Leśniak et al., 2008). At the 1-year follow-up, Leśniak et al. (2008) found that attention deficits are still the most frequent symptom, while executive dysfunctions are significantly less frequent than in the post-acute stage. Another longitudinal study also found a reduction in the proportion of patients with an executive deficit one-month post-stroke compared to one year after (Rasquin et al., 2004). All in all, the literature suggests a persistence of attentional deficits and the normalization of executive functions (only the inhibitory functions in our case) over the time course of recovery. Given that patients in the chronic stage were included in our study, it is not surprising that only a selective sustained attention (not executive) deficit was found.

that persist in chronic BIP (Mathias and Wheaton, 2007; Leśniak et al., 2008; Barker-Collo et al., 2010; Cumming et al., 2013). However, our results are consistent with a long-term (5-year) follow-up study of stroke patients (Barker-Collo et al., 2010) reporting significant deficits in the Integrated Visual and Auditory Continuous Performance Test known to involve sustained attention (Sandford and Turner, 2000). The sustained attention deficit seems to persist for a long time post-lesion.

Although executive function deficits are commonly reported in the literature on inhibition or executive control in BIP (Ballard et al., 2003; Rasquin et al., 2004; Sachdev et al., 2004; Roussel et al., 2016), we failed to find such deficits in our study. The absence of differences could be attributed to the number and characteristics of the BIP tested in our study. With regard to patient characteristics, most previous studies found deficits of attentional and executive functions during the subacute stage following

Increased amount and intensity of MM in BIP

In our study, the amount and intensity of MM was quantified using two variables: (1) the number of post-switching sEMG peaks during the switching motor task and (2) the amplitude of sEMG activity during the MVC task and the amplitude of post-switching sEMG peaks during the switching motor task. Overall, the amount and intensity of MM were exacerbated in BIP compared to healthy controls, for both tasks (MVC and switching motor task). Our findings are consistent with results of previous studies, showing that MM intensity was higher in BIP during unimanual contractions (Cernacek, 1961; Lazarus, 1992; Nelles et al., 1998; Hwang et al., 2005; Seo, 2013; Kim et al., 2015). However, two of our findings surprised us.

First, there was an asymmetry in the MM produced by BIP during the MVC task, with greater MM (larger

Table 3. Summary of linear stepwise regression analysis for neuropsychological scores predicting the average amplitude of sEMG activity (i.e. intensity of MM) during the *unimanual* MVC task (upper table) and the average number and amplitude of sEMG peaks (i.e. MM amount and intensity, respectively) during the switching motor task (lower table)

Model	Factor	Coefficients	Standard error	t (30)	p value
Maximal voluntary contraction task					
Average amplitude of sEMG activity	TMT	0.831	0.101	8.200	< 0.0001
$r = 0.831$ $\quad r2 = 0.691$					
Switching motor task					
Average number of sEMG peaks	TMT	0.502	0.157	3.182	0.003
$r = 0.502$ $\quad r2 = 0.252$					
Average amplitude of sEMG peaks	TMT	0.530	0.154	3.430	0.001
$r = 0.530$ $\quad r2 = 0.281$					

amplitude of the involuntary force and sEMG activity) in the weak (paretic) limb. The literature reports conflicting results on which side produces more MM in BIP. Some studies in chronic BIP reported a greater MM intensity in the paretic limb when the non-paretic limb was active (Chang et al., 2013; Kim et al., 2015). Other studies reported a greater MM intensity in the non-paretic limb when the paretic limb was active compared to the opposite case (Lazarus, 1992; Nelles et al., 1998; Seo, 2013). One hypothesis to explain this apparent contradiction is that the non-paretic limb could have a post-lesion deficit that generates a high level of MM in the paretic limb. This hypothesis is based on previous studies suggesting that a motor deficit of the non-paretic limb after unilateral stroke emerges acutely (Sunderland et al., 1999) and persists chronically (Yarosh et al., 2004; Wetter et al., 2005; Schaefer et al., 2007; Avila et al., 2013). However, in our study, MM in the strong limb during a unimanual isometric MVC task were comparable between BIP and healthy participants. Another hypothesis could be that our BIP had a good level of recovery. Given that previous findings showed that a good motor level in BIP was associated with high MM levels in the paretic limb (Nelles et al., 1998), the MM of the paretic limb may be similar (switching motor task) or even greater (MVC task) than MM of the non-paretic limb. Underlying this assumption, BIP tested in our study were in the post-injury chronic phase (63.62 months on average ± 48.62) and had a very good motor recovery (FMA-UE and ARAT score). Interestingly, a recent longitudinal case study reported a progressive MM decrease in the non-paretic limb during the process of motor recovery in a woman with a right-sided stroke (Ohtsuka et al., 2015). Similarly, a recent longitudinal study quantified MM and paretic hand function in 53 stroke patients in the year following unilateral stroke (Ejaz et al., 2017). These authors found that MM in the non-paretic hand were exaggerated early after damage (2 weeks) but progressively normalized over the following year, with a time-course that mimicked the recovery of the paretic hand function (Ejaz et al., 2017).

Another interesting finding is that asymmetry was not found in the switching task. For BIP as well as healthy adults, we found no asymmetry between the strong and weak limb during the switching motor task, neither in the force amplitude nor the MM amount and intensity. Hence, the degree of MM in the paretic and non-paretic limbs of BIP seems to depend not only on the motor recovery and the post-lesion delay, but also on the target force level (i.e. MVC or submaximal voluntary contractions) and perhaps the motor task type (Armatas and Summers, 2001). This suggestion is consistent with previous results showing that the level of MM is influenced by the required force level (Armatas et al., 1994, 1996; Arányi and Rösler, 2002).

Occurrence and intensity of MM were associated with executive control (TMT)

The three stepwise regression models with backward elimination between (1) the average amplitude of sEMG activity in the resting hand during the unimanual MVC task, (2) the average number and (3) amplitude of

post-switching sEMG peaks in the stopping hand during the switching motor task and the six neuropsychological variables assessing attentional and inhibitory functions revealed that in all participants, the level of MM can be explained by the B-A difference in the TMT. The B-A difference in the TMT reflects executive control mechanisms including several sub-functions such as inhibition, switching from one task to another or flexibility (Sánchez-Cubillo et al., 2009) and divided attention (Zomeren and Brouwer, 1994; Spikman et al., 2001; Zakzanis et al., 2005). It is doubtful that the level of MM would be linked to the inhibition or flexibility components of the TMT because of (1) the lack of correlation between MM and inhibitory functions (Stroop task and no-go test) and (2) the significant correlation between TMT and MM produced during the unimanual MVC task which does not imply switching or inhibition. Alternatively, the correlation between MM and the TMT score suggests that participants must divide their attention between each limb to contract one hand without contracting the other. In that sense, the amount and intensity of MM could be linked to divided attention rather than inhibition or flexibility. Participants with the lowest level of divided attention would have more MM than participants with the highest level of divided attention. Further investigations with a purer test of divided attention and a larger sample are required to confirm this hypothesis.

Clinical implications

As confirmed in this study, the assessment of MM in BIP is important because of their high prevalence in this population (Cernacek, 1961; Chaco and Blank, 1974; Lazarus, 1992; Nelles et al., 1998; Hwang et al., 2005; Kim et al., 2015) and also because MM has been identified as both a target for, and an aid in, evaluation and rehabilitation (Nelles et al., 1998; Bhakta et al., 2001).

With regard to evaluation, our results reveal that the amplitude of the involuntary force produced by the stopping hand was negligible in healthy participants (2.28% of the MVC). This result supports the idea that MM are inconspicuous in healthy adults: they do not produce directly observable behavioral manifestations and they can only be assessed by sEMG. In contrast, in BIP, the stopping limb produced a non-negligible involuntary force (16.97% of their MVC), which suggests that MM are an important clinical marker that should be evaluated and a potential rehabilitation target.

With regard to rehabilitation, several studies have reported that frequent involuntary movements – not restricted to homologous muscles (i.e. associated reactions) – could interfere with upper limb function in BIP (Bhakta et al., 2001, 2008; Kahn et al., 2016). In addition, many activities of daily living require two limbs to perform two different tasks simultaneously. Therefore, mirror activity can alter bimanual asymmetric coordination in BIP. The presence of associated movements during stroke recovery is said to hinder development of normal movement and therefore, the use of rehabilitation techniques targeting these abnormal movements have been proposed (Bhakta et al., 2001). Thus, therapists can train patients to perform strict unimanual movements (as in

constraint-induced therapy, e.g. Doussoulin et al., 2017) but also asymmetrical bimanual movements to prevent interference in functional activities (as in asymmetric training therapy, e.g. Lee et al., 2014).

In contrast, other studies suggest that post-stroke MM may act as a compensatory mechanism not only aiding voluntary movement, but also signifying recovery of motor function (Nelles et al., 1998). As noted earlier, patients with MM in the paretic limb tend to have better motor function than patients without MM in the paretic limb (Nelles et al., 1998). The goal would be to encourage the patient to perform the desired movement with his non-paretic hand to activate his paretic hand through mirror activity. In support of this hypothesis, a facilitation effect was demonstrated in the injured hemisphere during a movement with the non-paretic hand (Renner et al., 2005).

Finally, if the involvement of executive control abilities in the production of MM is confirmed, we could imagine that a cognitive rehabilitation or training program focused on this cognitive function in BIP could reduce MM and vice versa. There is good evidence that higher order cognitive processes such as executive control may modulate MM. Cognitive rehabilitation could improve the motor function of BIP. For example, inhibitory training programs that direct attention to involuntary force or sEMG production from the passive hand through feedback have been identified as relevant to reducing MM (Lazarus and Todor, 1991; Lazarus, 1992). Furthermore, a deficit in higher order cognitive process such as executive control hinder the sensorimotor learning (e.g. Dancause et al., 2002) required for successful physical rehabilitation and stroke recovery (Hyndman and Ashburn, 2003; Barker-Collo and Feigin, 2006; Barker-Collo et al., 2010; Mullick et al., 2015). Conversely, motor intervention could improve cognitive functioning. For example, a pilot study provided evidence that aerobic exercise improves cognition (the speed of information processing) in chronic stroke survivors (Quaney et al., 2009). A recent review confirmed that aerobic exercise may help to improve global cognitive ability (Zheng et al., 2016). Similar effects of aerobic exercise on executive functions have been found in healthy adults (e.g. Colcombe et al., 2004). These results are an example of the mutual interaction of cognitive and motor functions. On this basis, cognitive and motor rehabilitation should not be viewed as separate aspects; rehabilitation benefits from the interactions between cognitive and motor functions.

To our knowledge, this study is the first to highlight a relationship between MM and executive control in healthy adults and BIP. As in previous studies, we found a greater amount and intensity of MM in BIP compared to healthy adults during both MVC and switching motor tasks. More interestingly, the amount and intensity of MM were predicted by executive control (TMT) for all participants. Our results suggest that higher amount and greater intensity of MM is associated with lower divided attention. In this context, we can imagine that cognitive rehabilitation focused on attentional deficits could reduce MM in BIP, and vice versa.

CONFLICT OF INTEREST

The authors declare having no conflict of interest.

REFERENCES

Addamo PK, Farrow M, Hoy KE, Bradshaw JL, Georgiou-Karistianis N (2007) The effects of age and attention on motor overflow production—A review. Brain Res Rev 54:189–204.

Addamo PK, Farrow M, Hoy KE, Bradshaw JL, Georgiou-Karistianis N (2009a) The influence of task characteristics on younger and older adult motor overflow. Q J Exp Psychol 62:239–247.

Addamo PK, Farrow M, Hoy KE, Bradshaw JL, Georgiou-Karistianis N (2009b) A developmental study of the influence of task characteristics on motor overflow. Brain Cogn 69:413–419.

Addamo PK, Farrow M, Bradshaw JL, Moss S (2010) The effect of attending to motor overflow on its voluntary inhibition in young and older adults. Brain Cogn 74:358–364.

Amarantini D, Martin L (2004) A method to combine numerical optimization and EMG data for the estimation of joint moments under dynamic conditions. J Biomech 37:1393–1404.

Arányi Z, Rösler KM (2002) Effort-induced mirror movements: a study of transcallosal inhibition in humans. Exp Brain Res 145:76–82.

Armatas CA, Summers JJ (2001) The influence of task characteristics on the intermanual asymmetry of motor overflow. J Clin Exp Neuropsychol Neuropsychol Dev Cogn Sect A 23:557–567.

Armatas CA, Summers JJ, Bradshaw JL (1994) Mirror movements in normal adult subjects. J Clin Exp Neuropsychol 16:405–413.

Armatas CA, Summers JJ, Bradshaw JL (1996) Strength as a factor influencing mirror movements. Hum Mov Sci 15:689–705.

Avila MA, Romaguera F, Oliveira AB, Camargo PR, Salvini TF (2013) Bilateral impairments of shoulder abduction in chronic hemiparesis: electromyographic patterns and isokinetic muscle performance. J Electromyogr Kinesiol 23:712–720.

Baliz Y, Armatas C, Farrow M, Hoy KE, Fitzgerald PB, Bradshaw JL, Georgiou-Karistianis N (2005) The influence of attention and age on the occurrence of mirror movements. J Int Neuropsychol Soc 11:855–862.

Ballard C, Stephens S, Kenny R, Kalaria R, Tovee M, O'Brien J (2003) Profile of neuropsychological deficits in older stroke survivors without dementia. Dement Geriatr Cogn Disord 16:52–56.

Barker-Collo S, Feigin V (2006) The impact of neuropsychological deficits on functional stroke outcomes. Neuropsychol Rev 16:53–64.

Barker-Collo S, Feigin VL, Parag V, Lawes CMM, Senior H (2010) Auckland stroke outcomes study part 2: cognition and functional outcomes 5 years poststroke. Neurology 75:1608–1616.

Bhakta BB, Cozens JA, Chamberlain MA, Bamford JM (2001) Quantifying associated reactions in the paretic arm in stroke and their relationship to spasticity. Clin Rehabil 15:195–206.

Bhakta B, O'Connor R, Cozens J (2008) Associated reactions after stroke: a randomized controlled trial of the effect of botulinum toxin type A. J Rehabil Med 40:36–41.

Bodwell JA, Mahurin RK, Waddle S, Price R, Cramer SC (2003) Age and features of movement influence motor overflow. J Am Geriatr Soc 51:1735–1739.

Brickenkamp R (1962) Test d2: Aufmerksamkeits-Belastungs-Test. Verlag für Psychologie Hogrefe.

Cernacek J (1961) Contralateral motor irradiation-cerebral dominance: its changes in hemiparesis. Arch Neurol 4:165–172.

Chaco J, Blank A (1974) Mirror movements in hemiparesis. Stereotact Funct Neurosurg 36:1–4.

Chang S-H, Durand-Sanchez A, DiTommaso C, Li S (2013) Interlimb interactions during bilateral voluntary elbow flexion tasks in chronic hemiparetic stroke. Physiol Rep 1. Available at: http://physreports.physiology.org/cgi/doi/10.1002/phy2.10 [Accessed May 19, 2017].

Colcombe SJ, Kramer AF, Erickson KI, Scalf P, McAuley E, Cohen NJ, Webb A, Jerome GJ, Marquez DX, Elavsky S (2004)

Cardiovascular fitness, cortical plasticity, and aging. Proc Natl Acad Sci USA 101:3316–3321.

Conners CK (1994) The Conners continuous performance test. Multi-Health Systems, Toronto, Canada.

Cumming TB, Marshall RS, Lazar RM (2013) Stroke, cognitive deficits, and rehabilitation: still an incomplete picture. Int J Stroke 8:38–45.

Dancause N, Ptito A, Levin MF (2002) Error correction strategies for motor behavior after unilateral brain damage: short-term motor learning processes. Neuropsychologia 40:1313–1323.

Doussoulin A, Arancibia M, Saiz J, Silva A, Luengo M, Salazar AP (2017) Recovering functional independence after a stroke through Modified Constraint-Induced Therapy. NeuroRehabilitation 40:243–249.

Ejaz N, Xu J, Branscheidt M, Hertler B, Schambra H, Widmer M, Faria AV, Harran M, Cortes JC, Kim N, Kitago T, Celnik PA, Luft A, Krakauer JW, Diedrichsen J (2017) Finger recruitment patterns during mirror movements suggest two systems for hand recovery after stroke. bioRxiv. Available at: http://biorxiv.org/content/early/2017/04/22/129510 [Accessed May 26, 2017].

Fugl-Meyer AR, Jääskö L, Leyman I, Olsson S, Steglind S (1974) The post-stroke hemiplegic patient. 1. A method for evaluation of physical performance. Scand J Rehabil Med 7:13–31.

Hermens HJ, Freriks B, Disselhorst-Klug C, Rau G (2000) Development of recommendations for SEMG sensors and sensor placement procedures. J Electromyogr Kinesiol 10:361–374.

Hopf HC, Schlegel HJ, Lowitzsch K (1974) Irradiation of voluntary activity to the contralateral side in movements of normal subjects and patients with central motor disturbances. Eur Neurol 12:142–147.

Hoy KE, Fitzgerald PB, Bradshaw JL, Armatas CA, Georgiou-Karistianis N (2004) Investigating the cortical origins of motor overflow. Brain Res Rev 46:315–327.

Hübers A, Orekhov Y, Ziemann U (2008) Interhemispheric motor inhibition: its role in controlling electromyographic mirror activity. Eur J Neurosci 28:364–371.

Hwang S, Li-Chen T, Jeng-Feng Y, Chen Y-C (2005) Electromyographic analyses of global synkinesis in the paretic upper limb after stroke. Phys Ther 85:755–765.

Hyndman D, Ashburn A (2003) People with stroke living in the community: attention deficits, balance, ADL ability and falls. Disabil Rehabil 25:817–822.

Kahn MB, Mentiplay BF, Clark RA, Bower KJ, Williams G (2016) Methods of assessing associated reactions of the upper limb in stroke and traumatic brain injury: a systematic review. Brain Inj 30:252–266.

Kim Y, Kim W-S, Shim JK, Suh DW, Kim T, Yoon B (2015) Difference of motor overflow depending on the impaired or unimpaired hand in stroke patients. Hum Mov Sci 39:154–162.

Koerte I, Eftimov L, Laubender RP, Esslinger O, Schroeder AS, Ertl-Wagner B, Wahllaender-Danek U, Heinen F, Danek A (2010) Mirror movements in healthy humans across the lifespan: effects of development and ageing. Dev Med Child Neurol 52:1106–1112.

Lazarus J-AC (1992) Associated movement in hemiplegia: the effects of force exerted, limb usage and inhibitory training. Arch Phys Med Rehabil 73:1044–1049.

Lazarus J-AC, Todor JI (1991) The role of attention in the regulation of associated movement in children. Dev Med Child Neurol 33:32–39.

Lee D, Lee M, Lee K, Song C (2014) Asymmetric training using virtual reality reflection equipment and the enhancement of upper limb function in stroke patients: a randomized controlled trial. J Stroke Cerebrovasc Dis 23:1319–1326.

Leśniak M, Bak T, Czepiel W, Seniów J, Czonkowska A (2008) Frequency and prognostic value of cognitive disorders in stroke patients. Dement Geriatr Cogn Disord 26:356–363.

Mathias JL, Wheaton P (2007) Changes in attention and information-processing speed following severe traumatic brain injury: a meta-analytic review. Neuropsychology 21:212–223.

Mayston MJ, Harrison LM, Stephens JA (1999) A neurophysiological study of mirror movements in adults and children. Ann Neurol 45:583–594.

McDonald JH (2009) Handbook of biological statistics. Maryland, USA: Sparky House Publishing Baltimore.

Mullick AA, Subramanian SK, Levin MF (2015) Emerging evidence of the association between cognitive deficits and arm motor recovery after stroke: a meta-analysis. Restor Neurol Neurosci 33:389–403.

Nelles G, Cramer SC, Schaechter JD, Kaplan JD, Finklestein SP (1998) Quantitative assessment of mirror movements after stroke. Stroke 29:1182–1187.

Netz J, Lammers T, Hömberg V (1997) Reorganization of motor output in the non-affected hemisphere after stroke. Brain 120:1579–1586.

Nowak DA, Grefkes C, Ameli M, Fink GR (2009) Interhemispheric competition after stroke: brain stimulation to enhance recovery of function of the affected hand. Neurorehabil Neural Repair 23:641–656.

Ohtsuka H, Matsuzawa D, Ishii D, Shimizu E (2015) Longitudinal follow-up of mirror movements after stroke: a case study. Case Rep Neurol Med 2015:1–4.

Potvin JR, Norman RW, McGill SM (1996) Mechanically corrected EMG for the continuous estimation of erector spinae muscle loading during repetitive lifting. Eur J Appl Physiol 74:119–132.

Quaney BM, Boyd LA, McDowd JM, Zahner LH, He Jianghua, Mayo MS, Macko RF (2009) Aerobic exercise improves cognition and motor function poststroke. Neurorehabil Neural Repair 23:879–885.

Rasquin SMC, Lodder J, Ponds RWHM, Winkens I, Jolles J, Verhey FRJ (2004) Cognitive functioning after stroke: a one-year follow-up study. Dement Geriatr Cogn Disord 18:138–144.

Reitan RM (1958) Validity of the Trail Making Test as an indicator of organic brain damage. Percept Mot Skills 8:271–276.

Renner CIE, Woldag H, Atanasova R, Hummelsheim H (2005) Change of facilitation during voluntary bilateral hand activation after stroke. J Neurol Sci 239:25–30.

Ridderikhoff A, Daffertshofer A, Peper C (2005) Mirrored EMG activity during unimanual rhythmic movements. Neurosci Lett 381:228–233.

Roussel M, Martinaud O, Hénon H, Vercelletto M, Bindschadler C, Joseph P-A, Robert P, Labauge P, Godefroy O, on behalf of the GREFEX study group (2016) The behavioral and cognitive executive disorders of stroke: the GREFEX study Brucki S, ed.. PLoS ONE 11. Available at: http://dx.plos.org/10.1371/journal.pone.0147602 [Accessed May 18, 2017].

Sachdev PS, Brodaty H, Valenzuela MJ, Lorentz L, Looi JCL, Wen W, Zagami AS (2004) The neuropsychological profile of vascular cognitive impairment in stroke and TIA patients. Neurology 62:912–919.

Sánchez-Cubillo I, Periáñez JA, Adrover-Roig D, Rodríguez-Sánchez JM, Ríos-Lago M, Tirapu J, Barceló F (2009) Construct validity of the Trail Making Test: role of task-switching, working memory, inhibition/interference control, and visuomotor abilities. J Int Neuropsychol Soc 15:438–450.

Sandford JA, Turner A (2000) Integrated visual and auditory continuous performance test manual. Richmond VA BrainTrain.

Schaefer SY, Haaland KY, Sainburg RL (2007) Ipsilesional motor deficits following stroke reflect hemispheric specializations for movement control. Brain 130:2146–2158.

Seo NJ (2013) Involuntary contralateral upper extremity muscle activation pattern during unilateral pinch grip following stroke. J Hand Ther 26:272–278.

Shinohara M, Keenan KG, Enoka RM (2003) Contralateral activity in a homologous hand muscle during voluntary contractions is greater in old adults. J Appl Physiol 94:966–974.

Spikman JM, Kiers HAL, Deelman BG, van Zomeren AH (2001) Construct validity of concepts of attention in healthy controls and patients with CHI. Brain Cogn 47:446–460.

Stroop JR (1935) Studies of interference in serial verbal reactions. J Exp Psychol 18:643–662.

Sunderland A, Bowers MP, Sluman S-M, Wilcock DJ, Ardron ME (1999) Impaired dexterity of the ipsilateral hand after stroke and the relationship to cognitive deficit. Stroke 30:949–955.

Swinnen SP (2002) Intermanual coordination: from behavioural principles to neural-network interactions. Nat Rev Neurosci 3:348–359.

Tallet J, Barral J, Hauert C-A (2009) Electro-cortical correlates of motor inhibition: a comparison between selective and non-selective stop tasks. Brain Res 1284:68–76.

Tallet J, Albaret J-M, Barral J (2013) Developmental changes in lateralized inhibition of symmetric movements in children with and without Developmental Coordination Disorder. Res Dev Disabil 34:2523–2532.

Uttner I, Mai N, Esslinger O, Danek A (2005) Quantitative evaluation of mirror movements in adults with focal brain lesions. Eur J Neurol 12:964–975.

Vardy AN, Daffertshofer A, Ridderikhoff A, Beek PJ (2007) Differential after-effects of bimanual activity on mirror movements. Neurosci Lett 416:117–122.

Weiller C, Ramsay SC, Wise RJ, Friston KJ, Frackowiak RS (1993) Individual patterns of functional reorganization in the human cerebral cortex after capsular infarction. Ann Neurol 33:181–189.

Wetter S, Poole JL, Haaland KY (2005) Functional implications of ipsilesional motor deficits after unilateral stroke. Arch Phys Med Rehabil 86:776–781.

Yarosh CA, Hoffman DS, Strick PL (2004) Deficits in movements of the wrist ipsilateral to a stroke in hemiparetic subjects. J Neurophysiol 92:3276–3285.

Zakzanis KK, Mraz R, Graham SJ (2005) An fMRI study of the Trail Making Test. Neuropsychologia 43:1878–1886.

Zheng G, Zhou W, Xia R, Tao J, Chen L (2016) Aerobic exercises for cognition rehabilitation following stroke: a systematic review. J Stroke Cerebrovasc Dis 25:2780–2789.

Zimmermann P, Fimm B (2002) A test battery for attentional performance. Appl Neuropsychol Atten Theory Diagn Rehabil:110–151.

Zomeren AH, Brouwer WH (1994) Clinical neuropsychology of attention. USA: Oxford University Press.

SHORT COMMUNICATION

Check for updates

SPASTIC CO-CONTRACTION, RATHER THAN SPASTICITY, IS ASSOCIATED WITH IMPAIRED ACTIVE FUNCTION IN ADULTS WITH ACQUIRED BRAIN INJURY: A PILOT STUDY

Alexandre CHALARD, PT, MS[1,2], David AMARANTINI, PhD[1], Joseph TISSEYRE, MS[1], Philippe MARQUE, MD, PhD[1,3], Jessica TALLET, PhD[1] and David GASQ, MD, PhD[1,4]

From the [1]ToNIC, Toulouse NeuroImaging Center, Université de Toulouse, Inserm, UPS, [2]Ipsen Innovation, Les Ulis, [3]Department of Physical Medicine and Rehabilitation and [4]Department of Functional Physiological Explorations, University Hospital of Toulouse, Hôpital de Rangueil, Toulouse, France

Objective: To elucidate the adverse consequences of spasticity and spastic co-contraction of elbow flexors on motor impairment and upper limb functional limitation.
Design: A pilot case-controlled prospective observational study.
Subjects: Ten brain-injured adults, and 10 healthy controls.
Methods: The co-contraction index was computed from electromyographic recordings of elbow flexors during sub-maximal (25% Maximal Voluntary Contraction) isometric elbow extension. Spasticity was assessed with the Tardieu scale, upper limb limitation using a goniometer during active elbow extension, motor selectivity with the Fugl-Meyer Assessment for the upper limb, and motor function with the Action Research Arm Test.
Results: Greater co-contraction occurred in patients with brain injury compared with controls. In contrast to spasticity, strong associations were found between the co-contraction index, the limitation of active elbow extension, the Fugl-Meyer Assessment, and the Action Research Arm Test.
Conclusion: This pilot study suggests that spastic co-contraction rather than spasticity is an important factor in altered upper limb motricity in subjects with brain injury, leading to abnormal restricting arm movement patterns in subjects with more severe motor impairment. Practical applications directly concern the pre- and post-therapeutic evaluation of treatments aimed at improving motor skills in subjects with brain injury.

Key words: brain injury; hemiplegia; muscle hypertonia; upper extremity.

M uscle overactivity, including spasticity and spastic co-contraction in particular, describes involuntary motor unit recruitment, which occurs in spastic

LAY ABSTRACT

Spasticity and spastic co-contraction are expressions of muscle overactivity that occur in spastic paresis syndrome after a brain injury. The objective of the present pilot study was to improve our understanding of the respective adverse consequences of spasticity and spastic co-contraction on motor disability. In contrary to spasticity, spastic co-contraction is strongly associated with motor impairment in subjects with brain injury. Therapies should be directed toward reducing spastic co-contraction in order to improve motor function.

paresis syndrome after a brain injury, such as stroke or traumatic brain injury (1). Spasticity is defined as an increase in velocity-dependent stretch reflexes, and is clinically manifested by excessive responses to muscle stretch (2). Spasticity is used as a convenient way to assess muscle overactivity during passive and fast muscular stretch. Spastic co-contraction, as assessed by electromyography using the muscle co-contraction index (3), refers to increased antagonist muscle recruitment triggered by the volitional command of agonist muscles in the absence of a phasic stretch (1). It has been well established that spasticity and spastic co-contraction have different underlying physiological mechanisms (1), but their consequences on motor function remain to be confirmed and elucidated. It has been suggested that spastic co-contraction may contribute to limitations in active movement (4). However, to date, the impact of this disabling form of muscle overactivity on motor function in brain-injured adults has been only sparsely and indirectly studied (5). In addition, most treatments aimed at improving upper limb function, such as rehabilitation or botulinum toxin, focus on spasticity as the primary outcome in clinical practice (6).

The aim of the present pilot study was therefore to elucidate the adverse consequences of spasticity and spastic co-contraction of elbow flexors on upper limb motor impairment and disability. The results of this study may have direct application in improving the evaluation and implementation of treatments aimed at improving motor function in subjects with brain injury.

METHODS

Participants

This pilot case-controlled prospective observational study included 10 adults with brain injury (HEMI) and 10 control participants (CONTROL) (see Table I for participants' demographics). The inclusion criteria were: brain injury for at least 6 months caused by an acquired cerebral lesion (single stroke or traumatic brain injury); strength of paretic triceps brachii (rated at least at 3/5 on the Held-Deseilligny Scale, corresponding to extension of the forearm against slight resistance); and no anti-spastic treatment during the 3 previous months. Exclusion criteria were: severe cognitive disorders with limited comprehension of basic instructions; neurodegenerative conditions other than the acquired brain injury; elbow contracture (loss of passive elbow extension or flexion); and upper limb pain during movement. Ethics approval was obtained from the local institutional review board at Paul Sabatier University Hospital (No. 07-0716, Toulouse, France) and written informed consent was obtained from all participants. The study was conducted in accordance with the amended Declaration of Helsinki and conforms to all STROBE guidelines, reporting the required information accordingly.

Materials

Net torque around the elbow joint was recorded at 1 kHz using a Con-Trex MJ calibrated dynamometer (CMV AG, Dubendorf, Switzerland).

The surface electromyographic signal (EMG) was recorded at 1 kHz using Ag–AgCl bipolar electrodes in bipolar configuration with an inter-electrode distance of 20 mm,, using an MP150 system (Biopac Systems Inc., Goleta, CA, USA). The reference electrode was placed on the left ulnar head. Biceps brachii and brachioradialis were selected as the elbow flexors acting as antagonist muscles during elbow extension.

Recordings were made on the non-dominant side in the CONTROL group and on the paretic side in HEMI group.

Torque and EMG data were synchronized automatically using a rectangular triggering pulse signal and analysed offline.

Procedure

The experimental procedure comprised 2 steps.

First step. To perform the following clinical assessment (7): spasticity of elbow flexors, limitation to active elbow extension,
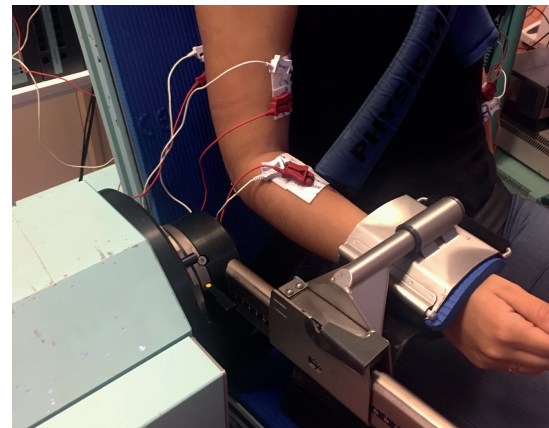
Fig. 1. Illustration of the arm and forearm positions used to perform torque and electromyographic recordings during isometric elbow extension on the calibrated dynamometer.

motor selectivity and motor function were assessed respectively, using the Tardieu scale, a goniometer during repetitive and dynamic voluntary elbow extensions at a preferred rate, the upper limb motor section of the Fugl-Meyer Assessment scale, and the Action Research Arm Test (Table I). Maximal net elbow extension torque value was taken as a functional marker of triceps brachii paresis, the Fugl-Meyer score as a motor selectivity assessment, and the Action Research Arm Test as a motor function assessment.

Second step. Participants were seated on the dynamometer chair with their upper body strapped firmly, the upper arm positioned along the trunk, and the elbow flexed at 90° (Fig. 1). The participants exerted 3 isometric maximal voluntary contractions of the elbow in flexion and in extension for a duration of 5 s, with 1 min rest between each contraction and 3 min rest between flexion and extension contractions. After collection of maximal voluntary contraction data, participants performed 2 sets of 5-s elbow isometric extension sub-maximal contractions while receiving visual feedback on their actual torque in relation to a target torque. Each set included 6 contractions at 25% Maximal Voluntary Contraction (MVC), corresponding to a level of force required for daily activities (8). The time between each contraction was 30 s; each set was separated by a 3-min rest period to minimize fatigue.

Table I. Participants' demographics

Participants	Sex	Age, year	Pathology	Side and location of cerebral injury	Disease course, month	Fugl-Meyer Assessment score (upper limb/66)	Action Research Arm Test (/57)
Control Group (*n*=10)	6 Males 4 Females	30 (15)*	–	–	–	–	–
Brain Injured Group							
1	Female	47	Ischaemic stroke	Left, cortical & subcortical	48	55	39
2	Male	66	Haemorrhagic stroke	Left, thalamic	14	51	36
3	Male	59	Ischaemic stroke	Left, latero-bulbar	27	59	55
4	Male	52	Ischaemic stroke	Left, subcortical	43	48	18
5	Male	64	Ischaemic stroke	Left, cortical & subcortical	39	60	57
6	Male	71	Ischaemic stroke	Right, cortical & subcortical	60	44	23
7	Male	33	Ischaemic stroke	Right, cortical & subcortical	146	54	51
8	Male	41	Traumatic brain injury	Left, cortical & subcortical	132	46	29
9	Male	57	Traumatic brain injury	Right, cortical & subcortical	360	18	0
10	Male	63	Haemorrhagic stroke	Left, subcortical	60	32	0

*Mean (standard deviation (SD)), indicates a significant difference in age between HEMI and CONTROL groups (*p* < 0.05).

Table II. Co-contraction index, net elbow extension torque during maximal voluntary contraction and clinical characteristics

Participants	Co-contraction index during sub-maximal elbow extension (%)	Net elbow extension torque (Nm) during maximal voluntary contraction	Limitation of active elbow extension (degree)	Elbow flexors spasticity (Tardieu scale, 0–4)
Control group (*n* = 10)				
Median (IQR)	1.7 (0.9)	27.4 (18.9)	–	–
Brain-injured group				
1	4.5	16.8	0	1
2	2.3	18.2	0	2
3	2.7	20.3	0	2
4	6.9	17.2	20	1
5	3.9	51.9	0	0
6	4.7	21.6	0	2
7	2.9	23.6	0	2
8	1.8	6.8	0	3
9	48.3	4.2	45	2
10	13.1	32.7	30	0
Median (IQR)	4.2 (2.7)*	19.3 (6.8)*	0 (20)	2 (1)

*Indicates a significant difference between HEMI and CONTROL groups ($p < 0.05$).
IQR: interquartile range.

Data processing

Net torque was low-pass filtered at 100 Hz with a 6th-order zero-lag Butterworth filter. EMG data were 10–400-Hz band-pass filtered (4th-order zero-lag Butterworth filter), full-wave rectified, and smoothed at 9 Hz to obtain the linear envelopes. The co-contraction index was determined as the ratio (expressed in percentage) between the root mean square value of the elbow flexors EMG envelopes during the sub-maximal elbow extensions and the root mean square of the same muscle during the highest maximal voluntary elbow flexion contraction (9).

Statistical analysis

Non-parametric analysis using Wilcoxon rank-sum test was performed to compare the co-contraction index and the maximal net elbow extension torque between HEMI and CONTROL groups.

Non-parametric Spearman's correlations (r_s) were performed to investigate the relationship between co-contraction index, elbow-flexor spasticity, maximal net elbow extension torque with: (*i*) limitation to active elbow extension, (*ii*) elbow-flexor spasticity, (*iii*) Fugl-Meyer Assessment score for the upper limb, and (*iiii*) Action Research Arm Test. It is notable that that there was a significant difference in age between the HEMI and CONTROL groups (Table I). However, preliminary analysis of the data showed a lack of any correlation with age ($p > 0.05$), enabling the results to be interpreted independently of age.

RESULTS

A higher co-contraction index occurred in the HEMI group compared with the CONTROL group ($w_{19} = 3.4$,

$p < 0.01$), with a mean difference (SD) of 7.6±12.9%. Lower net elbow extension torque during maximal voluntary contraction was found in the HEMI compared with the CONTROL group ($w_{19} = -2.34$, $p < 0.05$), with a mean difference (SD) of 17.6±17 Nm. Results of the Spearman's correlations are shown in Table III.

DISCUSSION

This pilot study aimed to elucidate the consequences of spasticity and spastic co-contraction of elbow flexors on limitation of active elbow extension in adults with brain injury. A strong association was found between the co-contraction index and (*i*) the limitation of active elbow extension, (*ii*) the Fugl-Meyer Assessment score, and (*iii*) the score on Action Research Arm Test. Conversely, no significant correlation was found between spasticity and any of the variables cited above.

These results are thus the first to show that spastic co-contraction primarily contributes to a deficit in active elbow extension in adults with brain injury, which occurs even in the absence of spasticity (see, for example, Table II, HEMI participants 5 and 10). These findings confirm the absence of an association between spasticity and spastic co-contraction, supporting the idea that they refer to different forms of overactivity with different underlying physiological mechanisms

Table III. Spearman correlations (95% confidence interval) for HEMI participants between co-contraction index, net elbow extension torque during maximal voluntary contraction and clinical variables

	Limitation of active elbow extension	Elbow flexors spasticity	Fugl-Meyer Assessment score (upper limb)	Action Research Arm Test
Co-contraction index during the sub-maximal elbow extension	0.88** [0.59, 0.97]	0.01 [–0.59, 0.60]	–0.86** [–0.96, –0.53]	–0.66* [–0.90, –0.09]
Elbow flexors spasticity	–0.23 [–0.72, 0.42]	–	0.10 [–0.53, 0.66]	0.06 [–0.63, 0.56]
Net elbow extension torque during maximal voluntary contraction	–0.26 [–0.74, 0.40]	–0.49 [–0.92, –0.08]	0.44 [–0.21, 0.82]	0.41 [–0.19, 0.80]

*Indicates a significant correlation at $p < 0.05$. **Indicates a significant correlation at $p < 0.01$.

(1). Most importantly, in agreement with a suggestion made in a previous report (10), these results unequivocally establish that spasticity and spastic co-contraction have different functional repercussions with regards to impaired motor function in adults with brain injury.

It is well known that selective muscle activation is necessary for skilled and coordinated upper limb movements, which implies concomitant activation of agonists and relaxation of antagonists. Lesions that damage the corticospinal pathways, such as stroke or traumatic brain injury, cause long-lasting impairment of the ability to produce selective patterns of EMG activity (11). However, it has been shown that, during rehabilitation, the decrease in co-contraction index is correlated with the improvement in Fugl-Meyer score among post-stroke subjects (12). In agreement with a previous study (4), our finding of a strong association between the co-contraction index and Fugl-Meyer Assessment score thus highlights the importance of impaired motor selectivity as a mechanism that contributes to greater spastic co-contraction.

The adverse consequence of the presence of spastic co-contraction on upper limb motor impairment is further supported by the significant association between the co-contraction index and the score on Action Research Arm Test, taken to reflect upper limb functional limitation. Furthermore, by analysing EMG-based assessment of spastic co-contraction in patients with a wide range of motor impairment, our results highlight that the more severe the motor impairment, the greater the co-contraction index.

These results also failed to show an association between the net elbow extension torque during maximal voluntary contraction, taken as a functional marker of triceps brachii paresis, and either the limitation of active elbow extension, the score of Fugl-Meyer Assessment or of the Action Research Arm Test. These findings indicate that motor weakness is not a primary factor limiting active elbow extension, and lead to the conclusion that non-selective motricity and function impairment are not directly linked to motor weakness.

Taken together, the above results demonstrate the detrimental impact of spastic co-contraction on upper limb motor function, leading to abnormal restricting arm movement patterns, especially in subjects with more severe motor impairment.

Despite strong evidence of improvement in spasticity induced by botulinum toxin treatment, few studies have shown effectiveness in improving active function and active movement (13, 14). A limitation that may explain this lack of efficacy in active function is the use of spasticity, as assessed during passive stretching, as a marker of muscle overactivity during movement (15). In contrast, the change in spastic co-contraction after injection of botulinum toxin has been poorly studied. From a clinical perspective, these results are in line with the Subcommittee of the American Academy of Neurology (13), which recommend the use and development of a method and outcome regarding motor function and active movement. We support the requirement to report active range of motion as an outcome of muscle overactivity treatments (7), and the use of EMG-based quantification of spastic co-contraction as a relevant tool for providing effective interventions related to altered recruitment of antagonist muscles and limitation of active movement.

Study limitations

Although a limitation of this pilot study is the small sample size, significant findings were made relative to the link between spastic co-contraction and clinical scores. Any generalization of these results, however, should be viewed with caution, especially because hemiparetic subjects had different aetiologies of brain injury (i.e. stroke and traumatic brain injury) and that little is known about the influence of the type of brain injury on spastic co-contraction.

This pilot study assessed the co-contraction index during submaximal isometric contraction, while spastic co-contraction is sensitive to stretch (1). Thus, future research should investigate co-contraction during active elbow extension.

Conclusion and clinical implications

The results of this pilot study suggest that spastic co-contraction alters upper limb function in subjects with hemiparetic brain injury. These findings may partially explain the lack of data concerning the efficacy of treatments, such as botulinum toxin to improve upper limb function (6, 13, 14). Although measurement of spasticity is usually performed to assess muscle overactivity, these results highlight the importance of considering spastic co-contraction to assess active motor function, and support further studies on changes in spastic co-contraction after injection of botulinum toxin, in connection with the improvement in active function. Practical applications arising from this work are to improve the assessment of factors that restrict movement and implementation of treatments aimed at improving motor function in subjects with brain injury.

REFERENCES

1. Gracies J-M. Pathophysiology of spastic paresis. II: emergence of muscle overactivity. Muscle Nerve 2005; 31: 552–571.
2. Lance JW. The control of muscle tone, reflexes, and movement: Robert Wartenberg Lecture. Neurology 1980; 30: 1303–1313.
3. Kellis E, Arabatzi F, Papadopoulos C. Muscle co-activation around the knee in drop jumping using the co-contraction index. J Electromyogr Kinesiol 2003; 13: 229–238.
4. Chae J, Yang G, Park BK, Labatia I. Muscle weakness and cocontraction in upper limb hemiparesis: relationship to motor impairment and physical disability. Neurorehabil Neural Repair 2002; 16: 241–248.
5. Silva CC, Silva A, Sousa A, Pinheiro AR, Bourlinova C, Silva A, et al. Co-activation of upper limb muscles during reaching in post-stroke subjects: an analysis of the contralesional and ipsilesional limbs. J Electromyogr Kinesiol 2014; 24: 731–738.
6. Wissel J, Ward AB, Erztgaard P, Bensmail D, Hecht MJ, Lejeune TM, et al. European consensus table on the use of botulinum toxin type A in adult spasticity. J Rehabil Med 2009; 41: 13–25.
7. Yelnik AP, Simon O, Parratte B, Gracies JM. How to clinically assess and treat muscle overactivity in spastic paresis. J Rehabil Med 2010; 42: 801–807.
8. Marshall MM, Armstrong TJ. Observational assessment of forceful exertion and the perceived force demands of daily activities. J Occup Rehabil 2004; 14: 281–294.
9. Vinti M, Couillandre A, Hausselle J, Bayle N, Primerano A, Merlo A, et al. Influence of effort intensity and gastrocnemius stretch on co-contraction and torque production in the healthy and paretic ankle. Clin Neurophysiol 2013; 124: 528–535.
10. Sarcher A, Raison M, Ballaz L, Lemay M, Leboeuf F, Trudel K, et al. Impact of muscle activation on ranges of motion during active elbow movement in children with spastic hemiplegic cerebral palsy. Clin Biomech 2015; 30: 86–94.
11. Schieber MH, Lang CE, Reilly KT, McNulty P, Sirigu A. Selective activation of human finger muscles after stroke or amputation. Adv Exp Med Biol 2009; 629: 559–575.
12. Hu X, Tong KY, Song R, Tsang VS, Leung PO, Li L. Variation of muscle coactivation patterns in chronic stroke during robot-assisted elbow training. Arch Phys Med Rehabil 2007; 88: 1022–1029.
13. Simpson DM, Gracies J-M, Graham K, Hallett M, Miyasaki J, Naumann M, et al. Assessment: botulinum neurotoxin for the treatment of spasticity (an evidence-based review). Neurology 2009; 73: 736–747.
14. Foley N, Pereira S, Salter K, Fernandez MM, Speechley M, Sequeira K, et al. Treatment with botulinum toxin improves upper-extremity function post stroke: a systematic review and meta-analysis. Arch Phys Med Rehabil 2013; 94: 977–989.
15. Sheean G, Lannin NA, Turner-Stokes L, Rawicki B, Snow BJ, Cerebral Palsy Institute. Botulinum toxin assessment, intervention and after-care for upper limb hypertonicity in adults: international consensus statement. Eur J Neurol 2010; 17: 74–93.

A novel method to generalize time-frequency coherence analysis between EEG or EMG signals during repetitive trials with high intra-subject variability in duration

Maxime Fauvet[1], Sylvain Cremoux[2,3], Alexandre Chalard[1], Joseph Tisseyre[1], David Gasq[1,4,‡], David Amarantini[1,‡,*]

Abstract – **Time-frequency coherence analysis between EEG and EMG signals represents a valuable tool to gain insight into neural mechanisms underlying motor control. However, for self-paced movements, the variability of inter-trial duration limits its proper use. To overcome this obstacle, we propose a time-normalizing approach and test it on both simulated and experimental data recorded during elbow extension movements performed by a post-stroke subject. Results show that the proposed time-normalization improves both the consistency and the accuracy of time-frequency coherence calculation, detection and quantification. The proposed time-normalization overcomes a major limitation to generalization of coherence analysis and can be suggested as an essential step to perform for coherence in presence of high intra-subject variability in duration.**

I. INTRODUCTION

For more than twenty years, coherence analysis [1,2] is used to study synchrony between brain and muscle activities (corticomuscular coherence [3–6]), between muscle activities (intermuscular coherence [7–9]) or within the brain (corticocortical coherence [10,11]). Coherence in the alpha ([8-12] Hz) and beta ([13-32] Hz) frequency ranges is thought to reflect underlying mechanisms of long range communication through neural synchronization [12,13]. According to recent neuroscience studies (e.g., [14]), coherence can be considered as a powerful tool to investigate neural mechanisms responsible for motor control.

Appropriate calculation, detection and quantification of coherence require concatenation of EEG or EMG data recorded during either repetitive trials or single-trial segments with the same number of observation recorded at regularly spaced time points [15]. This methodological requirement can be easily met with consistent data during calibrated isometric contractions with a fixed duration [16,17]. However, it is a major obstacle to generalization of the use of coherence during experimental tasks with high inter-trial variability in duration, such as during dynamic contractions performed by participants with altered motor function.

1: ToNIC, Toulouse NeuroImaging Center, Université de Toulouse, Inserm, UPS, Toulouse, France
2: LAMIH, UMR CNRS 8201, Université Polytechnique des Hauts-de-France, Valenciennes, France
3: CerCo, Centre de Recherche Cerveau et Cognition, Université de Toulouse, CNRS, UPS, Toulouse, France
4: Department of Functional Physiological Explorations, University Hospital of Toulouse, Hôpital Rangueil, Toulouse, France

‡Co-last authors (both authors contributed equally to this work)
*Corresponding author e-mail address: david.amarantini@inserm.fr

The present study aims to overcome this limitation and introduces a novel data preprocessing method to properly calculate coherence between EEG and EMG signals measured during repetitive trials of different durations. Firstly, a simulation analysis was performed to investigate the advantages and abilities of the proposed method to achieve this objective. Secondly, the method was applied to experimental EEG and EMG data to illustrate its performance during elbow extension movements in one post-stroke subject.

II. METHODS

A. Simulation data

Two paired datasets of thirty independent time series with zero mean and a -5dB signal-to-noise ratio with sampling rate 1 kHz were simulated. In each signal, a central segment of interest contained 10 and 30 Hz frequency components to respectively represent physiological α and β rhythms. The duration of the segment of interest was ranging between 1.35 and 4.78 s, randomly drawn from a normal distribution with mean and variance coming from sample data in elbow flexion-extension movements in post-stroke subjects [18]. The segment of interest was surrounded by two segments containing pure Gaussian white noise. The duration of the first segment was randomly chosen between 1 and 2.1 s. The duration of the last segment was randomly chosen such as the whole signal duration does not exceed the maximum duration of the segment of interest plus 2.1s. An illustration of simulated signal is shown on Fig. 1 (left column).

'Aligned' signals were obtained by settling the 'raw' signals 1 s prior to the segment of interest. The duration of the signal with the longest segment of interest plus one second (1000 or 1024 points in experimental data depending on the sampling frequency) was used as a reference. Gaussian white noise was added at the end of aligned signal of each trial to match the reference duration (see Fig. 1, middle column).

The 'time-normalized' signals were then obtained by upsampling 'aligned' signals in order to deal with the different durations of the segment of interest across trials. Upsampling was performed using the Matlab (The MathWorks Inc., Natick, MA, USA) function *resample*, according to the longest segment of interest in the dataset (i.e., representing the longest movement in experimental data). The resampling rate was established for each trial such as the normalized duration of the segment of interest was of equal length among all trials (Fig. 1, right column) and the duration was expressed in percentage terms. Each trial was
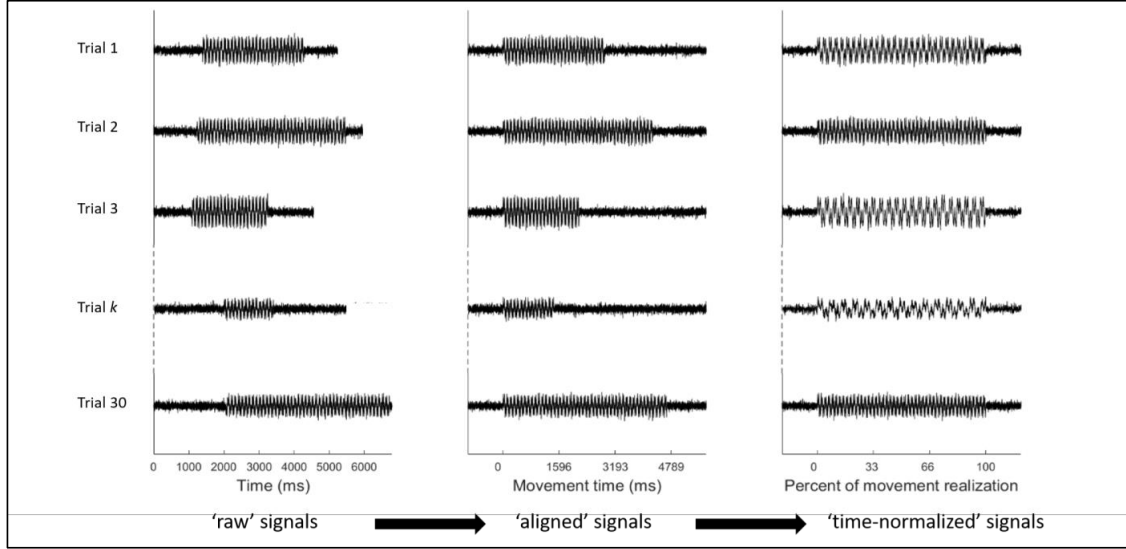
Figure 1. Steps taken to process simulated data and make them fit the coherence computation requirements. Left column: raw simulated signals at 1 KHz, minimal and maximal length of the segment of interest are respectively 1353 points and 4789 points. Middle column: raw signals aligned 1s prior to second segment onset. Right column: time-normalized signals with a fixed 7099 points length and individual sampling rate ranging from 1 kHz to 3817 Hz

first truncated to correct length according to the resampling rate; the segment of interest was preceded and followed by a duration of x_i from flanking segments computed with:

$$x_i = \frac{\frac{l_{1,i}}{l_{2,i}}(f_s + l_{2,i}) - l_{1,i}}{2} \qquad (1)$$

where $l_{1,i}$ is the length of the segment of interest, $l_{2,i}$ is the maximal length of segment of interest in the dataset and f_s is the original sample frequency. These two signal parts surrounding the segment of interest were then up-sampled at the same rate as the latter.

B. Experimental data

A post-stroke subject participated in the experiment and was seated in front of a table, the elbows 90° flexed. He was asked to perform two blocks of ten elbow extensions for each arm, in turn. A 1 min rest period was allowed after every block. The inter-trial movement duration (range: 1956 - 4393 ms) was variable enough to assess the robustness of the preprocessing steps for the coherence computation.

Activity of the brachial triceps was recorded at 1 kHz by a surface EMG system (Biopac, MP150 model, Acqknowledge, Biopac Systems Inc., Santa Barbara, USA). EEG signals were recorded at 1024 Hz by a 64-channel ActiveTwo System (Biosemi, Amsterdam, The Netherlands). Upper limbs movement kinematics was recorded at 250 Hz by eight infrared cameras (Optitrack, Natural Point, Corvallis, Oregon, USA).

Kinematic data were low-pass filtered at 6 Hz and elbow angular movement detection threshold was set to 0.01 °/s to assess movement onset and offset. EMG and EEG data were band-pass filtered (3-100 Hz). Continuous data were then epoched to trials from -1 s to +1 s relative to the movement onset and offset. Filtered EEG and EMG signals were then *time-normalized* according to the method described above for the simulated data (see: II.*A*).

C. Coherence analysis

For both simulated and experimental data, coherence was calculated, detected and quantified in the time-frequency domain from the respective above signals with the WaveCrossSpec software for wavelet coherence analysis [15]. For experimental data, corticomuscular coherence was computed between the right or left triceps brachii and contralateral C3 or C4 electrode, depending on the movement side. In WaveCrossSpec, the parameters 'nvoice', 'J1' and 'wavenumber' were respectively set to 7, 30 and 10 to yield accurate identification of oscillatory activity in the [0.0015:0.2232:47.9840] Hz frequency range. Magnitude-squared coherence was computed with:

$$R^2_{EEG,EMG} = \frac{|S_{EEG,EMG}|^2}{S_{EEG}S_{EMG}} \qquad (2)$$

where $S_{EEG,EMG}$ is the wavelet cross-spectrum between EEG and EMG signals and S_{EEG} and S_{EMG} are wavelet auto-spectrum of EEG and EMG. The magnitude-squared coherence was measured as the mean and its standard deviation in α ([8-12] Hz) and high β ([28-32] Hz) frequency bands over the segment of interest, excluding null values (i.e. non-significant coherence values). Coherence was quantified from the first movement onset to the last movement offset for 'raw' signals, from the movement onset to the last movement offset for 'aligned' signals and from 0 to 100% for 'time-normalized' signals.
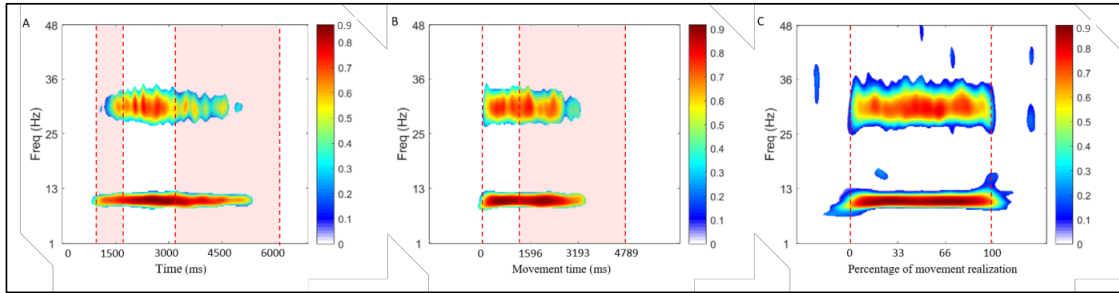
Figure 2. Time-frequency maps of magnitude-squared coherence of simulated signals. Non-significant values are whitened. Coherence computed from raw signals (A), aligned signals (B) and time-normalized signals (C). Red shaded area represent the range of movement onset and offset variability. Movement onset and offset are delimited by doted red lines in middle and right columns.

III. RESULTS AND DISCUSSION

A. Simulated data

Fig. 2 depicts coherence detection between two known simulated signals according to the preprocessing steps applied. Although significant coherence is detected for all three preprocessing steps, this detection is less accurate for 'raw' and 'aligned' signals than for 'time-normalized' signals. Mean±SD values of coherence magnitude are higher with 'time-normalized' signals (0.86 ± 0.06 and 0.72 ± 0.11 for α and β, respectively) than with 'aligned' (0.81 ± 0.18 and 0.66 ± 021 for α and β, respectively) or 'raw' signals (0.68 ± 0.22 and 0.52 ± 0.29 for α and β, respectively). Concurrently, the variance of magnitude of coherence is decreased with 'time-normalized' signals. For 'raw' signals, the magnitude of significant coherence areas is not consistent over time and the variability is high, especially at 30 Hz. For 'aligned' signals, the coherence detection is improved at the beginning of the segment of interest; as time goes on and number of controlled-frequency signals decreases, the accuracy of coherence detection decreases. For 'time-normalized' signals, coherence detection is improved over the whole signal length. The magnitude of coherence in the regions of interest are close to the maximum (Fig. 2A and 2B), meaning that the proposed method for time-normalizing signals does not alter the frequency contents while variability decreases, allowing a nearly optimal coherence computation. Even if false-positive points are detected with low magnitude values because of the strength of correlation between the two signals, the proposed time-normalization approach provides accurate coherence computation even in presence of high intra-subject variability in trials duration.
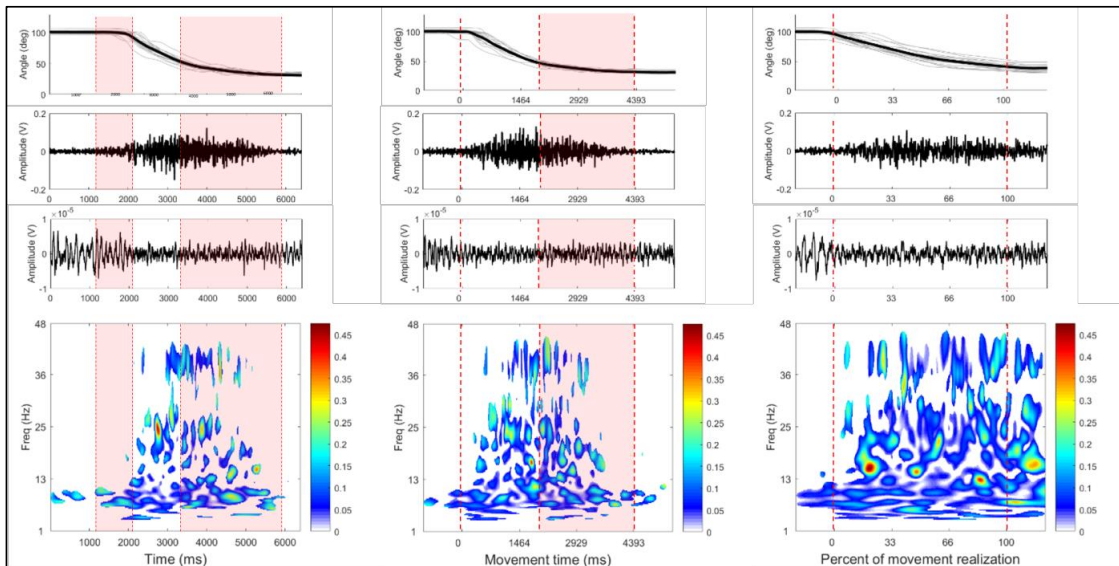
Figure 3. Processing steps from the post-stroke subject data corresponding to 17 trials. Left column is the raw signals dataset, middle is the aligned signals dataset and right column is the normalized signals dataset. Top row is the movement kinematics (mean in black and individual trials in grey), second row is the mean EMG signal, third row the mean EEG signal and bottom row is the magnitude-squared coherence maps. The varying movement onset and offset positions in raw and aligned signals are within the red shaded area. Movement onset and offset are delimited by doted red lines in middle and right columns.

Consequently, coherence detection and quantification is more accurate with 'time-normalized' signals obtained using the proposed method.

B. Experimental data

Fig. 3 presents corticomuscular coherence results obtained according to the proposed procedure using EEG and EMG data from the post-stroke subject performing elbow extension movements at spontaneous rate. The magnitude±SD of coherence in α band is 0.09±0.06 for 'raw' signals, 0.07±0.05 for 'aligned' signals and 0.05±0.03 for 'time-normalized' signals. Coherence in β band is null for 'raw' signals whereas it is 0.18±0.05 for 'aligned' signals and 0.16±0.04 for 'time-normalized' signals. As for simulated data, coherence detection is less important for 'raw' signals and is poorly consistent over time for both 'raw' and 'aligned' signals. It is remarkable to see that coherence variability decreases after each processing step applied to the data. Previous corticomuscular coherence studies involving post-stroke subjects [19]–[21] showed a modulation of coherence magnitude and a broader distribution of coherence in the β band. The lack of coherence detection within this band for 'raw' signals supports the need of the proposed time-normalization processing steps for a reliable and accurate coherence calculation in presence of variable inter-trial duration.

IV. CONCLUSION

Results from both simulated and experimental data show that the proposed time-normalization processing steps is a necessary and effective method for time-frequency coherence detection and quantification in presence of high inter-trial variability in duration. The proposed method overcomes a major limitation to generalization of time-frequency coherence analysis in various protocols involving repetitive trials of different durations, and also provides the advantage that it can be used either for corticocortical, corticomuscular or intermuscular coherence analysis.

REFERENCES

[1] D. M. Halliday, B. A. Conway, S. F. Farmer, and J. R. Rosenberg, "Using electroencephalography to study functional coupling between cortical activity and electromyograms during voluntary contractions in humans," *Neurosci. Lett.*, vol. 241, no. 1, pp. 5–8, Jan. 1998.

[2] T. Mima, J. Steger, A. E. Schulman, C. Gerloff, and M. Hallett, "Electroencephalographic measurement of motor cortex control of muscle activity in humans," *Clin. Neurophysiol.*, vol. 111, no. 2, pp. 326–337, Feb. 2000.

[3] R. Kristeva, L. Patino, and W. Omlor, "Beta-range cortical motor spectral power and corticomuscular coherence as a mechanism for effective corticospinal interaction during steady-state motor output," *NeuroImage*, vol. 36, no. 3, pp. 785–792, Jul. 2007.

[4] S. Cremoux, J. Tallet, F. D. Maso, E. Berton, and D. Amarantini, "Impaired corticomuscular coherence during isometric elbow flexion contractions in humans with cervical spinal cord injury," *Eur. J. Neurosci.*, vol. 46, no. 4, pp. 1991–2000, Aug. 2017.

[5] F. Dal Maso, M. Longcamp, S. Cremoux, and D. Amarantini, "Effect of training status on beta-range corticomuscular coherence in agonist vs. antagonist muscles during isometric knee contractions," *Exp. Brain Res.*, vol. 235, no. 10, pp. 3023–3031, Oct. 2017.

[6] G. Desmyttere, E. Mathieu, M. Begon, E. Simoneau-Buessinger, and S. Cremoux, "Effect of the phase of force production on corticomuscular coherence with agonist and antagonist muscles," *Eur. J. Neurosci.*, Aug. 2018.

[7] S. F. Farmer *et al.*, "Changes in EMG coherence between long and short thumb abductor muscles during human development," *J. Physiol.*, vol. 579, no. 2, pp. 389–402, Mar. 2007.

[8] C. Charissou, D. Amarantini, R. Baurès, E. Berton, and L. Vigouroux, "Effects of hand configuration on muscle force coordination, co-contraction and concomitant intermuscular coupling during maximal isometric flexion of the fingers," *Eur. J. Appl. Physiol.*, vol. 117, no. 11, pp. 2309–2320, Nov. 2017.

[9] E. Mathieu, G. Desmyttere, E. Simoneau, and S. Crémoux, "Modulation of intermuscular coherence between homologous muscles reflects different common neural drive regulating bilateral contractions," *Neurophysiol. Clin.*, vol. 48, no. 4, p. 227, Sep. 2018.

[10] L. M. Rueda-Delgado, E. Solesio-Jofre, D. J. Serrien, D. Mantini, A. Daffertshofer, and S. P. Swinnen, "Understanding bimanual coordination across small time scales from an electrophysiological perspective," *Neurosci. Biobehav. Rev.*, vol. 47, pp. 614–635, Nov. 2014.

[11] M. Blais, D. Amarantini, J. Albaret, Y. Chaix, and J. Tallet, "Atypical inter-hemispheric communication correlates with altered motor inhibition during learning of a new bimanual coordination pattern in developmental coordination disorder," *Dev. Sci.*, 2017.

[12] T. Mima, N. Simpkins, T. Oluwatimilehin, and M. Hallett, "Force level modulates human cortical oscillatory activities," *Neurosci. Lett.*, vol. 275, no. 2, pp. 77–80, Nov. 1999.

[13] F. Negro and D. Farina, "Linear transmission of cortical oscillations to the neural drive to muscles is mediated by common projections to populations of motoneurons in humans," *J. Physiol.*, vol. 589, no. 3, pp. 629–637, Feb. 2011.

[14] T. W. Boonstra, B. C. M. van Wijk, P. Praamstra, and A. Daffertshofer, "Corticomuscular and bilateral EMG coherence reflect distinct aspects of neural synchronization," *Neurosci. Lett.*, vol. 463, no. 1, pp. 17–21, Sep. 2009.

[15] J. Bigot, M. Longcamp, F. Dal Maso, and D. Amarantini, "A new statistical test based on the wavelet cross-spectrum to detect time-frequency dependence between non-stationary signals: application to the analysis of cortico-muscular interactions," *Neuroimage*, vol. 55, no. 4, pp. 1504–18, Apr. 2011.

[16] J. Gross, P. A. Tass, S. Salenius, R. Hari, H.-J. Freund, and A. Schnitzler, "Cortico-muscular synchronization during isometric muscle contraction in humans as revealed by magnetoencephalography," *J. Physiol.*, vol. 527, no. Pt 3, pp. 623–631, Sep. 2000.

[17] R. Kristeva-Feige, C. Fritsch, J. Timmer, and C.-H. Lücking, "Effects of attention and precision of exerted force on beta range EEG-EMG synchronization during a maintained motor contraction task," *Clin. Neurophysiol.*, vol. 113, no. 1, pp. 124–131, Jan. 2002.

[18] A. Chalard, D. Amarantini, M. Belle, E. Montane, and D. Gasq, "Impact of different EMG normalisation methods on muscle activations and cocontraction index in adults with chronic post-stroke hemiparesis," *Ann. Phys. Rehabil. Med.*, vol. 61, p. e444, Jul. 2018.

[19] Mima Tatsuya, Toma Keiichiro, Koshy Benjamin, and Hallett Mark, "Coherence Between Cortical and Muscular Activities After Subcortical Stroke," *Stroke*, vol. 32, no. 11, pp. 2597–2601, Nov. 2001.

[20] C. Braun, M. Staudt, C. Schmitt, H. Preissl, N. Birbaumer, and C. Gerloff, "Crossed cortico-spinal motor control after capsular stroke," *Eur. J. Neurosci.*, vol. 25, no. 9, pp. 2935–2945, 2007.

[21] Y. Fang *et al.*, "Functional corticomuscular connection during reaching is weakened following stroke," *Clin. Neurophysiol.*, vol. 120, no. 5, pp. 994–1002, May 2009.

Références bibliographiques

IX.   Références bibliographiques [15]

Aagaard, P., Simonsen, E. B., Andersen, J. L., Magnusson, P., & Dyhre-Poulsen, P. (2002). Increased rate of force development and neural drive of human skeletal muscle following resistance training. *J Appl Physiol*, 93(4), 1318-1326.

Aagaard, P., Simonsen, E. B., Andersen, J. L., Magnusson, S. P., Bojsen-Moller, F., & Dyhre-Poulsen, P. (2000). Antagonist muscle coactivation during isokinetic knee extension. *Scandinavian Journal of Medicine & Science in Sports*, 10(2), 58-67.

Abbruzzese, G., Morena, M., Spadavecchia, L., & Schieppati, M. (1994). Response of arm flexor muscles to magnetic and electrical brain stimulation during shortening and lengthening tasks in man. *The Journal of Physiology*, 481(2), 499-507.

Addamo, P. K., Farrow, M., Bradshaw, J. L., Moss, S., & Georgiou-Karistianis, N. (2010). The effect of attending to motor overflow on its voluntary inhibition in young and older adults. *Brain and Cognition*, 74(3), 358-364.

Addamo, P. K., Farrow, M., Hoy, K. E., Bradshaw, J. L., & Georgiou-Karistianis, N. (2007). The effects of age and attention on motor overflow production--A review. *Brain Research Reviews*, 54(1), 189-204.

Adrian, E. D., & Moruzzi, G. (1939). Impulses in the pyramidal tract. *The Journal of Physiology*, 97(2), 153-199.

Alkjaer, T., Simonsen, E. B., Magnusson, S. P., Aagaard, H., & Dyhre-Poulsen, P. (2002). Differences in the movement pattern of a forward lunge in two types of anterior cruciate ligament deficient patients: copers and non-copers. *Clinical Biomechanics*, 17(8), 586-593.

Allard, P., & Blanchi, J. P. (1996). *Analyse du mouvement humain par la biomécanique*. Ville Mont-Royal, Québec, Canada: Décarie Éditeur.

Allard, P., Duhaime, M., Thiry, P. S., & Drouin, G. (1981). Use of gait stimulation in the evaluation of a spring-loaded knee joint orthosis for Duchenne muscular dystrophy patients. *Med Biol Eng Comput*, 19(2), 165-170.

Allen, D. P., & MacKinnon, C. D. (2010). Time-frequency analysis of movement-related spectral power in EEG during repetitive movements: a comparison of methods. *Journal of Neuroscience Methods*, 186(1), 107-115.

Amarantini, D. (2003). *Estimation des efforts musculaires à partir de données périphériques : application à l'analyse de la coordination pluri-articulaire.* Université Joseph-Fourier Grenoble I.

Amarantini, D., Martin, L., & Blanchi, J. P. (1999). Biomechanical analysis of inter-joint coordination. *Archives of Physiology and Biochemistry*, 107(Suppl.), 93-93.

Amarantini, David, & Bru, B. (2015). Training-related changes in the EMG-moment

---

[15] A l'exception des références bibliographiques des publications jointes à ce mémoire dans le format de la revue.

relationship during isometric contractions: Further evidence of improved control of muscle activation in strength-trained men? *Journal of Electromyography and Kinesiology*, 25(4), 697-702.

Amarantini, David, & Martin, L. (2004). A method to combine numerical optimization and EMG data for the estimation of joint moments under dynamic conditions. *Journal of Biomechanics*, 37(9), 1393-1404.

Amarantini, David, Rao, G., & Berton, E. (2010). A two-step EMG-and-optimization process to estimate muscle force during dynamic movement. *Journal of Biomechanics*, 43(9), 1827-1830.

Amiridis, I. G., Martin, A., Morlon, B., Martin, L., Cometti, G., Pousson, M., & van Hoecke, J. (1996). Co-activation and tension-regulating phenomena during isokinetic knee extension in sedentary and highly skilled humans. *Eur J Appl Physiol Occup Physiol*, 73(1-2), 149-156.

Aranyi, Z., & Rosler, K. M. (2002). Effort-induced mirror movements - A study of transcallosal inhibition in humans. *Experimental Brain Research*, 145(1), 76-82.

Armatas, C. A., Summers, J. J., & Bradshaw, J. L. (1994). Mirror movements in normal adult subjects. *Journal of Clinical and Experimental Neuropsychology*, 16(3), 405-413.

Armatas, C. A., Summers, J. J., & Bradshaw, J. L. (1996a). Handedness and performance variability as factors influencing mirror movement occurrence. *Journal of Clinical and Experimental Neuropsychology*, 18(6), 823-835.

Armatas, C. A., Summers, J. J., & Bradshaw, J. L. (1996b). Strength as a factor influencing mirror movements. *Human Movement Science*, 15(5), 689-705.

Ashford, S., Slade, M., Malaprade, F., & Turner-Stokes, L. (2008). Evaluation of functional outcome measures for the hemiparetic upper limb: a systematic review. *Journal of Rehabilitation Medicine*, 40(10), 787-795.

Aumann, T. D., & Prut, Y. (2015). Do sensorimotor β-oscillations maintain muscle synergy representations in primary motor cortex? *Trends in Neurosciences*, 38(2), 77-85.

Baker, M. R., & Baker, S. N. (2003). The effect of diazepam on motor cortical oscillations and corticomuscular coherence studied in man. *J Physiol*, 546(3), 931-942.

Baliz, Y., Armatas, C., Farrow, M., Hoy, K. E., Fitzgerald, P. B., Bradshaw, J. L., & Georgiou-Karistianis, N. (2005). The influence of attention and age on the occurrence of mirror movements. *J Int Neuropsychol Soc*, 11(7), 855-862.

Baratta, R., Solomonow, M., Zhou, B. H., Letson, D., Chuinard, R., & D'Ambrosia, R. (1988). Muscular coactivation. The role of the antagonist musculature in maintaining knee stability. *The American Journal of Sports Medicine*, 16(2), 113-122.

Barrué-Belou, S., Marque, P., & Duclay, J. (2018). Recurrent inhibition is higher in eccentric compared to isometric and concentric maximal voluntary contractions. *Acta Physiologica (Oxford, England)*, 223(4), e13064.

Barrué-Belou, Simon, Amarantini, D., Marque, P., & Duclay, J. (2016). Neural adaptations to submaximal isokinetic eccentric strength training. *European Journal of Applied Physiology*, 116(5), 1021-1030.

Basmajian, J. V., & Deluca, C. J. (1985). *Muscles Alive: Their Functions Revealed by Electromyography* (5th edition). Baltimore: Lippincott Williams and Wilkins.

Bäumer, T., Dammann, E., Bock, F., Klöppel, S., Siebner, H. R., & Münchau, A. (2007).

Laterality of interhemispheric inhibition depends on handedness. *Experimental Brain Research*, 180(2), 195-203.

Beltman, J. G. M., Sargeant, A. J., Ball, D., Maganaris, C. N., & de Haan, A. (2003). Effect of antagonist muscle fatigue on knee extension torque. *Pflugers Archiv: European Journal of Physiology*, 446(6), 735-741.

Bergfeldt, U., Jonsson, T., Bergfeldt, L., & Julin, P. (2015). Cortical activation changes and improved motor function in stroke patients after focal spasticity therapy--an interventional study applying repeated fMRI. *BMC Neurology*, 15, 52.

Bernstein, N. A. (1967). *The co-ordination and regulation of movements,* (1st edition). Oxford: Pergamon Press.

Besier, T. F., Fredericson, M., Gold, G. E., Beaupre, G. S., & Delp, S. L. (2009). Knee muscle forces during walking and running in patellofemoral pain patients and pain-free controls. *J Biomech*, 42(7), 898-905.

Bigot, J., Longcamp, M., Dal Maso, F., & Amarantini, D. (2011). A new statistical test based on the wavelet cross-spectrum to detect time-frequency dependence between non-stationary signals: application to the analysis of cortico-muscular interactions. *NeuroImage*, 55(4), 1504-1518.

Billot, M., Duclay, J., Simoneau-Buessinger, E. M., Ballay, Y., & Martin, A. (2014). Is co-contraction responsible for the decline in maximal knee joint torque in older males? *Age (Dordrecht, Netherlands)*, 36(2), 899-910.

Blais, M., Amarantini, D., Albaret, J.-M., Chaix, Y., & Tallet, J. (2018). Atypical inter-hemispheric communication correlates with altered motor inhibition during learning of a new bimanual coordination pattern in developmental coordination disorder. *Developmental Science*, 21(3), e12563.

Blakemore, R. L., MacAskill', M. R., Shoorangiz, R., & Anderson, T. J. (2018). Stress-evoking emotional stimuli exaggerate deficits in motor function in Parkinson's disease. *Neuropsychologia*, 112, 66-76.

Bodwell, J. A., Mahurin, R. K., Waddle, S., Price, R., & Cramer, S. C. (2003). Age and features of movement influence motor overflow. *Journal of the American Geriatrics Society*, 51(12), 1735-1739.

Bogey, R. A., & Barnes, L. A. (2017). An EMG-to-Force Processing approach for estimating in vivo hip muscle forces in normal human walking. *IEEE Transactions on Neural Systems and Rehabilitation Engineering*, 25(8), 1172-1179.

Boonstra, T. W. (2013). The potential of corticomuscular and intermuscular coherence for research on human motor control. *Frontiers in Human Neuroscience*, 7, 855.

Boonstra, T. W., & Breakspear, M. (2012). Neural mechanisms of intermuscular coherence: implications for the rectification of surface electromyography. *J Neurophysiol*, 107(3), 796-807.

Boonstra, T. W., van Wijk, B. C. M., Praamstra, P., & Daffertshofer, A. (2009). Corticomuscular and bilateral EMG coherence reflect distinct aspects of neural synchronization. *Neuroscience Letters*, 463(1), 17-21.

Brand, R. A., Pedersen, D. R., & Friederich, J. A. (1986). The sensitivity of muscle force predictions to changes in physiologic cross-sectional area. *Journal of Biomechanics*, 19(8), 589-596.

Brittain, J.-S., Halliday, D. M., Conway, B. A., & Nielsen, J. B. (2007). Single-trial multiwavelet coherence in application to neurophysiological time series. *IEEE Transactions on Bio-Medical Engineering*, 54(5), 854-862.

Buchanan, T. S., Lloyd, D. G., Manal, K., & Besier, T. F. (2005). Estimation of muscle forces and joint moments using a forward-inverse dynamics model. *Medicine and Science in Sports and Exercise*, 37(11), 1911-1916.

Buchanan, T. S., & Shreeve, D. A. (1996). An evaluation of optimization techniques for the prediction of muscle activation patterns during isometric tasks. *Journal of Biomechanical Engineering*, 118(4), 565-574.

Buchanan, Thomas S., Lloyd, D. G., Manal, K., & Besier, T. F. (2004). Neuromusculoskeletal Modeling: Estimation of Muscle Forces and Joint Moments and Movements From Measurements of Neural Command. *Journal of applied biomechanics*, 20(4), 367-395.

Burke, M. J., Roman, V., & Wright, V. (1978). Bone and joint changes in lower limb amputees. *Annals of the Rheumatic Diseases*, 37(3), 252-254.

Buzsáki, G., & Draguhn, A. (2004). Neuronal oscillations in cortical networks. *Science (New York, N.Y.)*, 304(5679), 1926-1929.

Cahouet, V., Luc, M., & David, A. (2002). Static optimal estimation of joint accelerations for inverse dynamics problem solution. *Journal of Biomechanics*, 35(11), 1507-1513.

Carolan, B., & Cafarelli, E. (1992). Adaptations in coactivation after isometric resistance training. *J Appl Physiol*, 73(3), 911-917.

Carroll, T. J., Riek, S., & Carson, R. G. (2002). The sites of neural adaptation induced by resistance training in humans. *The Journal of Physiology*, 544(2), 641-652.

Carson, R. G. (2005). Neural pathways mediating bilateral interactions between the upper limbs. *Brain Research. Brain Research Reviews*, 49(3), 641-662.

Centomo, H. (2006). *Analyses comparatives des stratégies musculaires et des co-contractions chez des enfants sains et amputés trans-tibiaux lors de tâches dynamiques des membres inférieurs*. Université de Montréal.

Centomo, H., Amarantini, D., Martin, L., & Prince, F. (2007). Muscle adaptation patterns of children with a trans-tibial amputation during walking. *Clin Biomech*, 22(4), 457-463.

Centomo, H., Amarantini, D., Martin, L., & Prince, F. (2008). Differences in the coordination of agonist and antagonist muscle groups in below-knee amputee and able-bodied children during dynamic exercise. *Journal of Electromyography and Kinesiology*, 18(3), 487-494.

Cernacek, J. (1961). Contralateral motor irradiation--cerebral dominance. Its changes in hemiparesis. *Archives of Neurology*, 4, 165-172.

Chae, J., Yang, G., Park, B. K., & Labatia, I. (2002). Muscle weakness and cocontraction in upper limb hemiparesis: relationship to motor impairment and physical disability. *Neurorehabil Neural Repair*, 16(3), 241-248.

Chakarov, V., Naranjo, J. R., Schulte-Mönting, J., Omlor, W., Huethe, F., & Kristeva, R. (2009). Beta-range EEG-EMG coherence with isometric compensation for increasing modulated low-level forces. *Journal of Neurophysiology*, 102(2), 1115-1120.

Chalard, A., Amarantini, D., Belle, M., Montane, E., & Gasq, D. (2018). Impact of different

EMG normalisation methods on muscle activations and cocontraction index in adults with chronic post-stroke hemiparesis. *Annals of Physical and Rehabilitation Medicine*, 61, e444.

Chalard, A., Amarantini, D., Tisseyre, J., Marque, P., Tallet, J., & Gasq, D. (2018). Is spasticity or spastic cocontraction of the elbow flexors associated with the limitation of voluntary elbow extension in adults with acquired hemiparesis? *Annals of Physical and Rehabilitation Medicine*, 61, e439.

Chalard, Alexandre, Amarantini, D., Picaut, P., Pons, L., Marque, P., & Gasq, D. (2018). Assessment of upper limb active movement facilitation and neuromuscular plasticity induced by abobotulinumtoxinA in chronic poststroke: A study protocol. *Toxicon*, 156, S15-S16.

Chalard, Alexandre, Amarantini, D., Tisseyre, J., Marque, P., Tallet, J., & Gasq, D. (2019). Spastic co-contraction, rather than spasticity, is associated with impaired active function in adults with acquired brain injury: A pilot study. *Journal of Rehabilitation Medicine*.

Challis, J. H., & Kerwin, D. G. (1993). An analytical examination of muscle force estimations using optimization techniques. *Proceedings of the Institution of Mechanical Engineers. Part H, Journal of Engineering in Medicine*, 207(3), 139-148.

Challis, John H. (1997). Producing physiologically realistic individual muscle force estimations by imposing constraints when using optimization techniques. *Medical Engineering & Physics*, 19(3), 253-261.

Chao, E. Y., & An, K. N. (1978). Graphical Interpretation of the Solution to the Redundant Problem in Biomechanics. *Journal of Biomechanical Engineering*, 100(3), 159-167.

Charissou, C. (2018). *Etude de la contribution du couplage intermusculaire au contrôle de l'activité des muscles synergistes agonistes et antagonistes lors de contractions isométriques volontaires.* Université d'Aix-Marseille.

Charissou, Camille, Amarantini, D., Baurès, R., Berton, E., & Vigouroux, L. (2017). Effects of hand configuration on muscle force coordination, co-contraction and concomitant intermuscular coupling during maximal isometric flexion of the fingers. *European Journal of Applied Physiology*, 117(11), 2309-2320.

Charissou, Camille, Vigouroux, L., Berton, E., & Amarantini, D. (2016). Fatigue- and training-related changes in « beta » intermuscular interactions between agonist muscles. *Journal of Electromyography and Kinesiology*, 27, 52-59.

Chen, R., Cohen, L. G., & Hallett, M. (2002). Nervous system reorganization following injury. *Neuroscience*, 111(4), 761-773.

Cholewicki, J., McGill, S. M., & Norman, R. W. (1995). Comparison of muscle forces and joint load from an optimization and EMG assisted lumbar spine model: towards development of a hybrid approach. *Journal of Biomechanics*, 28(3), 321-331.

Cholewicki, J., Panjabi, M. M., & Khachatryan, A. (1997). Stabilizing function of trunk flexor-extensor muscles around a neutral spine posture. *Spine*, 22(19), 2207-2212.

Cincotta, M., & Ziemann, U. (2008). Neurophysiology of unimanual motor control and mirror movements. *Clinical Neurophysiology*, 119(4), 744-762.

Cohen, E. A. K., & Walden, A. T. (2010). A Statistical Study of Temporally Smoothed Wavelet Coherence. *IEEE Transactions on Signal Processing*, 58(6), 2964-2973.

Conway, B. A., Halliday, D. M., Farmer, S. F., Shahani, U., Maas, P., Weir, A. I., & Rosenberg, J. R. (1995). Synchronization between motor cortex and spinal motoneuronal

pool during the performance of a maintained motor task in man. *The Journal of Physiology*, 489(3), 917-924.

Corser, T. (1973). Cocontraction and reciprocal relaxation in the ankle plantar flexors and dorsiflexors during rapid stepping and jumping. *Electromyography and Clinical Neurophysiology*, 13(3), 289-306.

Coudrat, L., Rouis, M., Jaafar, H., Attiogbé, E., Gélat, T., & Driss, T. (2014). Emotional pictures impact repetitive sprint ability test on cycle ergometre. *Journal of Sports Sciences*, 32(9), 892-900.

Cremoux, S., Tallet, J., Berton, E., Maso, F. D., & Amarantini, D. (2012). Atypical EMG activation patterns of the elbow extensors after complete C6 tetraplegia during isometric contractions: a case report. *Computer Methods in Biomechanics and Biomedical Engineering*, 15(sup1), 266-268.

Cremoux, Sylvain. (2013). *Contrôle de la contraction musculaire volontaire après un traumatisme médullaire cervical : étude de la réorganisation des activations musculaires et corticales.* Université d'Aix-Marseille.

Cremoux, Sylvain, Amarantini, D., Tallet, J., Dal Maso, F., & Berton, E. (2016). Increased antagonist muscle activity in cervical SCI patients suggests altered reciprocal inhibition during elbow contractions. *Clin Neurophysiol*, 127(1), 629-634.

Cremoux, Sylvain, Charissou, C., Tallet, J., Abade-Moreira, A., Dal Maso, F., & Amarantini, D. (2018). T80. Alteration of intermuscular coherence in synergistic muscle pairs during actual elbow flexion contractions after cervical spinal cord injury. *Clinical Neurophysiology*, 129(Suppl. 1), e33-e33.

Cremoux, Sylvain, Tallet, J., Berton, E., Dal Maso, F., & Amarantini, D. (2013a). Does the force level modulate the cortical activity during isometric contractions after a cervical spinal cord injury? *Clinical Neurophysiology*, 124(5), 1005-1012.

Cremoux, Sylvain, Tallet, J., Berton, E., Dal Maso, F., & Amarantini, D. (2013b). Motor-related cortical activity after cervical spinal cord injury: multifaceted EEG analysis of isometric elbow flexion contractions. *Brain Research*, 1533, 44-51.

Cremoux, Sylvain, Tallet, J., Dal Maso, F., Berton, E., & Amarantini, D. (2017). Impaired corticomuscular coherence during isometric elbow flexion contractions in humans with cervical spinal cord injury. *The European Journal of Neuroscience*, 46(4), 1991-2000.

Crone, C., Nielsen, J., Petersen, N., Ballegaard, M., & Hultborn, H. (1994). Disynaptic reciprocal inhibition of ankle extensors in spastic patients. *Brain*, 117(5), 1161-1168.

Crone, N. E., Miglioretti, D. L., Gordon, B., Sieracki, J. M., Wilson, M. T., Uematsu, S., & Lesser, R. P. (1998). Functional mapping of human sensorimotor cortex with electrocorticographic spectral analysis. I. Alpha and beta event-related desynchronization. *Brain: A Journal of Neurology*, 121(12), 2271-2299.

Crowninshield, R. D., & Brand, R. A. (1981). A physiologically based criterion of muscle force prediction in locomotion. *J Biomech*, 14(11), 793-801.

d'Avella, A., Saltiel, P., & Bizzi, E. (2003). Combinations of muscle synergies in the construction of a natural motor behavior. *Nature Neuroscience*, 6(3), 300-308.

da Fonseca, S. T., Vaz, D. V., de Aquino, C. F., & Brício, R. S. (2006). Muscular co-contraction during walking and landing from a jump: comparison between genders and influence of activity level. *Journal of Electromyography and Kinesiology*, 16(3), 273-280.

Dai, C., Shin, H., Davis, B., & Hu, X. (2017). Origins of Common Neural Inputs to Different Compartments of the Extensor Digitorum Communis Muscle. *Scientific reports*, 7, 13960-13960.

Dakin, C. J., Dalton, B. H., Luu, B. L., & Blouin, J.-S. (2014). Rectification is required to extract oscillatory envelope modulation from surface electromyographic signals. *J Neurophysiol*, 112(7), 1685-91.

Dal Maso, F. (2012). *Implication du cortex moteur primaire dans la régulation de la coactivation musculaire : étude de la modulation des oscillations corticales et des interactions cortico-musculaires.* Université Toulouse III Paul Sabatier.

Dal Maso, F., Longcamp, M., & Amarantini, D. (2012). Training-related decrease in antagonist muscles activation is associated with increased motor cortex activation: evidence of central mechanisms for control of antagonist muscles. *Experimental Brain Research*, 220(3-4), 287-295.

Dal Maso, F., Longcamp, M., Cremoux, S., & Amarantini, D. (2017). Effect of training status on beta-range corticomuscular coherence in agonist vs. antagonist muscles during isometric knee contractions. *Experimental Brain Research*, 235(10), 3023-3031.

De Luca, C. J., & Mambrito, B. (1987). Voluntary control of motor units in human antagonist muscles: coactivation and reciprocal activation. *Journal of Neurophysiology*, 58(3), 525-542.

De Marchis, C., Severini, G., Castronovo, A. M., Schmid, M., & Conforto, S. (2015). Intermuscular coherence contributions in synergistic muscles during pedaling. *Experimental Brain Research*, 233(6), 1907-1919.

de Vries, I. E. J., Daffertshofer, A., Stegeman, D. F., & Boonstra, T. W. (2016). Functional connectivity in neuromuscular system underlying bimanual coordination. *Journal of neurophysiology*, 16(6), 2576-2585

Deiber, M. P., Caldara, R., Ibañez, V., & Hauert, C. A. (2001). Alpha band power changes in unimanual and bimanual sequential movements, and during motor transitions. *Clinical Neurophysiology*, 112(8), 1419-1435.

Delp, S. L., Anderson, F. C., Arnold, A. S., Loan, P., Habib, A., John, C. T., … Thelen, D. G. (2007). OpenSim: open-source software to create and analyze dynamic simulations of movement. *IEEE Trans Biomed Eng*, 54(11), 1940-1950.

Dewald, J. P., Pope, P. S., Given, J. D., Buchanan, T. S., & Rymer, W. Z. (1995). Abnormal muscle coactivation patterns during isometric torque generation at the elbow and shoulder in hemiparetic subjects. *Brain*, 118(2), 495-510.

Dideriksen, J. L., Negro, F., Falla, D., Kristensen, S. R., Mrachacz-Kersting, N., & Farina, D. (2018). Coherence of the Surface EMG and Common Synaptic Input to Motor Neurons. *Frontiers in Human Neuroscience*, 12, 207.

Duchateau, J., & Enoka, R. M. (2008). Neural control of shortening and lengthening contractions: influence of task constraints. *The Journal of physiology*, 586, 5853-5864.

Duchateau, J., & Enoka, R. M. (2016). Neural control of lengthening contractions. *The Journal of experimental biology*, 219, 197-204.

Duclay, J., & Martin, A. (2005). Evoked H-reflex and V-wave responses during maximal isometric, concentric, and eccentric muscle contraction. *J Neurophysiol*, 94(5), 3555-3562.

Duclay, J., Martin, A., Robbe, A., & Pousson, M. (2008). Spinal reflex plasticity during

maximal dynamic contractions after eccentric training. *Med Sci Sports Exerc*, 40(4), 722-734.

Duclay, J., Pasquet, B., Martin, A., & Duchateau, J. (2011). Specific modulation of corticospinal and spinal excitabilities during maximal voluntary isometric, shortening and lengthening contractions in synergist muscles. *J Physiol*, 589(11), 2901-2916.

Duclay, J., Pasquet, B., Martin, A., & Duchateau, J. (2014). Specific modulation of spinal and cortical excitabilities during lengthening and shortening submaximal and maximal contractions in plantar flexor muscles. *J Appl Physiol*, 117(12), 1440-1450.

Duclay, J., Robbe, A., Pousson, M., & Martin, A. (2009). Effect of angular velocity on soleus and medial gastrocnemius H-reflex during maximal concentric and eccentric muscle contraction. *J Electromyogr Kinesiol*, 19(5), 948-956.

Elliot, A. J. (2006). The Hierarchical Model of Approach-Avoidance Motivation. *Motivation and Emotion*, 30(2), 111-116.

Engelhorn, R. (1983). Agonist and Antagonist Muscle EMG Activity Pattern Changes with Skill Acquisition. *Research Quarterly for Exercise and Sport*, 54(4), 315-323.

Enoka, R. M. (1996). Eccentric contractions require unique activation strategies by the nervous system. *Journal of Applied Physiology*, 81(6), 2339-2346.

Erimaki, S., & Christakos, C. N. (2008). Coherent motor unit rhythms in the 6-10 Hz range during time-varying voluntary muscle contractions: neural mechanism and relation to rhythmical motor control. *Journal of Neurophysiology*, 99(2), 473-483.

Escamilla, R. F., Fleisig, G. S., Zheng, N. G., Barrentine, S. W., Wilk, K. E., & Andrews, J. R. (1998). Biomechanics of the knee during closed kinetic chain and open kinetic chain exercises. *Medicine and Science in Sports and Exercise*, 30(4), 556-569.

Espiau, B., Guigues, I., & Pissard-Gibollet, R. (1998). *Can an underactuated leg with a passive spring at the knee achieve a ballistic step ?* (Can an underactuated leg with a passive spring at the knee achieve a ballistic step ? No. 3544). Grenoble, France: Institut National de Recherche en Informatique et en Automatique.

Espiau, B., & Oudeyer, P.-Y. (2008). Robotique : de l'automate à l'humanoïde par Bernard Espiau. Un robot très curieux, entretien avec Pierre-Yves Oudeyer, propos recueillis par Dominique Chouchan. [Les Cahiers de l'INRIA - La Recherche, INRIA].

Falconer, K., & Winter, D. A. (1985). Quantitative assessment of co-contraction at the ankle joint in walking. *Electromyography and Clinical Neurophysiology*, 25(2-3), 135-149.

Falvo, M. J., Sirevaag, E. J., Rohrbaugh, J. W., & Earhart, G. M. (2010). Resistance training induces supraspinal adaptations: evidence from movement-related cortical potentials. *European Journal of Applied Physiology*, 109(5), 923-933.

Fang, Y., Siemionow, V., Sahgal, V., Xiong, F., & Yue, G. H. (2001). Greater movement-related cortical potential during human eccentric versus concentric muscle contractions. *Journal of Neurophysiology*, 86(4), 1764-1772.

Farina, D., Negro, F., & Jiang, N. (2013). Identification of common synaptic inputs to motor neurons from the rectified electromyogram. *J Physiol*, 591(10), 2403-2418.

Farmer, S F. (1998). Rhythmicity, synchronization and binding in human and primate motor systems. *The Journal of Physiology*, 509(1), 3-14.

Farmer, S. F., Bremner, F. D., Halliday, D. M., Rosenberg, J. R., & Stephens, J. A. (1993).

The frequency content of common synaptic inputs to motoneurones studied during voluntary isometric contraction in man. *J Physiol*, *470*, 127-155.

Farmer, Simon F., & Halliday, D. M. (2014). Reply to McClelland et al.: EMG rectification and coherence analysis. *J Neurophysiol*, 111(5), 1151-1152.

Fautrelle, L., Barbieri, G., Ballay, Y., & Bonnetblanc, F. (2011). Pointing to double-step visual stimuli from a standing position: motor corrections when the speed-accuracy trade-off is unexpectedly modified in-flight. A breakdown of the perception-action coupling. *Neuroscience*, 194, 124-135.

Fautrelle, L., Prablanc, C., Berret, B., Ballay, Y., & Bonnetblanc, F. (2010). Pointing to double-step visual stimuli from a standing position: very short latency (express) corrections are observed in upper and lower limbs and may not require cortical involvement. *Neuroscience*, 169(2), 697-705.

Fautrelle, Lilian, Ballay, Y., & Bonnetblanc, F. (2010). Muscular synergies during motor corrections: investigation of the latencies of muscle activities. *Behavioural Brain Research*, 214(2), 428-436.

Fauvet, M., Cremoux, S., Chalard, A., Tisseyre, J., Gasq, D., & Amarantini, D. (2019). A novel method to generalize time-frequency coherence analysis between EEG or EMG signals during repetitive trials of different durations. In *2019 9th International IEEE/EMBS Conference on Neural Engineering (NER)*. San Francisco, CA, USA.

Felson, D. T., Lawrence, R. C., Dieppe, P. A., Hirsch, R., Helmick, C. G., Jordan, J. M., … Fries, J. F. (2000). Osteoarthritis: new insights. Part 1: the disease and its risk factors. *Annals of Internal Medicine*, 133(8), 635-646.

Flor, H., Elbert, T., Knecht, S., Wienbruch, C., Pantev, C., Birbaumer, N., … Taub, E. (1995). Phantom-limb pain as a perceptual correlate of cortical reorganization following arm amputation. *Nature*, 375(6531), 482-484.

Foley, N., Pereira, S., Salter, K., Fernandez, M. M., Speechley, M., Sequeira, K., … Teasell, R. (2013). Treatment with botulinum toxin improves upper-extremity function post stroke: a systematic review and meta-analysis. *Archives of Physical Medicine and Rehabilitation*, 94(5), 977-989.

Fries, P. (2005). A mechanism for cognitive dynamics: neuronal communication through neuronal coherence. *Trends in Cognitive Sciences*, 9(10), 474-480.

Gagnon, D., Lariviere, C., & Loisel, P. (2001). Comparative ability of EMG, optimization, and hybrid modelling approaches to predict trunk muscle forces and lumbar spine loading during dynamic sagittal plane lifting. *Clinical Biomechanics*, 16(5), 359-372.

Gagnon, Denis, Arjmand, N., Plamondon, A., Shirazi-Adl, A., & Larivière, C. (2011). An improved multi-joint EMG-assisted optimization approach to estimate joint and muscle forces in a musculoskeletal model of the lumbar spine. *J Biomech*, 44(8), 1521-1529.

Gasq, D. (2015). *Application de l'analyse temps-fréquence à l'évaluation de l'instabilité posturale chez le patient neurologique.* Université Toulouse III Paul Sabatier.

Gastaut, H. (1952). Electrocorticographic study of the reactivity of rolandic rhythm. *Revue Neurologique*, 87(2), 176-182.

Gastaut, H., Terzian, H., & Gastaut, Y. (1952). Study of a little electroencephalographic activity: rolandic arched rhythm. *Marseille Medical*, 89(6), 296-310.

Gélat, T., Coudrat, L., & Le Pellec, A. (2011). Gait initiation is affected during emotional conflict. *Neuroscience Letters*, 497(1), 64-67.

Gelfand, I. M., & Latash, M. L. (1998). On the problem of adequate language in motor control. *Motor Control*, 2(4), 306-313.

Goislard de Monsabert, B., Rossi, J., Berton, E., & Vigouroux, L. (2012). Comparison of muscle loadings between power and pinch grip tasks. *Computer methods in biomechanics and biomedical engineering*, 15(Suppl. 1), 159-161.

Goscinny, R., & Uderzo, A. (1966). *Astérix chez les Bretons* (Hachette).

Grabiner, M. D., Campbell, K. R., Hawthorne, D. L., & Hawkins, D. A. (1989). Electromyographic study of the anterior cruciate ligament-hamstrings synergy during isometric knee extension. *Journal of Orthopaedic Research*, 7(1), 152-155.

Gracies, J.-M. (2005). Pathophysiology of spastic paresis. I: Paresis and soft tissue changes. *Muscle & Nerve*, 31(5), 535-551.

Gracies, J.-M., Brashear, A., Jech, R., McAllister, P., Banach, M., Valkovic, P., … International AbobotulinumtoxinA Adult Upper Limb Spasticity Study Group. (2015). Safety and efficacy of abobotulinumtoxinA for hemiparesis in adults with upper limb spasticity after stroke or traumatic brain injury: a double-blind randomised controlled trial. *The Lancet. Neurology*, 14(10), 992-1001.

Graimann, B., Huggins, J. E., Levine, S. P., & Pfurtscheller, G. (2002). Visualization of significant ERD/ERS patterns in multichannel EEG and ECoG data. *Clinical Neurophysiology*, 113(1), 43-47.

Granata, K. P., & Marras, W. S. (1993). An EMG-assisted model of loads on the lumbar spine during asymmetric trunk extensions. *Journal of Biomechanics*, 26(12), 1429-1438.

Granata, K. P., & Marras, W. S. (2000). Cost-benefit of muscle cocontraction in protecting against spinal instability. *Spine*, 25(11), 1398-1404.

Gribble, P. L., Mullin, L. I., Cothros, N., & Mattar, A. (2003). Role of cocontraction in arm movement accuracy. *Journal of Neurophysiology*, 89(5), 2396-2405.

Griffin, L., & Cafarelli, E. (2005). Resistance training: cortical, spinal, and motor unit adaptations. *Can J Appl Physiol*, 30(3), 328-340.

Grinsted, A., Moore, J. C., & Jevrejeva, S. (2004). Application of the cross wavelet transform and wavelet coherence to geophysical time series. *Nonlinear Processes in Geophysics*, 11(5/6), 561-566.

Grosse, P., Cassidy, M. J., & Brown, P. (2002). EEG-EMG, MEG-EMG and EMG-EMG frequency analysis: physiological principles and clinical applications. *Clin Neurophysiol*, 113(10), 1523-1531.

Gruber, M., Linnamo, V., Strojnik, V., Rantalainen, T., & Avela, J. (2009). Excitability at the motoneuron pool and motor cortex is specifically modulated in lengthening compared to isometric contractions. *Journal of Neurophysiology*, 101(4), 2030-2040.

Haaland, K. Y., Elsinger, C. L., Mayer, A. R., Durgerian, S., & Rao, S. M. (2004). Motor sequence complexity and performing hand produce differential patterns of hemispheric lateralization. *Journal of Cognitive Neuroscience*, 16(4), 621-636.

Hagood, S., Solomonow, M., Baratta, R., Zhou, B. H., & D'Ambrosia, R. (1990). The effect of joint velocity on the contribution of the antagonist musculature to knee stiffness and

laxity. *The American Journal of Sports Medicine*, 18(2), 182-187.

Hajcak, G., Dunning, J. P., & Foti, D. (2007). Neural response to emotional pictures is unaffected by concurrent task difficulty: an event-related potential study. *Behavioral Neuroscience*, 121(6), 1156-1162.

Häkkinen, K., Alen, M., Kallinen, M., Newton, R. U., & Kraemer, W. J. (2000). Neuromuscular adaptation during prolonged strength training, detraining and re-strength-training in middle-aged and elderly people. *European Journal of Applied Physiology*, 83(1), 51-62.

Häkkinen, K., Kallinen, M., Izquierdo, M., Jokelainen, K., Lassila, H., Mälkiä, E., … Alen, M. (1998). Changes in agonist-antagonist EMG, muscle CSA, and force during strength training in middle-aged and older people. *Journal of Applied Physiology*, 84(4), 1341-1349.

Hansen, N. L., Conway, B. A., Halliday, D. M., Hansen, S., Pyndt, H. S., Biering-Sørensen, F., & Nielsen, J. B. (2005). Reduction of common synaptic drive to ankle dorsiflexor motoneurons during walking in patients with spinal cord lesion. *Journal of Neurophysiology*, 94(2), 934-942.

Hari, R., & Salenius, S. (1999). Rhythmical corticomotor communication. *Neuroreport*, 10(2), R1-10.

Hasan, Z. (1986). Optimized movement trajectories and joint stiffness in unperturbed, inertially loaded movements. *Biol Cybern*, 53(6), 373-382.

Heald, J. B., Franklin, D. W., & Wolpert, D. M. (2018). Increasing muscle co-contraction speeds up internal model acquisition during dynamic motor learning. *Scientific Reports*, 8(1), 16355.

Herzog, W., & Binding, P. (1992). Predictions of antagonistic muscular activity using nonlinear optimization. *Math Biosci*, 111(2), 217-229.

Herzog, W., & Binding, P. (1993). Cocontraction of pairs of antagonistic muscles: analytical solution for planar static nonlinear optimization approaches. *Mathematical Biosciences*, 118(1), 83-95.

Hoang, H. X., Diamond, L. E., Lloyd, D. G., & Pizzolato, C. (2019). A calibrated EMG-informed neuromusculoskeletal model can appropriately account for muscle co-contraction in the estimation of hip joint contact forces in people with hip osteoarthritis. *Journal of Biomechanics*, 83, 134-142.

Hoang, H. X., Pizzolato, C., Diamond, L. E., & Lloyd, D. G. (2018). Subject-specific calibration of neuromuscular parameters enables neuromusculoskeletal models to estimate physiologically plausible hip joint contact forces in healthy adults. *Journal of Biomechanics*, 80, 111-120.

Hoy, K. E., Fitzgerald, P. B., Bradshaw, J. L., Armatas, C. A., & Georgiou-Karistianis, N. (2004). Investigating the cortical origins of motor overflow. *Brain Research Reviews*, 46(3), 315-327.

Hübers, A., Orekhov, Y., & Ziemann, U. (2008). Interhemispheric motor inhibition: its role in controlling electromyographic mirror activity. *The European Journal of Neuroscience*, 28(2), 364-371.

Huynh, W., Krishnan, A. V., Lin, C. S.-Y., Vucic, S., Katrak, P., Hornberger, M., & Kiernan, M. C. (2013). Botulinum toxin modulates cortical maladaptation in post-stroke spasticity. *Muscle Nerve*, 48(1), 93-99.

Issa, S. N., & Sharma, L. (2006). Epidemiology of osteoarthritis: an update. *Current Rheumatology Reports*, 8(1), 7-15.

Jaafar, H., Rouis, M., Coudrat, L., Gélat, T., Noakes, T. D., & Driss, T. (2015). Influence of Affective Stimuli on Leg Power Output and Associated Neuromuscular Parameters during Repeated High Intensity Cycling Exercises. *PloS One*, 10(8), e0136330.

Jahangir, A. W., Tan, H. J., Norlinah, M. I., Nafisah, W. Y., Ramesh, S., Hamidon, B. B., & Raymond, A. A. (2007). Intramuscular injection of botulinum toxin for the treatment of wrist and finger spasticity after stroke. *The Medical Journal of Malaysia*, 62(4), 319-322.

Jasper, H. H., & Andrews, H. L. (1938). Electroencephalography. III. Normal differentiation of occipital and precentral regions in man. *Archives of Neurology & Psychiatry*, 39, 96-115.

Jesunathadas, M., Laitano, J., Hamm, T. M., & Santello, M. (2013). Across-muscle coherence is modulated as a function of wrist posture during two-digit grasping. *Neurosci Lett*, 553, 68-71.

Kattla, S., & Lowery, M. M. (2010). Fatigue related changes in electromyographic coherence between synergistic hand muscles. *Experimental Brain Research*, 202(1), 89-99.

Keenan, K. G., Massey, W. V., Walters, T. J., & Collins, J. D. (2012). Sensitivity of EMG-EMG coherence to detect the common oscillatory drive to hand muscles in young and older adults. *J Neurophysiol*, 107(10), 2866-2875.

Kellis, E. (1998). Quantification of quadriceps and hamstring antagonist activity. *Sports Medicine*, 25(1), 37-62.

Kellis, E. (1999). The effects of fatigue on the resultant joint moment, agonist and antagonist electromyographic activity at different angles during dynamic knee extension efforts. *J Electromyogr Kinesiol*, 9(3), 191-199.

Kellis, E., Arabatzi, F., & Papadopoulos, C. (2003). Muscle co-activation around the knee in drop jumping using the co-contraction index. *Journal of Electromyography and Kinesiology*, 13(3), 229-238.

Kellis, Eleftherios, Zafeiridis, A., & Amiridis, I. G. (2011). Muscle coactivation before and after the impact phase of running following isokinetic fatigue. *J Athl Train*, 46(1), 11-19.

Kilner, J. M., Baker, S. N., Salenius, S., Hari, R., & Lemon, R. N. (2000). Human cortical muscle coherence is directly related to specific motor parameters. *The Journal of Neuroscience*, 20(23), 8838-8845.

Kilner, J. M., Baker, S. N., Salenius, S., Jousmaki, V., Hari, R., & Lemon, R. N. (1999). Task-dependent modulation of 15-30 Hz coherence between rectified EMGs from human hand and forearm muscles. *J Physiol*, 516(2), 559-570.

Kim, S. G., Ashe, J., Hendrich, K., Ellermann, J. M., Merkle, H., Uğurbil, K., & Georgopoulos, A. P. (1993). Functional magnetic resonance imaging of motor cortex: hemispheric asymmetry and handedness. *Science (New York, N.Y.)*, 261(5121), 615-617.

Kingma, I., Aalbersberg, S., & van Dieen, J. H. (2004). Are hamstrings activated to counteract shear forces during isometric knee extension efforts in healthy subjects? *Journal of Electromyography and Kinesiology*, 14(3), 307-315.

Kluka, V., Martin, V., Vicencio, S. G., Giustiniani, M., Morel, C., Morio, C., … Ratel, S. (2016). Effect of muscle length on voluntary activation of the plantar flexors in boys and men. *European Journal of Applied Physiology*, 116(5), 1043-1051.

Kluka, V., Martin, V., Vicencio, S. G., Jegu, A.-G., Cardenoux, C., Morio, C., … Ratel, S. (2015). Effect of muscle length on voluntary activation level in children and adults. *Medicine and Science in Sports and Exercise*, 47(4), 718-724.

Knecht, S., Henningsen, H., Elbert, T., Flor, H., Höhling, C., Pantev, C., … Taub, E. (1995). Cortical reorganization in human amputees and mislocalization of painful stimuli to the phantom limb. *Neuroscience Letters*, 201(3), 262-264.

Knikou, M. (2012). Plasticity of corticospinal neural control after locomotor training in human spinal cord injury. *Neural Plast*, 2012, 254948.

Koerte, I., Eftimov, L., Laubender, R. P., Esslinger, O., Schroeder, A. S., Ertl-Wagner, B., … Danek, A. (2010). Mirror movements in healthy humans across the lifespan: effects of development and ageing. *Developmental Medicine and Child Neurology*, 52(12), 1106-1112.

Kubo, K., Tsunoda, N., Kanehisa, H., & Fukunaga, T. (2004). Activation of agonist and antagonist muscles at different joint angles during maximal isometric efforts. *Eur J Appl Physiol*, 91(2-3), 349-352.

Laine, C. M., & Valero-Cuevas, F. J. (2017). Intermuscular Coherence Reflects Functional Coordination. *Journal of neurophysiology*, 18(3), 1775-1783.

Lajante, M., Droulers, O., Dondaine, T., & Amarantini, D. (2012). Opening the "Black Box" of Electrodermal Activity in Consumer Neuroscience Research. *Journal of Neuroscience, Psychology, and Economics*, 5(4), 238-249.

Lajante, M. M. P., Droulers, O., & Amarantini, D. (2017). How Reliable Are State-of-the-Art Facial EMG Processing Methods? *Journal of Advertising Research*, 57(1), 28-37.

Lang, P. J. (1995). The emotion probe. Studies of motivation and attention. *The American Psychologist*, *50*(5), 372-385.

Lang, Peter J. (2000). Emotion and Motivation: Attention, Perception, and Action. *Journal of Sport and Exercise Psychology*, 22(S1), S122-S140.

Lasseter, J. (1995). *Toy Story*. Buena Vista International.

Latash, M. L. (2012). The bliss (not the problem) of motor abundance (not redundancy). *Experimental Brain Research*, 217(1), 1-5.

Latash, M. L. (2016). Biomechanics as a window into the neural control of movement. *Journal of Human Kinetics*, 52, 7-20.

Lazarus, J. A., & Todor, J. I. (1991). The role of attention in the regulation of associated movement in children. *Developmental Medicine and Child Neurology*, 33(1), 32-39.

Leocani, L., Cohen, L. G., Wassermann, E. M., Ikoma, K., & Hallett, M. (2000). Human corticospinal excitability evaluated with transcranial magnetic stimulation during different reaction time paradigms. *Brain: A Journal of Neurology*, 123(6), 1161-1173.

Les Inconnus. (1991). Youpi Matin. *3ème Télé des Inconnus*.

Levine, M. G., Knott, M., & Kabat, H. (1952). Electrical stimulation of antagonist muscles in the relaxation of spasticity. *Permanente Foundation Medical Bulletin*, 10(1-4), 205-211.

Li, G., Rudy, T. W., Sakane, M., Kanamori, A., Ma, C. B., & Woo, S. L. Y. (1999). The importance of quadriceps and hamstring muscle loading on knee kinematics and in-situ forces in the ACL. *Journal of Biomechanics*, 32(4), 395-400.

Licari, M. K., Billington, J., Reid, S. L., Wann, J. P., Elliott, C. M., Winsor, A. M., … Bynevelt, M. (2015). Cortical functioning in children with developmental coordination disorder: a motor overflow study. *Experimental Brain Research*, 233(6), 1703-1710.

Liederman, J., & Foley, L. M. (1987). A modified finger lift test reveals an asymmetry of motor overflow in adults. *Journal of Clinical and Experimental Neuropsychology*, 9(5), 498-510.

Lloyd, D. G., Buchanan, T. S., & Besier, T. F. (2005). Neuromuscular biomechanical modeling to understand knee ligament loading. *Medicine and Science in Sports and Exercise*, 37(11), 1939-1947.

Macneil, L. K., Xavier, P., Garvey, M. A., Gilbert, D. L., Ranta, M. E., Denckla, M. B., & Mostofsky, S. H. (2011). Quantifying excessive mirror overflow in children with attention-deficit/hyperactivity disorder. *Neurology*, 76(7), 622-628.

Makeig, S. (1993). Auditory event-related dynamics of the EEG spectrum and effects of exposure to tones. *Electroencephalography and Clinical Neurophysiology*, 86(4), 283-293.

Mayston, M. J., Harrison, L. M., & Stephens, J. A. (1999). A neurophysiological study of mirror movements in adults and children. *Annals of Neurology*, 45(5), 583-594.

McClelland, V. M., Cvetkovic, Z., & Mills, K. R. (2012). Rectification of the EMG is an unnecessary and inappropriate step in the calculation of Corticomuscular coherence. *Journal of Neuroscience Methods*, 205(1), 190-201.

McClelland, V. M., Cvetkovic, Z., & Mills, K. R. (2014a). EMG rectification has inconsistent effects on coherence analysis even in single motor unit studies. *Journal of Neurophysiology*, 111(5), 1150.

McClelland, V. M., Cvetkovic, Z., & Mills, K. R. (2014b). Inconsistent effects of EMG rectification on coherence analysis. *The Journal of Physiology*, 592(1), 249-250.

McIntyre, A., Lee, T., Janzen, S., Mays, R., Mehta, S., & Teasell, R. (2012). Systematic review of the effectiveness of pharmacological interventions in the treatment of spasticity of the hemiparetic lower extremity more than six months post stroke. *Topics in Stroke Rehabilitation*, 19(6), 479-490.

McLean, L., Chislett, M., Keith, M., Murphy, M., & Walton, P. (2003). The effect of head position, electrode site, movement and smoothing window in the determination of a reliable maximum voluntary activation of the upper trapezius muscle. *J Electromyogr Kinesiol*, 13(2), 169-180.

Mehrkanoon, S., Breakspear, M., Daffertshofer, A., & Boonstra, T. W. (2011). Generalized time-frequency coherency for assessing neural interactions in electrophysiological recordings. *Nature Precedings*.

Melzer, I., Yekutiel, M., & Sukenik, S. (2001). Comparative study of osteoarthritis of the contralateral knee joint of male amputees who do and do not play volleyball. *The Journal of Rheumatology*, 28(1), 169-172.

Mengarelli, A., Gentili, A., Strazza, A., Burattini, L., Fioretti, S., & Di Nardo, F. (2018). Co-activation patterns of gastrocnemius and quadriceps femoris in controlling the knee joint during walking. *Journal of Electromyography and Kinesiology*, 42, 117-122.

Miller, J. P., Croce, R. V., & Hutchins, R. (2000). Reciprocal coactivation patterns of the medial and lateral quadriceps and hamstrings during slow, medium and high speed isokinetic movements. *Journal of Electromyography and Kinesiology*, 10(4), 233-239.

Mima, T., & Hallett, M. (1999). Corticomuscular coherence: a review. *Journal of Clinical Neurophysiology*, 16(6), 501-511.

Mima, T., Simpkins, N., Oluwatimilehin, T., & Hallett, M. (1999). Force level modulates human cortical oscillatory activities. *Neuroscience Letters*, 275(2), 77-80.

Minetti, A. E. (1994). Contraction dynamics in antagonist muscles. *J Theor Biol*, 169(3), 295-304.

Mirabella, G. (2018). The Weight of Emotions in Decision-Making: How Fearful and Happy Facial Stimuli Modulate Action Readiness of Goal-Directed Actions. *Frontiers in Psychology*, 9, 1334.

Moissenet, F., Chèze, L., & Dumas, R. (2016). Contribution of individual musculo-tendon forces to the axial compression force of the femur during normal gait. *Movement Sport Sciences*, 93(3), 63-69.

Molteni, E., Rigoldi, C., Morante, M., Rozbaczylo, C., Haro, M., Albertini, G., … Bianchi, A. M. (2015). Quantification of long-term effects of botulinum injection in a case of cerebral palsy affecting the upper limb movement. *Dev Neurorehabil*, 18(3), 145-148.

Mora, I., Quinteiro-Blondin, S., PÈrot, C., Isabelle, M., Sylvie, Q.-B., & Chantal, Pè. (2003). Electromechanical assessment of ankle stability. *Eur J Appl Physiol*, 88(6), 558-564.

Morita, H., Crone, C., Christenhuis, D., Petersen, N. T., & Nielsen, J. B. (2001). Modulation of presynaptic inhibition and disynaptic reciprocal Ia inhibition during voluntary movement in spasticity. *Brain*, 124(4), 826-837.

Müller-Putz, G. R., Zimmermann, D., Graimann, B., Nestinger, K., Korisek, G., & Pfurtscheller, G. (2007). Event-related beta EEG-changes during passive and attempted foot movements in paraplegic patients. *Brain Research*, 1137(1), 84-91.

Myers, L. J., Lowery, M., O'Malley, M., Vaughan, C. L., Heneghan, C., St Clair Gibson, A., … Sreenivasan, R. (2003). Rectification and non-linear pre-processing of EMG signals for cortico-muscular analysis. *J Neurosci Methods*, 124(2), 157-165.

Naugle, K. M., Joyner, J., Hass, C. J., & Janelle, C. M. (2010). Emotional influences on locomotor behavior. *Journal of Biomechanics*, 43(16), 3099-3103.

Nazarpour, K., Barnard, A., & Jackson, A. (2012). Flexible cortical control of task-specific muscle synergies. *The Journal of Neuroscience*, 32(36), 12349-12360.

Neptune, R. R., Wright, I. C., & Van Den Bogert, A. J. (2000). A Method for Numerical Simulation of Single Limb Ground Contact Events: Application to Heel-Toe Running. *Computer Methods in Biomechanics and Biomedical Engineering*, 3(4), 321-334.

Neto, O. P., & Christou, E. A. (2010). Rectification of the EMG signal impairs the identification of oscillatory input to the muscle. *Journal of Neurophysiology*, 103(2), 1093-1103.

Netz, J., Ziemann, U., & Hömberg, V. (1995). Hemispheric asymmetry of transcallosal inhibition in man. *Experimental Brain Research*, 104(3), 527-533.

Newton, J. M., Sunderland, A., & Gowland, P. A. (2005). fMRI signal decreases in ipsilateral primary motor cortex during unilateral hand movements are related to duration and side of movement. *NeuroImage*, 24(4), 1080-1087.

Nikooyan, A. A., Veeger, H. E. J., Westerhoff, P., Bolsterlee, B., Graichen, F., Bergmann, G., & van der Helm, F. C. T. (2012). An EMG-driven musculoskeletal model of the shoulder.

Human Movement Science, 31(2), 429-447.

Nordlund, M. M., Thorstensson, A., & Cresswell, A. G. (2002). Variations in the soleus H-reflex as a function of activation during controlled lengthening and shortening actions. *Brain Research*, 952(2), 301-307.

Norton, J. A., & Gorassini, M. A. (2006a). Changes in cortically related intermuscular coherence accompanying improvements in locomotor skills in incomplete spinal cord injury. *Journal of Neurophysiology*, 95(4), 2580-2589.

Norton, J. A., & Gorassini, M. A. (2006b). Changes in cortically related intermuscular coherence accompanying improvements in locomotor skills in incomplete spinal cord injury. *Journal of Neurophysiology*, 95(4), 2580-2589.

Okamoto, T., Okamoto, K., & Andrew, P. D. (2003). Electromyographic developmental changes in one individual from newborn stepping to mature walking. *Gait & Posture*, *17*(1), 18-27.

Olney, S. J., & Winter, D. A. (1985). Predictions of knee and ankle moments of force in walking from EMG and kinematic data. *Journal of Biomechanics*, 18(1), 9-20.

Osternig, L. R., Hamill, J., Lander, J. E., & Robertson, R. (1986). Co-activation of sprinter and distance runner muscles in isokinetic exercise. *Med Sci Sports Exerc*, 18(4), 431-435.

Patino, L., Chakarov, V., Schulte-Mönting, J., Hepp-Reymond, M.-C., & Kristeva, R. (2006). Oscillatory cortical activity during a motor task in a deafferented patient. *Neuroscience Letters*, 401(3), 214-218.

Pedrosa, D. J., Quatuor, E.-L., Reck, C., Pauls, K. A. M., Huber, C. A., Visser-Vandewalle, V., & Timmermann, L. (2014). Thalamomuscular coherence in essential tremor: hen or egg in the emergence of tremor? *The Journal of Neuroscience*, 34(43), 14475-14483.

Peterson, B., & Docter, P. (2009). *Là-haut*.

Pfurtscheller, G. (1977). Graphical display and statistical evaluation of event-related desynchronization (ERD). *Electroencephalography and Clinical Neurophysiology*, 43(5), 757-760.

Pfurtscheller, G. (1981). Central beta rhythm during sensorimotor activities in man. *Electroencephalography and Clinical Neurophysiology*, 51(3), 253-264.

Pfurtscheller, G. (1992). Event-related synchronization (ERS): an electrophysiological correlate of cortical areas at rest. *Electroencephalography and Clinical Neurophysiology*, 83(1), 62-69.

Pfurtscheller, G. (2001). Functional brain imaging based on ERD/ERS. *Vision research*, 41, 1257-1260.

Pfurtscheller, G., & Aranibar, A. (1977). Event-related cortical desynchronization detected by power measurements of scalp EEG. *Electroencephalography and Clinical Neurophysiology*, 42(6), 817-826.

Pfurtscheller, G., & Aranibar, A. (1979). Evaluation of event-related desynchronization (ERD) preceding and following voluntary self-paced movement. *Electroencephalography and Clinical Neurophysiology*, 46(2), 138-146.

Pfurtscheller, G., Graimann, B., Huggins, J. E., Levine, S. P., & Schuh, L. A. (2003). Spatiotemporal patterns of beta desynchronization and gamma synchronization in corticographic data during self-paced movement. *Clinical Neurophysiology*, 114(7),

1226-1236.

Pfurtscheller, G., & Lopes da Silva, F. H. (1999). Event-related EEG/MEG synchronization and desynchronization: basic principles. *Clinical Neurophysiology*, *110*(11), 1842-1857.

Pfurtscheller, G., Neuper, C., Andrew, C., & Edlinger, G. (1997). Foot and hand area mu rhythms. *International Journal of Psychophysiology*, 26(1-3), 121-135.

Pierrot-Deseilligny, E., & Burke, D. (2005). *The Circuitry of the Human Spinal Cord: Its Role in Motor Control and Movement Disorders*. Cambridge: Cambridge University Press.

Pincivero, D. M., Coelho, A. J., & Campy, R. M. (2008). Contraction mode shift in quadriceps femoris muscle activation during dynamic knee extensor exercise with increasing loads. *Journal of Biomechanics*, 41(15), 3127-3132.

Pincivero, D. M., Gandhi, V., Timmons, M. K., & Coelho, A. J. (2006). Quadriceps femoris electromyogram during concentric, isometric and eccentric phases of fatiguing dynamic knee extensions. *Journal of Biomechanics*, 39(2), 246-254.

Pitof. (2004). *Catwoman*. Warner.

Poston, B., Danna-Dos Santos, A., Jesunathadas, M., Hamm, T. M., & Santello, M. (2010). Force-independent distribution of correlated neural inputs to hand muscles during three-digit grasping. *Journal of Neurophysiology*, 104(2), 1141-1154.

Potvin, J. R., & O'Brien, P. R. (1998). Trunk muscle co-contraction increases during fatiguing, isometric, lateral bend exertions. Possible implications for spine stability. *Spine*, 23(7), 774-781.

Prilutsky, B. I. (2000). Muscle coordination: the discussion continues. *Motor Control*, 4(1), 97-116.

Prilutsky, B. I., & Zatsiorsky, V. M. (2002). Optimization-based models of muscle coordination. *Exercise and Sport Sciences Reviews*, 30(1), 32-38.

Psek, J. A., & Cafarelli, E. (1993). Behavior of coactive muscles during fatigue. *J Appl Physiol*, 74(1), 170-175.

Raethjen, J., Lindemann, M., Dümpelmann, M., Wenzelburger, R., Stolze, H., Pfister, G., … Deuschl, G. (2002). Corticomuscular coherence in the 6-15 Hz band: is the cortex involved in the generation of physiologic tremor? *Experimental Brain Research*, 142(1), 32-40.

Raikova, R. T., & Prilutsky, B. I. (2001). Sensitivity of predicted muscle forces to parameters of the optimization-based human leg model revealed by analytical and numerical analyses. *Journal of Biomechanics*, 34(10), 1243-1255.

Rao, G. (2006). *Biomécanique de la coordination motrice : modélisations et analyses en réponse à une perturbation interne ou externe.* Université d'Aix-Marseille II.

Rao, G., Amarantini, D., & Berton, E. (2009). Influence of additional load on the moments of the agonist and antagonist muscle groups at the knee joint during closed chain exercise. *Journal of Electromyography and Kinesiology*, 19(3), 459-466.

Rao, G., Berton, E., Amarantini, D., Vigouroux, L., & Buchanan, T. S. (2010). An EMG-driven biomechanical model that accounts for the decrease in moment generation capacity during a dynamic fatigued condition. *Journal of Biomechanical Engineering*, 132(7), 071003.

Rasmussen, J., Damsgaard, M., & Voigt, M. (2001). Muscle recruitment by the min/max

criterion -- a comparative numerical study. *Journal of Biomechanics*, 34(3), 409-415.

Remaud, A., Guével, A., & Cornu, C. (2007). Antagonist muscle coactivation and muscle inhibition: effects on external torque regulation and resistance training-induced adaptations. *Neurophysiol Clin*, 37(1), 1-14.

Remaud, Anthony, Cornu, C., & Guével, A. (2005). A methodologic approach for the comparison between dynamic contractions: influences on the neuromuscular system. *Journal of Athletic Training*, 40(4), 281-287.

Reyes, A., Laine, C. M., Kutch, J. J., & Valero-Cuevas, F. J. (2017). Beta Band Corticomuscular Drive Reflects Muscle Coordination Strategies. *Frontiers in computational neuroscience*, 11, 17-17.

Ridderikhoff, A., Daffertshofer, A., Peper, C. E., & Beek, P. J. (2005). Mirrored EMG activity during unimanual rhythmic movements. *Neuroscience Letters*, 381(3), 228-233.

Riehle, A., Vaadia, E., & Vaadia, E. (2004). *Motor Cortex in Voluntary Movements : A Distributed System for Distributed Functions*. CRC Press.

Roby-Brami, A., Hoffmann, G., Laffont, I., Combeaud, M., & Hanneton, S. (2005). Redondance du membre supérieur et compensation des déficiences motrices. In S. C. et C. M. Yann Coello (Éd.), *vision, espace et cognition : fonctionnement normal et pathologique* (p. 143-160). Presses Universitaires du Septentrion.

Romanò, C., & Schieppati, M. (1987). Reflex excitability of human soleus motoneurones during voluntary shortening or lengthening contractions. *The Journal of Physiology*, 390, 271-284.

Rosenberg, J. R., Amjad, A. M., Breeze, P., Brillinger, D. R., & Halliday, D. M. (1989). The Fourier approach to the identification of functional coupling between neuronal spike trains. *Prog Biophys Mol Biol*, 53(1), 1-31.

Rudolph, K. S., Axe, M. J., Buchanan, T. S., Scholz, J. P., & Snyder-Mackler, L. (2001). Dynamic stability in the anterior cruciate ligament deficient knee. *Knee Surgery Sports Traumatology Arthroscopy*, 9(2), 62-71.

Salenius, S., Portin, K., Kajola, M., Salmelin, R., & Hari, R. (1997). Cortical control of human motoneuron firing during isometric contraction. *Journal of Neurophysiology*, 77(6), 3401-3405.

Salenius, Stephan, & Hari, R. (2003). Synchronous cortical oscillatory activity during motor action. *Current Opinion in Neurobiology*, 13(6), 678-684.

Sallard, E., Tallet, J., Thut, G., Deiber, M.-P., & Barral, J. (2014). Post-switching beta synchronization reveals concomitant sensory reafferences and active inhibition processes. *Behavioural Brain Research*, 271, 365-373.

Salmelin, R., & Hari, R. (1994). Spatiotemporal characteristics of sensorimotor neuromagnetic rhythms related to thumb movement. *Neuroscience*, 60(2), 537-550.

Sartori, M., Reggiani, M., Farina, D., & Lloyd, D. G. (2012). EMG-driven forward-dynamic estimation of muscle force and joint moment about multiple degrees of freedom in the human lower extremity. *PLoS One*, 7(12), e52618-e52618.

Sartori, M., Reggiani, M., Lloyd, D. G., & Pagello, E. (2010). An EMG-driven Musculoskeletal Model of the Human Lower Limb for the Estimation of Muscle Forces and Moments at the Hip, Knee and Ankle Joints in vivo. In *Proceedings of SIMPAR 2010*

Workshops (p. 137-146). Darmstadt, Germany.

Schieppati, M. (1987). The Hoffmann reflex: a means of assessing spinal reflex excitability and its descending control in man. *Progress in Neurobiology*, 28(4), 345-376.

Semmler, J. G., Ebert, S. A., & Amarasena, J. (2013). Eccentric Muscle Damage Increases Intermuscular Coherence During a Fatiguing Isometric Contraction. *Acta Physiol*, 208(4), 362-75.

Serrien, D. J., Cassidy, M. J., & Brown, P. (2003). The importance of the dominant hemisphere in the organization of bimanual movements. *Human Brain Mapping*, 18(4), 296-305.

Shao, Q., Bassett, D. N., Manal, K., & Buchanan, T. S. (2009). An EMG-driven model to estimate muscle forces and joint moments in stroke patients. *Comput Biol Med*, 39(12), 1083-1088.

Shelburne, K. B., Torry, M. R., & Pandy, M. G. (2005). Effect of muscle compensation on knee instability during ACL-deficient gait. *Med Sci Sports Exerc*, 37(4), 642-648.

Shinohara, M., Keenan, K. G., & Enoka, R. M. (2003). Contralateral activity in a homologous hand muscle during voluntary contractions is greater in old adults. *Journal of Applied Physiology*, 94(3), 966-974.

Simpson, D. M., Gracies, J.-M., Graham, K., Hallett, M., Miyasaki, J., Naumann, M., … So, Y. (2009). Assessment: botulinum neurotoxin for the treatment of spasticity (an evidence-based review). *Neurology*, 73(9), 736-737.

Singh, L. N., Higano, S., Takahashi, S., Kurihara, N., Furuta, S., Tamura, H., … Yamada, S. (1998). Comparison of ipsilateral activation between right and left handers: a functional MR imaging study. *Neuroreport*, 9(8), 1861-1866.

Solomonow, M., Baratta, R., Zhou, B. H., & D'Ambrosia, R. (1988). Electromyogram coactivation patterns of the elbow antagonist muscles during slow isokinetic movement. *Experimental Neurology*, 100(3), 470-477.

Stancák, A., Riml, A., & Pfurtscheller, G. (1997). The effects of external load on movement-related changes of the sensorimotor EEG rhythms. *Electroencephalography and Clinical Neurophysiology*, 102(6), 495-504.

Sun, W., Liang, J., Yang, Y., Wu, Y., Yan, T., Song, R., … Song, R. (2016). Investigating Aging-Related Changes in the Coordination of Agonist and Antagonist Muscles Using Fuzzy Entropy and Mutual Information. *Entropy*, 18(6), 229.

Tallet, J., Albaret, J.-M., & Barral, J. (2013). Developmental changes in lateralized inhibition of symmetric movements in children with and without Developmental Coordination Disorder. *Research in Developmental Disabilities*, 34(9), 2523-2532.

Tallet, J., Barral, J., & Hauert, C.-A. (2009). Electro-cortical correlates of motor inhibition: A comparison between selective and non-selective stop tasks. *Brain Research*, 1284, 68-76.

Tanaka, R. (1974). Reciprocal Ia inhibition during voluntary movements in man. *Experimental Brain Research*, 21(5), 529-540.

Theorin, A., & Johansson, R. S. (2007). Zones of bimanual and unimanual preference within human primary sensorimotor cortex during object manipulation. *NeuroImage*, 36 *Suppl 2*, T2-T15.

Thomas, C. K., Tucker, M. E., & Bigland-Ritchie, B. (1998). Voluntary muscle weakness

and co-activation after chronic cervical spinal cord injury. *J Neurotrauma*, 15(2), 149-161.

Tillin, N. A., Pain, M. T. G., & Folland, J. P. (2011). Short-term unilateral resistance training affects the agonist-antagonist but not the force-agonist activation relationship. *Muscle & Nerve*, 43(3), 375-384.

Tisseyre, J., Amarantini, D., Chalard, A., Marque, P., Gasq, D., & Tallet, J. (2018). Mirror Movements are Linked to Executive Control in Healthy and Brain-injured Adults. *Neuroscience*, 379, 246-256.

Tisseyre, J., Marquet-Doléac, J., Barral, J., Amarantini, D., & Tallet, J. (2019). Lateralized inhibition of symmetric contractions is associated with motor, attentional and executive processes. *Behavioural Brain Research*, 361, 65-73.

Todor, J. I., & Lazarus, J. A. (1986). Exertion level and the intensity of associated movements. *Developmental Medicine and Child Neurology*, 28(2), 205-212.

Tome, & Janry. (2010). *Tiens-toi droit !* (Dupuis, Vol. 15).

Unnithan, V. B., Dowling, J. J., Frost, G., & Bar-Or, O. (1996). Role of cocontraction in the O2 cost of walking in children with cerebral palsy. *Med Sci Sports Exerc*, 28(12), 1498-1504.

Unnithan, V. B., Dowling, J. J., Frost, G., Volpe Ayub, B., & Bar-Or, O. (1996). Cocontraction and phasic activity during GAIT in children with cerebral palsy. *Electromyogr Clin Neurophysiol*, 36(8), 487-494.

Ushiyama, J., Masakado, Y., Fujiwara, T., Tsuji, T., Hase, K., Kimura, A., … Ushiba, J. (2012). Contraction level-related modulation of corticomuscular coherence differs between the tibialis anterior and soleus muscles in humans. *Journal of Applied Physiology*, 112(8), 1258-1267.

Ushiyama, J., Takahashi, Y., & Ushiba, J. (2010). Muscle dependency of corticomuscular coherence in upper and lower limb muscles and training-related alterations in ballet dancers and weightlifters. *Journal of Applied Physiology, 109*(4), 1086-1095.

Uttner, I., Kraft, E., Nowak, D. A., Müller, F., Philipp, J., Zierdt, A., & Hermsdörfer, J. (2007). Mirror movements and the role of handedness: isometric grip forces changes. *Motor Control*, 11(1), 16-28.

van Soest, A. J., Haenen, W. P., & Rozendaal, L. A. (2003). Stability of bipedal stance: the contribution of cocontraction and spindle feedback. *Biological Cybernetics*, 88(4), 293-301.

Vardy, A. N., Daffertshofer, A., Ridderikhoff, A., & Beek, P. J. (2007). Differential after-effects of bimanual activity on mirror movements. *Neuroscience Letters*, 416(2), 117-122.

Vernazza-Martin, S., Fautrelle, L., Vieillard, S., Longuet, S., & Dru, V. (2017). Age-related differences in processes organizing goal-directed locomotion toward emotional pictures. *Neuroscience*, 340, 455-463.

Verstynen, T., Diedrichsen, J., Albert, N., Aparicio, P., & Ivry, R. B. (2005). Ipsilateral motor cortex activity during unimanual hand movements relates to task complexity. *Journal of Neurophysiology*, 93(3), 1209-1222.

Vigouroux, L., Devise, M., Cartier, T., Aubert, C., & Berton, E. (2019). Performing pull-ups with small climbing holds influences grip and biomechanical arm action. *Journal of Sports Sciences*, 37(8), 886-894.

Vigouroux, L., Quaine, F., Labarre-Vila, A., Amarantini, D., & Moutet, F. (2007). Using EMG data to constrain optimization procedure improves finger tendon tension estimations

during static fingertip force production. *Journal of Biomechanics*, 40(13), 2846-2856.

Vila-Chã, C., Falla, D., Correia, M. V., & Farina, D. (2012). Changes in H reflex and V wave following short-term endurance and strength training. *Journal of Applied Physiology*, 112(1), 54-63.

Vinti, M., Costantino, F., Bayle, N., Simpson, D. M., Weisz, D. J., & Gracies, J.-M. (2012). Spastic cocontraction in hemiparesis: effects of botulinum toxin. *Muscle & Nerve*, 46(6), 926-931.

Vinti, M., Couillandre, A., Hausselle, J., Bayle, N., Primerano, A., Merlo, A., … Gracies, J.-M. (2013). Influence of effort intensity and gastrocnemius stretch on co-contraction and torque production in the healthy and paretic ankle. *Clin Neurophysiol*, 124(3), 528-535.

Ward, N. J., Farmer, S. F., Berthouze, L., & Halliday, D. M. (2013). Rectification of EMG in low force contractions improves detection of motor unit coherence in the beta-frequency band. *J Neurophysiol*, 110(8), 1744-1750.

Weidner, N., Ner, A., Salimi, N., & Tuszynski, M. H. (2001). Spontaneous corticospinal axonal plasticity and functional recovery after adult central nervous system injury. *Proc Natl Acad Sci U S A*, 98(6), 3513-3518.

Westing, S. H., Cresswell, A. G., & Thorstensson, A. (1991). Muscle activation during maximal voluntary eccentric and concentric knee extension. *European Journal of Applied Physiology and Occupational Physiology*, 62(2), 104-108.

Winges, S. A., Kornatz, K. W., & Santello, M. (2008). Common input to motor units of intrinsic and extrinsic hand muscles during two-digit object hold. *Journal of Neurophysiology*, 99(3), 1119-1126.

Winter, D. A. (1979). A new definition of mechanical work done in human movement. *Journal of Applied Physiology*, 46(1), 79-83.

Winter, David A. (1990). *Biomechanics and Motor Control of Human Movement* (Wiley-Interscience). Toronto, Ontario.

Wolff, P. H., Gunnoe, C. E., & Cohen, C. (1983). Associated movements as a measure of developmental age. *Developmental Medicine and Child Neurology*, 25(4), 417-429.

Yanagawa, T., Shelburne, K., Serpas, F., & Pandy, M. (2002). Effect of hamstrings muscle action on stability of the ACL-deficient knee in isokinetic extension exercise. *Clinical Biomechanics*, 17(9-10), 705-712.

Yeadon, M. R., & Challis, J. H. (1994). The future of performance-related sports biomechanics research. *Journal of Sports Sciences*, 12(1), 3-32.

Yelnik, A. P., Simon, O., Bensmail, D., Chaleat-Valayer, E., Decq, P., Dehail, P., … Agence française de sécurité sanitaire des produits de santé. (2009). Drug treatments for spasticity. *Ann Phys Rehabil Med*, 52(10), 746-756.

Neuro-biomécanique de la redondance musculaire – Modélisation musculo-squelettique et contrôle moteur de la co-contraction agoniste / antagoniste

——

David AMARANTINI

Rapport de synthèse, Habilitation à Diriger des Recherches – 2019
Graphical abstract
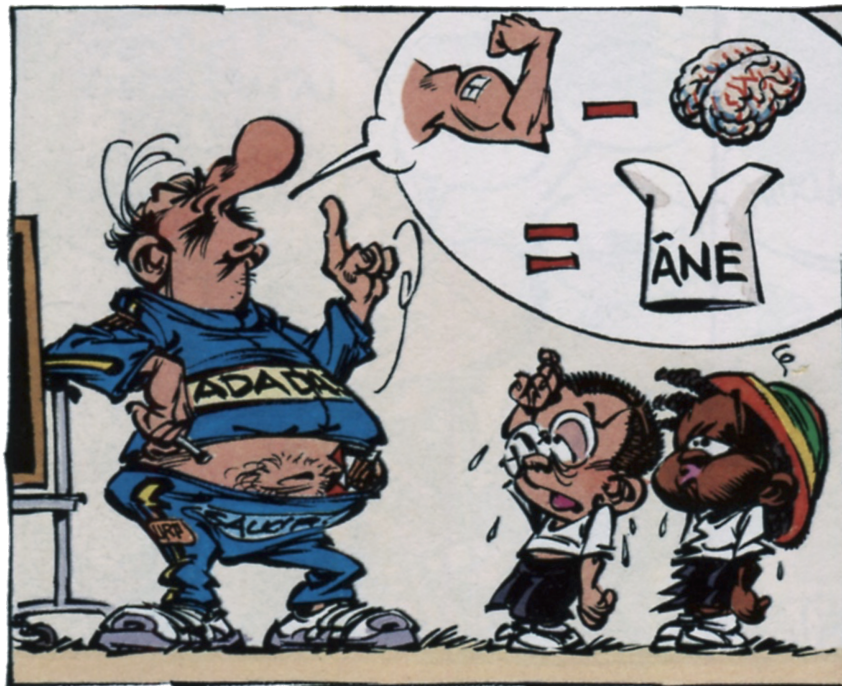
Le petit Spirou, Tome 15 – Tiens-toi droit ! (2010)

Neuro-biomécanique de la redondance musculaire – Modélisation musculo-squelettique et contrôle moteur de la co-contraction agoniste / antagoniste

————

David AMARANTINI

Rapport de synthèse, Habilitation à Diriger des Recherches – 2019
Résumés français et anglais

Résumé : Ce document est la synthèse du cheminement scientifique que j'ai suivi depuis 2003 pour développer mes activités de recherche sur la question de la redondance musculaire. Tout au long de mon parcours, j'ai approfondi ce sujet en m'intéressant aux rôles fonctionnels de la co-contraction agoniste / antagoniste et aux mécanismes nerveux centraux de contrôle de l'activité musculaire antagoniste lors de contractions volontaires et involontaires chez l'homme, avec des visées dans les domaines entrecroisés de l'optimisation de la performance motrice chez le sujet sain et l'amélioration de la fonction motrice chez le patient cérébro- ou médullo-lésé. Pour traiter cette question, ma démarche scientifique m'a fait passer d'une approche strictement biomécanique à une approche multimodale réellement pluridisciplinaire au croisement de la biomécanique, des neurosciences et du traitement du signal. Les principales thématiques de recherche que j'ai développées concernent la modélisation musculo-squelettique de la redondance musculaire, l'étude des facteurs de modulation de la co-contraction agoniste / antagoniste saine et pathologique, l'étude des corrélats cérébraux de l'activité des muscles antagonistes, et enfin la contribution des interactions cortico-musculaires et intermusculaires au contrôle de la co-contraction agoniste / antagoniste. En poursuivant la démarche originale dans laquelle je m'inscris dans le domaine de la neuro-biomécanique, ces travaux approfondiront l'analyse de la co-contraction à travers une définition élargie et une vision ouverte à de nouveaux champs scientifiques. Ils contribueront également à mieux comprendre le rôle fonctionnel et les mécanismes impliqués dans le contrôle de la redondance musculaire dans une double perspective fondamentale et clinique.

Mots clés : biomécanique, neuroscience, traitement du signal, cohérence, mouvement humain, EEG, EMG.

————————————

Neuro-biomechanics of muscular redundancy – Musculoskeletal modeling and motor control of agonist/antagonist co-contraction

Abstract: This document summarizes the scientific route that I have followed since 2003 to develop my research activities on the issue of muscular redundancy. Throughout my career, I have deepened this subject by focusing on the functional roles of agonist/antagonist co-contraction and on the central nervous mechanisms controlling antagonist muscles activity during voluntary and involuntary contractions in man, with the aims to optimize motor performance in the healthy subject and to improve motor function in the brain or spinal cord injured subjects. To address this issue, my scientific works shifted from a strictly biomechanical approach to a multidisciplinary multimodal approach at the intersection of biomechanics, neuroscience and signal processing. The main research topics that I have developed relate to musculoskeletal modeling of muscular redundancy, to the study of the factors of modulation of healthy and pathological agonist/antagonist co-contraction, to the study of the cerebral correlates of antagonist muscles activity, and finally to the contribution of cortico-muscular and intermuscular interactions to the control of agonist/antagonist co-contraction. By pursuing the original approach in which I am engaged in the field of neuro-biomechanics, this work will deepen the analysis of co-contraction through a broader definition and an open vision to new scientific fields. It will also contribute to a better understanding of the functional role and the mechanisms involved in the control of muscular redundancy from both a fundamental and clinical perspective.

Keywords: biomechanics, neuroscience, signal processing, coherence, human movement, EEG, EMG.